ASYMMETRIC INDUCTION IN THE PHOTOCHEMISTRY OF

α-OXOAMIDES AND BICYCLIC ARYL KETONES

by

KEYAN WANG

B.Sc., Hangzhou University, P.R.China, 1989
M.Sc., Tsinghua University, P.R.China, 1995

A THESIS SUBMITTED IN PARTIAL FULFILMENT OF

THE REQUIREMENTS FOR THE DEGREE OF

DOCTOR OF PHILOSOPHY

in

THE FACULTY OF GRADUATE STUDIES

(DEPARTMENT OF CHEMISTRY)

We accept this thesis as conforming

to the required standard

THE UNIVERSITY OF BRITISH COLUMBIA

May 2004

Canadä

Abstract

Enantioselective photochemical synthesis of a β-lactam (methyl 4-[3-hydroxy-2,2-dimethyl-1-(1-methylethyl)-4-oxo-3-azetidinyl]benzoate) was investigated *via* the ionic chiral auxiliary method. Solid state photolysis of the chiral salts formed from optically pure amines and the achiral α-oxoamide reactant containing a carboxylic acid functional group gave variable results, but through the use of a number of auxiliaries it was possible to achieve a high degree of enantioselectivity in the β-lactam (up to 99 % ee at 99 % conversion of the starting α-oxoamide). Suspension of the prolinamide salt in hexane allowed the photoreaction to be carried out on a 500 mg scale, thus demonstrating the synthetic utility of the solid state ionic chiral auxiliary approach to asymmetric synthesis.

The covalent chiral auxiliary method was also investigated for asymmetric synthesis of the β-lactam. Solid state photolysis of a chiral ester formed from an optically pure alcohol and the achiral α-oxoamide gave up to 95% de at 100 % conversion. Suspension of the chiral ester in water allowed the photoreaction to be carried out on a 200 mg scale.

X-ray crystallographic data from a number of α-oxoamides provided insight on the origin of the observed enantioselectivity/diastereoselectivity. The prediction of the absolute configuration of the β-lactam based on the topochemical control principle was validated by crystal structure-reactivity correlations.

Asymmetric induction in the Norrish/Yang photochemistry of a series of three bicyclic aryl ketones, bicyclo[2.2.2]octyl ketones, bicyclo[2.2.1]heptyl ketones and dimethylated bicyclo[2.2.1]heptyl ketones, was also studied by using the ionic chiral auxiliary method. Photolysis of the chiral salts in the crystalline state gave high ee's for bicyclo[2.2.2]octyl ketones, high de's for bicyclo[2.2.1]heptyl ketones, and both high ee's and de's for dimethylated bicyclo[2.2.1]heptyl ketones.

Through the use of X-ray crystallography, the solid state reactivities were rationalized based on topochemical expectations with the aid of strain energy calculations on the photoproducts. Non-topochemical reactions were also found in this study.

Molecular mechanics calculations were conducted to predict the solid state conformations of the substrates prior to the laboratory work. The calculations were successful in the prediction of enantioselectivity for the three bicyclic aryl ketones investigated. In this way, molecular mechanics serves as a basis for crystal engineering in asymmetric synthesis.

Table of Contents

List of Figures

List of Tables

List of Symbols and Abbreviations

ν_{max}	absorption maxima (IR spectroscopy)
λ_{max}	absorption maxima (UV spectroscopy)
Å	angstrom
Δ	heat
δ	chemical shift (ppm)
°C	degrees Celsius
ε	molar extinction coefficients
anal.	analysis
APT	attached proton test
Ar	aryl
aq.	aqueous
bp	boiling point
br	broad
calcd	calculated
conc.	concentrated
conv	conversion
COSY	^{1}H-^{1}H correlation spectroscopy
d	doublet
dd	doublet of doublets
de	diastereomeric excess
DCI	desorption chemical ionization
DMF	dimethylformamide
DMPU	*N,N'*-dimethylpropyleneurea
ee	enantiomeric excess
EI	electron impact
ESI	Electrospray ionization
GC	gas chromatography
h	hour(s)
hept	heptet

hv	light
HMBC	heteronuclear multiple bond connectivity
HMQC	heteronuclear multiple quantum coherence
HPLC	high performance liquid chromatography
HRMS	high resolution mass spectrometry
Hz	hertz
ID	inner diameter
IPA	isopropanol
IR	infrared
J	coupling constant (Hz)
LDA	lithium diisopropylamine
LRMS	low resolution mass spectrometry
LSIMS	liquid secondary ionization mass spectra
M	molarity
Me	methyl
MHz	megahertz
MOM	methoxymethyl
m	multiplet
mg	milligram
min	minute
mL	milliliter
mp	melting point
mmol	millimole
mol	mole
NMR	nuclear magnetic resonance
NOE	nuclear Overhauser enhancement
NOESY	two-dimensional nuclear Overhauser spectroscopy
nm	nanometer
ORTEP	Oak Ridge Thermal Ellipsoid Program
Ph	phenyl
^{i}Pr	isopropyl

ppm	parts per million
psi	pounds per square inch
q	quartet
quint	quintet
RT	room temperature
s	singlet
SEM	2-(trimethylsilyl)ethoxymethyl
t	triplet
temp	temperature
THF	tetrahydrofuran
TMS	trimethylsilyl
Tol	tolyl
UV / VIS	ultraviolet / visible

Acknowledgements

I would like to express my deepest gratitude to Professor John Scheffer for his valuable guidance, encouragement, and support on my research and study over the last five years. I appreciate his patience and understanding in helping me write this thesis.

I am grateful to Dr Brian Patrick (UBC X-ray crystallography laboratory), Professor Menahem Kaftory and Dr. Mark Botoshansky (Department of Chemistry, Technion, Israel), Professor Dario Braga and Dr. Lucia Maini (Department of Chemistry, University of Bologna, Italy), and Shuang Chen for their help on X-ray crystal structure determinations.

I would like to express my appreciation to the staff in the NMR laboratory, mass spectrometry facilities, and the Chemistry Department at the University of British Columbia.

Finally, I would like to thank the current and past members of the Scheffer group for their help and encouragement.

Dedications

To

My Parents, Molly and Aaron

with Love

INTRODUCTION

Chapter 1 Introduction

1.1 Preamble

The history of solid state chemistry can be traced back to the beginning of the nineteenth century. Wöhler's synthesis of urea in 1828,[1] the milestone event in organic chemistry, was the first solid state reaction. Trommsdorff's 1834 discovery[2] that sunlight caused santonin crystals to become yellow and shatter, was the first solid state organic photochemical reaction. However, in-depth research in both solid state chemistry and solid state organic photochemistry was hampered by a poor understanding of the crystal structures that are the essential governing factor in solid state reactions. Computers made crystallography accessible to everyone. The combination of X-ray crystallography and photochemistry has contributed greatly to our understanding of photoreaction mechanisms and enabled photochemistry to be used as a synthetic tool.[3] The solid state chemistry of drugs[4] and crystal engineering[5] in material sciences played an important role in the development of solid state chemistry/photochemistry. Photochemical techniques have greatly simplified the synthesis of numerous highly strained organic molecules, which are inaccessible by ground state chemistry.[6]

One of the fundamental features of the living world is its chirality. Chirality centres are common in the building blocks of the living world: amino-acids, carbohydrates and nucleic acids. For the most part, physiological processes are homochiral, i.e., they show 100% stereoselectivity and involve only one stereoisomer. Differential interactions with chiral targets, such as receptors, enzymes and ion channels, lead to chiral discrimination in physiological processes. The debate about the relative merits of racemic drugs and single-enantiomer drugs was short lived. Since 1992, the U.S. Food and Drug Administration (FDA) and the European Committee for Proprietary Medicinal Products have required manufacturers to research and characterize each enantiomer of a potential drug.[7] Single-enantiomer drugs are rapidly growing from ~20 % of new drugs ten years ago to almost 75 % in 2002.[8(a)] Drug molecules approved by the U.S. FDA in 1998-2001 show the following approximate distribution: 52 % achiral; 30 % single enantiomer with several chirality centres; 7 % single enantiomer with one chirality centre; 7 % racemates; and 4 % multiple diastereomers.[8(a)] Drugs are now marketed or being developed as single

enantiomers in place of previous racemic mixtures, a popular process in the pharmaceutical industry known as "chiral switching".[8] Asymmetric synthesis is the main source of chiral drugs. Ground state chemistry is dominant in the field of asymmetric synthesis. Asymmetric synthesis in organic photochemistry, a subject that has been seen considerable recent activity,[9] is still undeveloped compared to asymmetric synthesis in the ground state.

The combination of solid state chemistry and photochemistry has two advantages: higher selectivity in solid state reactions and construction of highly strained molecules through photochemistry. Utilization of these two advantages in asymmetric synthesis (Figure 1.1) is the major subject of the present thesis.
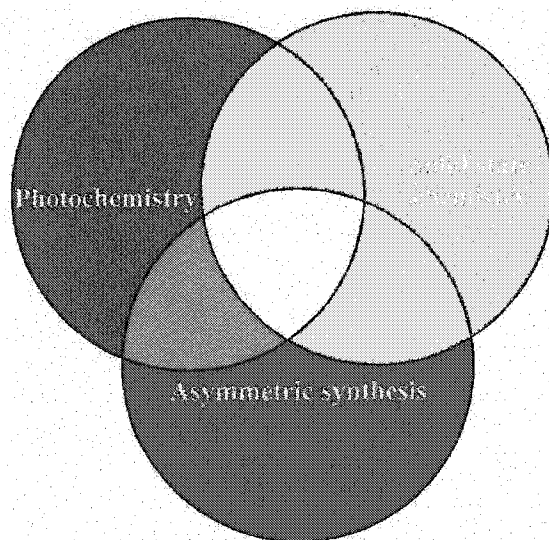
Figure 1.1 Pictorial representation of asymmetric synthesis in solid state photochemistry: (a) photochemistry (blue), a builder of highly strained molecules; (b) solid state chemistry (green), a highly selective chemical transformation; (c) asymmetric synthesis (red), a major source of enantiomerically pure molecules.

1.2 Crystal Engineering

The term "crystal engineering" was coined by Schmidt[10] in the 1970s with his pioneering work on the topochemical reactions of crystalline cinnamic acids. This term was widened in the 1990s by Desiraju[5] with the following definition: "Crystal engineering is defined as the understanding of intermolecular interactions in the context of crystal packing and in the utilization of such understanding in the design of new solids with desired physical and chemical properties".

Polymorphism is defined as the existence of the same chemical substance in more than one crystalline form and pseudopolymorphism refers to solvent inclusion in crystals.[11] Polymorphs have different physical and chemical properties, such as different melting points, different chemical reactivities, different dissolution rates and different bioavailabilities. They can be interconverted by phase transformations induced by heat or mechanical stress, or by solvent-mediated processes. The existence of polymorphism means the free energy difference between the different forms is quite small, which obviously hinders the prediction of crystal structures. In this case polymorphism is a distinct roadblock to crystal engineering. Polymorphism is very common in many drugs. The polymorphism of cinnamic acid will be described in greater detail in the next section of this chapter.

Amorphous solids have no regular crystal packing or shape. When a crystal is reduced to the size of 10^{-8} cm, the region of atomic dimensions, it is no longer an ordered array of atoms or molecules, i.e., it is no longer a crystal! An amorphous solid gives no X-ray diffraction pattern. Amorphous solids have a rapid dissolution rate, which is pharmaceutically desirable, but they are also relatively unstable, a pharmaceutically undesirable property.[4(a)]

Several techniques have been used in crystal engineering: X-ray crystallography, statistical analysis of the Cambridge Structural Database (the advantage of this method is that any distortion in individual X-ray structures is averaged), spectroscopy (NMR, IR), thermal analysis, and computation.

The ultimate step in crystal engineering must be the prediction of the crystal structure. To date, precise prediction of crystal structures is still a daunting task, even with the most powerful computational methods, because crystal packing is governed by many weak,

noncovalent intermolecular forces. Hydrogen bonding and metal-ligand coordination, the strong intermolecular interactions in crystals, were successfully utilized to engineer the assembly of supramolecular networks.[12] The most recent review of hydrogen bonding in the solid state was reported by Steiner.[13] To date, understanding of the intra- and intermolecular interactions leading to an observed crystal packing is incomplete, and attempts at engineering crystals have largely been a process of trial and error, as solid state chemistry itself is still in the stage of "Chem Is Try".

With the current limitations of crystal engineering in the design of multiple-component systems, solid state studies have focussed primarily on the reactions of single component crystals, e.g., rearrangements and dimerizations. An effective strategy for performing heterobimolecular solid state reactions comes from the growth of mixed crystals formed by co-crystallization of two structurally similar molecules such as the amides shown in Figure 1.2, or by host-guest complexes formed through hydrogen bonding. Compounds 1 and 2 crystallize together. Upon photolysis the co-crystal was transformed into the mixed dimer 3 as well as the *anti* head-to-tail homodimer 4 with excellent regio- and stereocontrol.[14] Host-guest chemistry will be described in more detail in a later part of this chapter.
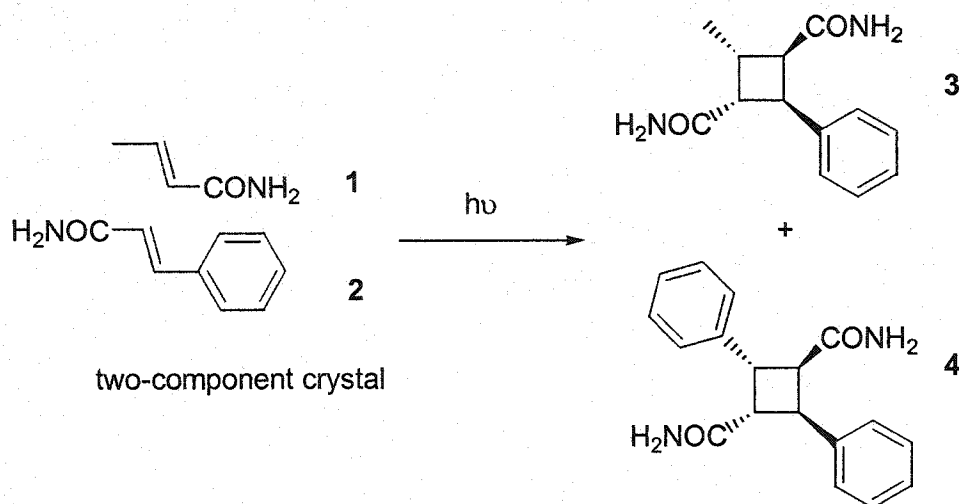
Figure 1.2 A solid state bimolecular reaction of a mixed crystal.

Today crystal engineering is expanding to the self-assembly of both organic and inorganic systems and more: molecular crystals,[15] nanostructures,[16] metal-organic frameworks,[17] solid state pharmaceutical chemistry,[4] coordination polymers,[18] theoretical

chemistry, crystallography, and crystal growth. A quote from Braga et al.[19] is used to conclude this section: "In the materials chemistry area, crystal engineering is perceived as a working strategy, a utilitarian method with relevant interdisciplinary interactions with biology, informatics and physics; in the supramolecular chemistry area, crystal engineering is perceived as a way to exploit non-covalent interactions to assemble molecules in solid supermolecules; in the area of solid state reactivity, crystal engineering is seen as the tool that allows topochemical control of reactivity and stereochemistry, as well as the understanding and exploitation of solvent-free, environmentally more friendly reactions, and/or heterogeneous reactions with potentials for sensing and trapping of molecules or for the preparation of otherwise elusive molecules; in the theoretical chemistry area, the challenge of crystal engineering is to predict the outcome of a crystallization process, hoping that this knowledge will then suggest methods of control; in the area of biology and biotechnology, crystal engineering is the investigation of the interaction between biological matrices and crystalline phases; For crystallography, crystal engineering provides the push and additional motivation to improve methods of data collection, data storage, data mining and most importantly, to develop friendly and portable methods for direct structure determination from powder diffraction data; in the field of polymorphism, crystal engineering is perceived as a conceptual (and practical) way to tackle the relationship between kinetics and thermodynamics, to generate polymorphs and pseudo-polymorphs *on purpose* by a judicious choice of the crystallization conditions, and to practise ways to *trick* nature into doing what the researcher needs".

1.3 Solid State Chemistry and the Topochemical Postulate

The field of crystal engineering began with the study of organic solids. Far from being a "chemical cemetery",[20] a crystal provides a more selective chemical reaction medium than conventional isotropic fluid media. Generally, solid state reactions tend to occur with minimum atomic/molecular motion, the so-called *topochemical principle*. This concept was first formulated by Kohlshütter in 1918.[21] It was not until the advent of modern X-ray crystallographic techniques in the 1960's that the fundamental *topochemical rules* finally emerged thanks to the pioneering work of Schmidt and

co-workers on the intermolecular [2 + 2] photocycloaddition reactions of *trans*-cinnamic acid derivatives.[22]
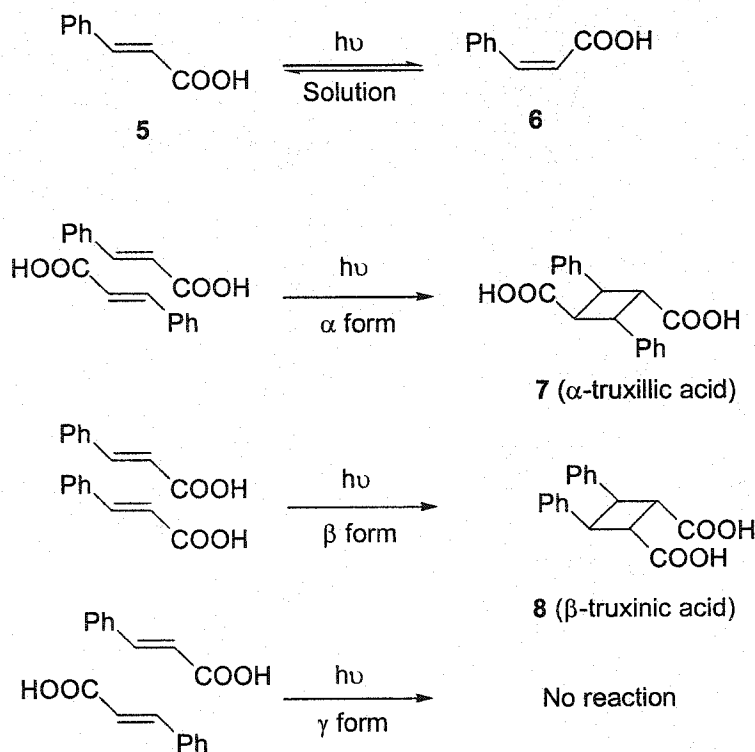
Figure 1.3 *trans*-Cinnamic acid photochemistry in solution and three polymorphic crystal forms

As shown in Figure 1.3, photolysis of *trans*-cinnamic acid (**5**) in solution affords *cis*-cinnamic acid (**6**). In the solid state, *trans*-cinnamic acid crystallizes in three polymorphic forms: α, β, and γ. Irradiation of the α form, in which the molecules are packed with a head-to-tail pattern and a center-to-center distance between the two nearest parallel double bonds of 3.8 Å, gives a head-to-tail dimer, α-truxillic acid (**7**). The molecules in the metastable β form are packed head-to-head with a nearest neighbor contact between two parallel double bonds of 3.9 Å. The mirror symmetric β-truxinic acid (**8**) is formed upon photolysis of the β form of *trans*-cinnamic acid in the solid state. The γ form, in which the adjacent and parallel double bonds are offset with a center-to-center distance of 4.7 Å, is photochemically stable. This photostability was interpreted as being due to lattice constraints which do not permit the potentially reactive centres to move

sufficiently close together to form a photodimer. Interestingly, the metastable β form of

trans-cinnamic acid undergoes a thermal phase transition to give the more stable α form

in the solid state at about 50 °C. Irradiation of β form crystals at high temperature (>50

°C) gave both α truxillic acid and β truxinic acid.[22(b)] This example shows both the

topochemical control of solid state reactions and the reactivity differences among

polymorphs. It should also be noted that solid-state photochemical reactions may offer

distinct advantages over the corresponding solution reactions, because they allow control

of the regio- and stereochemistry of the products (such as truxillic and truxinic acids) and

control of the course of the reaction. After studying the [2 + 2] photocycloaddition of

trans-cinnamic acid and its derivatives, Schmidt proposed that the centre-to-centre

distance between two adjacent double bonds should be less than a critical distance of

approximately 4.2 Å for the occurrence of [2 + 2] photocycloaddition in the solid state.

The distance between the reacting double bonds is not the only determining factor for

solid state [2 + 2] photocycloaddition. Parallel alignment of the reacting double bonds is

also required. There are examples in which the distance between the centres of adjacent

double bonds is within the proposed reaction limit, but the double bonds are not parallel

to each other. In these cases, no photodimerization reaction was observed in the solid

state.[23]

Nonetheless, a few cases have been reported where the reacting double bonds were

not exactly parallel but the photodimerization reaction was observed. For example, in

crystals of 7-methoxycoumarin, the reactive double bonds are rotated by about 65 ° with

respect to each other, and the centre-to-centre distance between them is 3.83 Å. In spite

of this unfavorable arrangement, solid state photodimerization did occur.[24] Another

exception was found in the [2 + 2] photocyclization of 4-formylcinnamic acid, where

photocyclization did occur upon irradiation even though the parallel double bonds are

more than 4.8 Å apart in the crystal.[25] Most exceptions to the topochemical rules were

explained by crystal disorder or defects.[4,5] Such exceptions should not be considered as

serious violations of Schmidt's original concepts in the topochemical postulate, but

should be integrated into the original basic idea by widening its scope. More recently, it

was suggested that orbital overlap rather than double bond centre-to-centre distance

might be considered.[26] Hydrogen abstraction geometric parameters defined by Scheffer

and co-workers in solid state Norrish type II reactions are directly concerned with orbital overlap, which will be described in the following section of this thesis.

Following Schmidt's topochemical postulate based on the solid state [2 + 2] photocyclization of cinnamic acid derivatives, another general concept called the "reaction cavity"[27] was introduced by Cohen as an aid in interpreting the course of solid state reactions. According to Cohen, each individual molecule within a crystal is located in a cavity composed of the neighboring molecules. As the reaction proceeds, the physical geometry of the reactant changes as the product is formed. As shown in Figure 1.4, only the reaction involving minimal changes in geometry is allowed; the reactions with transition state geometries incompatible with the cavity will be disfavored. Recently, Ramamurthy et al.[28] expanded the reaction cavity concept to include other organized media, leading to the development of solution-like photochemical behavior in organized media (such as polymer films, liquid crystals, zeolites, glasses, micelles, cyclodextrins, clays)
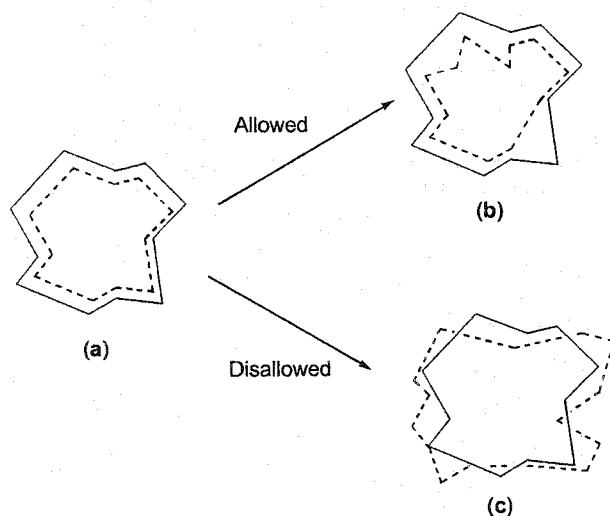
Figure 1.4 Pictorial representation of Cohen's "reaction cavity" concept: (a) starting material (dashed line) fits within the reaction cavity (solid line); (b) allowed solid state reaction where the product (dashed line) fits within the cavity; (c) disallowed reaction where the product (dashed line) does not fit within the cavity.

The concept of the reaction cavity is based on the assumption that topochemically controlled reactions occur in the bulk of the crystal rather than at defect sites. Lattice

defects, disorder, amorphous solids, and phase transitions have frequently been used to explain deviations from topochemical behavior.

A topotactic[29] reaction involves a single-crystal-to-single-crystal transformation in which a single crystal of the reactant is converted into a single crystal of the product without any phase separation during the reaction. A recent example within the Scheffer group is shown in Figure 1.5. X-ray diffraction studies showed that during photolysis a single crystal of the starting material underwent Yang photocyclization to form the cyclobutanol photoproduct in up 93 % conversion without breaking the crystal lattice.[30]

Starting material in single crystal

Mixture of starting material and photoproduct in single crystal

Photoproduct in single crystal
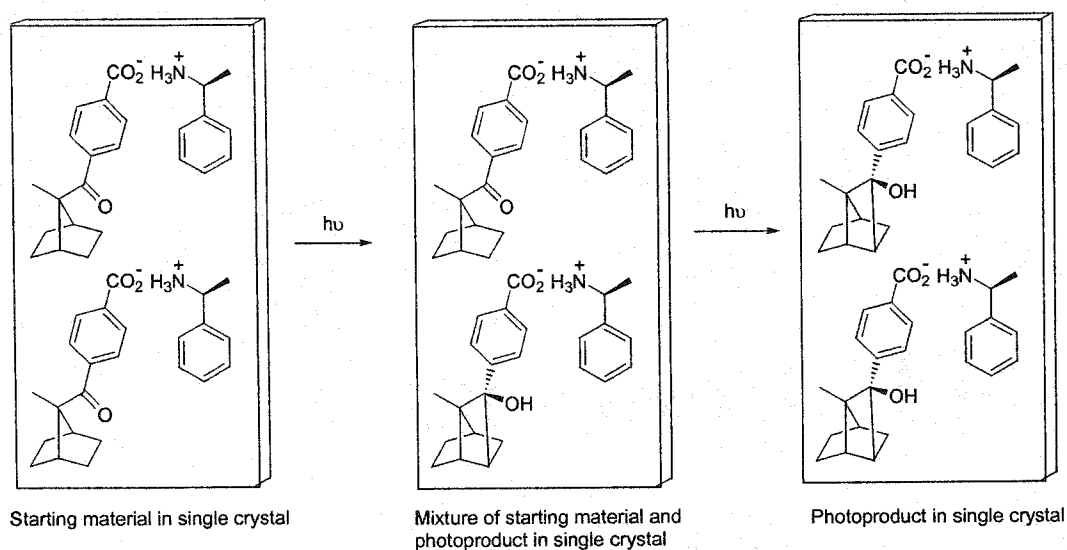
Figure 1.5 Representation of a single crystal to single crystal photoreaction of a norbornane derivative

Several other concepts such as molecular volume and free space,[31] local stress,[32] steric compression,[33] and "latent" reactivity[34] have been utilized to interpret solid state reactivity.

1.4 Type II Photochemistry of Ketones[35]

1.4.1 General Aspects of Type II Photochemistry

Ketones have attracted more photochemical research than any other compound.[36] Both aliphatic and aromatic ketones absorb ultraviolet light in the 290-330 nm region.[37] Following $n \rightarrow \pi^*$ excitation, three major types of reaction can occur: Norrish Type I, Norrish Type II and photoreduction.[38] The Norrish type I reaction is also known as α-fission (or α-cleavage), in which the cleavage of the bond between the carbonyl carbon and the α-carbon results in an acyl radical and an alkyl radical (Figure 1.6). The radicals can undergo a variety of subsequent reactions (decarbonylation and/or radical coupling, or hydrogen abstraction) to achieve stability. Photoreduction, which involves an intermolecular hydrogen atom abstraction, is rare in solid state photochemistry and will not be discussed in this thesis.
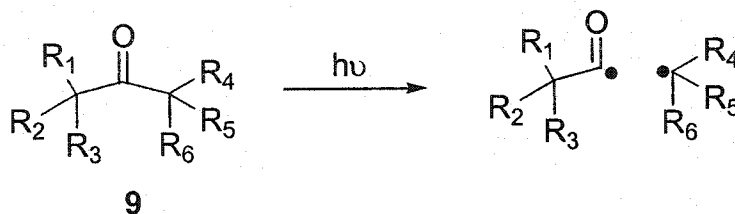
Figure 1.6 The Norrish type I reaction.

The Norrish type II reaction is among the most thoroughly investigated of all photoreactions and has been reviewed a number of times.[39] A Norrish type II reaction involves abstraction of a γ hydrogen atom by the (n, π^*) excited ketone to give either a Norrish type II cleavage product, or a Yang cyclization[40] product as shown in Figure 1.7. The excited state of ketone **10** may undergo γ hydrogen atom abstraction to form 1,4-hydroxybiradical intermediate **11**, which has been detected by laser flash photolysis and trapped by S-deuterated thiols or oxygen.[41] 1,4-Hydroxybiradical **11** has three fates: (1) reverse hydrogen transfer (disproportionation) to regenerate ketone **10**, (2) cleavage of the central carbon-carbon bond to form alkene **12** and enol **13** (ketone **14** formed by tautomerization), or (3) Yang cyclization to form cyclobutanol **15**. Type II reactions may occur from either the singlet or triplet excited state of the molecule; however, phenyl ketones have been found to react exclusively from the triplet excited state.[42]
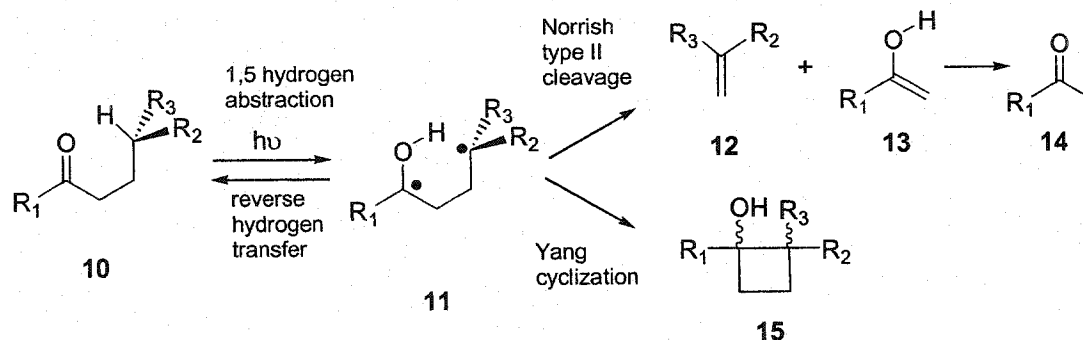
Figure 1.7 Type II photochemistry of ketones

Abstraction of a γ-hydrogen atom to form a 1,4-biradical is favored because it proceeds *via* a six-membered transition state; however, β-, δ-, ϵ- or even further long-range hydrogen abstraction may be observed, especially when no γ-hydrogen atoms are available.[35(b)] It was first suggested by Wagner that chair-like six-membered transition states for γ-hydrogen abstraction are favorable.[43] However, crystallographic studies by Scheffer *et al.* disclosed that a boat-like transition state is often favored in the solid state.[30,44]

It is well known that some photochemical reactions[6] like [2 + 2] photocyclization and the di-π-methane reaction are synthetically useful. Type II photochemistry was also used in the synthesis of a variety of natural and/or non-natural products. Examples include: Taxane precursors (type I and II cleavage),[45] the Aflatoxin family (1,6-hydrogen abstraction and Yang cyclization),[46] Enediynes,[47] Lignan paulownin (1,6-hydrogen abstraction and Yang cyclization),[48] and Dodecahedrane.[49] The synthetic utility of 1,9-, 1,12-, and other remote hydrogen atom abstractions was explored by Breslow[50] and Kraus *et al.*[51] The synthetic uses and other applications of the type II reaction were briefly reviewed by Wagner[35(b)] and Kraus *et al.*[52] A few examples are given below. Paquette's synthesis of Punctatin A (**19**) was accomplished using the Yang cyclization as a key step to make cyclobutanol **18** from ketone **16** (Figure 1.8).[53]
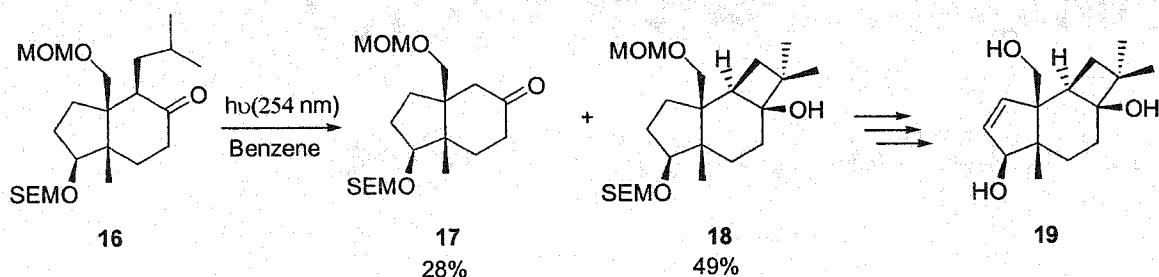
Figure 1.8 Yang photocyclization as a key step in the synthesis of Punctatin A

Compound **22** (Figure 1.9) was synthesized by a [2 + 2] cycloaddition followed by a type II photocyclization in 50 % yield.[54] Six years later this methodology was used in the synthesis of Filiformin by another research group, although the previous study was not cited.[55] As in this case, it is little wonder that people think the type II reaction has only a few uses in natural product synthesis.[30] Some reactions in the area of hydrogen abstraction are reported without the key words of Norrish type II, Yang cyclization or even photochemistry/photochemical.
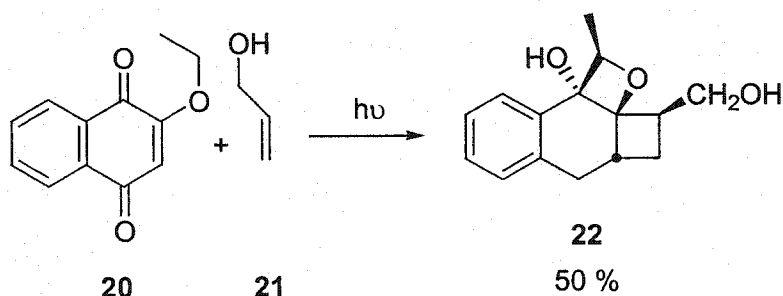
Figure 1.9 A [2 + 2] cycloaddition followed by a type II photocyclization

Coumestrol **25**, a phytoestrogen, was synthesized in five steps *via* a key step involving photochemical cyclization of glyoxylate ester **23** as shown in Figure 1.10. [56]

13
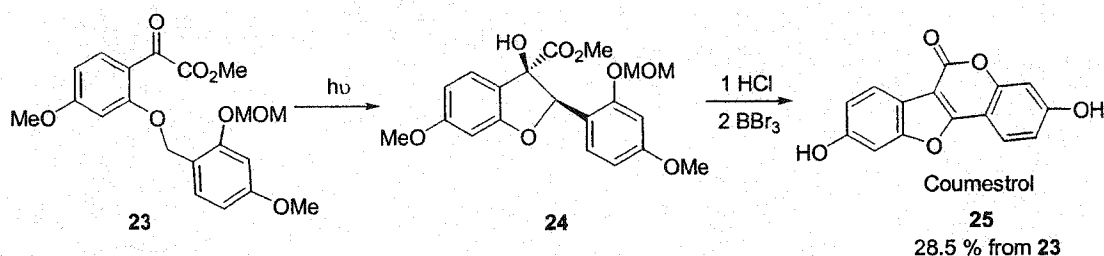
Figure 1.10 The synthesis of Coumestrol

In solution, triplet 1,4-hydroxybiradicals are long enough lived to experience conformational interchange. Thus, the products derived from these intermediates will be strongly influenced by the geometry at which triplet-to-singlet intersystem crossing occurs, and may not necessarily correlate with the geometry of the initially formed biradical, or its lowest energy conformer.

In the solid state, correlation of (n, π*) excited state reactivity with the geometry of the ground state ketone is valid for aromatic ketones because the excitation is known to be highly localized in the carbonyl group such that geometric changes in the rest of the molecule are negligible, with only a slight lengthening (*ca.* 0.1 Å) of the carbonyl double bond.[57] It is not the case for aliphatic ketones because the carbonyl carbon of the (n, π*) excited state becomes pyramidalized.[58] It is important to emphasize that such structure-reactivity relationships are only approximate using *ground state* structures correlated with *excited state* reactivity.

From the triplet excited state, the Norrish type II reaction is a two step process, hydrogen abstraction followed by cyclization and/or cleavage of the resulting biradical. The geometric parameters for each process are also broken down into different sections for the purpose of discussion.

1.4.2 Hydrogen Abstraction Geometric Parameters[30,59]

As with Schmidt's work on the topochemical postulate, which started with the definition of a set of geometric parameters describing the relative geometry necessary for solid state [2 + 2] photocycloaddition, hydrogen abstraction geometric parameters were also defined by Scheffer for the solid state Norrish type II reaction.[60]
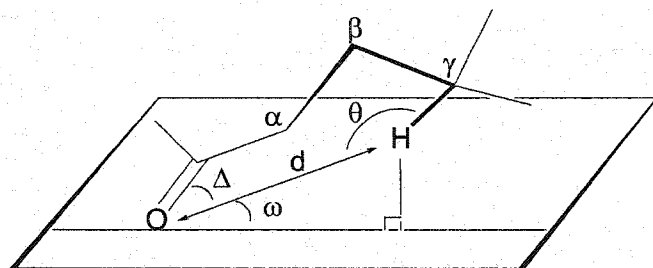
Figure 1.11 Geometric parameters for hydrogen abstraction

Four geometric parameters associated with the abstraction process are shown in Figure 1.11. The first, **d**, is the distance between the carbonyl oxygen and the γ-hydrogen. The second parameter Δ is defined as the C=O...H angle. The third parameter is θ, defined as the C-H...O angle. The fourth parameter is ω, the angle by which the γ-hydrogen atom lies outside the mean plane of the carbonyl group.

From a theoretical standpoint, ideal values for the four parameters have been proposed. The ideal value of d is 2.72 Å, the sum of the van der Waals radii for a hydrogen and an oxygen atom.[61] Because hydrogen abstraction involves the n-orbital on oxygen, the ideal value of ω, the deviation of the γ-hydrogen atom from the mean plane of the carbonyl group, is 0°. On the basis of mathematical and experimental kinetic studies, Wagner has proposed that the abstraction rate is proportional to $\cos^2\omega$.[62] *Ab initio* calculations by Houk have likewise shown that the enthalpy of activation increases significantly as θ deviates from 180°, suggesting that a linear O...H-C arrangement (θ = 180°) is preferred.[63] The ideal value for the Δ parameter is complicated by the fact that two models of the (n, π^*) excited state ketone exist. In the so-called "rabbit ear" conception, the atomic orbitals on oxygen are hybridized, and the two non-bonding sp^2 hybrids are degenerate, each forming a 120° angle with the carbonyl C=O bond axis. In the model proposed by Kasha,[64] the oxygen atom is not hybridized, resulting in non-degenerate non-bonding orbitals, one largely of 2s character, and the other 2p-like. The latter, which forms an angle of 90° with respect to the C=O bond axis, contains the

unpaired electron in the excited state. In general, therefore, the ideal Δ angle is thought to lie in the 90-120° range.

Inspection of the above data reveals that it is geometrically impossible for all of the atoms to be ideally aligned in a six-membered transition state; some of the parameters must deviate significantly from their optimum values. The solid state study of 3 series of compounds by Scheffer *et al.* has provided average values for γ-hydrogen atom abstraction (Figure 1.12 and Table 1.1).[59,60]
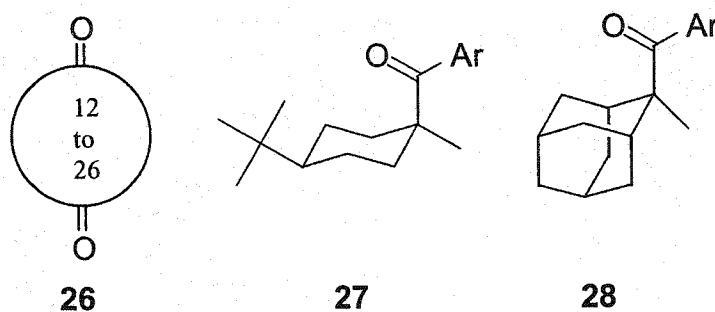
Figure 1.12 Previous studies of γ-hydrogen abstraction parameters in Yang photocyclization

Table 1.1 Ideal and crystallographically determined γ-hydrogen abstraction parameters

	d (Å)	ω (°)	θ (°)	Δ (°)
Ideal	<2.72	0	180	90-120
26	2.73 ± 0.03	52 ± 5	115 ± 2	83 ± 4
27/28	2.63 ± 0.06	58 ± 3	114 ± 1	81 ± 4

1.4.3 Geometric Requirements for Cleavage and Cyclization[30,59]

For a better understanding of the structure-reactivity relationships involved in 1,4-hydroxybiradical cleavage and/or cyclization, other geometrical parameters were defined by Scheffer *et al.* Cleavage parameters φ_1 and φ_4 are shown in Figure 1.13. The dihedral angle φ_1 represents the overlap angle between the *p*-orbital on the carbonyl carbon C_1, with the C_2-C_3 σ bond that would be fragmented in a cleavage reaction. Another dihedral angle φ_4 represents the overlap angle between the *p*-orbital on C_4 with the C_2-C_3 σ bond. The overlap between these orbitals is proportional to $\cos\varphi_1$ and $\cos\varphi_4$.[65] The ideal

geometry for cleavage is with both φ_1 and φ_4 equal to $0°$, the angle at which maximum overlap would be achieved. Those angles are only available from X-ray crystallography when the following assumptions are met: (1) the C_1 and C_4 carbons are sp^2 hybridized and (2) no conformational changes occur in the molecule following hydrogen abstraction. It seems likely that these assumptions are valid for solid state reactions, where conformational motions are severely restricted.
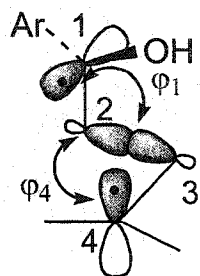
Figure 1.13 Cleavage parameters φ_1 and φ_4

There are two parameters (Figure 1.14) related to the cyclization reaction. One is D, the distance between the radical centers (equal to the distance between the two reacting centers in the ground state). The ideal value of D should be less than 3.4 Å, the sum of the van der Waals radii for two carbon atoms. Another parameter β is the dihedral angle between the p-orbital on C_1 and the C_2-C_4 vector. The ideal situation for cyclization is when $\beta = 0°$, i.e., the p-orbital on C_1 is pointed directly toward the p-orbital on the on C_4 carbon, allowing for closure of the cyclobutane ring.
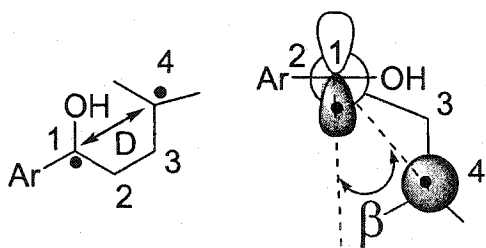
Figure 1.14 Cyclization parameters D and β

1.5 Asymmetric Induction

1.5.1 Asymmetric Induction in Solid State Chemistry and Photochemistry

There are a number of ways to obtain optically pure compounds. Pasteur resolution, which was developed 150 years ago, is used to separate racemates using acid-base reactions followed by crystallization of diastereomeric salts.[66] The obvious limitations of the Pasteur approach are that it is labor-intensive and gives only a 50 % maximum yield. Isolation of natural products and manufacture by enzymatic processes also provide single enantiomers. Asymmetric synthesis, however, is the most powerful and general tool to produce optically pure compounds.[67]

Asymmetric synthesis in a photochemical reaction can be achieved by conducting a reaction in a chiral environment. The chiral environment could be a chiral solvent, reactant, sensitizer, auxiliary or circularly polarized light.[68] Yang photocyclization of α-amido alkylaryl ketones in solution was reported by Griesbeck et al.[69] with >95% de using an intramolecular hydrogen bonding strategy (Figure 15a). An intermolecular hydrogen bonding strategy was used by Bach et al. in a Norrish/Yang photoreaction in solution and 26 % ee was achieved (Figure 15b).[70] Attempts at photochemical asymmetric synthesis in solution usually give photoproducts with low enantiomeric excess.

(a)

(b)
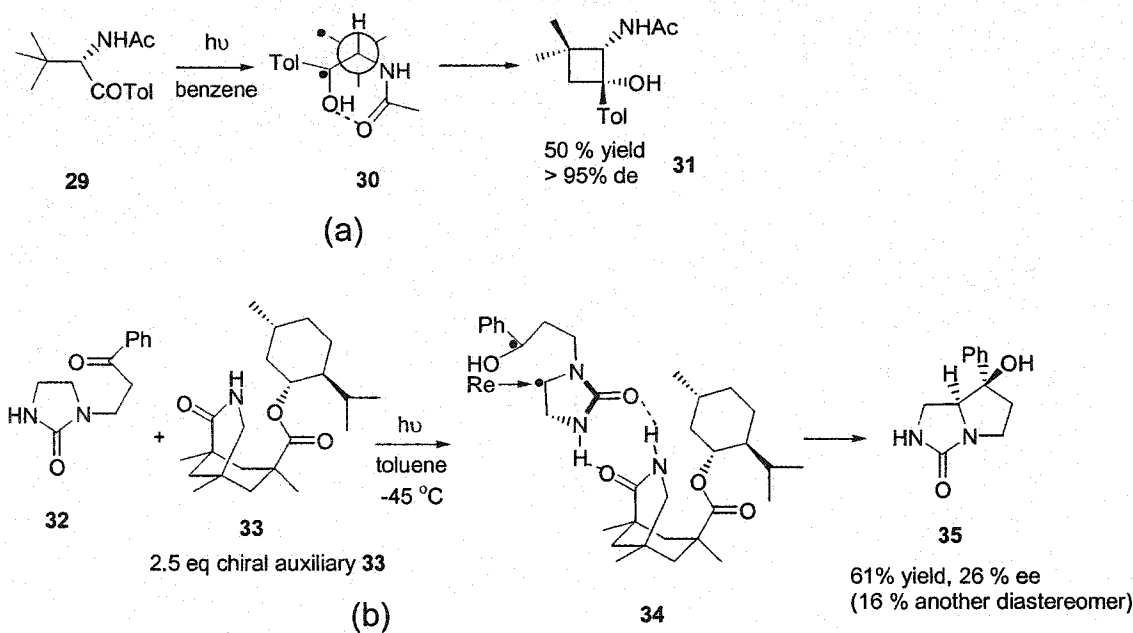
Figure 1.15 Examples of asymmetric synthesis *via* Yang photocyclization in solution: (a) Griesbeck's intramolecular hydrogen bonding strategy; (b) Bach's intermolecular hydrogen bonding strategy.

Asymmetric syntheses in "organized" media include:[71] (1) zeolites with chiral inductors or chiral auxiliaries; (2) cyclodextrins; (3) chiral crystals. The chiral crystalline state is the most organized chiral medium and often leads to high ee's. Several approaches have been studied in the chiral crystalline state: (1) absolute asymmetric synthesis; (2) host-guest method; (3) covalent chiral auxiliary method; (4) ionic chiral auxiliary method. The host-guest method, in which an achiral guest molecule forms a chiral inclusion complex with an optically pure host compound, will be described in a later section of this chapter. The covalent chiral auxiliary method is used commonly in ground state chemistry.

Achiral molecules may spontaneously crystallize in one of the 65 chiral space groups, thereby providing a chiral environment for asymmetric induction in solid state photoreactions, a process known as "absolute asymmetric synthesis", i.e. without the imposition of an external asymmetric source.[72] The first absolute asymmetric synthesis was reported by Schmidt and co-workers over three decades ago on the gas-solid bromination of *p,p*-dimethylchalcone.[73] The first photochemical studies in absolute

asymmetric synthesis were done by Schmidt[74] (bimolecular [2 + 2] addition) and Scheffer[75] (unimolecular di-π-methane reaction). However, crystallization of achiral compounds in chiral space groups is rare and unpredictable.[76,77] At present, absolute asymmetric synthesis is generally an unreliable method of making enantiomerically enriched substances. A method of guaranteeing the presence of a chiral space group is needed and will be synthetically useful in organic chemistry, especially for the preparation of compounds unavailable by common ground state chemistry. The ionic chiral auxiliary method was developed with this in mind.

1.5.2 The Ionic Chiral Auxiliary Method

An achiral reactant molecule containing a carboxylic acid (or an amine) is reacted with an optically pure amine (or an optically pure acid), which becomes the so-called ionic chiral auxiliary,[78] to form an optically pure salt. Such salts must crystallize in chiral space groups, which provide the asymmetric environment necessary for chiral induction. After photolysis, the chiral ammonium ion can be easily removed by diazomethane (CH_2N_2) workup, giving the desired photoproduct as its methyl ester, which is easily purified by chromatography. The following (Figure 1.16) is one example.[79] Salt **36**, formed between an achiral acid and an optically pure amine, was photolyzed in the solid state and afforded ester **37** with an enantiomeric excess of 97 % after diazomethane workup for removing the chiral amine.
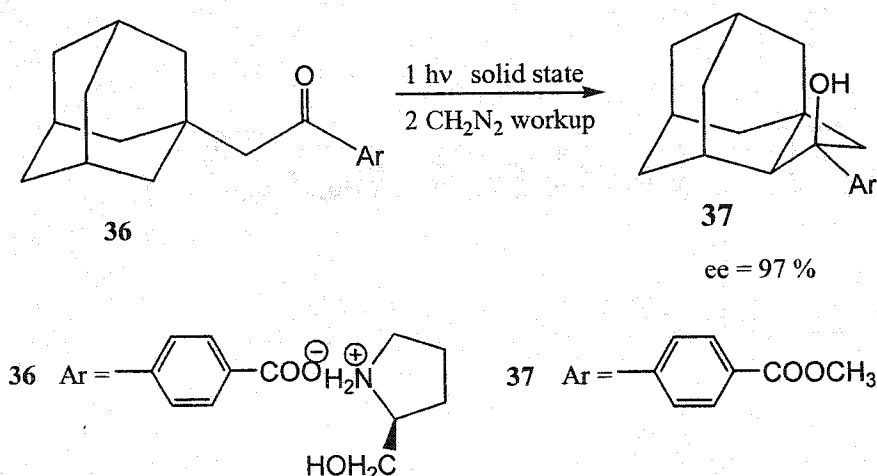
Figure 1.16 An example of the solid state ionic chiral auxiliary method for photochemical asymmetric synthesis

The energy level diagram shown in Figure 1.17 demonstrates the general concept. Since the crystalline environment is chiral, reaction of the photolabile salt can proceed *via* either of two diastereomeric transition states of different energy. The pathway with the lowest kinetic barrier proceeds at a greater rate, and the product of this photoreaction will predominate.
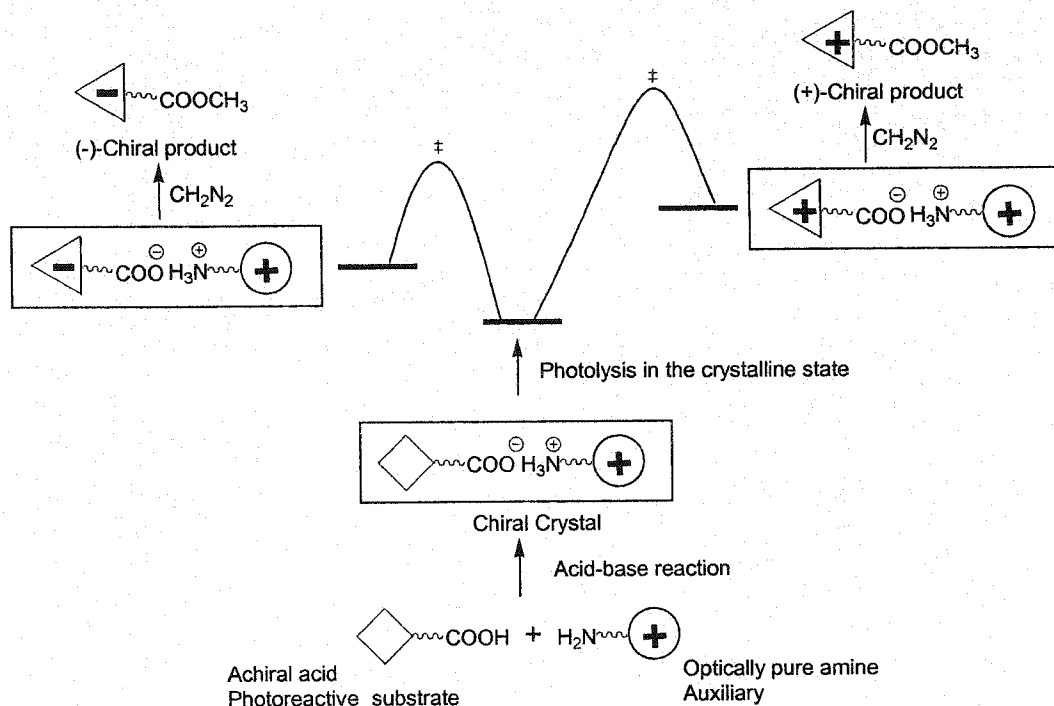
Figure 1.17 Schematic representation of the ionic chiral auxiliary approach to asymmetric induction in the solid state.

The ionic chiral auxiliary method utilizes "remote" chiral induction, unlike the traditional ground state method of asymmetric synthesis in which the chiral auxiliary is tightly bound to the reactive substrate near the site of reaction. It is the chiral crystalline environment that controls molecular conformation and packing in the crystals and determines the asymmetric induction. This will be discussed in greater detail in the next part of this thesis.

Three conditions must be met in studies of asymmetric induction in the Yang photocyclization reaction using ionic chiral auxiliaries: (1) Straight-chain aryl alkyl ketones, which crystallize in extended conformations with inaccessible γ-hydrogen atoms, are ruled out. Only ketones that crystallize in conformations favorable for hydrogen abstraction can be investigated. (2) The chiral auxiliary must be easily attached prior to reaction and easily removed after reaction. (3) The substrates must crystallize in chiral space groups.

Compared to the traditional covalent auxiliary approach, the ionic chiral auxiliary method has a variety of advantages, including ease of introduction and removal of the

chiral auxiliary and the fact that salts form robust ionic crystals with high melting points (resisting crystal breakdown during the reaction).

The ionic chiral auxiliary method joins the two concepts of absolute asymmetric synthesis and Pasteur resolution in one procedure; moreover, it overcomes the drawbacks that absolute asymmetric synthesis is not general and that the maximum yield for Pasteur resolution is only 50 % (Figure 1.18). The ionic chiral auxiliary method has been applied by the Scheffer group to a wide variety of photochemical reactions to achieve near-quantitative de's and ee's.[78] It is worth noting that both methods employ crystalline ammonium carboxylate salts.
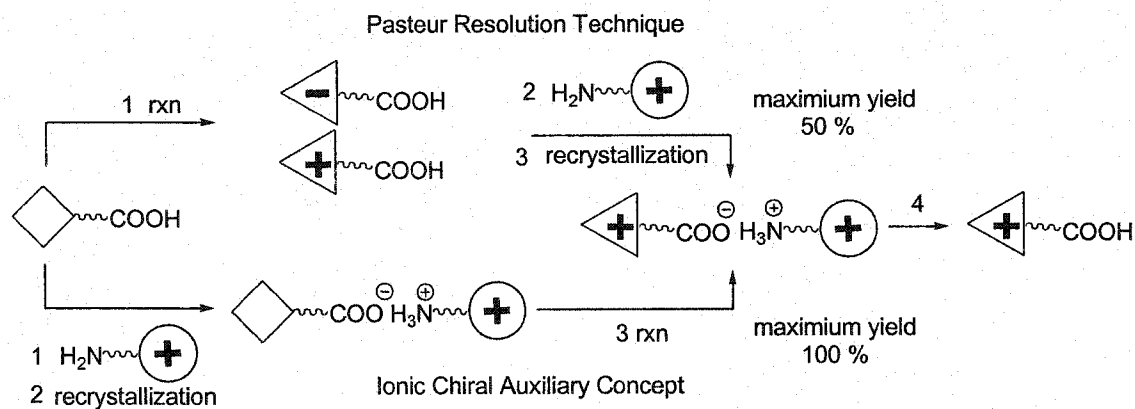
Figure 1.18 Comparison of the ionic chiral auxiliary approach to asymmetric induction and the Pasteur resolution method.

1.6 Photochemistry of α-Oxoamides

The photochemistry of α-oxoamides (N,N-dialkylarylglyoxylamides) in the solid state was originally investigated by Aoyama *et al.*[80] and studied extensively by Toda *et al.*[81]
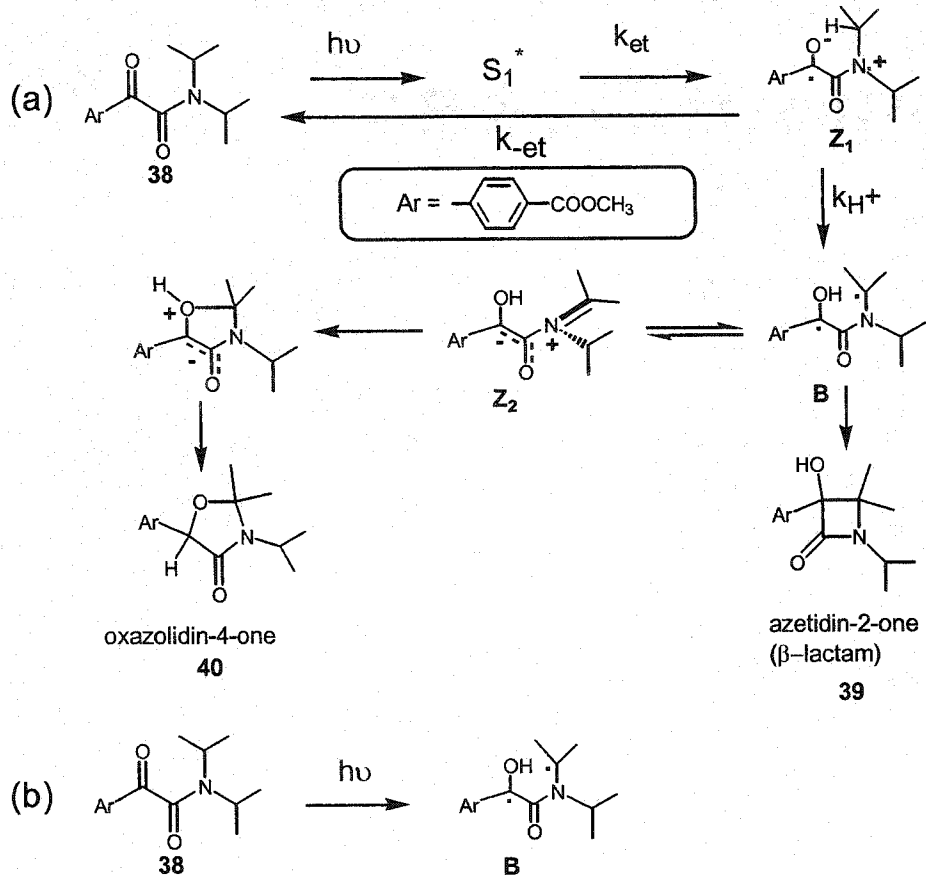
Figure 1.19 Proposed mechanism for the formation of azetidinone and oxazolidinone. (a) Whitten's single electron transfer (SET) mechanism.[82] (b) Aoyama's biradical mechanism.[80(c)]

Two mechanisms have been proposed for β-lactam (azetidinone) formation. One suggested by Whitten et al.[82] is depicted in Figure 1.19(a), in which β-lactam formation is thought to involve photoinduced single electron transfer from nitrogen to the benzoyl group (forming zwitterion Z_1) followed by transfer of a tertiary γ-proton (k_H^+) from one of the isopropyl groups to the carbonyl oxygen. This generates 1,4-hydroxybiradical **B**, which closes to form β-lactam (azetidinone) **39**. In this mechanism, oxazolidinone **40** is formed via a second intramolecular electron transfer to produce zwitterion Z_2 followed by ring-closure. The second mechanism was proposed by Aoyama[80(c)] (Figure 1.19(b)), in which the 1,4-hydroxybiradical (**B**, triplet or singlet) is formed directly upon photolysis of **38**. The subsequent steps are same as Whitten's mechanism. The most recent studies on the mechanism of β-lactam formation were carried out by Mariano et al.[83] in which he

concluded that Aoyama's mechanism (the hydrogen atom abstraction route) is more probable than Whitten's mechanism (SET-proton-transfer route) based on studies of the photoreactions of *N*-trimethylsilylmethyl- and *N*-tributylstannylmethyl-substituted α-oxoamides.

Photolysis of α-oxoamides in solution usually yields oxazolidinones as the chief products, while photolysis in the solid state affords azetidinones as the major photoproducts. Biradical **B** and zwitterionic intermediate Z_2 exist as two different conformers in which the intramolecular electronic distribution is controlled by the molecular geometry. Zwitterionic intermediate Z_2 adopts a different conformation from biradical **B**, which reduces the steric hindrance in the latter (By MMX molecular mechanics calculations it was found that the plane containing the hydroxyl group, the anionic carbon and the carbonyl group is twisted from the plane defined by N-alkyl group and the N=C bond).[82] In solution the extended conformer Z_2 is energetically favorable and the formation of oxazolidinone **40** *via* nucleophilic ring closure, in which large motions are necessary, is preferred. In the solid state, on the other hand, biradical **B** can not twist to form zwitterion Z_2, and therefore azetidinone **39** is produced *via* this biradical intermediate.

A variety of α-oxoamides has been explored photochemically by Toda and others to make β-lactams and penicillin derivatives (Figure 1.20).[84]
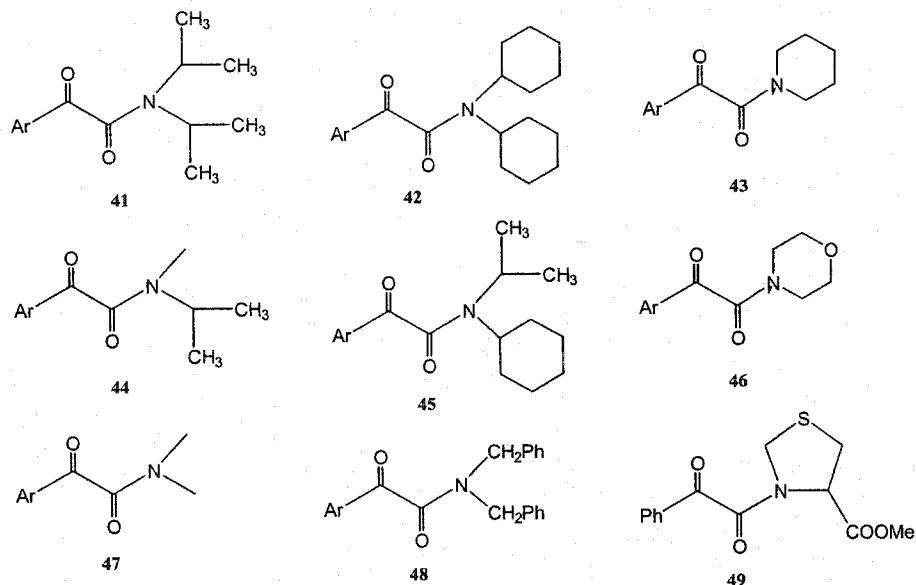
Figure 1.20 α-Oxoamides studied by Toda and others.

Photochemical asymmetric synthesis from α-oxoamides was first studied by Aoyama *et al.*[80(e)] and subsequently by Toda *et al.*[81] Toda and coworkers were the first to report that compounds **41a** and **41b** serendipitously crystallize in the chiral space group $P2_12_12_1$.[81(g)] The absolute asymmetric synthesis method was used successfully for α-oxoamides **41a** and **41b**, but it did not work for *ortho-* (**41c**) and *para-* (**41d**) substituted α-oxoamides owing to their crystal packing in centrosymmetric space groups (Figure 1.21).
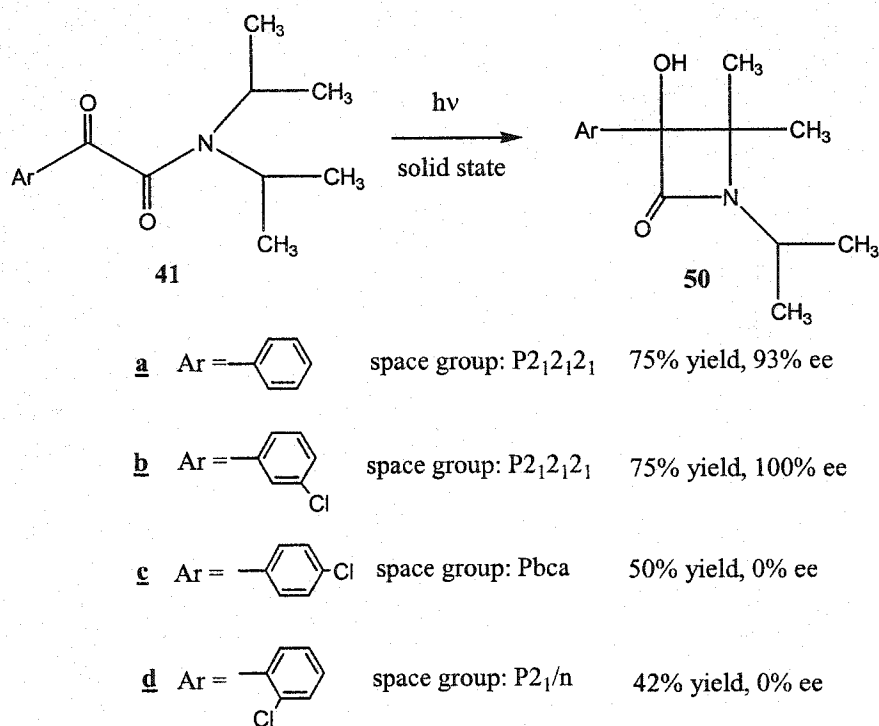
Figure 1.21 Absolute asymmetric synthesis of β-lactams

Enantioselective photocyclization of α-oxoamides to β-lactams was also achieved in nearly quantitative ee by the "inclusion complex method" (Figure 1.22), in which a 1:2 inclusion complex of α-oxoamide **51** with the optically pure host **52** can be crystallized in a chiral space group.[81(a)]
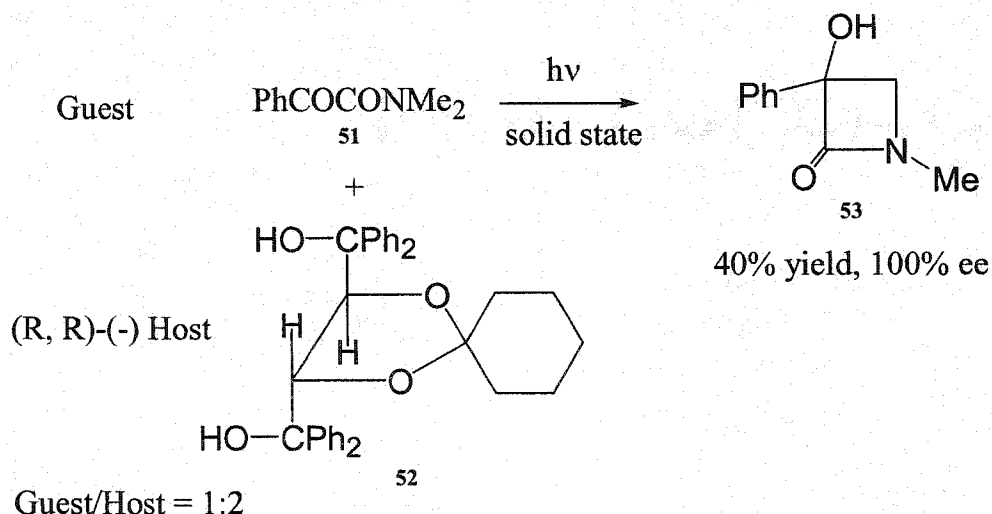
Figure 1.22 Toda's host-guest approach to make enantiomerically enriched β-lactams

Some drawbacks of the host-guest approach are the following: (1) only certain combinations of host and guest can form crystalline complexes suitable for photolysis; (2) the optically active host molecules are time-consuming and expensive to prepare; (3) separation of the host molecules from reaction mixture following photolysis is much more difficult than the diazomethane workup in the ionic chiral auxiliary approach.

1.7 Research Objectives

The first project to be described in this thesis deals with the solid state asymmetric photochemical transformation of α-oxoamides to β-lactams. A number of α-oxoamides have been studied by Toda and others as shown in Figure 1.20. Compound **38**, a derivative of oxoamide **41** which has been studied intensively by Toda, was selected as a target molecule in this project for the following reasons: to use the ionic chiral auxiliary method, and to compare the results with Toda's methods. Photocyclization of α-oxoamides in the solid state is a Norrish/Yang reaction, which has been the focus of much recent work in Dr. Scheffer's laboratory using the ionic chiral auxiliary approach. The goals of this project are: (1) to further explore the generality and synthetic utility of the ionic chiral auxiliary method; (2) to show that the ionic chiral auxiliary method can be carried out on a 100-500 mg scale, making the procedure synthetically useful. Although the two methods (absolute asymmetric synthesis and host-guest inclusion

complex) described in last section lead to β-lactams in respectable ee, both lack generality. The solid state covalent chiral auxiliary method was also applied to the photochemistry of α-oxoamide derivatives in this thesis. Unlike traditional ground state asymmetric synthesis using covalent chiral auxiliaries, the solid state covalent auxiliary method is a long-range asymmetric induction in which the chiral crystalline environment rather than the covalent auxiliary itself is responsible for asymmetric induction.

The second project to be described in this thesis deals with the study of the solid state asymmetric photocyclization of derivatives of bicyclic aryl ketones **55, 58** and **61** (Figure 1.23). These bicyclic aryl ketone systems were selected as targets for continued studies on the Yang photocyclization similar to those on admantyl ketone **36**, in which high ee was achieved. Like ketone **36**, ketones **56, 59, 62** can not undergo type II cleavage, since anti-Bredt olefins would be generated. The photochemistry of these bicyclic aryl ketones has not been studied previously. All three target molecules are achiral and their cyclization products are chiral molecules, allowing for asymmetric induction to be studied. In bicyclo[2.2.1]heptyl ketones, regioselectivity could also be studied because the γ-hydrogens on the one- and two-carbon bridges are potentially abstractable. All three target molecules were equipped with a carboxylic acid group in the phenyl ring, making it possible to apply the ionic chiral auxiliary method in the asymmetric induction. Two diastereomeric cyclobutanols are possible from photolysis of the ketones, and therefore diastereoselectivity could also be studied in this project.
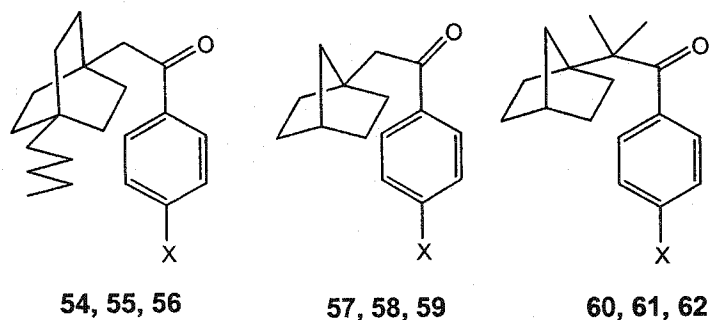
54, 55, 56   **57, 58, 59**   **60, 61, 62**

For compounds **54, 57, 60**, X = COOH
For compounds **55, 58, 61**, X = COOCH$_3$
For compounds **56, 59, 62**, X = COO$^{\ominus}$ $^{\oplus}$NH$_3$R

Figure 1.23 Bicyclic aryl ketones selected for photochemical studies

Solid state X-ray structure-reactivity correlation studies were carried out to rationalize the results in both projects. Molecular mechanics has been shown to provide information useful for the crystal engineering of type II photochemistry.[30] Therefore, HyperChem MM$^+$ calculations[85] were conducted throughout these projects.

RESULTS AND DISCUSSION

Chapter 2 Asymmetric Synthesis of β-Lactam Derivatives

2.1 Preparation of Substrates

2.1.1 Preparation of α-Oxoamides 38, 66 and 68

The target molecules **66** and **68** were synthesized in an expeditious and straightforward fashion as shown in Figure 2.1.
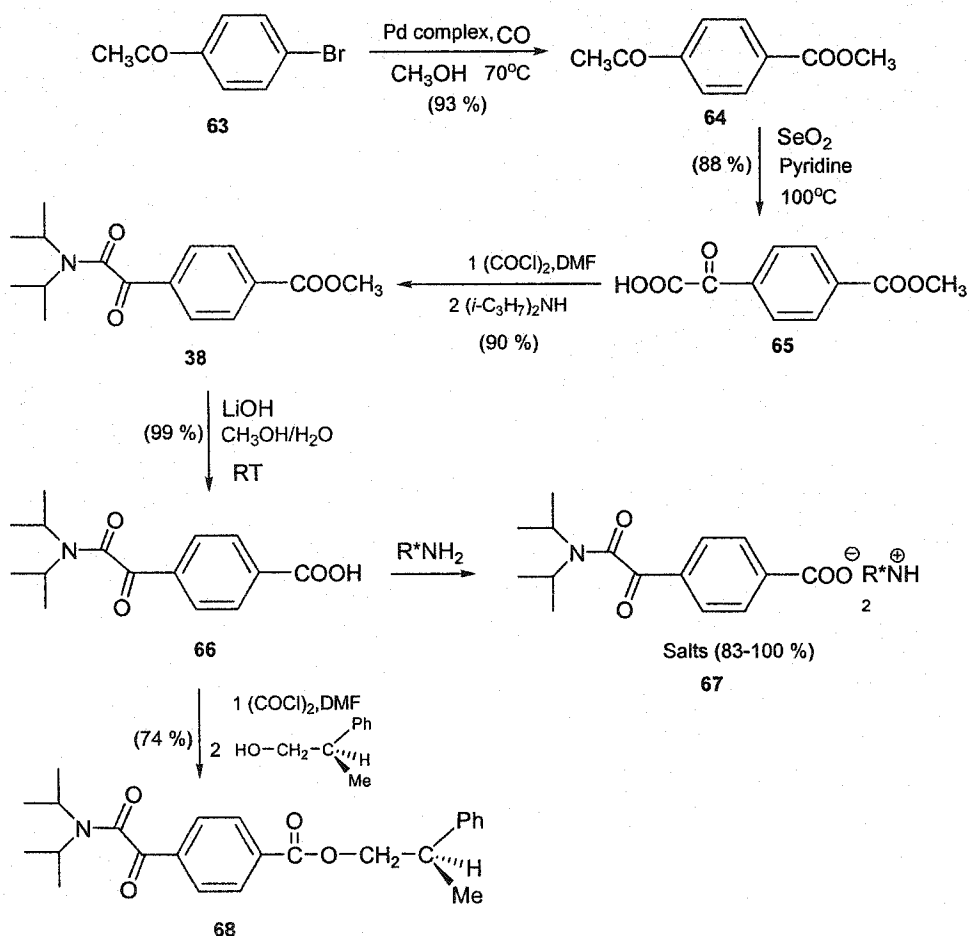
Figure 2.1 Synthesis of α-oxoamides **38, 66, 68**

Commercially available bromide **63** was converted into ester **64** in a yield of 93 % by palladium (0)-catalyzed methoxycarbonylation.[86] α-Oxoacid **65** was prepared by one-step oxidation with selenium dioxide[87] in pyridine in 88 % yield. It was interesting to find

that α-ketocarboxylic acid **65** was a previously unknown compound and was recently claimed as an inhibitor of phosphoryl tyrosine phosphases in a U.S. patent.[88] Using a standard synthetic method, the target molecule **38** was synthesized from acid **65**. Quantitative hydrolysis of ester **38** with lithium hydroxide afforded the target acid **66**. The crude product thus obtained was an analytically pure pale yellow solid without further purification. Acid **66** was linked with chiral amines by ionic bonding and a chiral alcohol by covalent bonding. Recrystallization of chiral ester **68** or chiral salts **67a-l** gave chiral crystals for asymmetric induction and X-ray crystallographic studies. Esters **38** and **68** gave spectra fully in agreement with assigned structures, which were confirmed by X-ray crystallography.

2.1.2 Preparation of Chiral Salts 67a-l

Chiral salts **67a-l** were prepared with acid **66** and various optically pure, commercially available amines as outlined in Table 2.1. The detailed procedure to make crystalline salts is given in the Experimental Section. All salts were characterized by NMR, IR, MS and elemental analysis.[89] The 1:1 stoichiometric ratio of acid to chiral amine was confirmed by ^{1}H-NMR, elemental analysis and MS. The formation of an ammonium carboxylate bond was evidenced by changes in the IR spectra for the salts. Asymmetric and symmetric stretches consistent with carboxylates[90] were observed in the salts with two intense bands from 1300 to 1650 cm^{-1}. The structures of salts **67a, 67c, 67e, 67f,** and **67g** were confirmed by X-ray crystallography.

Table 2.1 Preparation of chiral salts of acid **66**

salt	amine	recryst solvent	cryst morphol	mp(°C)
67a	L-prolinamide	MeOH	plates[a]	202-206
67b	R-(+)-bornylamine	MeOH	needles	183-185
67c	R-(-)-1-cyclohexylethylamine	MeOH	needles[a]	178-182
67d	S-(+)-1-aminoindane	MeOH	plates	192-195
67e	(1R, 2S)-(+)-*cis*-1-amino-2-indanol	MeOH	plates[a]	180-182
67f	R-(+)-1-phenylethylamine	MeOH	needles[a]	178-181
67g	S-(-)-1-phenylethylamine	MeOH	needles[a]	179-181
67h	(1S, 2R)-(+)-norephedrine	MeOH	needles	145-148
67i	(1R, 2R)-(-)-pseudoephedrine	MeOH	needles	168-172
67j	(-)-*cis*-myrtanylamine	MeOH	plates	127-130
67k	S-(+)-2-pyrrolidinemethanol	CH$_3$CN	prisms	116-119
67l	S-(+)-*N*-methyl-1-phenylethylamine	ethyl acetate	needles	126-128

[a] X-ray crystal structure obtained.

2.2 Photochemical Studies of Ester 38

Although α-oxoamide **38** is a previously unknown compound, its photochemistry is similar to that of α-oxoamide **41** (Figure 1.21), which was extensively studied by Toda.[81] The photochemical results are outlined in Figure 2.2 and Table 2.2.

Figure 2.2 The photoreaction of α-oxoamide **38**

33

All solution photolyses were performed in benzene at room temperature following Toda's procedure.[81] Both solid state and solution photolyses are very efficient, with 100 % conversion in 2 hours. The crystals of α-oxoamide **38** were photolyzed to 100 % conversion at room temperature without melting. α-Oxoamide **38** shows different photochemical behavior in solution and in the solid state. Azetidinone **39** is the major photoproduct in the solid state photolysis of α-oxoamide **38**. In solution, however, oxazolidinone **40** is the major photoproduct. The photoproduct ratio **39/40** is consistent between GC analysis and isolated yield (Table 2.2). The different photochemical behavior in solution and the solid state has been discussed in the Introduction of this thesis. Both photoproducts **39** and **40** were isolated and fully characterized by the spectroscopic techniques outlined in the Experimental Section. For photoproduct **39**, particularly diagnostic were a broad OH stretch in the infrared spectrum at 3441 cm^{-1} and two methyl singlets at 1.59 and 0.91 ppm in the ^{1}H-NMR spectrum. Photoproduct **40** also has two methyl singlets at 1.58 and 1.53 ppm in the ^{1}H-NMR spectrum, and has an additional one methine singlet hydrogen at 5.21 ppm rather than an OH peak in the IR spectrum. The structure of photoproduct **39** was also confirmed by X-ray crystallography. The preparative scale photolysis of **38** in solution provided isolated racemic **39** and **40**, not only for characterization of the photoproducts, but also for the chiral HPLC analysis in the resolution of the enantiomers.

Table 2.2 Photolyses of α-oxoamide **38** in solution and solid state

medium	time (h)	conv (%)^a	**39/40**
crystal	2	100	73/27^b
benzene	2	100	25/75^b
crystal	2	100	66/34^c
benzene	2	100	29/71^c

^{a} Percentage of total GC integral due to the disappearance of the corresponding starting material. ^{b} Products ratio from GC analysis. ^{c} Products ratio from isolated yields.

2.3 Asymmetric Induction by the Ionic Chiral Auxiliary Method

2.3.1 Determination of the Enantioselectivity

Following the preparative scale photolysis of α-oxoamide **38** in solution, photoproducts **39** and **40**, which are presumably racemic, were used to test the resolution conditions with chiral HPLC. The enantiomeric excess of each sample was determined using a HPLC column containing a chiral stationary phase, a Chiralcel® OD® column for β-lactam **39** and a Chiralpak® AD® column for oxazolidinone **40**. The chromatographic conditions for **39** and **40** are outlined in Table 2.3, and typical HPLC traces are shown in Figures 2.3 and 2.4.
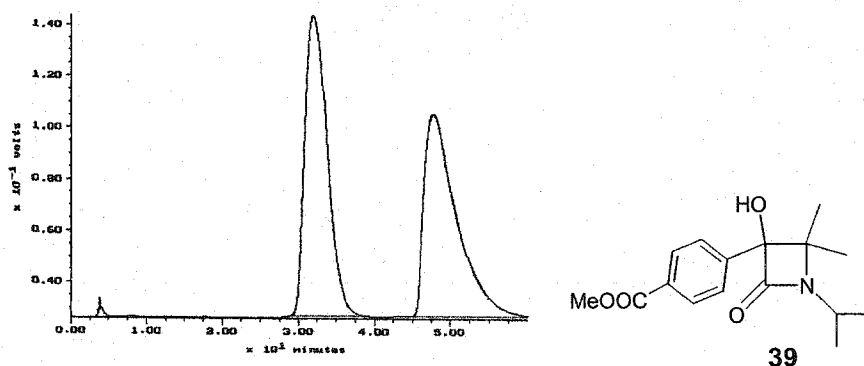
Figure 2.3 HPLC trace for the resolution of racemic **39** on Chiralcel® OD® column (eluting solvents, hexanes/isopropanol 99/1; flow rate, 1.0 mL/min)
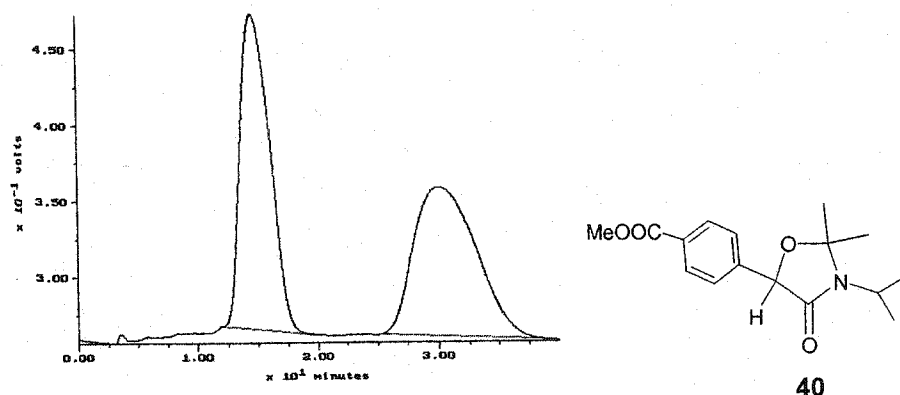
Figure 2.4 HPLC trace for the resolution of racemic **40** on Chiralpak® AD® column (eluting solvents, hexanes/ethanol 93/7; flow rate, 1.0 mL/min)

Table 2.3 Chromatographic data for enantiomeric excess determination of photoproducts **39** and **40**.

compound	column	HPLC conditions			Retention Time (min)[a]
		UV detector (nm)	Solvents	Flow rate (mL/min)	
39	OD[b]	254	99/1 hexanes/IPA	1.0	A: 31.8 B: 47.7
40	AD[c]	254	93/7 hexanes/EtOH	1.0	A: 14.7 B: 30.0

[a] A refers to the first eluted peak, B to the second. [b] Chiralcel® OD® (25 cm × 0.46 cm ID), Chiral Technologies Inc. [c] Chiralpak® AD® (25 cm × 0.46 cm ID), Chiral Technologies Inc.

2.3.2 Asymmetric Induction Results

The α-oxoamide salts **67a-l** were photolyzed in the solid state on an analytical scale (2-5 mg). The salt **67a** was also photolyzed in solution (CH$_3$OH and CH$_3$CN) and as a crystalline powder suspended in hexane (5 mg scale, 100 mg scale and 500 mg scale). The time of photolysis for each solid state reaction was controlled to different lengths so that the enantiomeric excess could be determined at a variety of conversions. Some salts, especially those that melted during photolysis at room temperature, were photolyzed at low temperature (-20 °C). Following photolysis, the salt sample was treated with ethereal diazomethane, converting the carboxylate anions to the corresponding methyl esters, and filtered through a short plug of silica gel to remove the chiral auxiliary. The photolysis and workup are described in detail in the Experimental Section. The conversion percentage as well as the product composition was determined by GC analysis. Isolated yields are reported for the photolyses in 100 and 500 mg scale. Isolation of each photoproduct by silica gel column chromatography was required before the ee determination by chiral HPLC owing to the overlapping of the two photoproduct peaks on chiral HPLC.

Because compound **39** is the major photoproduct in the solid state photochemistry of α-oxoamides, the asymmetric induction study was focused mainly on this substance. For convenience, the 12 salts can be divided into 2 groups: 5 salts with high ee (> 90 % ee for

39) and 7 salts with low ee (< 65 % ee for **39**). Four of the five salts in the high ee group shown in Table 2.4 (**67a, 67b, 67c, 67d**) stayed at a high ee level without significant decrease when the conversion was increased. This photochemical behavior suggests a possible single-crystal-to-single-crystal reaction. Unfortunately, attempts at crystallographic study for a single-crystal-to-single-crystal transformation were not successful. After photolysis the neat single crystal became cloudy and was not suitable for X-ray crystallographic analysis. A dramatic decrease of ee with increasing conversion was found for the (1R, 2S)-(+)-*cis*-1-amino-2-indanol salt (**67e**); this is probably due to crystal breakdown during the course of photolysis, leading to loss of asymmetric induction in the crystalline state.

Table 2.4 Asymmetric induction in the photolysis of chiral salts **67a-e**

salt	amine	temp (°C)	conv[a] (%)	39/40[b]	ee[c] (%) for 39
67a	L-prolinamide	RT	58	53/1	+99
67a	L-prolinamide	RT	88	82/1	>+99
67a	L-prolinamide	RT	92	89/0	+99
67a	L-prolinamide	RT	100	97/3	+99
67b	R-(+)-bornylamine	-20	78	74/3	-98
67b	R-(+)-bornylamine	RT	37	36/1	-98
67b	R-(+)-bornylamine	RT	73	70/3	-98
67b	R-(+)-bornylamine	RT	89	84/4	-98
67b	R-(+)-bornylamine	RT	100	92/7	-96
67c	R-(-)-1-cyclohexylethylamine	-20	22	15/7	-91
67c	R-(-)-1-cyclohexylethylamine	RT	32	24/4	-85
67c	R-(-)-1-cyclohexylethylamine	RT	60	38/15	-83
67d	S-(+)-1-aminoindane	-20	84	78/3	+95
67d	S-(+)-1-aminoindane	RT	80	74/3	+88
67d	S-(+)-1-aminoindane	RT	100	94/5	+89
67e	(1R, 2S)-(+)-*cis*-1-amino-2-indanol	-20	92	68/9	+81
67e	(1R, 2S)-(+)-*cis*-1-amino-2-indanol	RT	23	15/1	+91
67e	(1R, 2S)-(+)-*cis*-1-amino-2-indanol	RT	58	44/7	+71
67e	(1R, 2S)-(+)-*cis*-1-amino-2-indanol	RT	75	59/9	+58
67e	(1R, 2S)-(+)-*cis*-1-amino-2-indanol	RT	88	70/8	+53
67e	(1R, 2S)-(+)-*cis*-1-amino-2-indanol	RT	98	75/10	+45

[a] Percentage of total GC integral due to the disappearance of the corresponding starting material. [b] Percentage yield of products from GC analysis; the total percentage yield of **39** and **40** is less than the percentage of conversion due to other side products. [c] Enantiomeric excess (ee) values measured on a chiral OD column. Sign of rotation was obtained at the sodium D-line (589 nm).

The seven salts in the low ee group are shown in Table 2.5. The reasons for the low ee's, which could be crystal breakdown, crystal melting (**67k, 67l**), and conformational enantiomerism, will be discussed in the next section.

Table 2.5 Asymmetric induction in the photolysis of chiral salts **67f-l**

salt	amine	temp (°C)	conv[a] (%)	39/40[b]	ee[c] (%) for 39
67f	R-(+)-1-phenylethylamine	RT	98	81/10	+3
67g	S-(-)-1-phenylethylamine	RT	99	79/10	-3
67h	(1S, 2R)-(+)-norephedrine	RT	59	30/15	-60
67h	(1S, 2R)-(+)-norephedrine	RT	78	41/22	-49
67h	(1S, 2R)-(+)-norephedrine	RT	100	54/31	-43
67i	(1R, 2R)-(-)-pseudoephedrine	RT	28	15/6	-60
67i	(1R, 2R)-(-)-pseudoephedrine	RT	44	21/7	-55
67i	(1R, 2R)-(-)-pseudoephedrine	RT	79	37/14	-41
67i	(1R, 2R)-(-)-pseudoephedrine	RT	100	47/17	-36
67j	(-)-*cis*-myrtanylamine	RT	52	25/8	+47
67j	(-)-*cis*-myrtanylamine	RT	89	50/17	+39
67j	(-)-*cis*-myrtanylamine	RT	100	63/21	+37
67k	S-(+)-2-pyrrolidinemethanol	-20	23	18/5	-62
67k	S-(+)-2-pyrrolidinemethanol	RT	56[d]	29/27	-49
67k	S-(+)-2-pyrrolidinemethanol	RT	100[d]	62/38	-47
67l	S-(+)-N-methyl-1-phenylethylamine	-20	84	80/3	-10
67l	S-(+)-N-methyl-1-phenylethylamine	RT	39[d]	33/3	-29
67l	S-(+)-N-methyl-1-phenylethylamine	RT	69[d]	64/5	-14
67l	S-(+)-N-methyl-1-phenylethylamine	RT	100[d]	86/11	-8

[a] Percentage of total GC integral due to the disappearance of the corresponding starting material. [b] Percentage yield of products from GC analysis; the total percentage yield of **39** and **40** is less than the percentage of conversion due to other side products. [c] Enantiomeric excess (ee) values measured on a chiral OD column. Sign of rotation was obtained at the sodium D-line (589 nm). [d] Crystal melting observed.

In a dramatic demonstration of the synthetic potential of the ionic chiral auxiliary approach, a large scale solid state photoreaction was carried. Suspending the crystalline powder in a solvent in which it is insoluble, like HPLC grade hexanes, solves the problem of large scale solid state photochemistry. First, small scale hexane suspensions were investigated to see if there was any different photochemical behavior between the pure crystal and suspension in hexanes. Table 2.6 shows the photochemical similarity between the pure crystal and crystalline powder suspension in hexanes. A hexane suspension of 500 mg of the prolinamide salt was irradiated to 99 % conversion to afford a 91 % isolated yield of photoproduct **39** with an ee of > 99 %.

Table 2.6 Photochemistry of chiral salts **67a** suspended in hexanes

scale (mg)	isolated 39(%)	temp(°C)	conv (%)[a]	39/40[b]	ee[c] (%) for 39
5	-	RT	48	48/0	>+99
5	-	RT	99	92/2	+99
100	86	RT	98	93/3	+98
100	84	RT	99	88/3	+98
500	91	RT	99	94/2	>+99

[a] Percentage of total GC integral due to the disappearance of the corresponding starting material.
[b] Percentage yield of products from GC analysis; the total percentage yield of **39** and **40** is less than the percentage of conversion due to other side products. [c] Enantiomeric excess (ee) values measured on a chiral OD column. Sign of rotation was obtained at the sodium D-line (589 nm).

Emphasizing the importance of the crystalline state to asymmetric induction, photolysis of the salts in solution gave negligible enantiomeric excess, e.g., 5-6 % shown in Table 2.7.

Table 2.7 Solution phase photolyses of chiral salt **67a**

solvent	conv[a] (%)	39/40[b]	ee[c] (%) for **39**
CH_3CN	100	64/16[d]	+6.2
MeOH	100	29/68	+5.1

[a] Percentage of total GC integral due to the disappearance of the corresponding starting material. [b] Percentage yield of products from GC analysis. The total percentage yield of **39** and **40** is less than the percentage of conversion due to other side products. [c] Enantiomeric excess (ee) values measured on a chiral OD column. Sign of rotation was obtained at the sodium D-line (589 nm). [d] Becomes cloudy after photolysis.

The enantiomeric excess of the minor photoproduct **40** was only measured in a few cases owing to its low yield. Essentially, racemic photoduct **40** was obtained in all measured cases (Table 2.8), and a possible explanation will be given in the next section.

Table 2.8 Determination of the enantiomeric excess (ee) of photoproduct **40**

salt	amine/medium	temp (°C)	conv (%)[a]	39/40[b]	ee (%)[c] for **39**	ee (%)[d] for **40**
67a	L-prolinamide/ MeOH	RT	100	29/68	+5	6
67a	L-prolinamide/100mg suspended in hexanes	RT	100	76/18	+99	4
67a	L-prolinamide/100mg suspended in hexanes	RT	100	78/15	+95	0
67c	R-(-)-1-cyclohexylethylamine	RT	100	92/5	-80	0
67k	S-(+)-2-pyrrolidinemethanol[e]	RT	60	38/20	-44	0
67k	S-(+)-2-pyrrolidinemethanol[e]	RT	56	29/27	-49	0
67k	S-(+)-2-pyrrolidinemethanol[e]	RT	100	62/38	-47	0
67m	S-(+)-2-(methoxymethyl)pyrrolidine[e]	RT	100	49/40	+13	3

[a] Percentage of total GC integral due to the disappearance of the corresponding starting material. [b] Percentage yield of products from GC analysis; the total percentage yield of **39** and **40** is less than the percentage of conversion due to other side products. [c] Enantiomeric excess (ee) values measured on a chiral OD column. Sign of rotation was obtained at the sodium D-line (589 nm). [d] Enantiomeric excess (ee) values measured on a chiral AD column. Sign of rotation was undetermined due to unavailability of enantiomeric-enriched **40**. [e] Crystal melting observed.

2.4 Asymmetric Induction by the Covalent Chiral Auxiliary Method

The traditional covalent chiral auxiliary method, which has been extensively used for asymmetric synthesis in ground state chemistry, was also applied here to solid state photochemistry. In compound **68**, the covalent chiral auxiliary R-(+)-2-phenyl-1-propanol was introduced *via* ester formation with *N,N*-bis(1-methylethyl)-α-oxo-benzeneacetamide-4-carboxylic acid (**66**). The photoreactive portion of the α-carbonyl in the α-oxoamide moiety was at the *para* position of the aromatic ring, that is, far away from the chiral auxiliary. Thus this covalent chiral auxiliary is a remote chiral auxiliary.
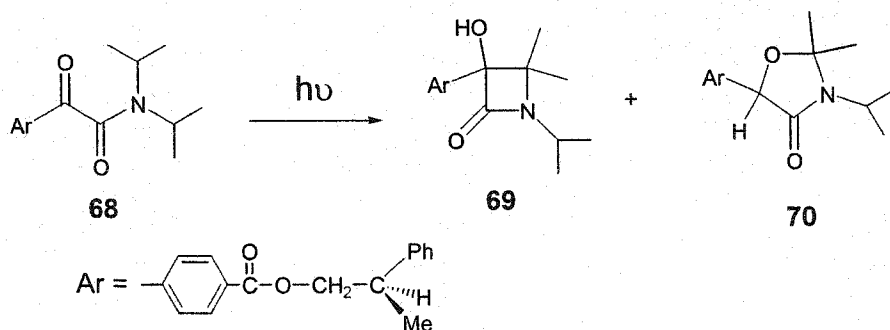
Figure 2.5 Photochemistry of α-oxoamide **68**

The solution phase photochemistry of α-oxoamide **68** proceeded to give **70** oxazolidinone as a major photoproduct and azetidinone **69** as a minor photoproduct as shown in Figure 2.5 and Table 2.10. These photoproducts, having a diastereomeric excess (de) of 0 % owing to the remote chiral auxiliary, were used to test the separation conditions on chiral HPLC. The solution phase photolysis also served as a method of producing sufficient amounts of the photoproducts for characterization. The identification of photoproducts **69** and **70** was virtually identical to that of photoproducts **39** and **40** described previously. The percentage conversion as well as the product composition was determined by GC. Isolated yields are reported for the 200 mg scale photolysis. Isolation of each photoproduct through silica gel chromatography was necessary owing to the overlapping of the two photoproduct peaks on chiral HPLC. Following purification, the diastereomeric excess of azetidinone **69** was determined using a HPLC column containing a chiral stationary phase, Chiralcel® OD® (Figure 2.6). Unfortunately, the diastereomers of photoproduct **70** could not be separated by all in-house chiral HPLC

columns, and best results were obtained using the OD column with hexanes/EtOH as the eluting solvents (Figure 2.7). It was found that the chiral HPLC trace of oxazolidinone **70** from the photolysis of oxoamide **68** in the solid state showed two peaks indicating a de of approximately 0 %. This result is in agreement with the previous study, which showed an enantiomeric excess for oxazolidinone **40** of 0 % in the solid state using the ionic chiral auxiliary approach. Therefore other methods to separate the diastereomers of compound **70** were not attempted. The detailed conditions of chromatographic separation for photoproducts **69** and **70** are outlined in Table 2.9.

Table 2.9 Chromatographic data for enantiomeric excess determination of photoproducts **69** and **70**.

Compound	Column	HPLC conditions			Retention Time (min)[a]
		UV detector (nm)	Solvents	Flow rate (mL/min)	
69	OD[b]	254	99/1 hexanes/IPA	1.0	A: 37.0 B: 50.3
70	OD[b]	254	99/1 hexanes/EtOH	0.5	A: 45.5 B: 49.0

[a] A refers to the first eluted peak, B to the second. [b] Chiralcel® OD® (25 cm × 0.46 cm ID), Chiral Technologies Inc

Figure 2.6 HPLC trace for the resolution of photoproduct **69** on Chiralcel OD (eluting solvents, hexanes/isopropanol 99/1; flow rate, 1.0 mL/min)
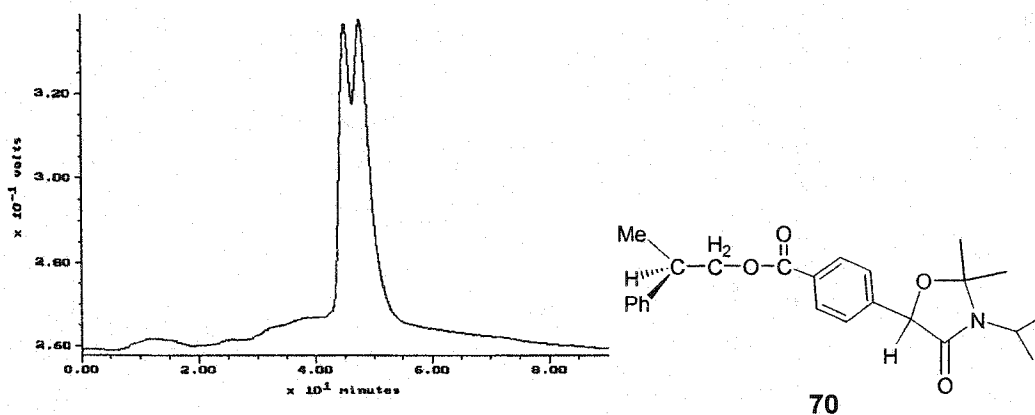
Figure 2.7 HPLC trace for the unsuccessful resolution of photoproduct **70** on Chiralcel OD (eluting solvents, hexanes/ethanol 99/1; flow rate, 0.5 mL/min)

Table 2.10 shows that excellent diastereomeric excess (> 84 % de for photoproduct **69**) was obtained even at quantitative conversion by the solid state covalent chiral auxiliary approach. The de was enhanced to 92% at low temperature. Once again, to demonstrate the synthetic utility of solid state photochemistry in asymmetric synthesis, a large scale solid state photoreaction was achieved by the suspension of powdered crystalline oxoamide **68** in a solvent in which it is insoluble, such as water. Surprisingly, suspension in water gave higher de's than pure crystal photoreaction on both the 5 mg and 200 mg scales. An obvious explanation of this result is lacking at the present time. With increasing of conversion, the de remains in the 95 % level without significant

decrease. Once again, a single-crystal-to-single-crystal experiment was not successful in the photolysis of oxoamide **68**. The single crystal of oxoamide **68** also became cloudy after photolysis.

Table 2.10 Asymmetric induction in the photolyses of chiral ester **68**

medium	temp (°C)	conv [a] (%)	69/70 [b]	de [c] (%) for **69**	Peak [d]
pure crystals	-25	26	18/4	92	B
pure crystals	RT	26	16/6	85	B
pure crystals	RT	81	53/16	85	B
pure crystals	RT	98	66/17	84	B
Suspension in H_2O	RT	46	38/4	94	B
Suspension in H_2O	RT	94	75/10	95	B
200 mg suspension in H_2O	RT	100	67/8 [e]	95	B
MeOH	RT	100	12/65	6	B
MeOH	RT	100	14/63	13	B
Benzene	RT	100	8/77	0	B

[a] Percentage of total GC integral due to the disappearance of the corresponding starting material. [b] Percentage yield of products from GC analysis. The total percentage yield of **69** and **70** is less than the percentage of conversion due to other side products. [c] Diastereomeric excess (de) values measured on a chiral OD column. [d] Peaks A and B represent two diastereomers of **69**; Peak A refers to the first peak eluted as the predominant diastereomer in the HPLC analysis, B to the second. [e] Isolated yields.

The photolysis of oxoamide **68** in solution (MeOH and benzene) also gave negligible diastereomeric excess as shown in Table 2.10. Once again, this demonstrates the importance of the crystalline state to asymmetric induction using remote chiral auxiliaries. The covalent chiral auxiliary method is not applied to the second project in this thesis because ionic chiral auxiliary method has obvious advantages: (a) it is easier to add and easier to remove ionic chiral auxiliaries than covalent chiral auxiliaries; (b) ionic bonding makes salts potentially high melting point.

2.5 Structure-Reactivity Correlations

2.5.1 Crystallographic Studies and Molecular Modeling

As expected according to the previous studies of Aoyama and Toda[80,81], photolysis of α-oxoamides in the solid state produced β-lactam **39** as a major product and oxazolidinone **40** as a minor product and unisolated trace amounts of type II cleavage products (<5%, detected by GCMS) as shown in Figure 2.8. In solution photolyses, the major product is oxazolidinone **40** rather than β-lactam **39**. The photochemical results for α-oxoamide **38** are shown in Table 2.2. As described in the introduction section of this thesis, the different photochemical behavior of α-oxoamide **38** in the solid state and in solution can be attributed to the presence of intermediates Z_2 and **B**. The extended zwitterion Z_2 is unfavorable in the solid state and rapid ring closure from biradical **B** affords β-lactam **39**. However, in solution the extended zwitterion Z_2 is energetically favorable and ring closure produces oxazolidinone **40**. Type II photocleavage also occurs *via* zwitterionic intermediate Z_2 (Figure 2.9).[80(c)]
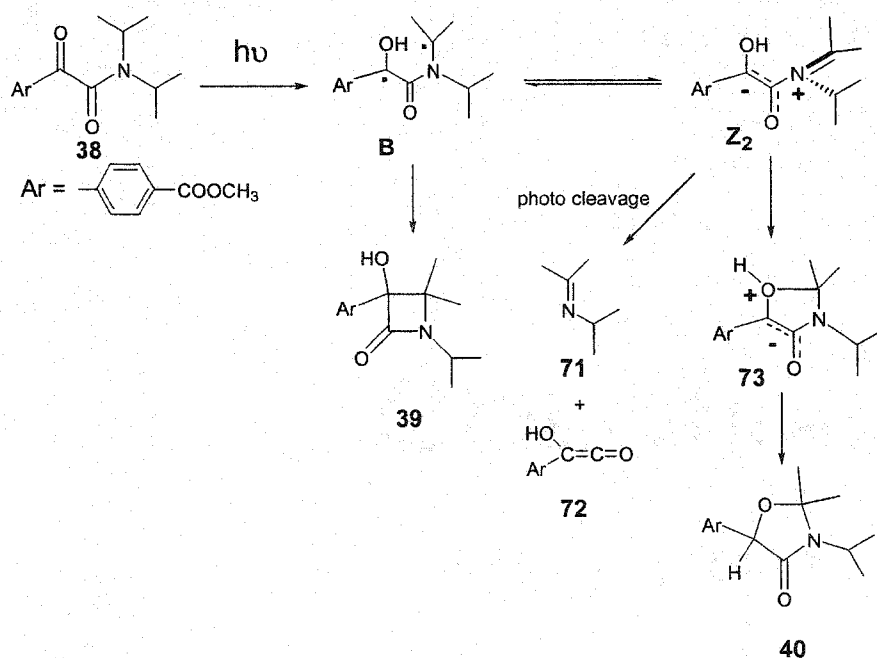
Figure 2.8 Photochemistry of α-oxoamide **38**
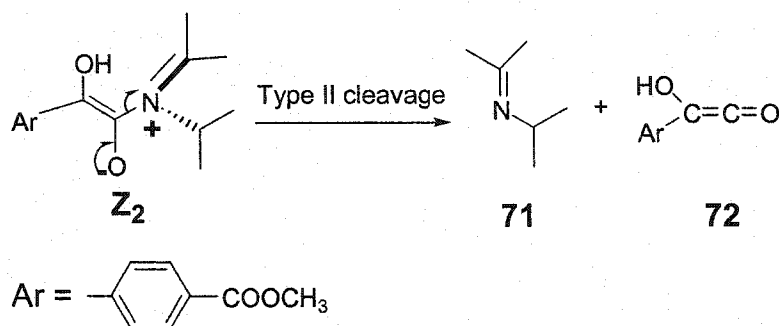
Figure 2.9 Photocleavage from zwitterionic intermediate.

The photoreactions of α-oxoamides provide the first example of type II reactions that involve zwitterionic intermediates. The intermediacy of 1,4-hydroxybiradicals in normal type II reactions is well established.[91] The geometric requirements for hydrogen atom abstractability[60] and 1,4-hydroxybiradical reactivity[92] in the Norrish type II reaction were intensively explored in the Scheffer group using X-ray crystallography and molecular modeling. However, the geometric requirements for hydrogen atom abstractability, 1,4-hydroxybiradical reactivity (for the formation of azetidinones) and zwitterion reactivity (for the formation of oxazolidinones and photocleavage products) in the type II reactions of α-oxoamides have not been previously studied. The formation of oxazolidinones and

photocleavage products *via* zwitterionic intermediate Z_2 is not a topochemically controlled process since large motions are involved.

Table 2.11 shows that the hydrogen abstraction parameters d, ω, Δ, and θ for six crystalline α-oxoamides (average shown in entry 7) are very close to the MM^+ calculation values (entry 9) and also close to the data obtained from previous studies of normal Norrish/Yang photoreactions studied in the Scheffer group (entry 8). This explains the efficiency of hydrogen abstraction in the type II reactions of α-oxoamides. The average β (entry 7) is $6°$, which is favorable for photocyclization from biradicals to form azetidinones (ideal value, $\beta = 0°$). Experimentally, all compounds in entries 1-6 were photolyzed in solid state to form azetidinones as the major products. The biggest difference between entries 7 (current studies in α-oxoamides) and 8 (previous studies in regular ketones) are φ_1 and φ_4. The values of $\varphi_1 = 8°$ and $\varphi_4 = 5°$ in entry 7 suggest the photocleavage should be favorable (ideal values, φ_1 and $\varphi_4 = 0°$) for compounds in entries 1-6. However, there were no significant amounts of cleavage products obtained from the photolysis of the oxoamides in the current studies and in the previous studies by Aoyama and Toda.[80,81] The angles of φ_1 and φ_4 might not be applicable to the judgement of the efficiency of the photocleavage and the reason could be due to the fact that the photocleavage of oxoamides is not *via* biradical intermediate but *via* a zwitterion intermediate. For the same reason, the efficiency of the formation of oxazolidinones might be unpredictable by parameters measured from X-ray crystal structures of ground state α-oxoamides.

Table 2.11 Crystallographic studies and molecular modeling[a]

entry	compound	H[d]	β(°)	φ$_1$(°)	φ$_4$(°)	d(Å)	ω(°)	Δ(°)	θ(°)	D(Å)
1		a	18	20	7	2.58	53	66	119	2.91
		a'				5.00				
		b	10	11	7	2.67	54	62	120	2.88
		b'				5.06				
2		a	2	1	9	2.77	52	54	113	2.84
		a'				5.09				
		b	2	0	2	2.74	52	54	119	2.81
		b'				5.08				
3		a	0	1	1	2.73	54	56	124	2.85
		a'				5.12				
4		a	3	9	3	2.71	53	56	117	2.82
		a'				4.93				
5		a	10	11	6	2.65	54	62	120	2.87
		a'				5.02				
6		a	6	7	2	2.65	56	60	123	2.85
		a'				5.07				
7[b]	average 1-6	a	6	8	5	2.69	54	59	119	2.85
		a'				5.05				
8[c]		a	22	56	56	2.68	62	82	106	2.88
9		a	2	8	12	2.68	60	62	104	2.84
	MM$^+$ calculation	a'				4.31				

[a] See the Introduction of this thesis for the definition of all parameters in this table. [b] Entry 7 is the average data from entries 1-6. [c] Data from the previous studies in the Scheffer group. See reference.[30] [d] In entries 1 and 2, there are two independent conformers in the asymmetric unit. Hydrogens a and a' are enantiotopic in one conformer; hydrogens b and b' are also enantiotopic but in the other conformer.

2.5.2 Enantioselectivity/Diastereoselectivity in the Photolysis of α-Oxoamides

Asymmetric synthesis *via* the solid state ionic chiral auxiliary method and the covalent chiral auxiliary method was described in sections 2.3 and 2.4. Near-quantitative ee's and de's were achieved in a number of salts and in ester **68**. One chiral ester (**68**) and four chiral salts were studied by X-ray crystallography as shown in Table 2.11 (entries 2-6). The data in entries 3-6 show that one chiral conformation of the α-oxoamide is preorganized for reaction in the crystalline state. The photoexcited carbonyl oxygen is much closer to one abstractable γ hydrogen (O-H_a, within 2.72 Å) than the other (O-$H_{a'}$, ~5.03 Å), so only the hydrogen abstraction from H_a is favorable to form biradical **B**. Assuming that biradical **B** has a conformation similar to that of its α-oxoamide precursor and reacts with least motion (topochemical control), ring closure from biradical **B** with retention of configuration at the carbonyl carbon is favored to produce the major enantiomer of the β-lactam. A specific example is salt **67a** shown in Figures 2.10 and 2.11. This salt crystallizes in a unique pro-S conformation. It is apparent that γ hydrogen H_a (in green), which lies at a distance of 2.73 Å from the carbonyl oxygen (in red), is much more favorably disposed for hydrogen transfer than is γ hydrogen $H_{a'}$ (in green, O-$H_{a'}$ distance 5.12 Å), and there can be little doubt that H_a is preferentially abstracted in the solid state. The stereochemistry of biradical closure can also be reasonably interpreted in terms of the molecular conformation shown in Figure 2.11. Again, assuming that the biradical has a conformation similar to that of its α-oxoamide precursor, least motion closure of the biradical should lead to the (S) absolute configuration at the newly generated chirality center (retention). Formation of the (R) enantiomer requires rotation around the C_1-C_2 bond (Figure 2.10). Such a process is associated with its concomitant large amplitude motions of the pendant aryl and hydroxyl groups, and is expected to be topochemically forbidden in the rigid, close-packed environment of the crystal.
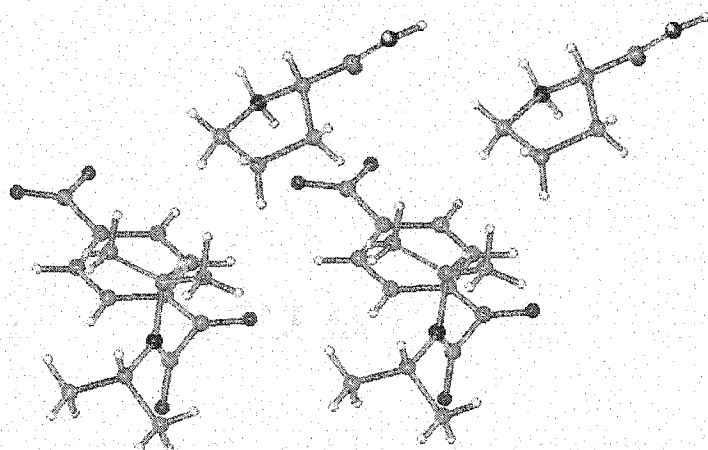
(a) Unique Pro-S conformation in the crystals of salt **67a**
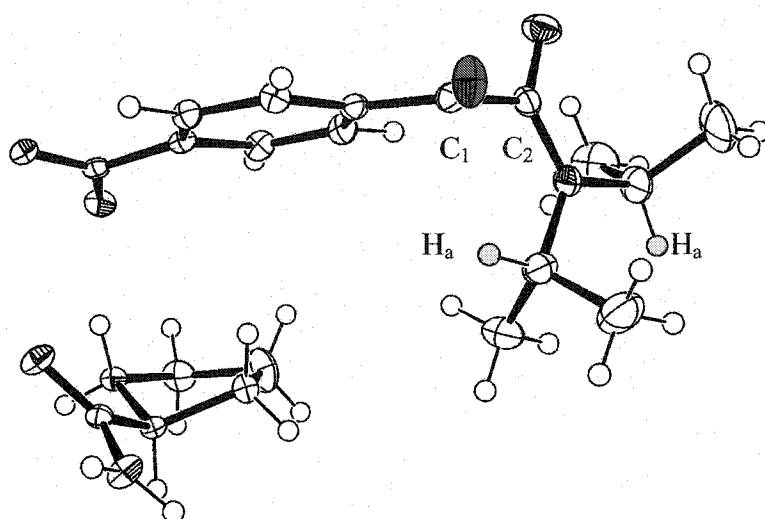
(b) ORTEP representation of salt **67a**. Carbonyl oxygen is colored red, γ hydrogens H_a and $H_{a'}$ green.

Figure 2.10 Molecular conformation in crystals of salt **67a**.

Pro-S conformation
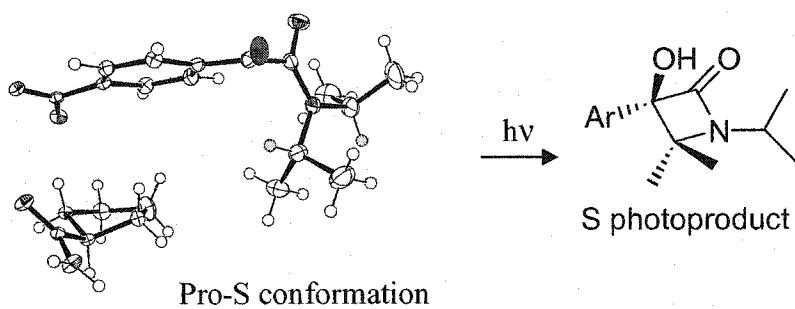
Figure 2.11 The reaction course of salt **67a** in the crystalline state. In the ORTEP

representation of salt **67a,** carbonyl oxygen is colored red, γ hydrogens H_a and $H_{a'}$ green.

In solution, rotation around the C_1-C_2 bond is allowed and enantiomeric/ diastereomeric excess was not obtained. A number of salts in Table 2.5 showed low ee in the solid state asymmetric induction studies. An obvious reason in the case of salts 67k and 67l is crystal breakdown, because the crystals melted during photolysis. The reason for the low ee in salts 67f and 67g is "conformational enantiomerism", which will be described in next section. Due to the unavailability of crystal structures there is no firm evidence to explain the low ee in the case of salts 67h, 67i, 67j. From previous studies in the Scheffer group,[44,78] it is a typical result that a number of salts lead to low ee's while others lead to near-quantitative ee's in the solid state asymmetric induction studies, and a number of reasons can account for the low ee: (1) crystal melting and crystal breakdown; (2) conformational enantiomerism; (3) disorder in the crystal where two or more conformations of the reactive ion are distributed randomly in the crystal (static disorder) or are thermally interconverting (dynamic disorder).[93]

In the solid state photolysis of salts, the minor oxazolidinone product 40 is virtually racemic. The mechanism in Figure 2.8 shows the chirality center on oxazolidinone 40 is formed upon proton transfer from zwitterion 73. Because racemic oxazolidinone was obtained in the solid state photoreaction, the proton transfer apparently occurs with equal ease from the *re-* and *si-* faces in the chiral crystalline environment. This is the same reason that a de of 0 % for oxazolidinone 70 was obtained in the solid state photoreaction.

2.5.3 Conformational Enantiomerism and Absolute Configuration

Low ee (3 %) was observed in the solid state photolysis of salts 67f and 67g (Table 2.5). The X-ray crystal structure of salt 67f (Figure 2.12) shows that it contains equal amounts of two independent and mirror image related anion moieties (carboxylate ions) in the asymmetric unit, while the cation moieties (phenylethylammonium ions) retain their absolute configuration. The near-perfect enantiomeric relationship between the carboxylate ions was disclosed by computationally inverting one and overlapping it with the other, which leads to a root-mean-square error (RMSE) of 0.06 Å (Figure 2.13). Half of the molecules in the crystal have conformations that lead to the (R)-β-lactam, while the other half are conformationally poised to form (S). Two facts account for the low but

measurable 3% ee: (1) the two sets of conformers are not perfect mirror images of one another; (2) they are diastereomerically related when the presence of the (R)-ammonium ion is considered, so they react at slightly different rates (the molecular packing in the crystal is in a chiral space group: C_2). Similar conformational effects have been reported by Scheffer *at al.* and termed "conformational enantiomerism".[94]

Pro-R   Pro-S

X = -COO H_3N—

R-(+)-phenylethyllamine salt
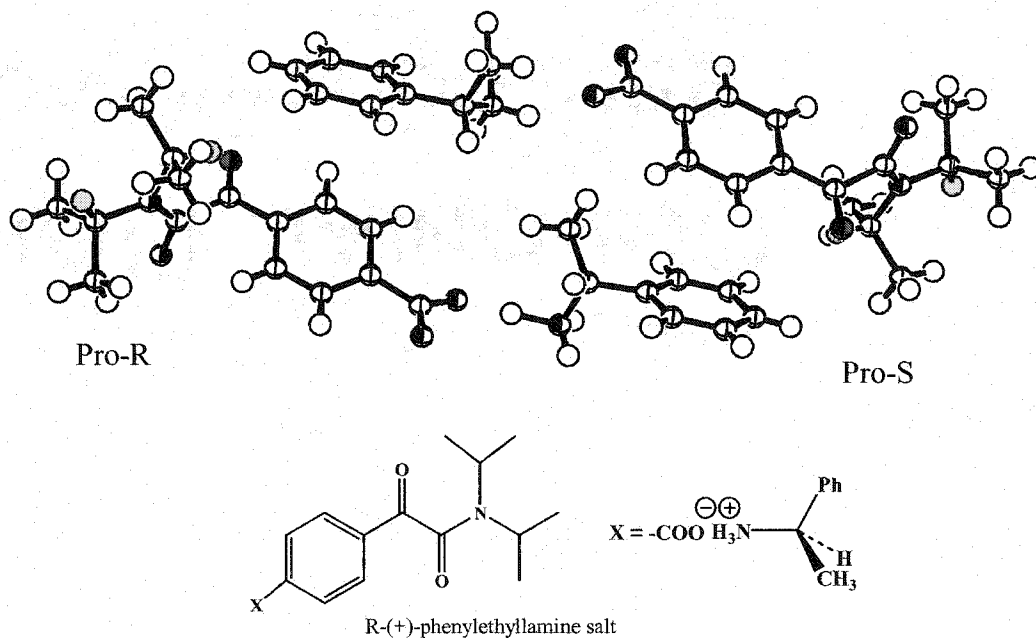
Figure 2.12 Conformational enantiomerism in crystals of salt **67f**.
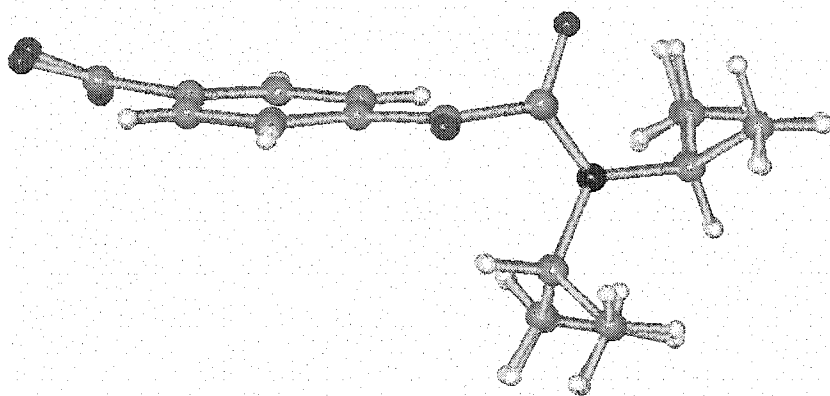
Figure 2.13 Inverting the pro-R conformer and overlapping it with the pro-S conformer in the crystal of salt **67f**

The X-ray crystallographic studies on the photolysis of α-oxoamide **68** allow the determination of the absolute configuration. Using the same method as described in section 2.5.2 and Figure 2.11, photoproduct **69** should have the (R) configuration at the newly formed chirality center (Figure 2.14). The (R) configuration was confirmed by X-ray structure determination of photoproduct **69**. Thus we see that the concepts of conformational control (preorganization with a unique conformation during the crystallization) and topochemical control (least motion during the ring closure) are successful in rationalizing the asymmetric induction and predicting the absolute configuration of the product(s) in the solid state photolysis of α-oxoamides.
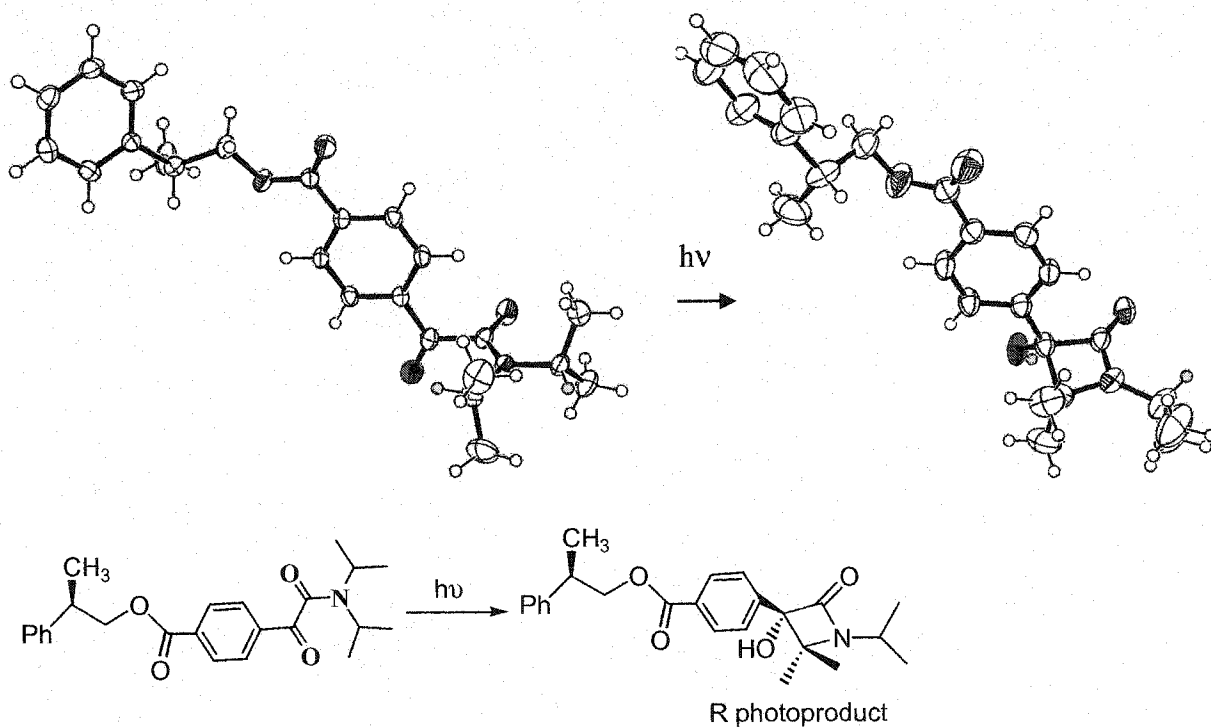
Figure 2.14 The reaction course of ester **68** in crystalline state. In the ORTEP

representation of ester **68**, carbonyl oxygen is colored red, γ hydrogens H_a and $H_{a'}$ green.
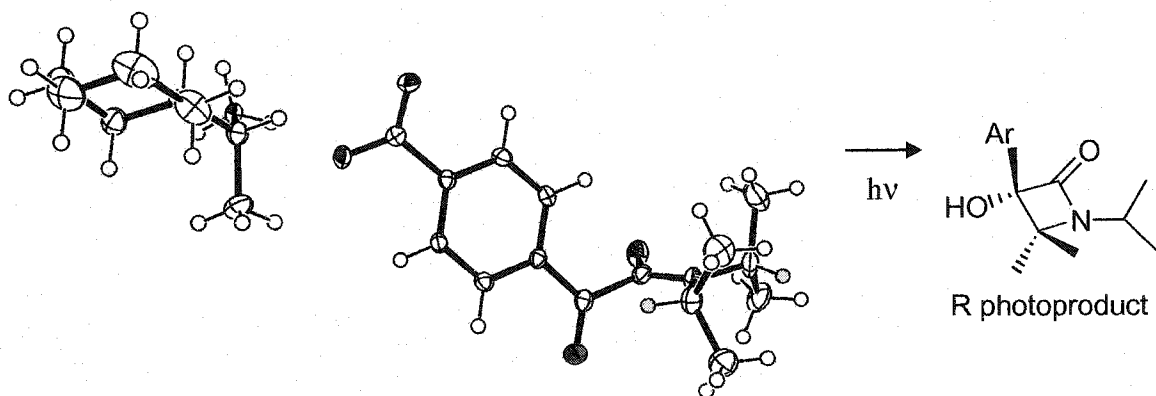
Figure 2.15 The reaction course of salt **67c** in crystalline state. In the ORTEP

representation of salt **67c**, carbonyl oxygen is colored red, γ hydrogens H_a and $H_{a'}$ green.

By the same method, the absolute configuration of the photoproduct of salt **67c** was also predicted to be (R) (Figure 2.15). The absolute configurations of photoproducts from **67a**, **67c** and **67e** were predicted as (S), (R), (S), and their signs of rotation were measured as (+), (-) and (+) respectively. The predicted configurations were completely consistent with the signs of rotation of the photoproduct β-lactams as shown in Table 2.12.

Table 2.12 Comparison of the predicted configuration and sign of rotation

α-oxoamide	measured $[\alpha]^a$	predicted absolute configuration of C_1
67a	+	S
67c	-	R
67e	+	S

^{a} Signs of rotation were determined at the sodium D-line.

2.6 Summary

1. By using the solid state ionic chiral auxiliary approach and the solid state covalent chiral auxiliary approach, nearly quantitative enantiomeric/diastereomeric excesses were obtained in the photolysis of α-oxoamides.

2. By suspension in hexanes (or water), asymmetric synthesis in solid state photochemistry can be carried out on a preparative scale without loss of ee (or de). Therefore, the ionic chiral auxiliary method and the covalent chiral auxiliary method were demonstrated to be synthetically useful in the asymmetric synthesis of β-lactams *via* solid state photoreaction of α-oxoamides.

3. X-ray crystallography and molecular modeling were used for the first time in the study of hydrogen atom abstraction and 1,4-hydroxybiradical reactivity in the type II reactions of α-oxoamides. Using X-ray crystallography, the conformational and topochemical control in the enantiomeric/diastereomeric induction was also studied and the absolute configuration of the β-lactams determined.

4. Using the ionic chiral auxiliary method, some salts led to low ee's in the solid state asymmetric induction studies. It is a typical result that a number of salts lead to low ee's while others lead to near-quantitative ee's in the solid state asymmetric induction studies. Crystal breakdown and conformational enantiomerism were used to rationalize the results.

Chapter 3 Asymmetric Synthesis in the Photocyclization of Bicyclic Aryl Ketones

3.1 General Considerations

Asymmetric induction studies in type II reactions have been the focus of much recent work in the Scheffer laboratory.[44] One example is shown in Figure 3.1.
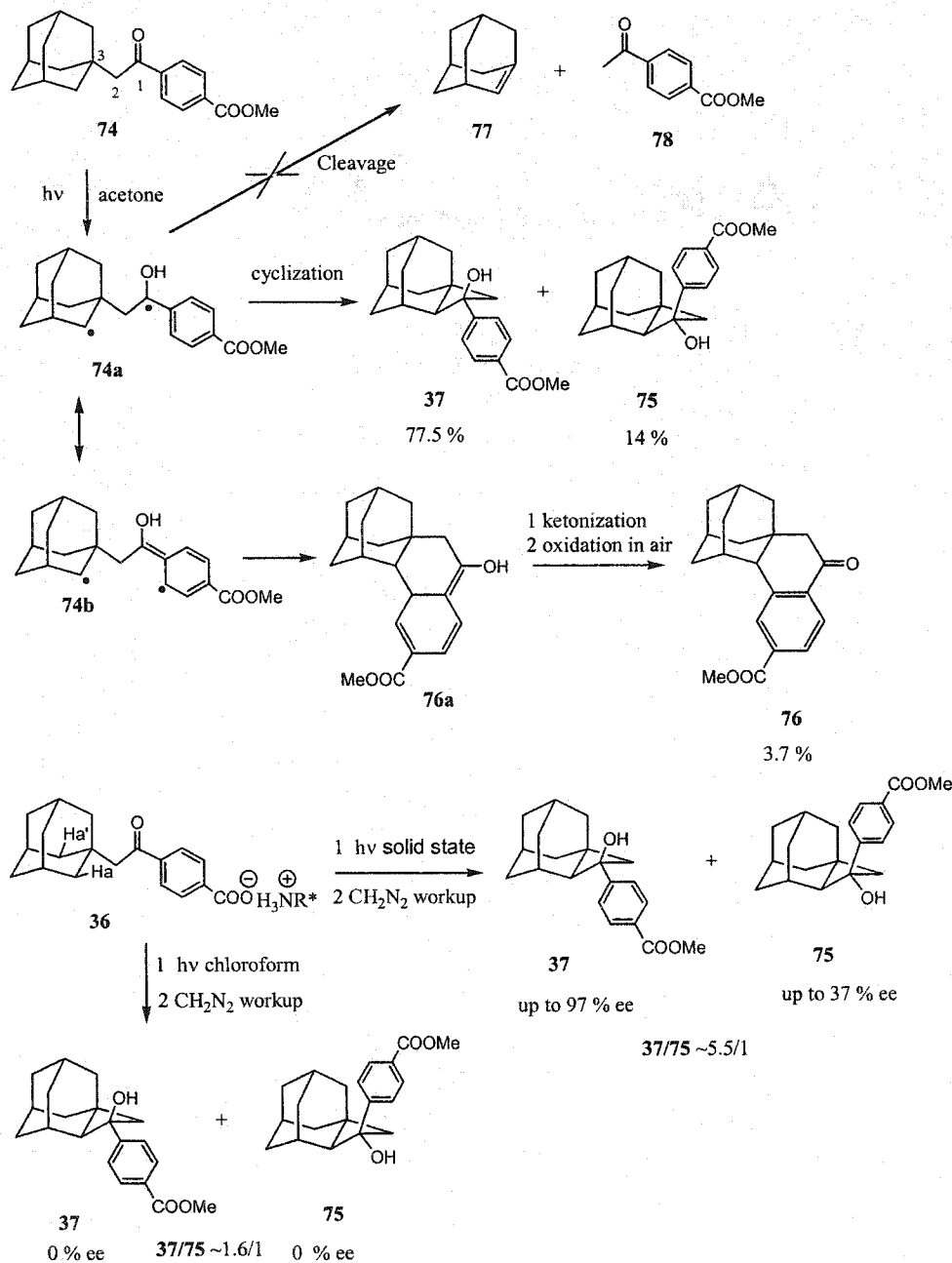
Figure 3.1 Previous studies in α-adamantyl acetophenones[79]

α-Adamantyl acetophenone **74** was photolyzed in acetone, producing photocyclization products **37** (major product), **75** (minor product) and **76** (trace), which is formed from the biradical following ketonization and oxidation in air (Figure 3.1). No cleavage photoproduct **77**, a bridgehead alkene (anti-Bredt olefin), was found in this reaction. Using the ionic chiral auxiliary method, cyclobutanol **37** was formed with up to 97 % ee.[79] The X-ray crystal structure of salt **36** showed the distances from the carbonyl oxygen to the six γ-hydrogens are: O-H_a, 2.70 Å; O-$H_{a'}$, 3.14, 3.47, 4.5, 4.74, 4.91 Å (For clarity only one of the five γ-hydrogens $H_{a'}$ is shown in Figure 3.1). Enantiomeric excess was achieved owing to the fact that only one γ-hydrogen (H_a in Figure 3.1) is within 3.0 Å of the carbonyl oxygen, and hydrogen abstraction of H_a (followed by the radical coupling under the rule of topochemical control described in section 2.5.2 in the oxoamide project) is favored. The second project of this thesis is an extension of the project of Yang photocyclization of α-adamantyl acetophenone derivatives.

54, 55, 56   **57, 58, 59**   **60, 61, 62**

For compounds **54, 57, 60**, X = COOH
For compounds **55, 58, 61**, X = COOCH$_3$
For compounds **56, 59, 62**, X = COO $\ominus\oplus$ NH$_3$R
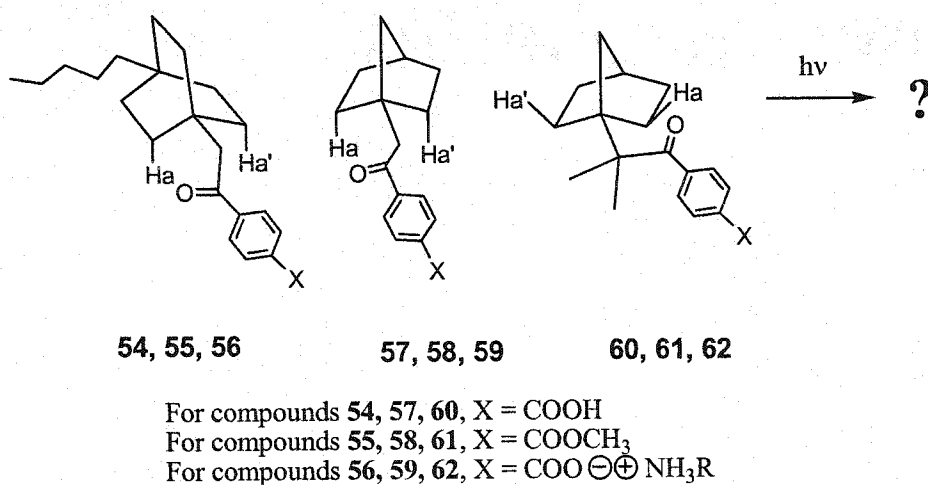
Figure 3.2 α-Bicycloalkylacetophenone compounds selected for study.

In total, three bicyclic aryl ketone systems (Figure 3.2) were chosen for asymmetric induction studies using the ionic chiral auxiliary method. First bicyclo[2.2.2]octyl ketones **54-56** were studied and the long alkyl chain substrates were selected owing to the simplicity of synthesizing the substrates from commercially available 4-pentylbicyclo[2.2.2]octyl carboxylic acid. Like adamantyl ketone **74**, there are six γ-hydrogens in the bicyclo[2.2.2]octyl ketones. This project also rules out the possibility of

type II cleavage, in which an anti-Bredt olefin would be generated. Secondly, the bicyclo[2.2.1]heptyl ketones **57-59** were selected as research targets, in which regioselectivity could also be studied because the γ-hydrogens on both the one- and two-carbon bridges are potentially abstractable. The dimethylated bicyclo[2.2.1]heptyl ketones **60-62** have similar abstractable γ-hydrogens as ketones **57-59**. However, the solid state conformations of ketones **60-62** should be different from those of ketones **60-62**; therefore, their photochemical diastereoselectivity and/or enantioselectivity might be different.

The photochemistry of these bicyclic aryl ketones has not been studied previously. All three target molecules are achiral and their cyclization products are chiral molecules, allowing for asymmetric induction to be studied. All three target molecules incorporate a carboxylic acid group in the phenyl ring, making it possible to apply the ionic chiral auxiliary method in the asymmetric induction. Two diastereomeric cyclobutanols were possible from photolysis of each substrate and therefore diastereoselectivity was also studied in this project.

3.2 Substrate Preparation

3.2.1 Synthesis of Bicyclo[2.2.2]octyl Ketones 85, 54-56
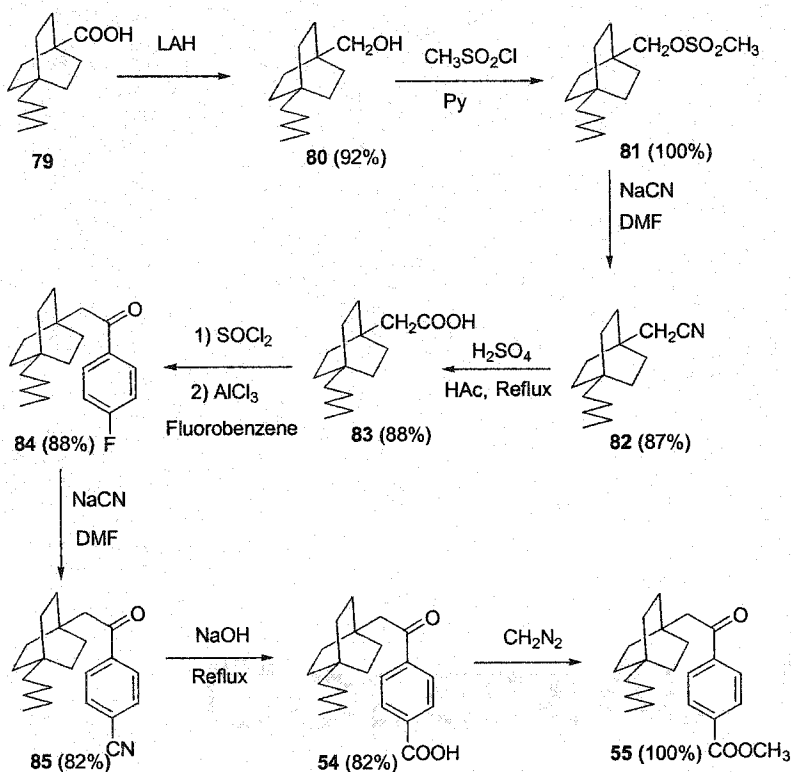
Figure 3.3 Synthesis of bicyclo[2.2.2]octyl ketones **85, 54-55**

As shown in Figure 3.3, bicyclo[2.2.2]octyl ketones **54** and **55** were synthesized according to a method based on a modification of literature procedures.[95] Starting from commercially available 4-pentylbicyclo[2.2.2]octyl carboxylic acid (**79**), 4-pentylbicyclo[2.2.2]octylmethanol (**80**) was prepared in a yield of 92 % by reduction with lithium aluminum hydride. The methanesulfonyl group (a good leaving group) was introduced into alcohol **80** to form 4-pentylbicyclo[2.2.2]octane-1-methanol methanesulfonate (**81**) quantitatively. 4-Pentylbicyclo[2.2.2]octane-1-acetonitrile (**82**) was prepared from compound **81** in 87 % yield using S$_N$Ar reaction through treatment with sodium cyanide in refluxing anhydrous DMF. Hydrolysis of the cyano group in compound **82** was accomplished using the harsh condition of sulfuric acid (50 %). Following acid chloride formation from acid **83** with thionyl chloride, an attempt to make

ketone **55** in a one-pot procedure was unsuccessful by using nucleophilic addition to the acid chloride with a Grignard reagent, generated *in situ* from diisopropylmagnesium chloride and methyl *p*-iodobenzoate.[96] Following the traditional strategy used within our group,[95(b)] the synthesis of ketones **54** and **55** was completed from acid **83** in a total yield of 59 % in four steps. All new compounds gave spectra in agreement with the assigned structures.

Using commercially available optically pure amines, thirteen chiral crystalline salts **56a-m** were prepared from acid **54** as listed in Table 3.1. The detailed procedure to make the salts is given in the Experimental Section. All 13 salts were characterized by NMR, IR, MS and elemental analysis. The structures of salts **56a,b** were confirmed by X-ray crystallography.

Table 3.1 Preparation of chiral salts of acid **54**

salt	amine	recryst solvent	cryst morphol	mp(°C)
56a	R-(-)-1-cyclohexylethylamine	MeOH	plates[a]	173-176
56b	L-prolinamide	MeOH	plates[a]	170-172
56c	(1S, 2R)-(+)-norephedrine	MeOH	needles	170-173
56d	(1R, 2R)-(-)-pseudoephedrine	MeOH	needles	118-119
56e	R-(-)-1-aminoindane	MeOH	needles	182-185
56f	S-(+)-1-aminoindane	MeOH	needles	184-186
56g	(1S, 2R)-(-)-*cis*-1-amino-2-indanol	MeOH	needles	162-165
56h	S-(-)-*p*-tolylethylamine	MeOH	needles	187-189
56i	(1R, 2R)-(-)-amino-1-phenyl-1, 3-propanediol	MeOH	prisms	140-142
56j	S-(+)-2-(methoxymethyl)pyrrolidine	MeOH	powder	76-80
56k	R-(+)-1-phenylethylamine	MeOH	needles	185-187
56l	S-(-)-1-phenylethylamine	MeOH	needles	185-187
56m	(-)-*cis*-myrtanylamine	MeOH	prisms	155-157

[a] X-ray crystal structure obtained.

3.2.2 Synthesis of Bicyclo[2.2.1]heptyl Ketones 57-59
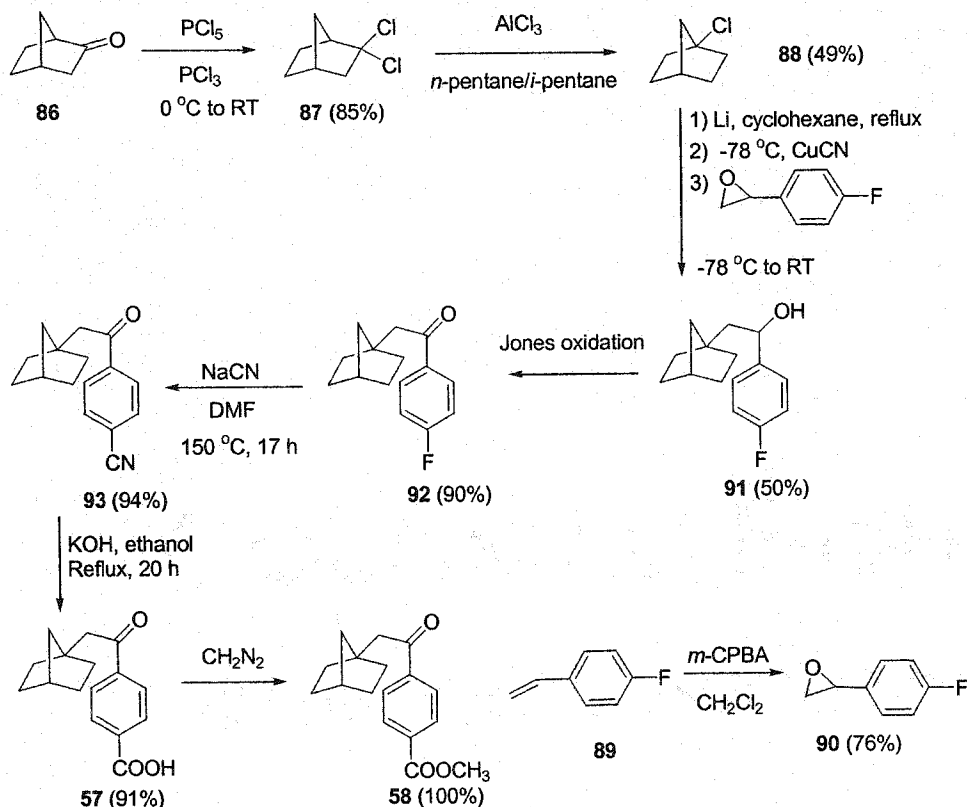
Figure 3.4 Synthesis of bicyclo[2.2.1]heptyl ketones **57-58**

Due to the commercial unavailability of bicyclo[2.2.1]heptyl carboxylic acid, the synthetic methodology used in the synthesis of the bicyclo[2.2.2] analogues could not be used to prepare bicyclo[2.2.1]heptyl ketones **57** and **58**, and an alternative methodology was sought (Figure 3.4). Following the chlorination of commercially available norcamphor (**86**) with phosphorus pentachloride to form 2,2-dichloronorcamphor (**87**), selective rearrangement of compound **87** with aluminum trichloride led to 1-chlorobicyclo[2.2.1]heptane (**88**) which served as the source of the bicyclo[2.2.1]heptane skeleton.[97] A lithium-halogen exchange[98] between chloride **88** and lithium wire was carried out in refluxing cyclohexane followed by the addition of cuprous cyanide to generate bicyclo[2.2.1]hept-1-yl lithium cuprate. This lithium cuprate was added with epoxide **90** (easily obtained from epoxidation of alkene **89** with

3-chloroperoxybenzoic acid) to produce alcohol **91** (the key step for preparing bicyclo[2.2.1]heptyl ketone **58**). The yield for this reaction was disappointingly low (50 % isolated) and is likely due in part to the steric hindrance of the tertiary carbanion involved in the substitution reaction. However, this reaction was a successful synthetic shortcut with two carbons and one aryl group added in one step. It is interesting to mention that when epoxide **90** was contaminated with ethyl acetate, the only isolated product was compound **94**. This three-component reaction was performed by mistake (Figure 3.5).
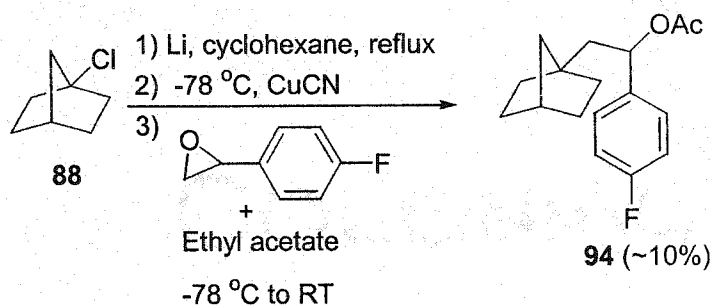
Figure 3.5 A three-component reaction in an unsuccessful synthesis of compound **91**

Following Jones oxidation of alcohol **91**, ketones **57** and **58** were again prepared by the traditional methods used within our group. Spectral data for all new compounds were in agreement with the assigned structures.

Using commercially available optically pure amines, thirteen chiral salts of acid **57** were prepared as outlined in Table 3.2. As described in section 2.1.2, all salts were characterized by NMR, IR, MS and elemental analysis. The structure of salt **59d** was confirmed by X-ray crystallography.

Table 3.2 Preparation of chiral salts of acid **57**

salt	amine	recryst solvent	cryst morphol	mp(°C)
59a	L-prolinamide	MeOH	plates	162-163
59b	(1S, 2R)-(-)-*cis*-1-amino-2-indanol	MeOH	needles	166-168
59c	S-(-)-*p*-tolylethylamine	MeOH	needles	177-179
59d	R-(-)-1-cyclohexylethylamine	MeOH	needles[a]	175-176
59e	(1S, 2R)-(+)-norephedrine	MeOH	needles	144-147
59f	R-(+)-1-phenylethylamine	MeOH	needles	166-167
59g	S-(-)-1-phenylethylamine	MeOH	needles	165-166
59h	(1R, 2R)-(-)-amino-1-phenyl-1, 3-propanediol	MeOH	powder	132-133
59i	(-)-*cis*-myrtanylamine	MeOH	needles	152-154
59j	S-(+)-2-(methoxymethyl)pyrrolidine	MeOH	powder	108-113
59k	R-(+)-Bornylamine	MeOH	needles	156-159
59l	S-(+)-1-aminoindane	MeOH	needles	172-174
59m	(1R, 2R)-(-)-pseudoephedrine	MeOH	powder	127-129

[a] X-ray crystal structure obtained.

3.2.3 Synthesis of Dimethylated Bicyclo[2.2.1]heptyl Ketones 60-62

The straightforward method to make substrate **62** would be a double methylation starting from ketone **58** as shown in the Figure 3.6.
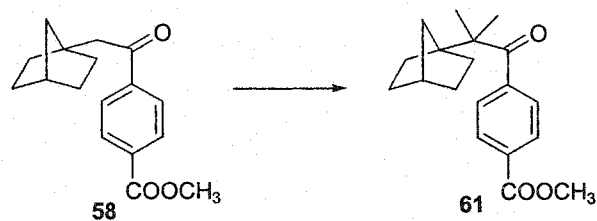
Figure 3.6 Proposed synthesis of ketone **61**

A variety of methylation methods were tried. The first attempt to make ketone **61** was to use lithium diisopropylamide and methyl iodide (LDA/CH₃I) for methylation. Ketone **58** was treated with LDA and DMPU followed by addition of methyl iodide. Unfortunately, reduced alcohol **95** was formed as a single product (Figure 3.7), which is in agreement with similar reports in literature.[99] Monitoring the reaction by GCMS showed that reduction of ketone **58** occurred before methyl iodide was added to the reaction mixture.
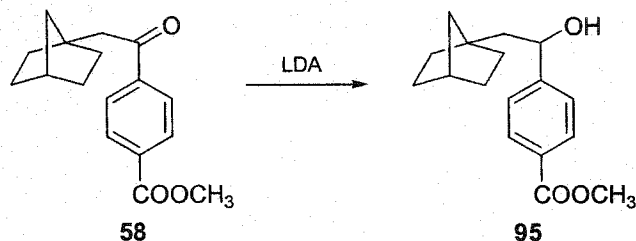
Figure 3.7 An unsuccessful attempt for the methylation of ketone **58**

Mono-methylation was easily achieved in 85 % yield by using sodium hydride and methyl iodide in THF, although the methyl ester was also converted to carboxylic acid **96** as shown in Figure 3.8. Monomethylated carboxylic acid **96** was easily transformed into methyl ester **97** through treatment with diazomethane.
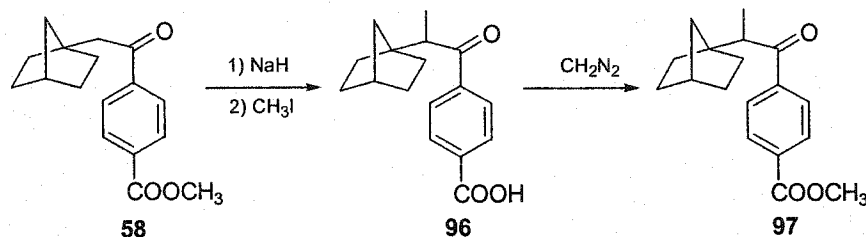
Figure 3.8 Synthesis of monomethylated bicyclo[2.2.1]heptyl ketone **97**

The second methylation was unsuccessful after numerous attempts were made. First, the LDA/CH₃I method was used for the second methylation which led 100 % recovery of the starting material. The starting material was also recovered when lithium

bis(trimethylsilyl)amide or sodium hydride was used in this reaction. Potassium *t*-butoxide and methyl iodide were used in the second methylation and gave 5-10 % of the desired dimethylated product **61**. In this reaction, improvement of the yield and separation of the mono-methylated and dimethylated products was unsuccessful. Based on this difficulty in making ketone **61**, it was decided to revert to the traditional synthetic strategy previously used in making bicyclo[2.2.2]octane derivatives.
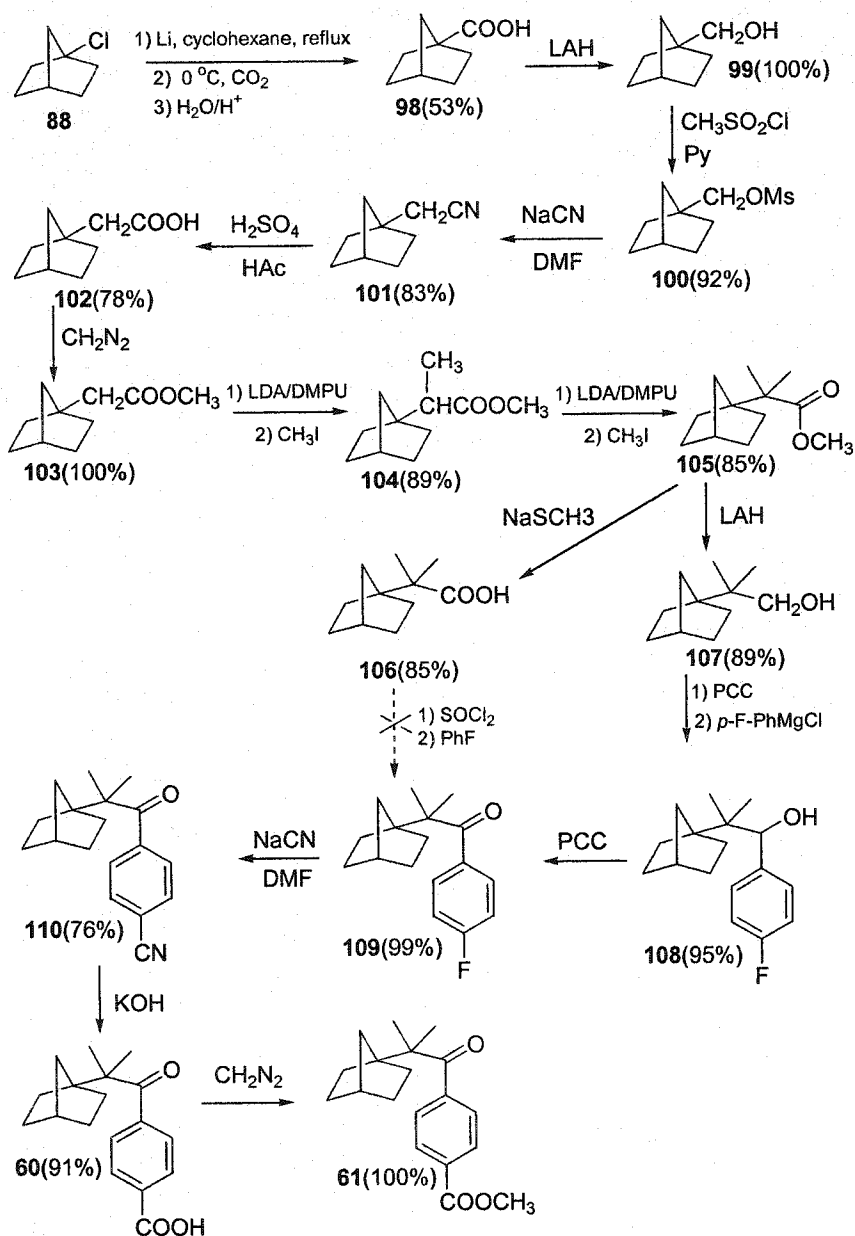
Figure 3.9 Synthesis of ketones **60** and **61**

As shown in Figure 3.9, starting from 1-chloronorbornane (**88**) the carboxylic acid **98** was produced with a yield of 53 % through a lithium-halogen exchange reaction followed by addition of gaseous carbon dioxide. Following the same procedures as used in the synthesis of bicyclo[2.2.2]octane derivatives, acid **102** was obtained in 4 steps from acid **98** with an overall yield of 60 %. Starting from ester **103**, the LDA/CH$_3$I method was applied twice to produce dimethylated ester **105** in an overall yield of 76 %. S$_N$2 displacement reaction of sterically hindered ester **105** was conducted using sodium thiomethoxide in DMF to obtain the desired acid **106** in 85 % yield. The method chosen for the synthesis of ketone **109** was Friedel-Crafts reaction using fluorobenzene and the acid chloride generated from acid **106**. This method had been used previously in the synthesis of bicyclo[2.2.2]octyl ketones. Unfortunately, it was found that the increased steric hindrance provided by the presence of the dimethyl substituents at the α carbon hindered the reaction. Therefore, the synthesis of ketones **60** and **61** proceeded through an even longer synthetic route as shown in Figure 3.9.

Alcohol **107** was synthesized by reduction of ester **105** with lithium aluminum hydride. Addition of the *p*-fluorophenyl ketone functionality was accomplished to form alcohol **108** by adding *p*-fluorophenylmagnesium bromide to the aldehyde generated from oxidation of alcohol **107** with PCC. Once again utilizing PCC oxidation of alcohol **108**, ketone **109** was prepared in 99 % yield. Following the same procedure used previously, the synthesis of ketone **61** was completed in 3 steps from ketone **109** with an overall yield of 69 %.

Again, using the acid-base reaction described in section 2.1.2, eight chiral salts of acid **60** were prepared as outlined in Table 3.3. All salts were characterized by NMR, IR, MS and elemental analysis. The structures of salts **62a, 62c, 62e** were confirmed by X-ray crystallography.

Table 3.3 Preparation of chiral salts of acid **60**

salt	amine	recryst solvent	cryst morphol	mp(°C)
62a	R-(-)-1-cyclohexylethylamine	MeOH	plates[a]	187-189
62b	(1R, 2R)-(-)-pseudoephedrine	MeOH	prisms	134-135
62c	(1R, 2S)-(+)- (-)-*cis*-1-amino-2-indanol	MeOH	needles[a]	202-204
62d	S-(-)-*p*-tolylethylamine	MeOH	prisms	181-184
62f	R-(-)-1-aminoindane	MeOH	needles	198-200
62e	L-prolinamide	MeOH	plates[a]	164-166
62g	R-(+)-1-phenylethylamine	MeOH	needles	175-177
62h	(1R, 2S)-(-)-norephedrine	MeOH	needles	157-159

[a] X-ray crystal structure obtained.

3.3 Photochemical Studies and Identification of Photoproducts

3.3.1 Photochemical Studies of Ketones 85, 54-55

85 X = CN
54 X = COOH
55 X = COOMe

111 X = CN
113 X = COOH
115 X = COOMe

112 X = CN
114 X = COOH
116 X = COOMe ← CH₂N₂
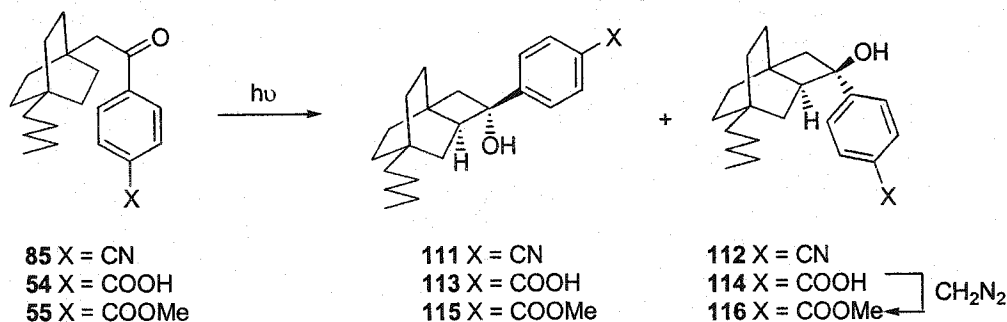
Figure 3.10 Photolysis of ketones **85, 54-55** in solution and the solid state

The photochemical studies of ketones **85, 54-55** were performed in both solution and the solid state. Figure 3.10, Table 3.4 and Table 3.5 summarize the photochemical results in both media. All photolyses in solution were conducted at room temperature with acetonitrile as a solvent. Low temperature (-10 or –25 °C) was applied to the solid state photolyses of ketones **54** and **55** to minimize crystal melting during the formation of

photoproducts. Product ratios were analyzed by chiral HPLC because the peaks of the two photoproducts were overlapped on GC.

Tables 3.4 and 3.5 show that all three ketones have similar photochemical behavior[100] in both solution and the solid state, producing two Yang photocyclization products (cyclobutanols 111, 113, 115 and 112, 114, 116). The *cis* photoproducts (112, 114, 116) are formed more favorably in the solid state than in solution. All photoproducts (acids 113 and 114 were converted into esters 115 and 116 through treatment with diazomethane) were isolated by column chromatography and fully characterized by spectroscopic analysis. The structure of photoproduct 111 was also confirmed by X-ray crystallography.

It was found that the crystalline state photolysis of ketone 85 produced racemic cyclobutanols 111 and 112 (resolution of the enantiomers was accomplished using a chiral AD column; eluting solvents, hexanes/isopropanol 95/5; flow rate, 1.0 mL/min).

Table 3.4 Photolysis of ketones **85, 54, 55** in solution (CH₃CN)

ketone	X	temp (°C)	time (h)	conv (%)[a]	photoproduct ratio
85	CN	RT	2	78	**112/111**
					57/43[b]
85	CN	RT	2	100	**112/111**
					64/36[c]
54	COOH	RT	2	71	**116/115**[d]
					73/27[b]
55	COOMe	RT	0.7	98	**116/115**
					68/32[b]
55	COOMe	RT	3	100	**116/115**
					69/31[c]

[a] Percentage of total GC integral due to the disappearance of the corresponding starting material. [b] Product ratio from chiral HPLC analysis. [c] Product ratio from isolated yields. [d] After diazomethane workup.
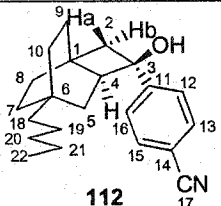
Table 3.5 Photolysis of ketones **85**, **54**, and **55** in the solid state

ketone	X	temp (°C)	time (h)	conv (%)[a]	photoproduct ratio
85	CN	RT	14	42	**112/111**
					78/22[b, c]
54	COOH	RT	13	87	**116/115**[d]
					88/12[b]
54	COOH	-10	9	45	**116/115**[d]
					93/7[b]
55	COOMe	RT	2	30	**116/115**
					93/7[b]
55	COOMe	-25	10	35	**116/115**
					97/3[b]

[a] Percentage of total GC integral due to the disappearance of the corresponding starting material. [b] Product ratio from chiral HPLC analysis. [c] Crystal melting observed. [d] After diazomethane workup.

3.3.2 Identification of Photoproducts 111, 112, 115 and 116

The identification of photoproduct **116** is virtually same as that of photoproduct **112**. For simplification, therefore, only the identification of cyclobutanol **112** is described in detail. The structure of cyclobutanol **112** was elucidated by NMR spectroscopy with the aid of IR, MS, and elemental analysis. The IR spectrum shows a broad O-H stretch around 3400 cm^{-1}. Mass spectroscopy and elemental analysis confirmed that the compound is a structural isomer of the starting material. On the basis of the NMR data, the structural assignments of cyclobutanol **112** are shown in Table 3.6.

Table 3.6 Comprehensive NMR assignments for cyclobutanol **112**

Carbon #	^{13}C δ (ppm)	^1H δ (ppm) from HMQC	^1H-^1H COSY	HMBC	^1H-^1H NOE
1	33.04	-	-	H_4, H_2	
2	44.96	H_a, 2.03, 1H, d, J=12.0Hz H_b, 2.23, 1H, d, J=12.0Hz	H_2	H_4	
3	79.22	-	-	H_{12}/H_{16}, H_2, H_5	
4	47.17	2.41, 1H, m	H_5	H_2, H_5	H_{12}/H_{16}, H_{2b}
5	29.50	1.64 and 1.41, 2H, m	H_4		
6	31.40	-	-	H_5	
11	110.98	-	-	H_{12}/H_{16}	
12/16	126.32	7.46, 2H, d, J=8.2Hz	H_{13}/H_{15}	H_{13}/H_{15}	
13/15	132.66	7.63, 2H, d, J=8.2Hz	H_{12}/H_{16}	H_{12}/H_{16}	
14	153.62	-	-	H_{13}/H_{15}	
17	119.23	-	-	H_{13}/H_{15}	
18	41.70	1.12, 2H, m			
21	23.08	1.35, 2H, m	H_{22}	H_{22}	
22	14.24	0.88 3H, t, J=7.2Hz	H_{21}	H_{21}	
OH	-	2.10, 1H, s, br	-	-	-

The presence of a *para* disubstituted aromatic ring was determined from the ^1H-NMR (7.46 ppm, 2H, d, J = 8.2 Hz and 7.63 ppm, 2H, d, J = 8.2 Hz) and COSY spectra. The COSY, HMQC and HMBC spectra are complicated by overlapping proton signals at carbons 7, 8, 9, 10, 19, 20. However the structure is still well-established from other parts of the spectra. From HMQC, the primary, secondary, tertiary and quaternary carbons and correlated hydrogens were elucidated. The chemical shift of quaternary carbon 3 is 79.22 ppm owing to the direct connection with oxygen. The carbon-carbon connections were established from HMBC and COSY. The relative stereochemistry was determined by

one-dimensional (1D) selective NOE (Figure 3.11). The NOE experiment shows the close proximity between H_4 and H_{12}/H_{16} as well as H_4 and H_{2b}.
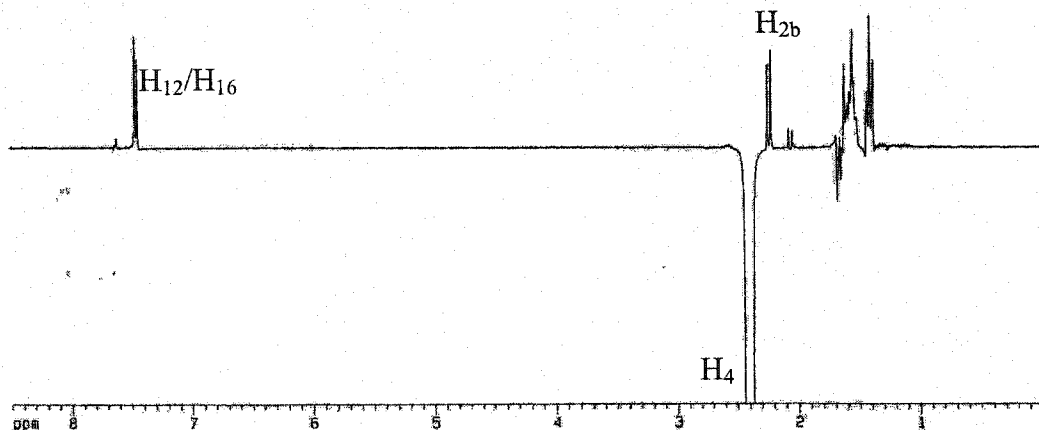
Figure 3.11 NOE spectrum for cyclobutanol **112** with irradiation at 2.41ppm (H_4)

The identification of photoproduct **115** is same as that of photoproduct **111**. Again for simplification, only the identification of cyclobutanol **111** is described in detail. The structure of cyclobutanol **111** was also elucidated mainly by NMR spectroscopy, with the aid of IR, MS, and elemental analysis and confirmed by X-ray crystallography (Figure 3.13). The IR spectrum shows abroad O-H stretch around 3400 cm^{-1}. Mass spectroscopy and elemental analysis confirmed that the compound is a structural isomer of the starting material. On the basis of the NMR data, the structural assignments for cyclobutanol **111** are shown in Table 3.7.

Table 3.7 Comprehensive NMR assignments for cyclobutanol **111**

111

Carbon #	^{13}C δ (ppm)	^1H δ (ppm) from HMQC	^1H-^1H COSY	HMBC	^1H-^1H NOE
1	32.68	-	-	H_4, H_2	
2	43.35	H_a, 2.72, 1H, d, J=12.2Hz H_b, 2.05, 1H, d, J=12.2Hz	H_2	H_4	
3	78.95	-	-	H_{12}/H_{16}, H_2, H_5	
4	52.13	2.58, 1H, m	H_5	H_2, H_5	OH, H_{2b}
5	33.20	1.62 and 1.10, 2H, m	H_4		
6	26.90	-	-	H_5	
11	111.51	-	-	H_{12}/H_{16}	
12/16	129.06	7.50, 2H, d, J=8.3Hz	H_{13}/H_{15}	H_{13}/H_{15}	
13/15	132.52	7.69, 2H, d, J=8.3Hz	H_{12}/H_{16}	H_{12}/H_{16}	
14	148.53	-	-	H_{13}/H_{15}	
17	119.23	-	-	H_{13}/H_{15}	
18	41.37	1.05, 2H, m			
21	23.02	1.25, 2H, m	H_{22}	H_{22}	
22	14.21	0.86 3H, t, J=7.3Hz	H_{21}	H_{21}	
OH	-	2.10, 1H, s, br	-	-	-

The presence of a *para* disubstituted aromatic ring was determined from the ^{1}H-NMR (7.50 ppm, 2H, d, J = 8.3 Hz and 7.69 ppm, 2H, d, J = 8.3 Hz) and COSY spectra. The COSY, HMQC and HMBC spectra are also complicated by overlapping proton peaks at carbons 7, 8, 9, 10, 19, 20, but the structure is well-established from the other part of the spectra and was confirmed by X-ray crystallography. From HMQC, the structure of the primary, secondary, tertiary and quaternary carbons, and correlated hydrogens was elucidated. The chemical shift of quaternary carbon 3 is 78.95 ppm owing to the direct connection with oxygen. The carbon-carbon connections were established from HMBC

and COSY. The relative stereochemistry was determined by 1D selective NOE (Figure 3.12). The NOE experiment shows the close proximity between H_4 and H_{2b} as well as H_4 and OH. From the X-ray structure (Figure 3.13), the aromatic ring is oriented close to one of hydrogens H_5 (1.10ppm, strong shielding effect from aromatic ring), and hydrogen H_{2a} (2.72 ppm) is strongly deshielded by the aromatic ring.
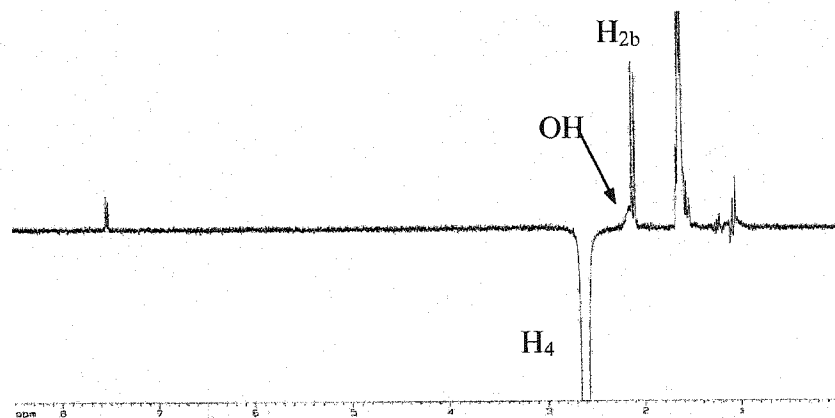
Figure 3.12 NOE spectrum for cyclobutanol **111** with irradiation at 2.58ppm (H_4)
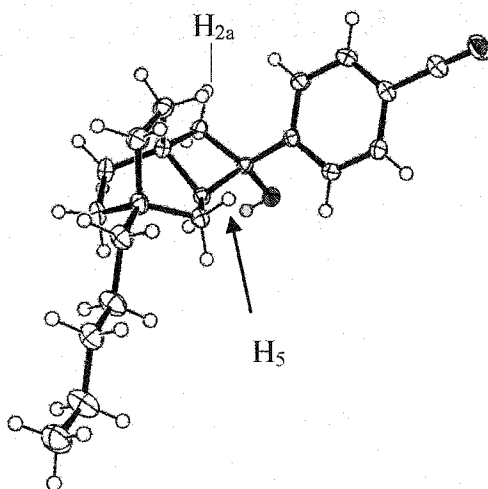
Figure 3.13 ORTEP representation of photoproduct **111**. In the hydroxyl group, the oxygen atom is colored red, the hydrogen atom green.

3.3.3 Photochemical Studies of Ketones 57 and 58

57 X = COOH	**117** X = COOH	**118** X = COOH
58 X = COOMe	**119** X = COOMe	**120** X = COOMe
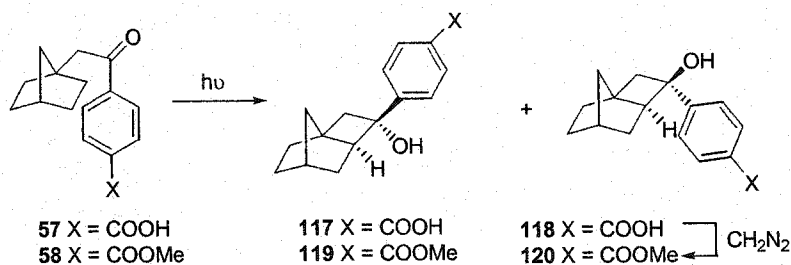
Figure 3.14 Photolysis of ketones **57** and **58** in solution and the solid state

Photochemical studies of ketones **57-58** were conducted in both solution and the solid state. Figure 3.14 and Tables 3.8 and 3.9 summarize the photochemical results in both media. All photolyses in solution were conducted at room temperature in acetonitrile. Product ratios were analyzed by chiral HPLC because the peaks of the two products were overlapped on GC.

Tables 3.8 and 3.9 show that ketones **57** and **58** have similar photochemical behavior in both solution and the solid state, producing two Yang photocyclization products (cyclobutanols **117**, **119** and **118**, **120**). The *trans* photoproduct **119** is formed in a greater yield in the solid state than in solution. Acid **57** is photochemically inert in the solid state. All photoproducts (products **117** and **118** were converted into products **119** and **120** through treatment with diazomethane) were isolated by flash chromatography and fully characterized by spectroscopic analysis.

Table 3.8 Photolysis of ketones **57-58** in solution (CH₃CN)

ketone	X	temp (°C)	time (h)	conv (%)[a]	photoproduct ratio
57	COOH	RT	4	99	**119/120**[b]
					51/49[c]
58	COOMe	RT	2	100	**119/120**
					53/47[c]
58	COOMe	RT	4	100	**119/120**
					56/44[d]

[a] Percentage of total GC integral due to the disappearance of the corresponding starting material. [b] After diazomethane workup. [c] Product ratio from chiral HPLC analysis.
[d] Product ratio from isolated yields.

Table 3.9 Photolysis of ketones **57-58** in the solid state

ketone	X	temp (°C)	time (h)	conv (%)[a]	photoproduct ratio
57	COOH	RT	70	0	**119/120**[b]
					-
58	COOMe	RT	1.5	17	**119/120**
					65/35[c]

[a] Percentage of total GC integral due to the disappearance of the corresponding starting material. [b] After diazomethane workup. [c] Product ratio from chiral HPLC analysis.

3.3.4 Identification of Photoproducts 119 and 120

The structure of cyclobutanol **119** was elucidated by NMR spectroscopy with the aid of IR, MS, and elemental analysis. The IR spectrum shows a broad O-H stretching vibration around 3400 cm⁻¹. Mass spectroscopy and elemental analysis confirmed that the compound is a structural isomer of the starting material. On the basis of the NMR data, the structural assignments for cyclobutanol **119** are shown in Table 3.10.

Table 3.10 Comprehensive NMR assignments for cyclobutanol **119**

119

Carbon #	^{13}C δ (ppm)	^1H δ (ppm) from HMQC	^1H-^1H COSY	HMBC	^1H-^1H NOE
1	41.84	-	-	H_{2a}, H_{2b}, H_4	
2	35.99	H_a 3.10, 1H, d, J = 12.6 Hz H_b 2.31, 1H, d, J = 12.6 Hz	H_{2a}/H_{2b}	-	H_{2a}-H_{11}/H_{15}
3	79.03	-	-	H_{2a}, H_{2b}, H_4	
4	56.93	2.23, 1H, m	H_5	H_{2a}, H_5, H_8	H_{2b}, H_{5b}
5	37.25	1.59 (H_{5b}) and 1.29 (H_{5a}), 2H, m	H_5, H_4, H_6	-	H_{11}/H_{15}
6	38.79	1.93, 1H, m	H_5, H_7	-	
7	28.49	1.54 and 1.20, 2H, m	H_7, H_6, H_8	H_8, H_9	
8	34.52	1.51 and 1.40, 2H, m	H_8, H_7	H_{2b}, H_4, H_9	
9	41.05	1.01 (H_{9a}) and 0.81(H_{9b}), 2H, m	H_9	-	H_{11}/H_{15}
10	129.47	-	-	H_{11}/H_{15}	
11/15	128.52	7.43, 2H, d, J = 8.4 Hz	H_{12}/H_{14}	H_{12}/H_{14}	H_{9b}(0.81ppm) H_{5a}(1.29ppm) H_{2a}(3.10ppm)
12/14	129.69	8.01, 2H, d, J = 8.4 Hz	H_{11}/H_{15}	H_{11}/H_{15}	
13	148.27	-	-	H_{12}/H_{14}	
16	167.11	-	-	H_{12}/H_{14}, H_{17}	
17	52.32	3.88, 3H, s	-	-	
OH	-	2.43, 1H, s, br	-	-	

The presence of a *para* disubstituted aromatic ring was determined from the ^1H-NMR (7.43 ppm, 2H, d, J = 8.4 Hz and 8.01 ppm, 2H, d, J = 8.4 Hz) and COSY spectra. From HMQC, the primary, secondary, tertiary and quaternary carbons, and correlated hydrogens were identified. The chemical shift of quaternary carbon 3 is 79.03 ppm owing to the direct connection with oxygen. The carbon-carbon connections were established from HMBC and COSY. The relative stereochemistry was determined by NOESY (Figure 3.15). The NOESY experiment shows the close proximity between H_4 and H_{2b},

H_4 and H_{5b}, H_{9b} and H_{11}/H_{15}, H_{2a} and H_{11}/H_{15}, H_{5a} and H_{11}/H_{15}. In compound **119**, hydrogens H_{5a} (1.29 ppm) and H_{9b} (0.81 ppm) are shielded by the aromatic ring and H_{2a} (3.10 ppm) is deshielded.
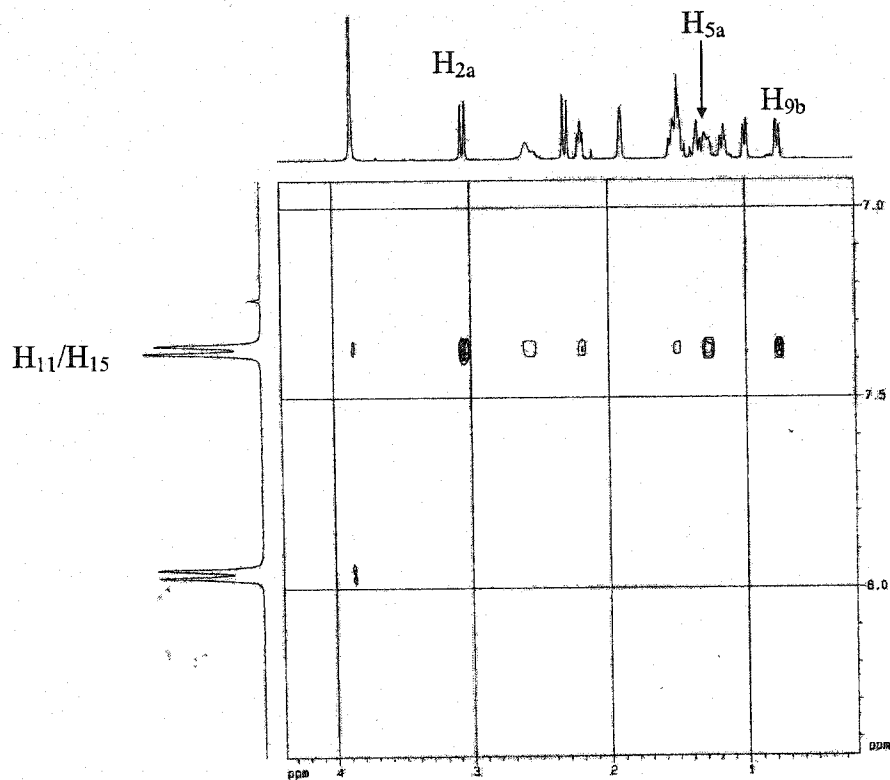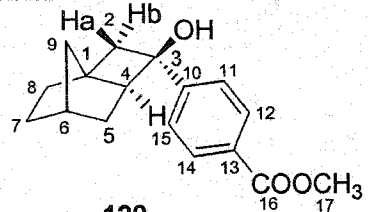
Figure 3.15 Partial NOESY spectrum for cyclobutanol **119**
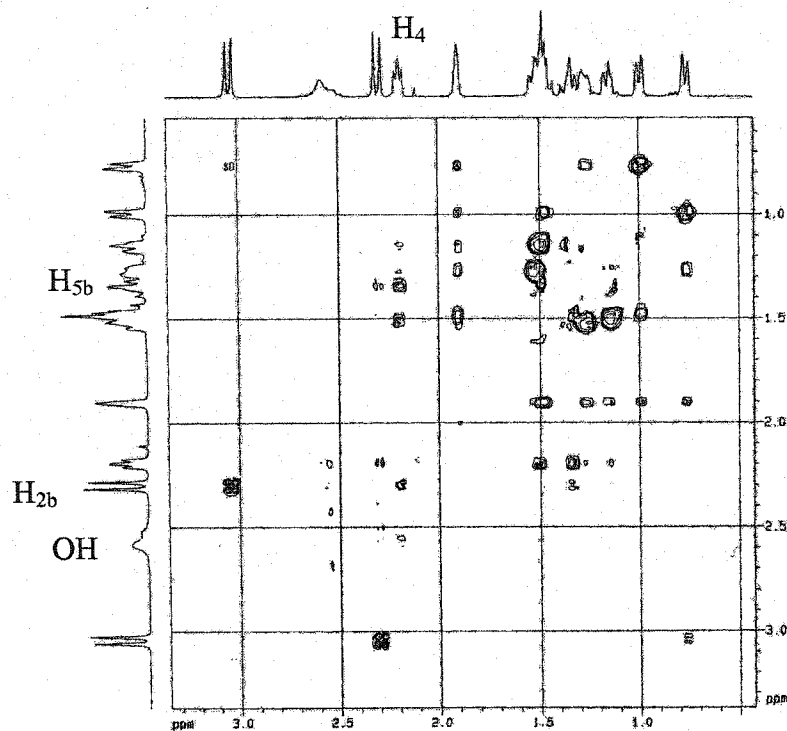
Figure 3.15 Partial NOESY spectrum for cyclobutanol **119** (Continued)

The structure of cyclobutanol **120** was also elucidated mainly by the NMR spectroscopy, with the aid of IR, MS, and elemental analysis. The IR spectrum shows a broad O-H stretching vibration around 3400 cm^{-1}. Mass spectroscopy and elemental analysis confirmed that the compound is a structural isomer of the starting material. On the basis of the NMR data, the structural assignments for cyclobutanol **120** are shown in Table 3.11.

**Table 3.11** Comprehensive NMR assignments for cyclobutanol **120**

120

Carbon #	^{13}C δ (ppm)	^1H δ (ppm) from HMQC	^1H-^1H COSY	HMBC	^1H-^1H NOE
1	45.14	-	-	H_{2a}, H_{2b} H_8, H_9	
2	38.28	H_a 2.36, 1H, d, J = 12.4 Hz H_b 2.51, 1H, d, J = 12.4 Hz	H_{2a}/H_{2b}	-	
3	77.25	-	-	H_{11}/H_{15}, H_{2a}, H_{2b}	
4	50.80	2.11, 1H, m	H_5	H_{2a}, H_5, H_8, H_9	H_{2b}, H_5, H_7, H_8
5	33.61	1.95 and 1.53, 2H, m	H_5, H_4	H_{2a}, H_{2b}, H_7	
6	37.45	2.22 1H, m	H_7	-	
7	28.75	1.67 and 1.22, 2H, m	H_7, H_6, H_8	H_9	
8	33.63	1.50 and 1.27, 2H, m	H_8, H_7	H_7, H_9	
9	42.09	2.00 and 1.36, 2H, m	H_9	H_{2a}, H_{2b}, H_8	
10	128.70	-	-	H_{11}/H_{15}	
11/15	125.13	7.40, 2H, d, J = 8.3 Hz	H_{12}/H_{14}	H_{12}/H_{14}	H_4, H_{2b}
12/14	129.77	7.97, 2H, d, J = 8.3 Hz	H_{11}/H_{15}	H_{11}/H_{15}	
13	153.12	-	-	H_{12}/H_{14}	
16	166.91	-	-	H_{12}/H_{14}, H_{17}	
17	52.04	3.88, 3H, s	-	-	
OH	-	1.87, br, 1H, s	-	-	

The presence of a *para* disubstituted aromatic ring was determined from the ^1H-NMR (7.40 ppm, 2H, d, J = 8.3 Hz and 7.97 ppm, 2H, d, J = 8.3 Hz) and COSY spectra. From HMQC, the primary, secondary, tertiary and quaternary carbons, and correlated hydrogens were identified. The chemical shift of quaternary carbon 3 is 77.25 ppm owing to the direct connection with oxygen. The carbon-carbon connections were established from HMBC and COSY. The relative stereochemistry was determined by NOESY (Figure 3.16). The NOESY experiment shows the close proximity between H_4 and H_{2b}, H_4 and H_{11}/H_{15}, H_{2b} and H_{11}/H_{15}.
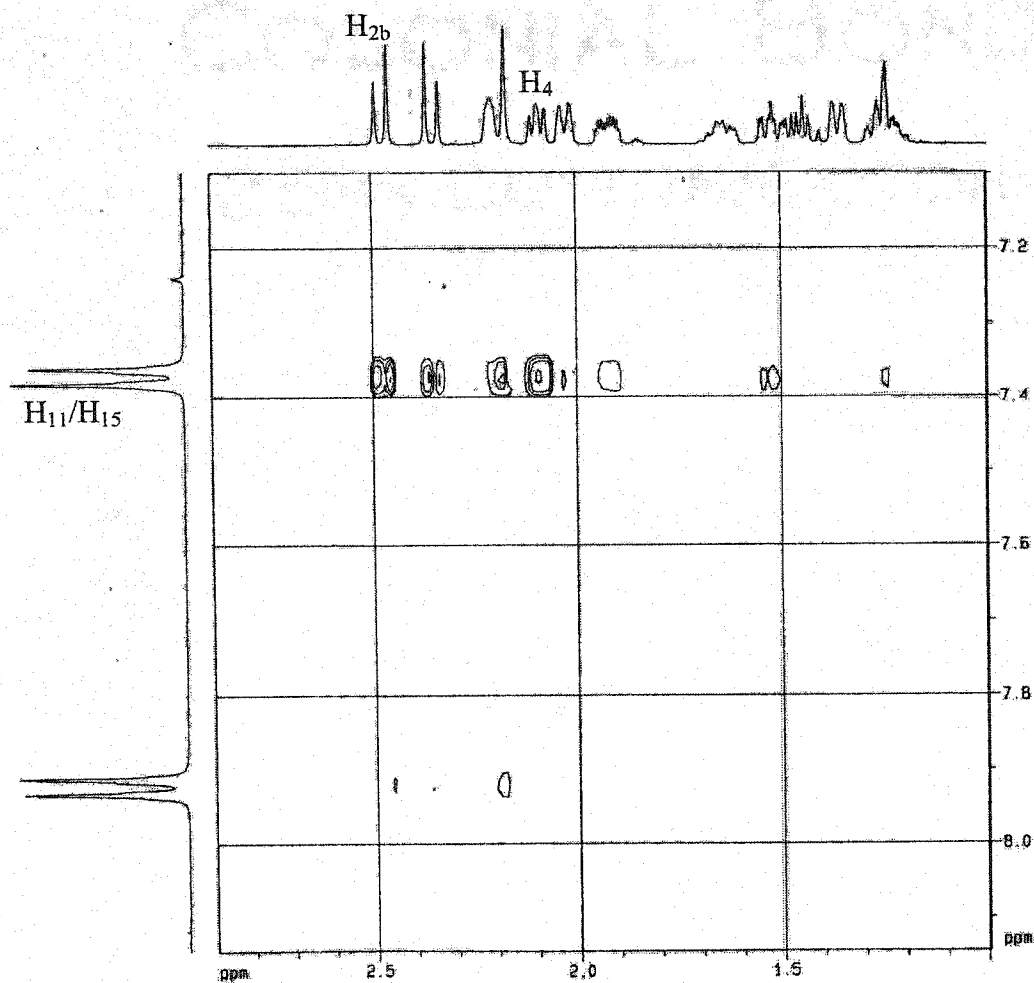
Figure 3.16 Partial NOESY spectrum for cyclobutanol **120**

3.3.5 Photochemical Studies of Ketones 60 and 61

60 X = COOH
61 X = COOMe

121 X = COOH
124 X = COOMe

122 X = COOH
125 X = COOMe

123 X = COOH
126 X = COOMe

(trace)

CH₂N₂
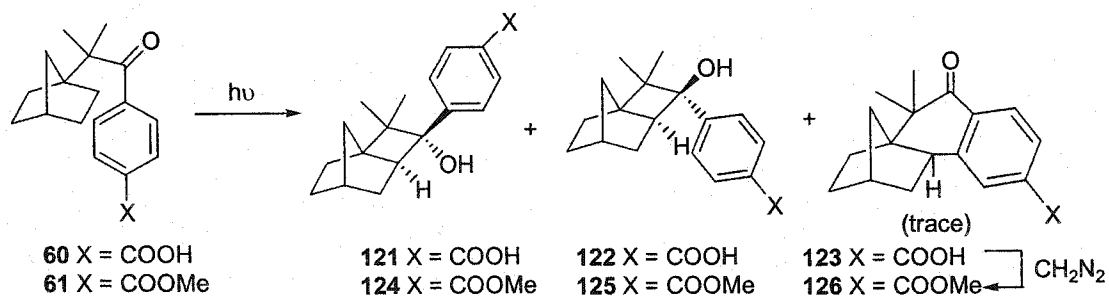
Figure 3.17 Photolysis of ketones **60** and **61** in solution and solid state

The photochemical studies of ketones **60-61** were conducted in both solution and the solid state. Figure 3.17 and Tables 3.12 and 3.13 summarize the photochemical results in both media. All photolyses in solution were performed at room temperature with acetonitrile as the solvent. The conversions and product ratios were analyzed from chiral HPLC because photoproducts **124** and **125** decomposed on the GC column. The percentage of minor ketone **126** was not recorded in the analytical scale photolysis owing to peak overlapping of ketones **61** and **126** on chiral HPLC.

As shown in Tables 3.12 and 3.13, photolysis of ketones **60-61** produced two Yang photocyclization products, **124** and **125** (by treatment with diazomethane in the case of ketone **60**). The *trans* photoproduct **124** is formed in a greater yield in the solid state than in solution. Photoproducts **124** and **125** were isolated by flash chromatography and fully characterized by spectroscopic analysis. The structure of cyclobutanol **125** was confirmed by X-ray crystallography.

Table 3.12 Photolysis of ketones **60-61** in solution (CH$_3$CN)

ketone	X	temp (°C)	time (h)	conv (%)[a]	photoproduct ratio
60	COOH	RT	2	85	**124/125**[b]
					68/32[c]
61	COOMe	RT	2	83	**124/125**
					64/36[c]
61	COOMe	RT	11	100	**124/125/126**
					64/32/4[d]

[a] Percentage of total chiral HPLC integral (response factors were applied) due to the disappearance of the corresponding starting material. [b] After diazomethane workup. [c] Product ratio from chiral HPLC analysis. [d] Product ratio from isolated yields.
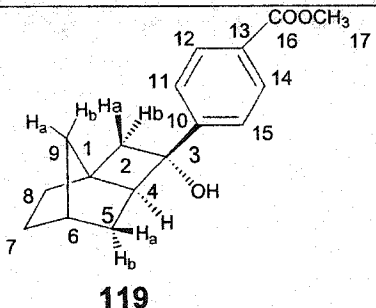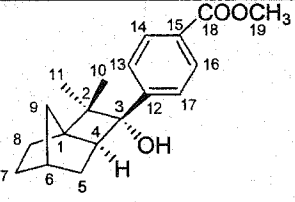
Table 3.13 Photolysis of ketones **60-61** in the solid state

ketone	X	temp (°C)	time (h)	conv (%)[a]	photoproduct ratio
60	COOH	RT	6	96	**124/125**[b]
					94/6[c]
60	COOH	-20	9	95	**124/125**[b]
					98/2[c]
61	COOMe	RT	14	98	**124/125**
					57/43[c,d]
61	COOMe	RT	4	50	**124/125**
					84/16[c]
61	COOMe	-10	13	20	**124/125**
					90/10[c]

[a] Percentage of total chiral HPLC integral (calibrated with response factors) due to the disappearance of the corresponding starting material. [b] After diazomethane workup. [c] Product ratio from chiral HPLC analysis. [d] Crystal melting observed.

## 3.3.6 Identification of Photoproducts 124 and 125

The structure of photoproduct **124** was elucidated by NMR spectroscopy with the aid of IR, MS, and elemental analysis. The IR spectrum showed a broad O-H stretching vibration around 3400 cm^{-1}. Mass spectroscopy and elemental analysis confirmed that the compound was a structural isomer of the starting material. Based on the NMR data, the structural assignments for cyclobutanol **124** are outlined in Table 3.14.

**Table 3.14** Comprehensive NMR assignments for cyclobutanol **124**

124

Carbon #	^{13}C δ (ppm)	^1H δ (ppm) from HMQC	^1H-^1H COSY	HMBC	^1H-^1H NOE
1	44.96	-	-	H_{10}, H_{11}	
2	52.19	-	-	H_4, H_{10}, H_{11}, H_8, H_9	
3	82.20	-	-	H_{13}/H_{17}, H_{11}, H_{10}, H_4	
4	54.65	2.26, 1H, m	H_5	H_5, H_8, H_9	H_{11}, H_8
5	37.01	2.07 and 1.68, 2H, m	H_5, H_4, H_6	H_7, H_9	
6	38.25	2.10, 1H, m	H_5, H_7	H_7, H_9	
7	28.39	1.58 and 1.21, 2H, m	H_7, H_6, H_8	H_6, H_5, H_8, H_9	
8	29.03	1.40, 2H, m	H_8, H_7	H_4, H_9	
9	39.82	1.10, 2H, m	H_9	H_4, H_5, H_8, H_7	
10	25.46	1.19, 3H, s	-	H_{11}	
11	23.48	1.33, 3H, s	-	H_{10}	
12	128.76	-	-	H_{13}/H_{17}	
13/17	129.16	7.58 2H, d, $J = 8.5$ Hz	H_{14}/H_{16}	H_{14}/H_{16}	H_{10}, H_5, H_9
14/16	129.27	7.95 2H, d, $J = 8.5$ Hz	H_{13}/H_{17}	H_{13}/H_{17}	
15	150.10	-	-	H_{14}/H_{16}	
18	166.92	-	-	H_{14}/H_{16}, H_{19}	
19	52.27	3.88, 3H, s	-	-	
OH	-	2.31, 1H, s, br	-	-	H_{11}
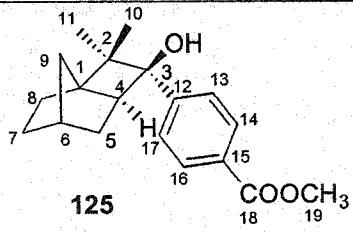
The presence of a *para* disubstituted aromatic ring was elucidated from the ^1H-NMR (7.58 ppm, 2H, d, $J = 8.5$ Hz and 7.95 ppm, 2H, d, $J = 8.5$Hz) and COSY spectra. From HMQC, it was easy to identify the primary, secondary, tertiary and quaternary carbons and their correlated hydrogens. Quaternary carbon 3 is distinguished an absorption at 82.20 ppm owing to the direct connection with oxygen. The carbon-carbon connections were deduced from HMBC and COSY. The relative stereochemistry was established by NOESY (Figure 3.18). Notable NOE interactions were found between H_4 and H_{11}, OH and H_{11}, H_{13}/H_{17} and H_{10}.
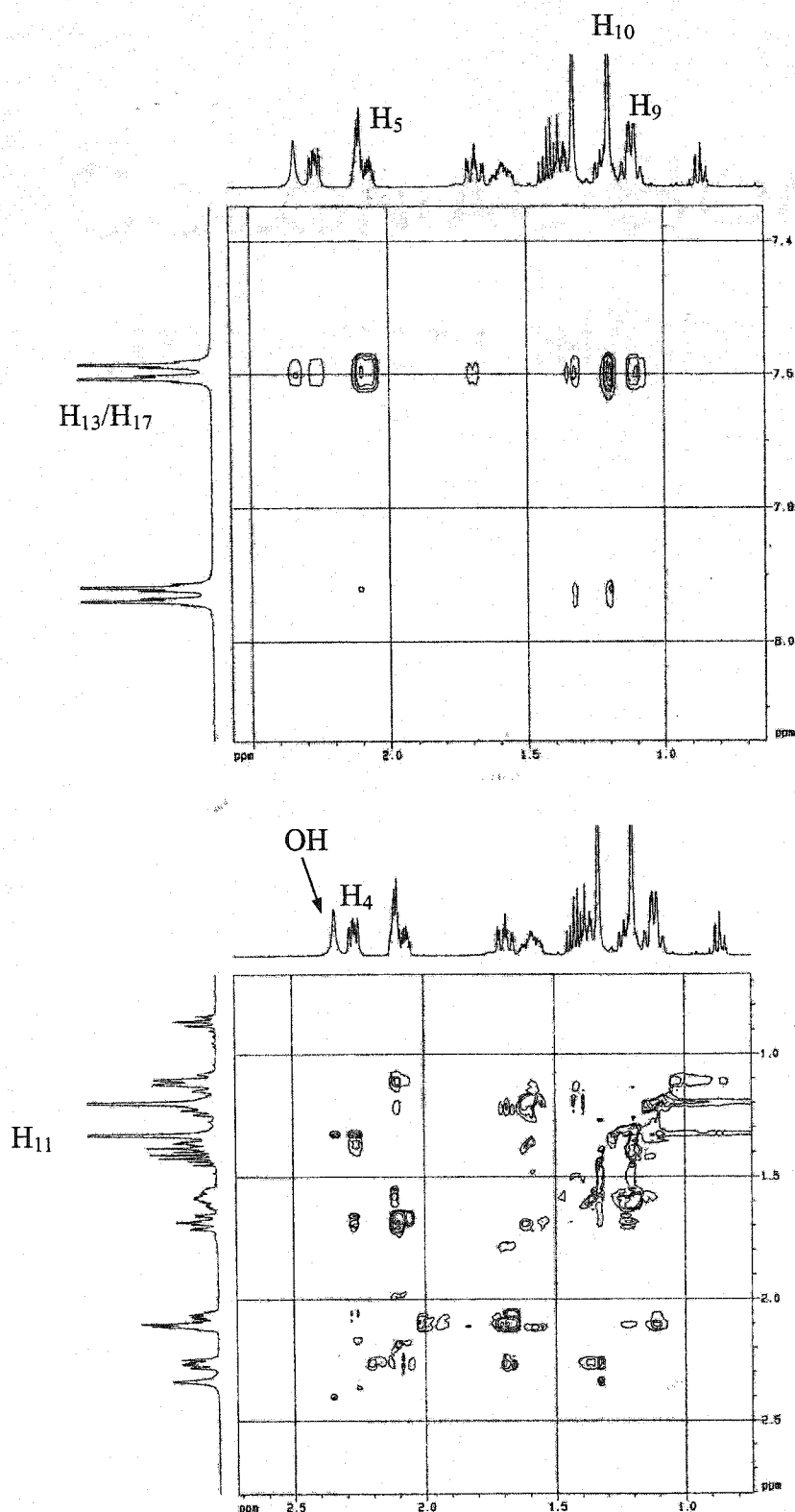
Figure 3.18 Partial NOESY spectrum for cyclobutanol **124**

Similarly, the structure of compound **125** was established by NMR spectroscopy with the aid of IR, MS, and elemental analysis. The IR spectrum of cyclobutanol **125** also

showed a broad O-H stretching vibration around 3400 cm^{-1}. Mass spectroscopy and elemental analysis were used to determine that the compound was a structural isomer of the starting material. From the NMR data, the structural assignments of compound **125** are given in Table 3.15.

Table 3.15 Comprehensive NMR assignments for cyclobutanol **125**

Carbon #	^{13}C δ (ppm)	^1H δ (ppm) from HMQC	^1H-^1H COSY	HMBC	^1H-^1H NOE
1	43.37	-	-	H_{10}, H_{11}	
2	54.34	-	-	H_4, H_8, H_{10}, H_{11}	
3	81.37	-	-	H_{13}/H_{17}, H_{10}, H_{11}, OH	
4	43.08	2.45, 1H, m	H_5	OH, H_8	H_{13}/H_{17}, H_{11}, H_5, H_8
5	32.64	1.77 and 1.56, 2H, m	H_5, H_4, H_6	H_9	
6	37.99	2.22, 1H, m	H_5, H_7, H_9	-	
7	28.54	1.63 and 1.31, 2H, m	H_7, H_6, H_8	H_8	
8	29.76	1.34 and 1.21, 2H, m	H_8, H_7	H_4	
9	39.31	2.03 and 1.30, 2H, m	H_6, H_9	H_4, H_5, H_8, H_7	
10	24.29	1.22, 3H, s	-	H_{11}	
11	20.02	0.74, 3H, s	-	H_{10}	
12	129.17	-	-	H_{13}/H_{17}	
13/17	126.87	7.35, 2H, d, J = 8.5 Hz	H_{14}/H_{16}	H_{14}/H_{16}	H_4, H_{11}
14/16	129.68	7.97, 2H, d, J = 8.5 Hz	H_{13}/H_{17}	H_{13}/H_{17}	
15	150.67	-	-	H_{14}/H_{16}	
18	166.98	-	-	H_{14}/H_{16}, H_{19}	
19	52.26	3.89, 3H, s	-	-	
OH	-	1.68, 1H, s, br	-	-	

The presence of a *para* disubstituted aromatic ring was elucidated from the ^1H-NMR (7.35 ppm, 2H, d, J = 8.5 Hz and 7.97 ppm, 2H, d, J = 8.5Hz) and COSY spectra. From HMQC, it was easy to identify the primary, secondary, tertiary and quaternary carbons and their correlated hydrogens. The chemical shift of quaternary carbon 3 is 81.37 ppm. The carbon-carbon connections were established by HMBC and COSY. The relative stereochemistry was determined by NOESY (Figure 3.20). The NOESY experiment shows the close proximity between H_4 and H_{11}, H_4 and H_{13}/H_{17}, H_{13}/H_{17} and H_{11}. The chemical shift of H_{11} is 0.74 ppm owing to the shielding effect of the aromatic ring. This

shielding effect is supported by the X-ray structure in which the aromatic ring is oriented to H_{11}. Compared to photoproduct **124**, H_4 in compound **125** is slightly deshielded by the aromatic ring (H_4 in compound **125**: 2.45 ppm; H_4 in compound **124**: 2.26 ppm). The structure of cyclobutanol **125** was confirmed by X-ray crystallography (Figure 3.19).
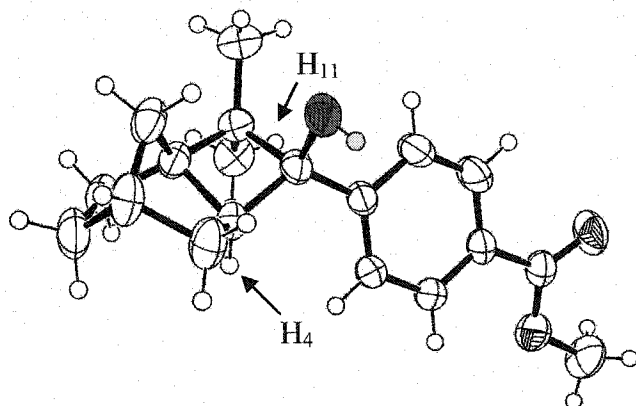
Figure 3.19 ORTEP representation of photoproduct **125**. In the hydroxyl group, the oxygen atom is colored red, the hydrogen atom green.
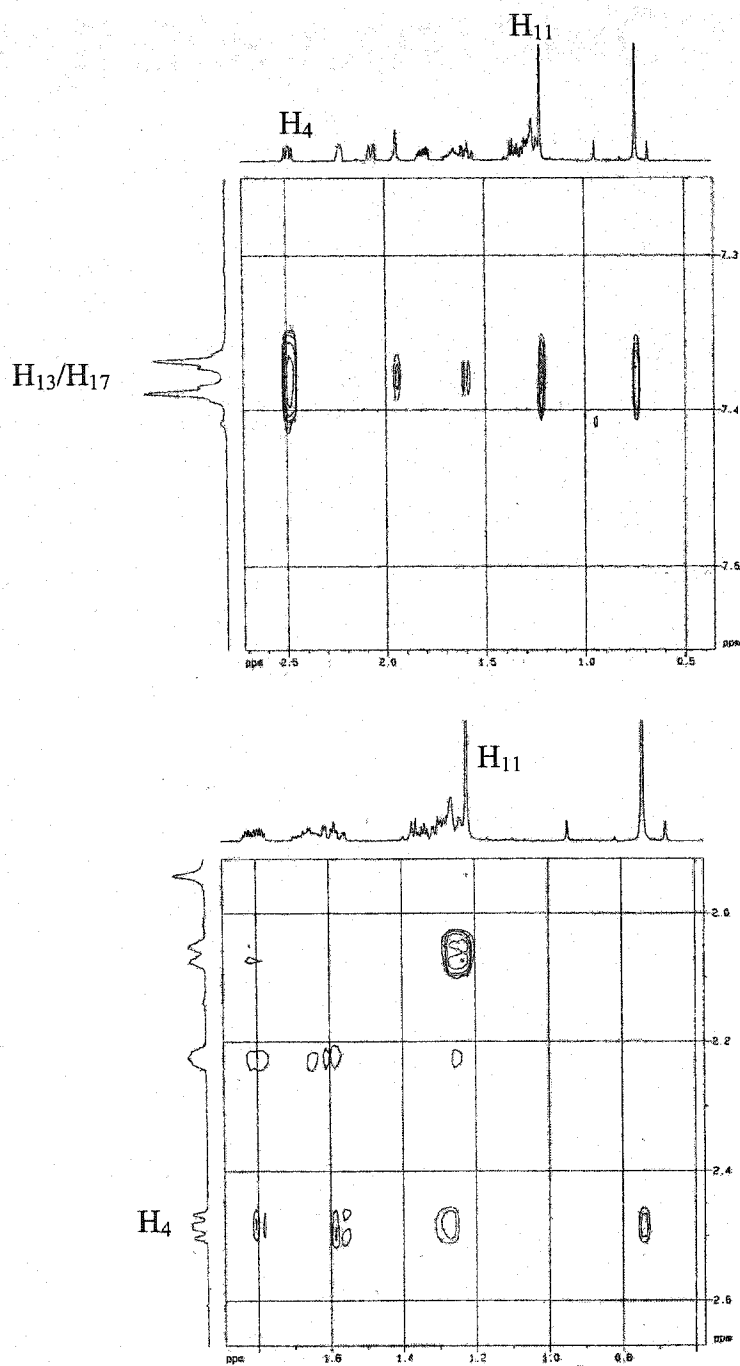
Figure 3.20 Partial NOESY spectrum for cyclobutanol **125**

The structure of photoproduct **126** was elucidated by NMR spectroscopy with the help of IR, MS, and elemental analysis. The IR spectrum shows an absorption at 1730 (ester) and 1681 (ketone) cm^{-1}. The presence of ester and ketone carbonyl carbons was

confirmed by ^{13}C-NMR, with peaks at 166.54 and 203.38 ppm respectively. Mass spectroscopy showed that the compound **126** has a mass of 298, two atomic units less than that of starting ketone **61** (the mass of ketone **61**: 300). Based on the NMR data, the structural assignments for compound **126** are given in Table 3.16.

Table 3.16 Comprehensive NMR assignments for ketone **126**

126

Carbon #	^{13}C δ (ppm)	^{1}H δ (ppm) from HMQC	^{1}H-^{1}H COSY	HMBC	^{1}H-^{1}H NOE
1	45.58	-	-	H_{13}, H_{12}	
2	54.11	-	-	H_{13}, H_{12}	
3	203.38	-	-	H_{13}, H_{12}, H_{14}	
4	132.90	-	-	H_{15}, H_{17}	
5	134.44	-	-	H_{14}	
6	42.60	3.09, 1H, m	H_7	H_{17}, H_{11}, H_7	H_{13}, H_{10}, H_7
7	41.70	2.26 and 1.64, 2H, m	H_7, H_6, H_8	H_9	
8	37.70	2.30, 1H, m	H_9, H_{11}, H_7	H_7, H_{10}	
9	29.75	1.77 and 1.70, 2H, m	H_9, H_{10}, H_8	H_{10}, H_{11}	
10	29.85	1.45, 2H, m	H_{10}, H_9	H_9, H_{11}	
11	37.38	1.28 and 1.04, 2H, m	H_{11}, H_8	H_{10}, H_8, H_7	
12	18.69	1.26, 3H, s	-	H_{13}	
13	23.33	1.10, 3H, s	-	H_{12}	H_6
14	126.64	7.92, 1H, d, J = 8.1Hz	H_{15}	-	
15	127.21	7.85, 1H, m	H_{14}, H_{17}	H_{17}	
16	148.34	-	-	H_{14}	
17	130.11	7.84, 1H, m	H_{15}	H_{15}	
18	166.53	-	-	H_{15}/H_{17}, H_{19}	
19	52.36	3.90, 3H, s	-	-	

^{1}H-NMR shows that ketone **126** no longer has a *para* disubstituted aromatic structure (the two doublet feature is lacking). From HMQC, the primary, secondary, tertiary and quaternary carbons and their correlated hydrogens were identified. The carbon-carbon connections were obtained from HMBC and COSY. The relative stereochemistry was established from 1D selective NOE (Figure 3.21). The NOE provided information on the close proximity between H_6 and H_{13}.
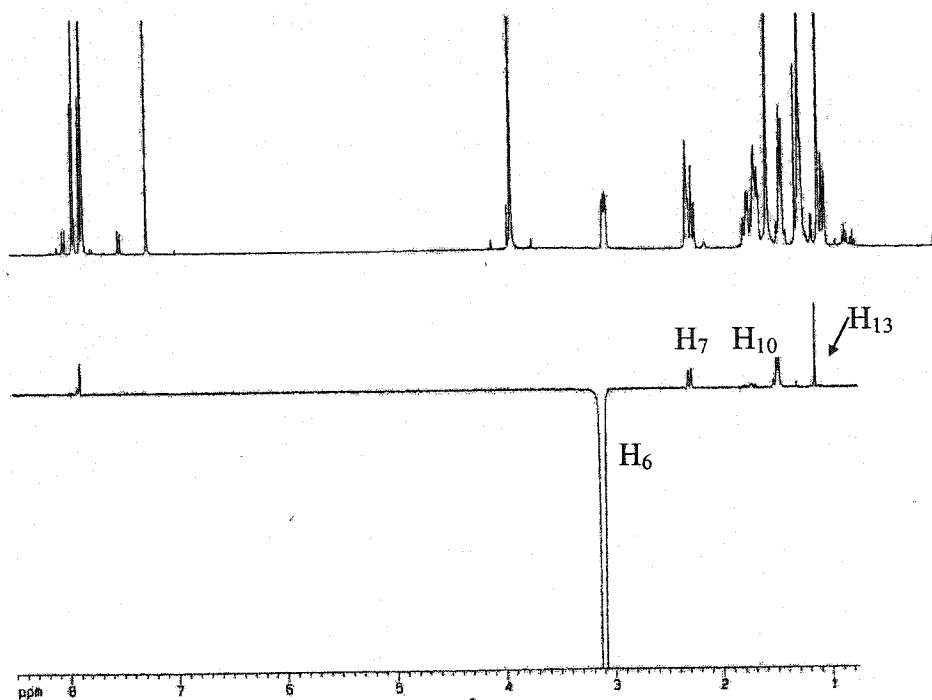
Figure 3.21 NOE spectrum for cyclobutanol **126** with irradiation at 3.09 ppm (H_6)

3.4 Asymmetric Induction Studies

3.4.1 Asymmetric Induction in the Solid State Photolysis of Bicyclo[2.2.2]octyl Ketones

3.4.1.1 Determination of the Enantioselectivity

The large scale solution phase photolysis of ketone **55** provided racemic photoproducts **115** and **116** used for testing the chiral HPLC resolution conditions. Manually premixed compounds **55**, **115** and **116** were injected onto a Chiralcel® OD® column to find 5 peaks as shown in Figure 3.22. The detailed chiral HPLC conditions are outlined in Table 3.17. The less polar ketone **55** was eluted from the chiral column at 8 minutes. The two enantiomers of cyclobutanol **116** were eluted at 25.1 minutes (peak A) and 33.2 minutes (peak B). The retention times of the two enantiomers of cyclobutanol **115** were 46.0 minutes (peak C) and 60.1 minutes (peak D).

55

116

115

116: A, B
115: C, D
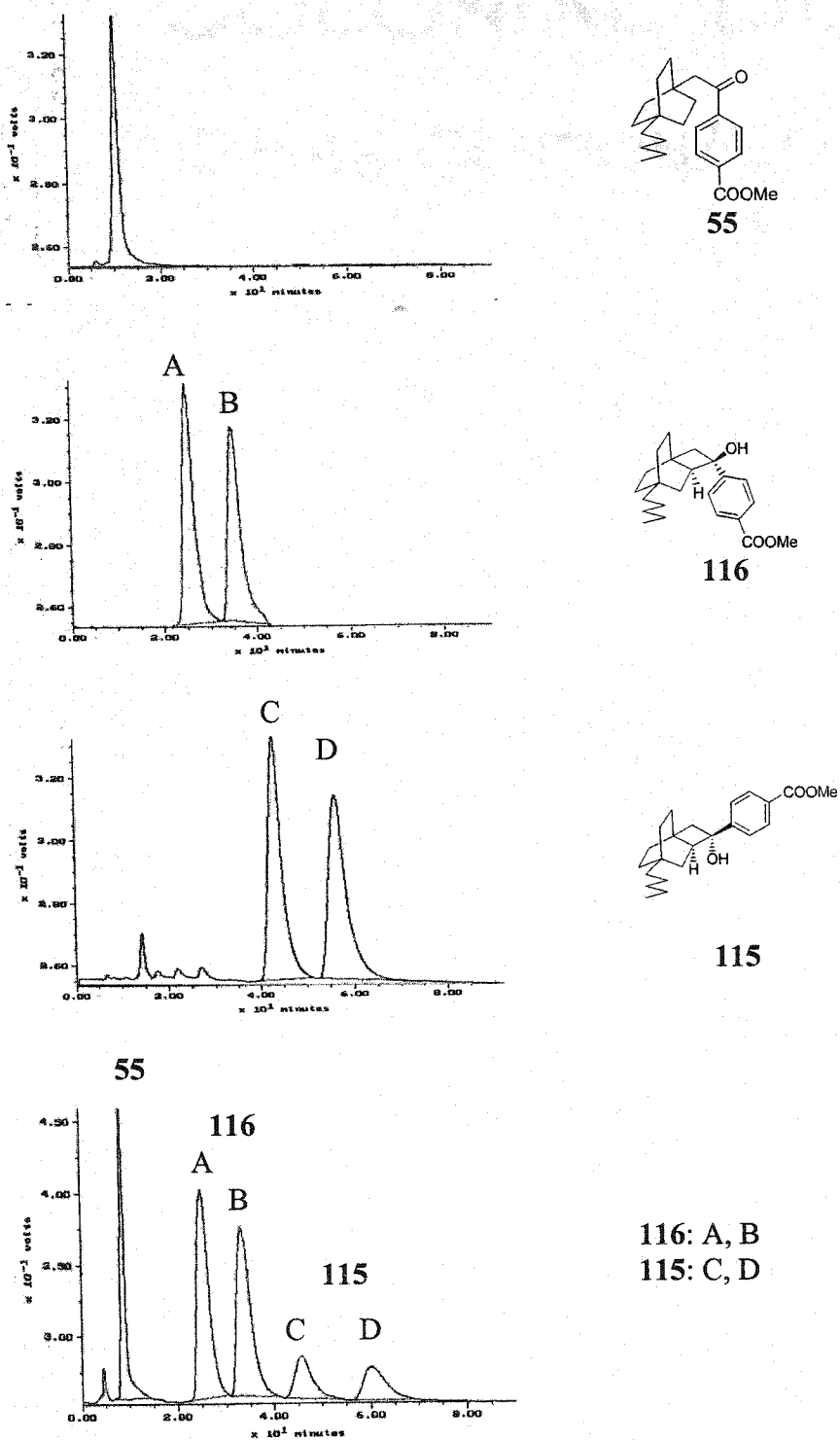
Figure 3.22 HPLC traces for the resolution of racemic cyclobutanols **115** and **116** on a Chiralcel OD column (eluting solvents, hexanes/isopropanol 99/1; flow rate, 1.0 mL/min)

Table 3.17 Chromatographic data for enantiomeric excess determination of cyclobutanols **115** and **116**.

Column	HPLC conditions			Retention Time (min)[a]
	UV detector (nm)	Solvents	Flow rate (mL/min)	
OD[b]	254	99/1 hexanes/IPA	1.0	**116:** A: 25.1 B: 33.2 **115:** C: 46.0 D: 60.1

[a] A refers to the first eluted peak, B to the second, C to the third and D to the fourth. [b] Chiralcel® OD® (25 cm × 0.46 cm ID), Chiral Technologies Inc.

3.4.1.2 Asymmetric Induction Results

Crystalline salts **56a-m** were photolyzed on an analytical scale (2-5 mg). The time of photolysis for each solid state reaction was controlled to different lengths so that the enantiomeric excess could be determined at a variety of conversions. Some salts were photolyzed at low temperature (-25°C). Following photolysis the salts were treated with ethereal diazomethane, which converted the carboxylate anions into methyl esters. The percentage conversion was determined by GC analysis. The de and ee were measured by chiral HPLC using a Chiralcel® OD® column as described above.

Asymmetric induction results for all 13 salts are shown in Table 3.18. Salts **56a-b** were found to be photochemically stable. Again, a number of salts lead to low ee's while others lead to near-quantitative ee's; this is a typical result in the solid state asymmetric induction studies. For salt **56c**, near quantitative ee's for both photoproducts were obtained at near quantitative conversions. These results will be discussed in section 3.5.

Table 3.18 Asymmetric induction in the photolysis of chiral salts **56a-m**

salt	amine	conv (%)[a]	temp	de[b] (%)	ee[b] for 116 (%)	ee[b] for 115 (%)
56a	R-(-)-1-cyclohexylethylamine	0	RT	-	-	-
56b	Prolinamide	0	RT	-	-	-
56c	(1S, 2R)-(+)-norephedrine	77	-25	+58	+95	-99
56c	(1S, 2R)-(+)-norephedrine	55	RT	+80	+96	-99
56c	(1S, 2R)-(+)-norephedrine	80	RT	+76	+93	-95
56c	(1S, 2R)-(+)-norephedrine	95	RT	+79	+88	-95
56d	(1R, 2R)-(-)-pseudoephedrine	70	-25	+16	-78	+98
56d	(1R, 2R)-(-)-pseudoephedrine	15	RT	+57	-84	+91
56d	(1R, 2R)-(-)-pseudoephedrine	98	RT	+48	-49	+56
56e	R-(-)-1-aminoindane	42	-25	+31	+90	-96
56e	R-(-)-1-aminoindane	35	RT	+28	+76	-94
56e	R-(-)-1-aminoindane	80	RT	+33	+54	-75
56f	S-(+)-1-aminoindane	70	-25	+21	-77	+93
56f	S-(+)-1-aminoindane	83	-25	+24	-78	+89
56f	S-(+)-1-aminoindane	30	RT	+23	-88	+93
56f	S-(+)-1-aminoindane	56	RT	+33	-64	+90
56f	S-(+)-1-aminoindane	85	RT	+32	-52	+74
56f	S-(+)-1-aminoindane	96	RT	+30	-45	+65
56g	(1S, 2R)-(-)-cis-1-amino-2-indanol	40	RT	+34	+82	-95
56g	(1S, 2R)-(-)-cis-1-amino-2-indanol	87	RT	+38	+65	-77
56h	S-(-)-tolylethylamine	50	-25	+76	+58	-26
56h	S-(-)-tolylethylamine	5	RT	+88	+72	-62
56h	S-(-)-tolylethylamine	95	RT	+81	+28	-13
56i	(1R, 2R)-(-)-2-amino-1-phenyl-1,3-propanediol	50	-25	+80	+49	-50
56i	(1R, 2R)-(-)-2-amino-1-phenyl-1,3-propanediol	30	RT	+69	+44	-49
56i	(1R, 2R)-(-)-2-amino-1-phenyl-1,3-propanediol	66	RT	+63	+38	-38
56j	S-(+)-2-(methoxymethyl)pyrrolidine	8	-25	+64	-56	+94
56j	S-(+)-2-(methoxymethyl)pyrrolidine	5	RT	+81	-77	+72
56j	S-(+)-2-(methoxymethyl)pyrrolidine	16	RT	+75	-71	+36
56j	S-(+)-2-(methoxymethyl)pyrrolidine	30[c]	RT	+75	-55	+30
56j	S-(+)-2-(methoxymethyl)pyrrolidine	60[c]	RT	+76	-42	+28
56k	R-(+)-1-phenylethylamine	60	RT	+69	+4	-29
56k	R-(+)-1-phenylethylamine	87	RT	+55	+8	-24
56l	S-(-)-1-phenylethylamine	36	RT	+66	-4	+27
56l	S-(-)-1-phenylethylamine	62	RT	+57	-9	+18
56m	(-)-cis-myrtanylamine	46	RT	+15	+19	-11
56m	(-)-cis-myrtanylamine	93	RT	+12	+7	-3

[a] Percentage of total GC integral due to the disappearance of the corresponding starting material.
[b] Diastereomeric excess (de) and enantiomeric excess (ee) values were measured on a Chiralcel OD column. The de values were calculated with the equation: de (%) = **116** (%) – **115** (%). Sign of rotation was obtained at the sodium D-line (589 nm). [c] Crystal melting observed.

3.4.2 Asymmetric Induction in the Solid State Photolysis of Bicyclo[2.2.1]heptyl Ketones

3.4.2.1 Determination of the Enantioselectivity

The large scale solution phase photolysis of ketone **58** provided racemic cyclobutanols **119** and **120** used for testing the chiral HPLC resolution conditions. The mixture of compounds **58**, **119** and **120** was separated into 5 peaks by a Chiralpak® AD® HPLC column as shown in Table 3.19 and Figure 3.23. Ketone **58** was eluted from the chiral HPLC at *ca.* 16 minutes. Cyclobutanol **120** was eluted at 52.6 minutes (peak A) and 72.2 minutes (peak C). The retention times of the two enantiomers of cyclobutanol **119** were 66.0 minutes (peak B) and 79.6 minutes (peak D).

Figure 3.23 HPLC traces for the resolution of racemic cyclobutanols **119** and **120** on a Chiralpak AD column (eluting solvents, hexanes/IPA 98/2; flow rate, 0.60 mL/min)

Table 3.19 Chromatographic data for enantiomeric excess determination of cyclobutanols **119** and **120**.

Column	HPLC conditions			Retention Time (min)[a]
	UV detector (nm)	Solvents	Flow rate (mL/min)	
AD[b]	254	98/2 hexanes/IPA	0.60	**120:** A: 52.6 C: 72.2 **119:** B: 66.0 D: 79.6

[a] A refers to the first eluted peak, B to the second, C to the third and D to the fourth. [b] Chiralpak® AD® (25 cm × 0.46 cm ID), Chiral Technologies Inc.

3.4.2.2 Asymmetric Induction Results

Salts **59a-m** were photolyzed in the solid state on an analytical scale (2-5 mg). The time of photolysis for each solid state reaction was controlled to different lengths so that the enantiomeric excess could be determined at a variety of conversions. Some salts were photolyzed at low temperature (-25°C). Following photolysis the salts were treated with diazomethane, converting the carboxylate anions into methyl esters. The percent conversion was determined by GC analysis. The de and ee were measured by chiral HPLC using a Chiralpak® AD® column as described above.

Asymmetric induction results for all 13 salts are outlined in Table 3.20. Salt **59a** proved to be photochemically inert after 33 hours of solid state photolysis at room temperature. However, the photolysis of salt **59a** in acetonitrile afforded racemic photoproducts **119** and **120** (**119/120** = 53/47) with a conversion of 71% in 4 hours. Two of the 13 salts (**59b,c**) showed near-quantitative de's. All 13 salts gave modest to low ee's (< 80 %). These results will be discussed in the section 3.5.

Table 3.20 Asymmetric induction in the photolysis of chiral salts **59a-m**

salt	amine	conv (%)[a]	temp	de[b]	ee[b] for 120 (%)	ee[b] for 119 (%)
59a	L-prolinamide	0	RT	-	-	-
59b	(1S, 2R)-(-)-cis-1-amino-2-indanol	43	RT	-95	-35	+39
59b	(1S, 2R)-(-)-cis-1-amino-2-indanol	84	RT	-95	-27	+39
59b	(1S, 2R)-(-)-cis-1-amino-2-indanol	94	RT	-94	-23	+33
59c	S-(-)-p-tolylethylamine	18	-25	-98	+51	-42
59c	S-(-)-p-tolylethylamine	94	-25	-92	-15	-13
59c	S-(-)-p-tolylethylamine	40	RT	-88	-64	-2
59c	S-(-)-p-tolylethylamine	93	RT	-82	-68	+17
59c	S-(-)-p-tolylethylamine	97	RT	-82	-73	+21
59d	R-(-)-1-cyclohexylethylamine	80	-25	-39	-37	+38
59d	R-(-)-1-cyclohexylethylamine	94	RT	-39	-30	+36
59e	(1S, 2R)-(+)-norephedrine	30	-25	0	-76	+62
59e	(1S, 2R)-(+)-norephedrine	54	RT	-23	-65	+63
59e	(1S, 2R)-(+)-norephedrine	78	RT	-39	-55	+45
59e	(1S, 2R)-(+)-norephedrine	82	RT	-42	-40	+39
59e	(1S, 2R)-(+)-norephedrine	96	RT	-59	-31	+36
59f	R-(+)-1-phenylethylamine	14	RT	-45	+11	-42
59f	R-(+)-1-phenylethylamine	18	RT	-50	+21	-45
59f	R-(+)-1-phenylethylamine	80	RT	-76	+24	-51
59f	R-(+)-1-phenylethylamine	94	RT	-76	+19	-50
59g	S-(+)-1-phenylethylamine	43	RT	-66	-5	+44
59g	S-(+)-1-phenylethylamine	78	RT	-76	-11	+42
59g	S-(+)-1-phenylethylamine	83	RT	-79	-10	+41
59g	S-(+)-1-phenylethylamine	92	RT	-76	-8	+43
59h	(1R, 2R)-(-)-2-amino-1-phenyl-1,3-propanediol	48	-25	-56	-53	+22
59h	(1R, 2R)-(-)-2-amino-1-phenyl-1,3-propanediol	63	RT	-60	-33	+22
59h	(1R, 2R)-(-)-2-amino-1-phenyl-1,3-propanediol	64	RT	-63	-30	+23
59h	(1R, 2R)-(-)-2-amino-1-phenyl-1,3-propanediol	81	RT	-62	-31	+28
59i	(-)-cis-myrtanylamine	8	-25	+50	+24	+19
59i	(-)-cis-myrtanylamine	28	RT	+37	+27	+23
59i	(-)-cis-myrtanylamine	91	RT	-12	+22	+1
59j	S-(+)-2-(methoxymethyl)pyrrolidine	7	-25	-22	+33	-19
59j	S-(+)-2-(methoxymethyl)pyrrolidine	23	RT	-43	+19	-15
59j	S-(+)-2-(methoxymethyl)pyrrolidine	61	RT	-46	+10	-6
59k	R-(+)-bornylamine	67	-25	-60	-3	+4
59k	R-(+)-bornylamine	45	RT	-60	-14	+5
59k	R-(+)-bornylamine	73	RT	-61	-3	+3
59k	R-(+)-bornylamine	91	RT	-64	-1	-1
59k	R-(+)-bornylamine	94	RT	-65	0	+2
59l	S-(+)-1-aminoindane	8	-25	-26	-5	+12
59m	(1R, 2R)-(-)-pseudoephedrine	68	RT	-11	+23	+6

[a] Percentage of total GC integral due to the disappearance of the corresponding starting material.
[b] Diastereomeric excess (de) and enantiomeric excess (ee) values were measured on a Chiralpak AD column. The de values were calculated with the equation: de (%) = **120** (%) – **119** (%). Sign of rotation was obtained at the sodium D-line (589 nm).

3.4.3 Asymmetric Induction in the Solid State Photolysis of Dimethylated Bicyclo[2.2.1]heptyl Ketones

3.4.3.1 Determination of the Enantioselectivity

The large scale solution phase photolysis of ketone **61** produced cyclobutanols **124** and **125** used for testing the chiral HPLC resolution conditions. Fortunately, cyclobutanols **124** and **125** could be resolved with good baseline separation on a Chiralpak® AD® column giving a total 5 peaks including the achiral starting material, ketone **61**. The detailed chiral HPLC separation is outlined in Table 3.21 and Figure 3.24.
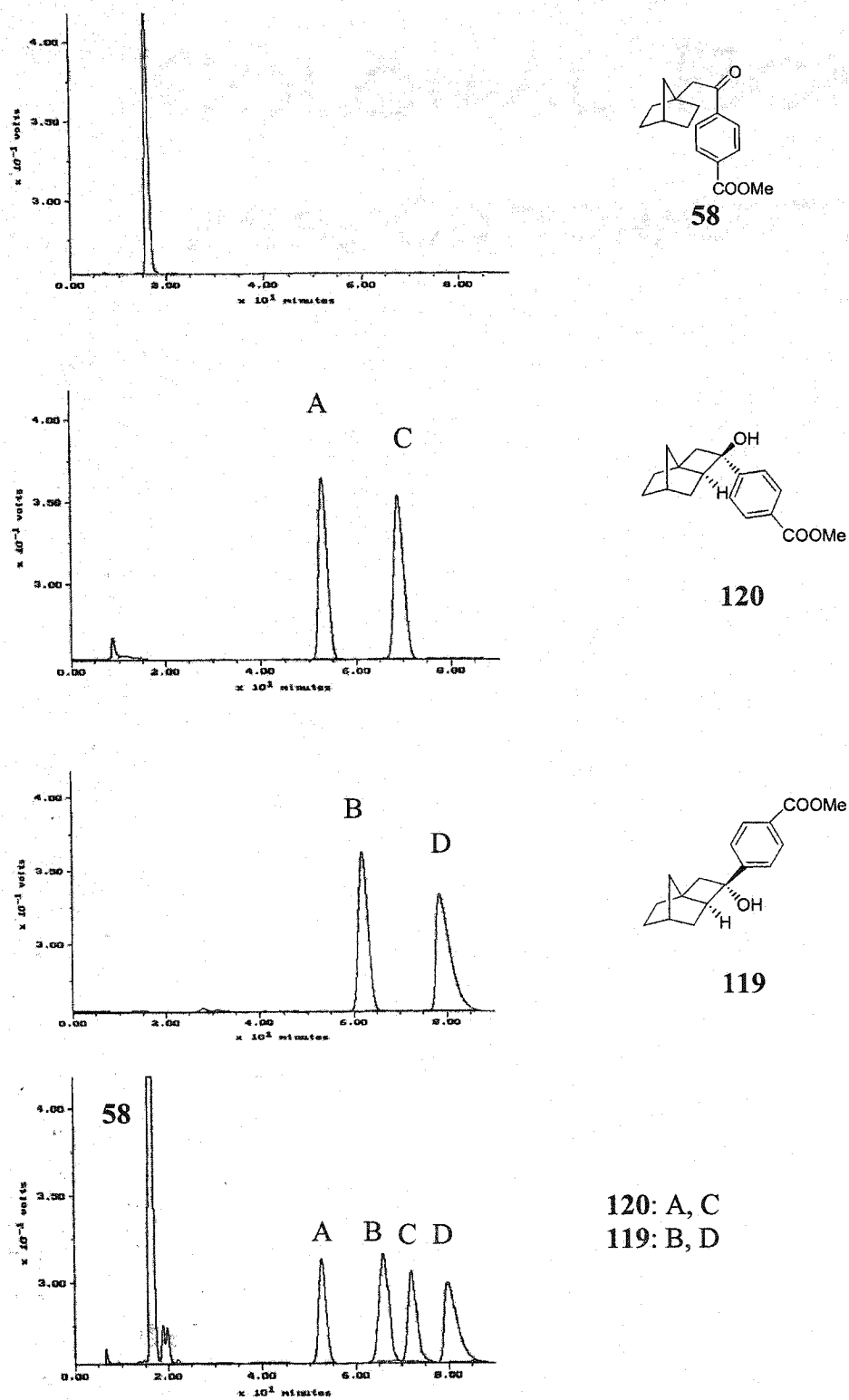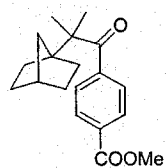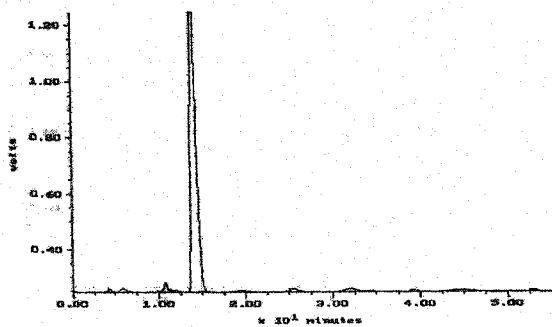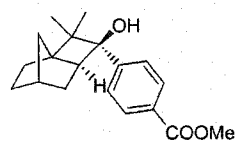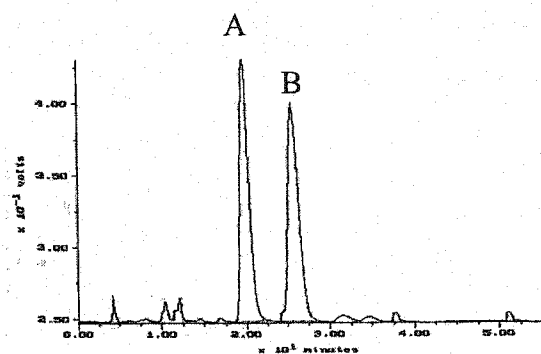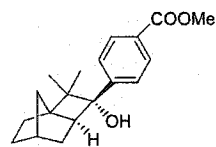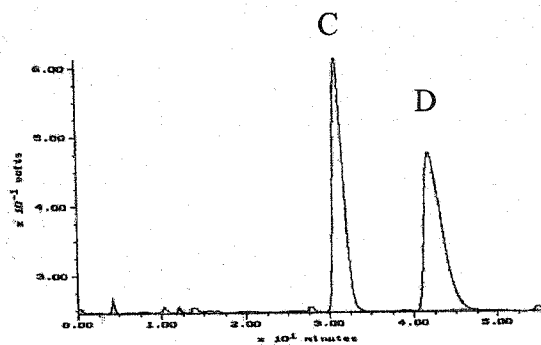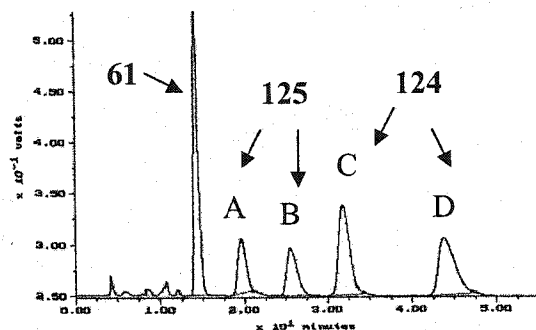
Figure 3.24 HPLC traces for the resolution of racemic cyclobutanols **124** and **125** on a Chiralpak AD column (eluting solvents, hexanes/ethanol 98/2; flow rate, 1.0 mL/min)

Table 3.21 Chromatographic data for enantiomeric excess determination of cyclobutanols **125** and **124**.

Column	HPLC conditions			Retention
	UV detector (nm)	Solvents	Flow rate (mL/min)	Time (min)[a]
AD[b]	254	98/2 hexanes/EtOH	1.0	**125:** A: 19.7 B: 25.6 **124:** C: 30.9 D: 43.0

[a] A refers to the first eluted peak, B to the second, C to the third and D to the fourth. [b] Chiralpak® AD® (25 cm × 0.46 cm ID), Chiral Technologies Inc.

3.4.3.2 Asymmetric Induction Results

Salts **62a-h** were photolyzed in the solid state on an analytical scale (2-5 mg). The time of photolysis for each solid state reaction was controlled to different lengths so that the enantiomeric excess could be determined at a variety of conversions. Each salt was also photolyzed at low temperature (-20 °C). After photolysis the salts were treated with ethereal diazomethane, converting the carboxylate anions into methyl esters, and filtered through a short plug of silica gel to remove the chiral auxiliary. The percent conversion as well as the product composition was determined by chiral HPLC due to the decomposition of the photoproducts on the GC column. Preweighed equal amounts of cyclobutanol **124** and starting material ketone **61** were injected onto the chiral HPLC column to find that their response factors are equal with the UV detector at 254 nm. The de and ee were obtained by HPLC using a Chiralpak® AD® column as described above.

Asymmetric induction results for all 8 salts are outlined in Table 3.22. Four of the eight salts (**62a-d**) showed near-quantitative ee for cyclobutanol **124**. Most salts gave good to excellent de's (> 80 %) in the solid state. Once again, a number of salts led to low ee's while others led to near-quantitative ee's, which is a typical result in the solid state asymmetric induction studies. These results will be discussed in section 3.5. The

103

photolysis of salt **62a** in methanol gave racemic cyclobutanols **124** and **125** (124/125 = 65/35) at 99 % conversion. This highlights the importance of the crystalline state in the asymmetric induction.

Table 3.22 Asymmetric induction in the photolysis of chiral salts **62a-h**

salt	amine	conv[a] (%)	temp	de[b] (%)	ee[b,c] for 125 (%)	ee[b] for 124 (%)
62a	R-(-)-1-cyclohexylethylamine	99	-20	-99	UM	-99
62a	R-(-)-1-cyclohexylethylamine	55	RT	-96	UM	-98
62a	R-(-)-1-cyclohexylethylamine	88	RT	-95	UM	-98
62a	R-(-)-1-cyclohexylethylamine	99	RT	-94	UM	-98
62a	R-(-)-1-cyclohexylethylamine	100	RT	-92	UM	-99
62b	(1R. 2R)-(-)-pseudoephedrine	18	-20	-97	-73	+93
62b	(1R. 2R)-(-)-pseudoephedrine	48	-20	-93	-65	+90
62b	(1R. 2R)-(-)-pseudoephedrine	55	RT	-85	-61	+61
62b	(1R. 2R)-(-)-pseudoephedrine	100	RT	-75	-42	+51
62c	(1R, 2S)-(+)-cis-1-amino-2-indanol	94	-20	-88	0	+86
62c	(1R, 2S)-(+)-cis-1-amino-2-indanol	65	RT	-84	-7	+84
62c	(1R, 2S)-(+)-cis-1-amino-2-indanol	97	RT	-80	-5	+80
62d	S-(-)-p-tolylethylamine	65	-20	-46	-56	+65
62d	S-(-)-p-tolylethylamine	76	-20	-58	-41	+42
62d	S-(-)-p-tolylethylamine	33	RT	-36	-19	+91
62e	L-prolinamide	25	-20	-82	+10	-60
62e	L-prolinamide	50	RT	-75	+5	-46
62e	L-prolinamide	70	RT	-61	+6	-46
62f	R-(-)-1-aminoindane	10	-20	-85	-3	-67
62f	R-(-)-1-aminoindane	16	RT	-87	+3	-48
62g	R-(+)-1-phenylethylamine	70	-20	-83	-4	-10
62g	R-(+)-1-phenylethylamine	50	RT	-87	0	-6
62h	(1R, 2S)-(-)-norephedrine	28	-20	-84	-18	-24
62h	(1R, 2S)-(-)-norephedrine	45	RT	-80	-8	-9

a Percentage of total HPLC integral (chiral AD column) due to the disappearance of the corresponding starting material (after calibration using the response factor). b Diastereomeric excess (de) and enantiomeric excess (ee) values were measured on a Chiralpak AD column. The de values were calculated with the equation: de (%) = **125** (%) – **124** (%). Sign of rotation for cyclobutanol **124** was obtained at the sodium D-line (589 nm). c For the high de cases, ee for the minor diastereomer **125** is unmeasurable (UM). The sign of ee for minor product **125** is not the sign of rotation, but calculated from the equation: ee (%) = peak A (%) – peak B (%). Peak A and peak B are shown in Figure 3.24.

3.5 Molecular Mechanics Calculations and X-ray Crystallographic Studies

3.5.1 Bicyclo[2.2.2]octyl Substrates

Ester **55** was studied by molecular mechanics calculations, and acid **54** and salts **56a-b** were studied by X-ray crystallography (Table 3.23 and Figure 3.25). Because there are no Norrish type II cleavage products formed in all bicyclic substrates, cleavage parameters (φ_1 and φ_4) will not be discussed in this section. The lowest energy conformation (**55-1**, Figure 3.25(A)) of ester **55** is similar to the X-ray structure of acid **54** (Figure 3.25(a)), because there is a similarity in the carbonyl oxygen position (the carbonyl oxygen is situated much closer to γ hydrogen H_a than $H_{a'}$) and in the aryl group orientation (the phenyl ring faces $H_{a'}$). From the hydrogen abstraction and cyclization parameters described in the Introduction section, it was found that the crystal structure of acid **54** and conformer **55-1** (the lowest energy conformer) presented in Table 3.23 have parameters (ω, Δ, θ) within favorable limits of the "ideal" values. Because there is no significant difference in the values of the angles ω, Δ and θ among different crystal structures studied in this project, in the following part of this thesis, only the d, β and D values among hydrogen abstraction and cyclization parameters are discussed to rationalize the enantioselectivity, diastereoselectivity and photostability.

Although hydrogen abstractions have been observed at distances (d) up to 3.15 Å,[101] studies of Norrish type II abstraction have shown that, in a competitive situation, a difference in the distance (d) of only 0.27 Å will lead to exclusive abstraction of one hydrogen over the other.[102] There are no crystal structures of salts **56d-g** obtained; however, it is reasonable to assume that salts **56d-g** might crystallize in a conformation similar to conformer **55-1** and the differentiation between the two enantiotopic γ hydrogens and topochemical control account for the high enantiomeric excess observed for these compounds, which will be described in the following section.

The second lowest energy conformation (**55-2**) of ester **55** is similar to the X-ray structures of salts **56a** and **56b**, because there is a similarity among them in the carbonyl oxygen position (the carbonyl oxygen is located nearly equidistant from γ hydrogens H_a and $H_{a'}$ as shown in Figure 3.25 and Table 3.23) and in the aryl group orientation (the phenyl ring bisects H_a-$H_{a'}$). Salts **56a** and **56b** are photochemically inert. The reason

could be that the large β and D values retard the rate of ring closure of the biradical. Previous studies in the Scheffer group showed that reverse hydrogen transfer is dominant when the D value is as large as ~3.2 Å[103] *or* the β value is as large as 68°.[30] For salts **56a** and **56b**, both β and D values are very close to these critical upper limit values as shown in Table 3.23.

Table 3.23 Hydrogen abstraction and cyclization parameters for bicyclo[2.2.2]octyl substrates

conformer	notes	γ-H	β(°)	d(Å)	ω(°)	Δ(°)	θ(°)	D(Å)	
55-1	the lowest energy conformer	a	34	2.71	63	84	100	3.08	
		a'		3.56					
55-2	the second lowest energy conformer	a	61	2.43	28	105	112	3.19	
		a'	60	2.47	38	97	116	3.24	
54	X-ray structure	a	29	2.65	62	78	114	3.02	similar to **55-1**
		a'		3.71					
56a	X-ray structure	a	57	2.46	35	94	123	3.14	similar to **55-2**
		a'	65	2.55	25	98	118	3.20	
56b[a]	X-ray structure	a	68	2.46	24	97	123	3.20	similar to **55-2**
		a'	52	2.58	36	94	118	3.17	
		b	69	2.46	24	98	122	3.19	
		b'	52	2.59	36	94	117	3.16	

[a] There are two independent conformers in the asymmetric unit; γ hydrogens H_a and $H_{a'}$ are enantiotopic in one conformer; γ hydrogens b and b' are also enantiotopic but in the other conformer.
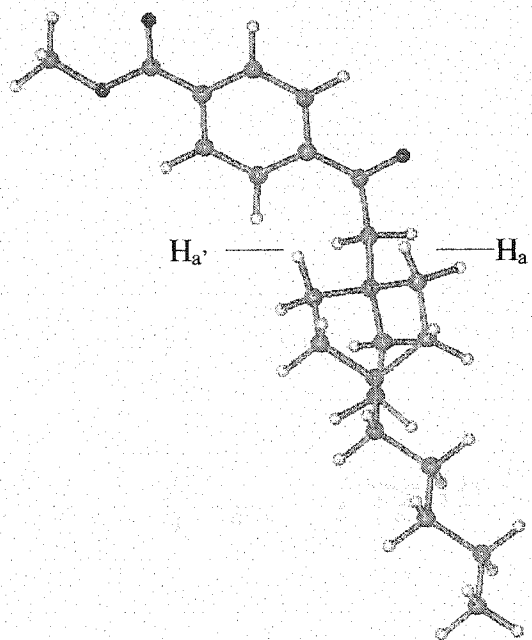
(A): **55-1**
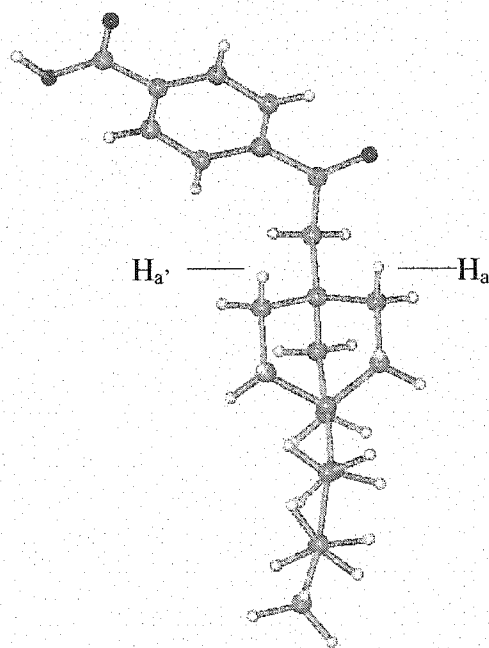
(a): **54**

Figure 3.25 Conformers obtained by MM$^+$ calculations and X-ray crystallographic studies for bicyclo[2.2.2]octyl ketones. (A) Conformer **55-1**, the lowest energy (36.00 Kcal/mol) conformer of ester **55** (MM$^+$); (a) the conformer from the crystal structure of acid **54**.
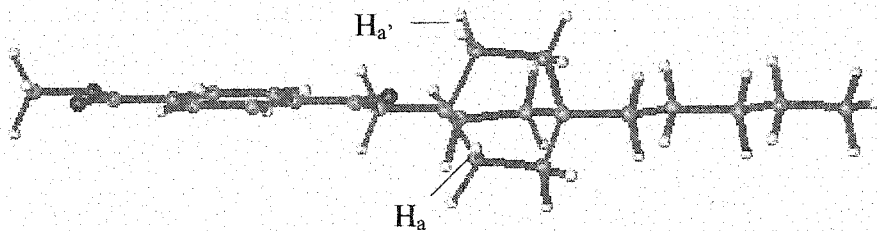
(B): **55-2**
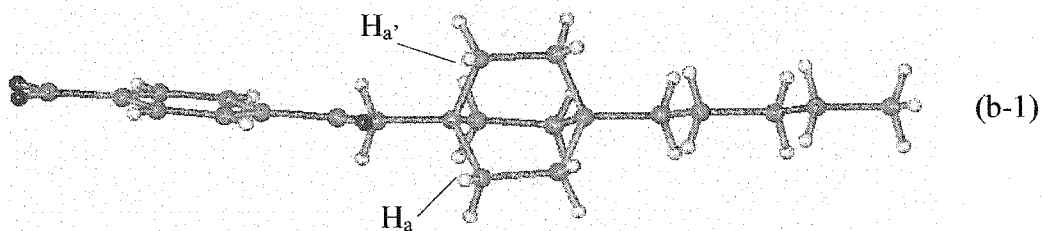
(b-1)
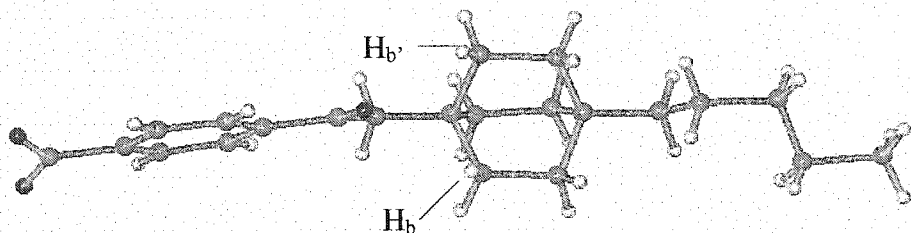
(b-2)
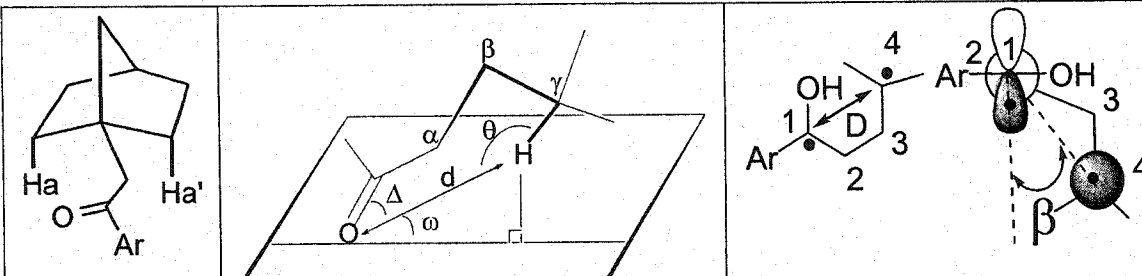
(b): **56b**

Figure 3.25 (Continued) (B) conformer **55-2**, the second lowest energy (36.26 Kcal/mol) conformer of ester **55** (MM$^+$); (b) the two conformers (b-1 and b-2) in the crystal structure of salt **56b**; the conformation of crystal **56a** (not shown in the Figure) is virtually same as b-1 in crystal **56b** and the conformer **55-2** (MM$^+$).
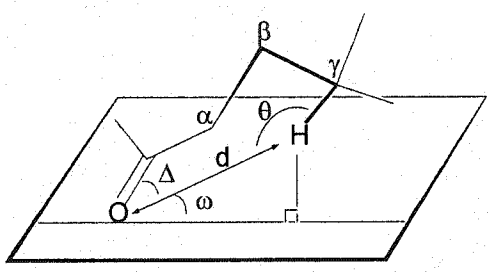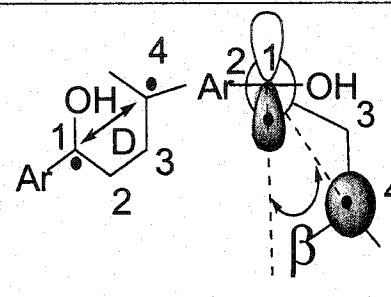
3.5.2 Bicyclo[2.2.1]heptyl Substrates

Ester **58** was studied by molecular mechanics calculations, and ester **58** and salt **59d** were studied by X-ray crystallography (Table 3.24 and Figure 3.26). It was found that the lowest energy conformation (**58-1**) of ester **58** predicted by MM$^+$ is similar to its X-ray structure and that of salt **59d**, because there is a similarity among them in the carbonyl oxygen position (the carbonyl oxygen is located nearly equidistant from γ hydrogens H_a and $H_{a'}$ as shown in Figure 3.26 and Table 3.24) and in the aryl group orientation (the phenyl ring bisects H_a-$H_{a'}$). It is thus not surprising that salt **59d** gave modest ee ($\sim$ 38%) as shown in Table 3.20. The rationale for this result will be described in the following section. The higher energy conformations (**58-2, 58-3, 58-4**) as shown in Figure 3.26 have not been found by X-ray crystallography. Although only one salt (**59d**) has had its X-ray crystal structure determined, all 13 salts of acid **57** gave moderate to low ee's, which suggests most salts might crystallize in the lowest energy conformation (**58-1**). Due to the unavailability of an X-ray structure for acid **57** and salt **59a**, no evidence can be provided to explain their photostability. However, we may speculate that its photostability could also be due to high D and β values, the same reason as for salts **56a-b**. The lowest energy conformer **58-1** (MM$^+$) shows a D value of 3.23 Å (larger than 3.20 Å) and a β value of 61° (close to 68°). This result is also consistent with the low photocyclization rate of other salts of acid **57** (Their quantum yield were not determined, but the solid state photocyclizations were completed after 24 hours for most bicyclo[2.2.1]heptyl ketones; most of the other Yang photocyclizations in this thesis can be finished in less than 5 hours).

Table 3.24 Hydrogen abstraction and cyclization parameters for bicyclo[2.2.1]heptyl substrates

conformer	notes	γ-H[*]	β(°)	d(Å)	ω(°)	Δ(°)	θ(°)	D(Å)	
58-1	the lowest energy conformer	2a	61	2.59	28	108	103	3.23	
		2a'	61	2.59	28	108	103	3.23	
58-2	the second lowest energy conformer	2a	27	2.99	39	90	91	3.10	
		2a'		4.48					
58-3	the third lowest energy conformer	2a	23	2.64	65	82	118	3.14	
		2a'		5.00					
58-4	the fourth lowest energy conformer	1a	29	2.85	64	84	102	3.17	
		1a'		3.43					
		2a	26	3.54	41	41	104	3.14	
		2a'		4.63					
58	X-ray structure	2a	55	2.63	20	103	107	3.20	similar to **58-1**
		2a'	67	2.74	32	97	108	3.21	
59d	X-ray structure	2a	60	2.58	12	102	108	3.16	similar to **58-1**
		2a'	64	2.71	11	100	108	3.14	

[*] H_{1a} and $H_{1a'}$ are two enantiotopic γ hydrogens in one-carbon bridge. H_{2a}, $H_{2a'}$ are enantiotopic γ hydrogens in two-carbon bridge.

(a₁): **58**   (a₂): **59d**   (A): **58-1**

(B): **58-2**   (C): **58-3**   (D): **58-4**
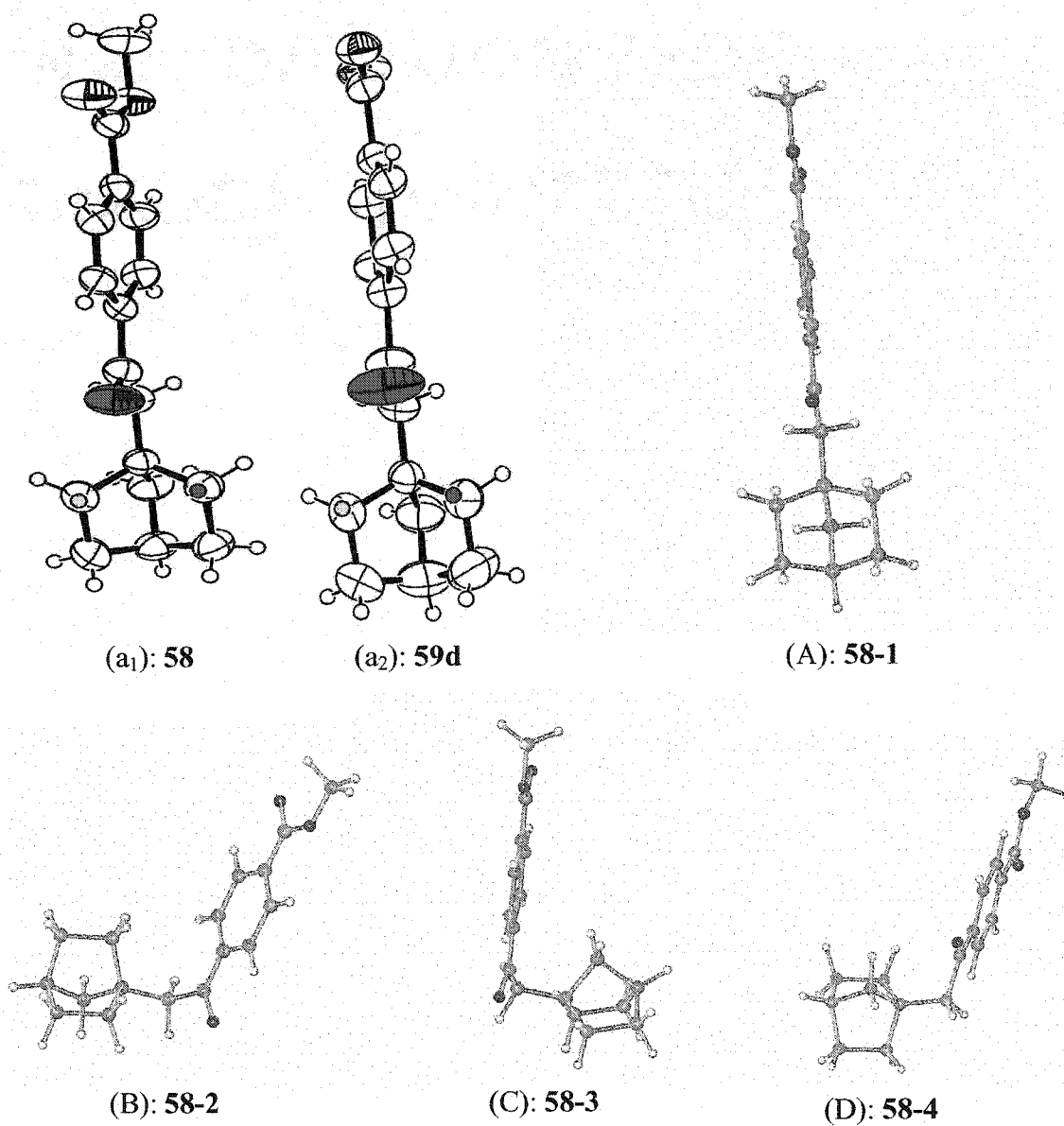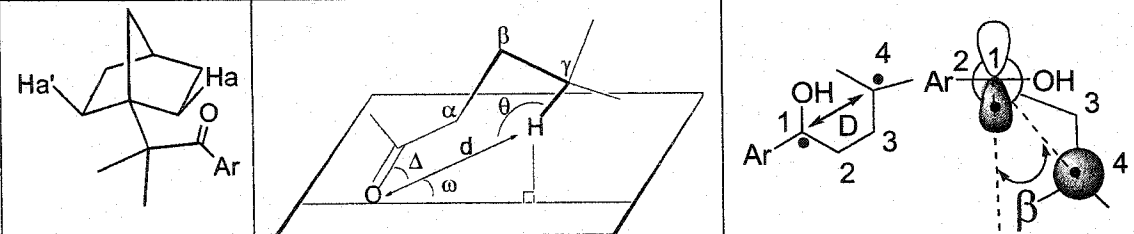
Figure 3.26 Conformers obtained by MM⁺ calculations and X-ray crystallographic studies for bicyclo[2.2.1]heptyl substrates. (a₁) The conformer in the crystal of ester **58**; (a₂) the conformer (anion part) in the crystal of salt **59d**; (A), (B), (C), (D) are calculated conformers of ester **58** with total energy 39.43, 39.49, 39.62, and 39.82 Kcal/mol, respectively. In the ORTEP representations a₁ and a₂, the carbonyl oxygen is colored red, γ-hydrogen H$_a$ green and H$_{a'}$ blue.

3.5.3 Dimethylated Bicyclo[2.2.1]heptyl Substrates

Ester **61** was studied by molecular mechanics calculations, and ester **61** (X=COOMe) and its derivatives **110** (X=CN), **109** (X=F), **60** (X=COOH), **62a** (R(-)-1-cyclohexylethylamine salt), **62c** ((1R, 2S)-(+)-cis-1-amino-2-indanol salt), **62e** (L-prolinamide salt) were studied by X-ray crystallography (Table 3.25 and Figure 3.27). It was interesting to find that the lowest energy conformation (**61-1**) of ester **61** is similar to the X-ray structures of compounds **110, 109, 60** and **62a**, because there is a similarity among them in the carbonyl oxygen position (the carbonyl oxygen is situated between the one-carbon bridge and the two-carbon bridge with a distance much closer to γ hydrogen H_a than $H_{a'}$) and in the aryl group orientation (the phenyl ring faces the hydrogens at the one-carbon bridge); the second lowest energy conformation (**61-2**) is similar to the X-ray structure of ester **61**, because there is a similarity between them in the carbonyl oxygen position (the carbonyl oxygen is close to a γ hydrogen at the one-carbon bridge) and in the aryl group orientation (the aryl group points to the two-carbon bridge side); and the third lowest energy conformation (**61-3**) is similar to the X-ray structures of salts **62c** and **62e**, because there is a similarity among them in the carbonyl oxygen position (the carbonyl oxygen is situated between the two two-carbon bridges and is much closer to γ hydrogen H_a than $H_{a'}$) and in the aryl group orientation (the phenyl ring faces hydrogen $H_{a'}$). No X-ray crystal structure was found with the fourth lowest energy conformation (**61-4**), in which the carbonyl oxygen is situated equidistant from γ hydrogens H_a and $H_{a'}$ between the two-carbon bridges. As shown in Table 3.25, the hydrogen abstraction and cyclization parameters for all substrates are within favorable limits of the "ideal" values. Upon photolysis, all substrates underwent rapid Norrish/Yang photocyclization to form cyclobutanols. The structure-reactivity correlation will be discussed in the following section. It is interesting to note that, as shown in Figure 3.28, conformations **58-1, 58-2, 58-3** and **58-4** of the bicyclo[2.2.1]heptyl ketones are similar (in carbonyl oxygen position and aryl group orientation) to conformers **61-4, 61-3, 61-1,** and **61-2** in the dimethylated bicyclo[2.2.1]heptyl ketones respectively.

Table 3.25 Hydrogen abstraction and cyclization parameters for dimethylated

bicyclo[2.2.1]heptyl substrates

conformer	notes	γ-H[*]	$\beta(°)$	$d(\text{Å})$	$\omega(°)$	$\Delta(°)$	$\theta(°)$	$D(\text{Å})$	
61-1	the lowest energy conformer	2a	19	2.59	67	78	118	3.06	
		2a'		5.07					
61-2	the second lowest energy conformer	1a	35	2.74	61	90	107	3.22	
		1a'		3.56					
		2a	18	3.26	48	48	108	3.03	
		2a'		4.79					
61-3	the third lowest energy conformer	2a	9	2.76	57	83	105	2.90	
		2a'		4.46					
61-4	the fourth lowest energy conformer	2a	59	2.38	30	114	103	3.14	
		2a'	65	2.47	30	112	104	3.23	
110	X-ray structure	2a	4	2.88	62	65	120	3.01	similar to **61-1**
		2a'		5.05					
109	X-ray structure	2a	3	2.96	59	60	119	2.99	similar to **61-1**
		2a'		5.03					
60	X-ray structure	2a	6	2.83	63	66	119	3.00	similar to **61-1**
		2a'		5.03					
61	X-ray structure	1a	46	2.61	42	96	112	3.20	similar to **61-2**
		1a'		3.40					
		2a	4	3.06	55	56	112	2.99	
		2a'		4.70					
62a	X-ray structure	2a	1	2.96	61	60	119	3.01	similar to **61-1**
		2a'		5.08					
62c	X-ray structure	2a	6	3.28	62	63	94	3.05	similar to **61-3**
		2a'		4.02					
62e	X-ray structure	2a	7	3.11	67	66	95	2.98	similar to **61-3**
		2a'		3.84					

[*] H_{1a} and $H_{1a'}$ are two enantiotopic γ hydrogens in the one-carbon bridge. H_{2a}, $H_{2a'}$ are enantiotopic γ hydrogens in the two-carbon bridge.

(a): **62a**

(A): **61-1**

(b): **61**

(B): **61-2**

(c₁): **62c**

(c₂): **62e**

(C): **61-3**

(D): **61-4**
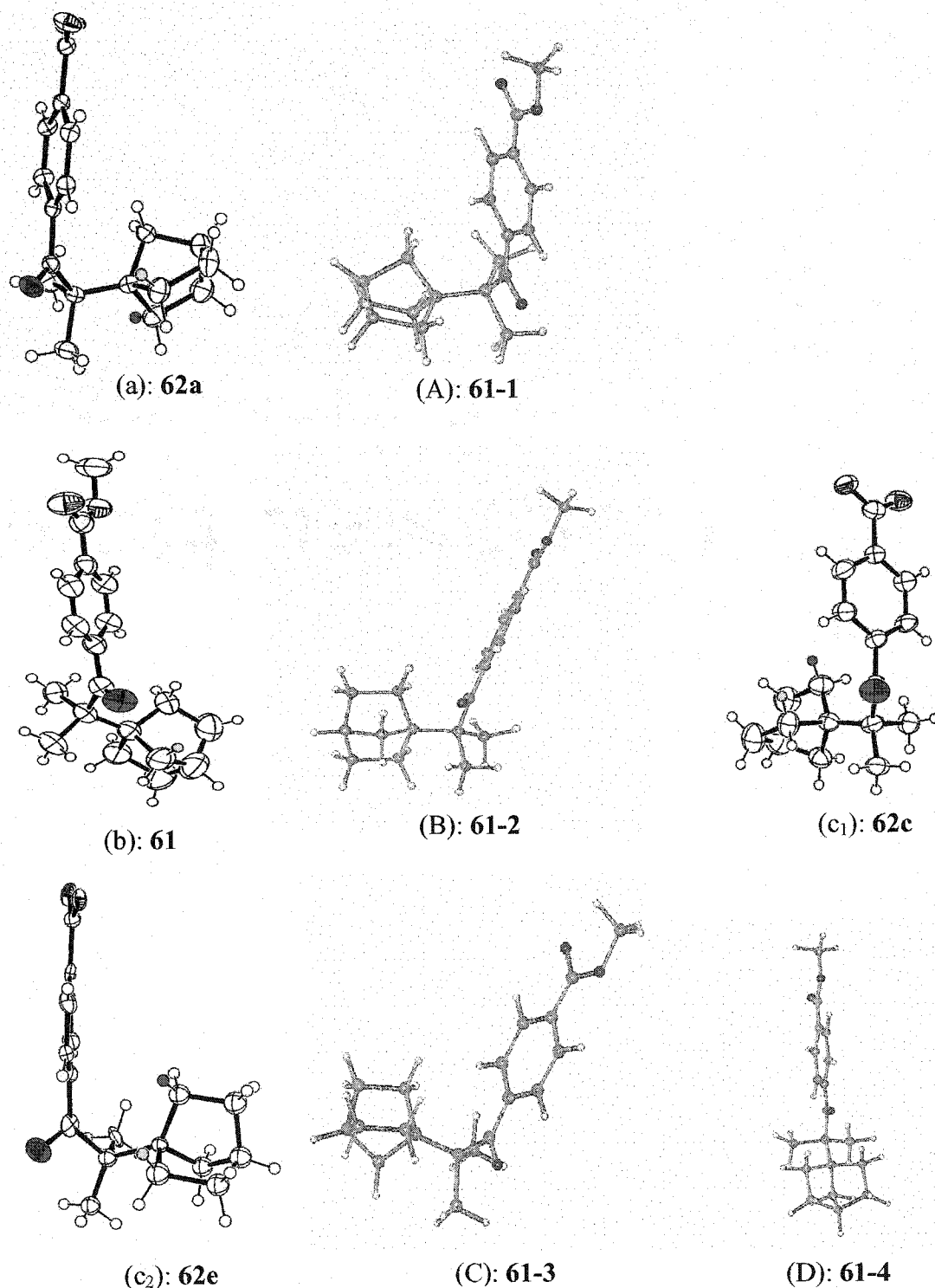
Figure 3.27 Conformers obtained by MM$^+$ calculations and X-ray crystallographic studies for dimethylated bicyclo[2.2.1]heptyl substrates. (a), (b), (c₁), (c₂) are the conformers in the crystals of compounds **62a** (anion part), **61**, **62c** (anion part), **62e** (anion part); (A), (B), (C), (D) are calculated conformers of ester **61** with energy 42.41, 43.20, 43.64, and 44.69 Kcal/mol respectively. In the ORTEP representations, the carbonyl oxygen is colored red, the γ hydrogen H$_a$ green and H$_{a'}$ blue.

Ketone **58**   Dimethylated ketone **61**

the fourth lowest energy conformer   **58-4**   **61-4**

the third lowest energy conformer   **58-3**   **61-3**

the second lowest energy conformer   **58-2**   **61-2**

the lowest energy conformer   **58-1**   **61-1**
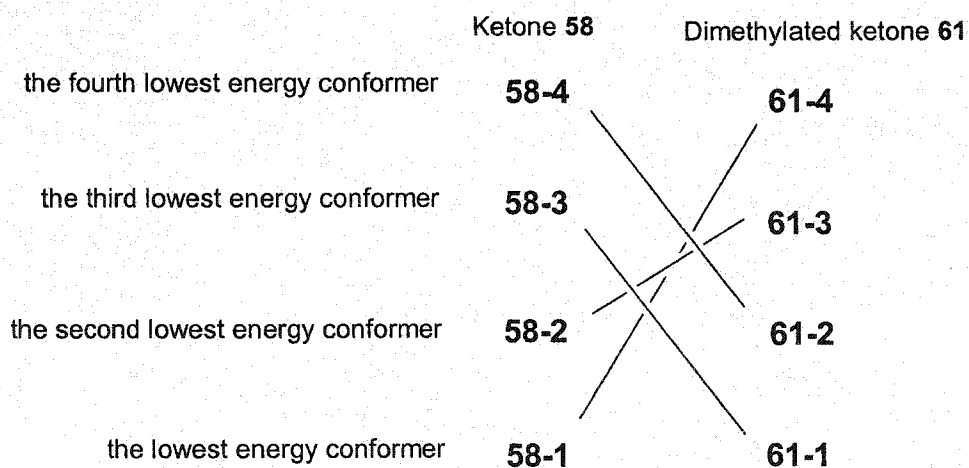
Figure 3.28 Conformational correlations between bicyclo[2.2.1]heptyl ketone **58** and dimethylated bicyclo[2.2.1]heptyl ketone **61** by MM^+ calculations.

3.5.4 Molecular Mechanics Calculations on Yang photocyclization Products
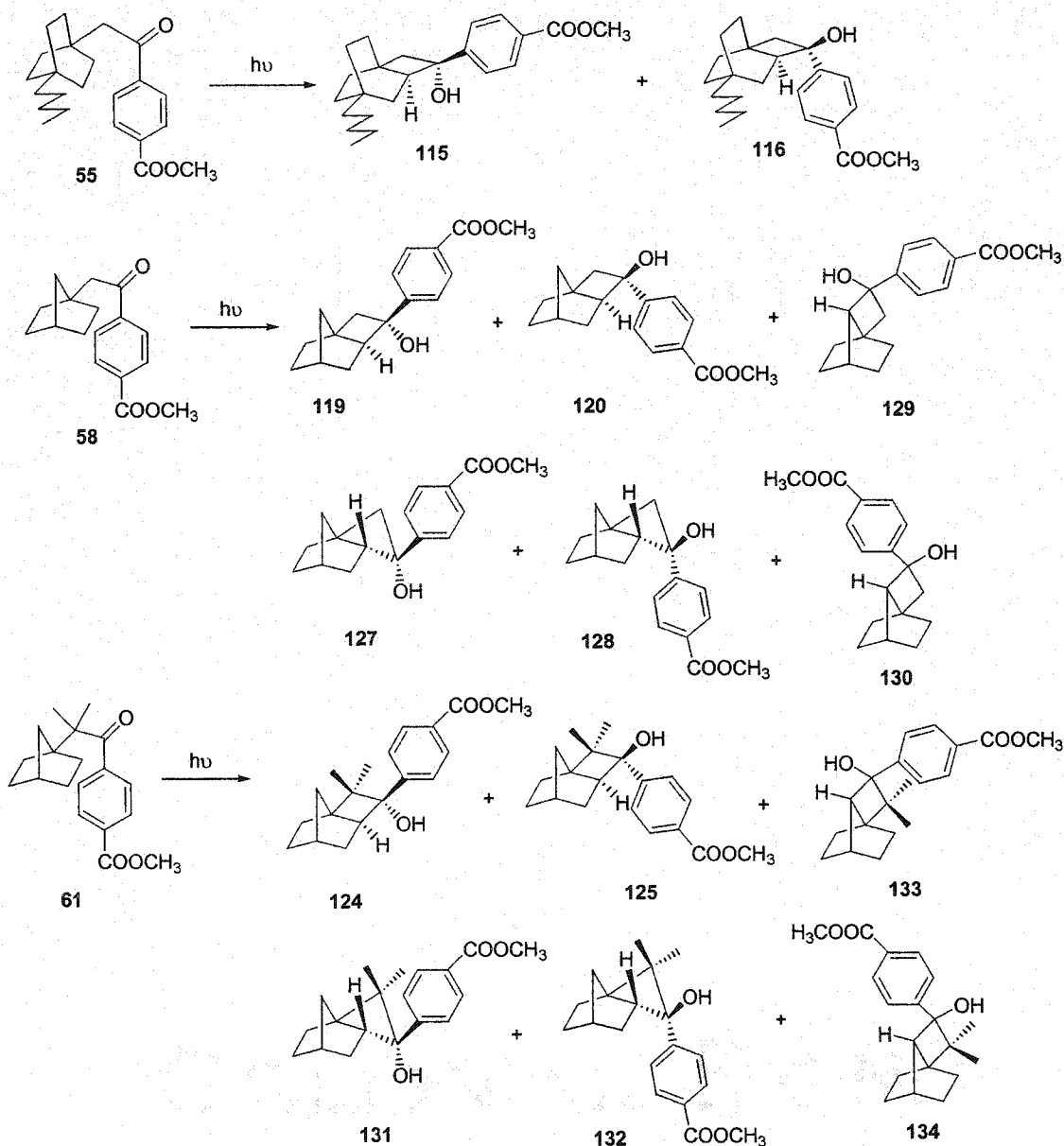
Figure 3.29 Possible Norrish type II photocyclization products.

The geometry (obtained from X-ray crystallography or predicted from molecular modeling) of the parent ketones has been used successfully in explaining 1,4-hydroxybiradical reactivity in solid state Norrish type II reactions.[60] However, previous studies in the Scheffer group showed that a full understanding of the results requires consideration of the strain energy of the cyclization products.[92] Molecular mechanics

116

calculations were also conducted to estimate the relative strain energy and total energy of (potential) Yang photocyclization products in this thesis.[104]

Ester **55** has 6 γ-hydrogens and in theory can (by the Norrish/Yang photocyclization mechanism shown in Figure 1.7) undergo γ-hydrogen abstraction to form cyclobutanols **115** and **116** (Figure 3.29). By MM$^+$ calculation, it was found that cyclobutanol **116** has a slightly lower total energy and strain energy than cyclobutanol **115** as shown in Table 3.26. The photochemical studies of ester **55** (See section 3.3.1) showed cyclobutanol **116** is the major photoproduct both in solution (**116/115**~ 68/32) and the solid state (**116/115**~ 93/7).

Ester **58** has 6 γ-hydrogens and its possible Yang photocyclization products are cyclobutanols **119-120**, **127-130**. However, only cyclobutanols **119-120** were isolated. This might be due to the fact that cyclobutanols **127-130** have significantly higher total energy and strain energy than cyclobutanols **119-120** as shown in Table 3.26. Cyclobutanol **119** has a slightly higher total energy and strain energy than cyclobutanol **120**; however, photochemical studies of ester **58** (section 3.3.3) showed that cyclobutanol **119** was formed preferentially both in solution (**119/120** ~ 53/47) and the solid state (**119/120**~ 65/35). This will be discussed in the next section of structure-reactivity studies using topochemical expectations.

Ester **61** also has 6 γ-hydrogens and its possible Norrish type II photocyclization products are cyclobutanols **124-125** and **131-134** as shown in Figure 3.29. However, only cyclobutanols **124-125** were isolated. This might also be due to the fact that cyclobutanols **131-134** have significantly higher total energy and strain energy than cyclobutanols **124-125** as shown in Table 3.26. Cyclobutanol **124** has a slightly higher total energy and strain energy than cyclobutanol **125**; however, photochemical studies of ester **61** (section 3.3.5) showed that cyclobutanol **124** was formed preferentially both in the solid state (**124/125**~ 64/36) and solution (**124/125**~ 84/16). This result will also be discussed in the next section.

The formation of minor photoproduct ketone **126** probably proceeds *via* the mechanism shown in Figure 3.30; a similar photoproduct was also formed in the photolysis of the adamantyl ketones studied by Jie Yang.[79] Although the formation of minor photoproduct **126** is thermodynamically favorable (total energy, 38.79 Kcal/mol;

strain energy, 25.80 Kcal/mol; angle strain, 14.44 Kcal/mol), it is not a topochemically favorable photoproduct. The nearest distance (D_{126}) from carbon 5 to carbon 6 (Figure 3.30) is greater than 3.20 Å (in conformer **61-1**, D_{126} = 4.87 Å; in conformer **61-2**, D_{126} = 3.32 Å; in conformer **61-3**, D_{126} = 4.55 Å; in conformer **61-4**, D_{126} = 5.16 Å).

Table 3.26 Molecular mechanics studies on possible cyclobutanol photoproducts

molecule	total energy (kcal/mol)	strain energy (kcal/mol)	angle strain (kcal/mol)
116	74.93	57.78	44.46
115	76.86	59.38	45.44
120	75.53	65.87	55.48
119	77.57	67.57	56.53
128	100.54	88.15	76.69
127	99.22	86.73	75.75
129	93.38	82.40	70.01
130	92.03	80.39	68.64
125	78.40	67.88	57.06
124	84.21	71.97	59.08
132	107.08	92.23	78.88
131	102.15	88.62	76.67
133	101.47	87.64	73.64
134	96.68	83.38	70.41
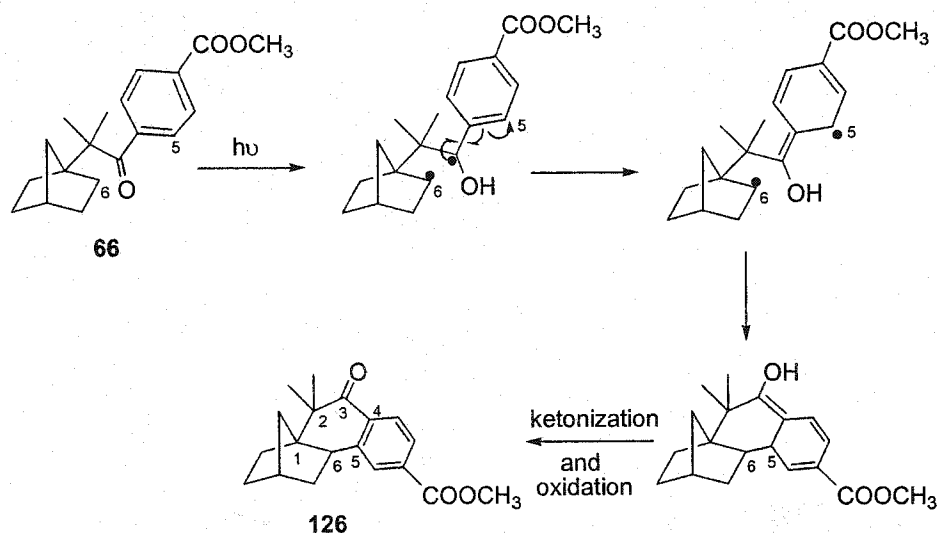
Figure 3.30 Proposed mechanism for the formation of ketone **126**

To conclude this section, highly strained cyclobutanols (**127-130** and **131-134** with high angle strain[105]) were not detected either in solution or the solid state.

3.6 Structure-reactivity Studies

3.6.1 Topochemical Control Reactions

3.6.1.1 Structure-reactivity Analysis of Bicyclo[2.2.2]octyl Substrates

No X-ray crystal structures were obtained for salts **56c-g** (high ee's achieved). However, organic molecules generally crystallize in or near their minimum energy conformations.[5] Assuming one of salts **56c-g** crystallized in the lowest energy conformation (**55-1**) in the asymmetric unit as shown in Figure 3.25(A), its solid state photochemical diastereoselectivity and enantioselectivity can be analyzed as follows. As shown in Table 3.24, only γ-hydrogen H_a is within the proposed hydrogen abstraction distance of 2.7 ± 0.2 Å (O-H_a, 2.71 Å). In conformer **55-1** (Figure 3.31), there are two diastereotopic carbonyl faces (*re* and *si*) and the carbonyl *si* face is closer to the reacting γ-hydrogen H_a than the corresponding *re* face. Upon photolysis, only γ-hydrogen H_a is abstracted to form biradical **55-1-BR-1**. In biradical **55-1-BR-1**, there are another two diastereotopic faces (*re* and *si*) at the radical-bearing carbon 6. As shown in Figure 3.31, there are four possible pathways for forming a single bond between the two radical centers in intermediate **55-1-BR-1**. Pathway 1 involves bond formation between the *si* face of the *p* orbital at C1 and the *si* face of the *p* orbital at C6 (C1 *si* + C6 *si*), to give *trans*-cyclobutanol **115(1S)** with the (S) absolute configuration at C1. Pathway 2, C1 *si* + C6 *re*, gives *cis*-cyclobutanol **116(1S)** with the C1(S) absolute configuration; pathway 3, C1 *re* + C6 *si*, gives *cis*-cyclobutanol **116(1R)** with the C1(R) absolute configuration; pathway 4, C1 *re* + C6 *re*, gives *trans*-cyclobutanol **115(1R)** with the C1(R) absolute configuration. Among these four possible pathways, pathway 1 involves the least motion (direct radical coupling without rotation (a) or (b)); therefore, *trans*-cyclobutanol **115(1S)** is the topochemically favored photoproduct. In contrast, pathways 2, 3 and 4 require certain molecular motions (rotation (a) and/or rotation (b)) to bring the corresponding *p* orbital lobes into position for bond formation. However, *cis*-cyclobutanol **116** is the major photoproduct for all salts **56**, ester **55** and acid **54**, both in the solid state and solution (sections 3.3.1 and 3.4.1.2). Previous studies on α-adamantyl acetophenones in the Scheffer group showed that the rotation of the adamantyl group (C3 symmetry) around the C2-C3 bond (called *rotation a*) is considered to involve the least hindrance

(Figure 3.32), because this movement does not require much void space.[79] On the other hand, the rotation of the phenone-salt moiety around C1-C2 bond (called *rotation b*), which requires more void space, is topochemically disallowed. Bicyclo[2.2.2]octyl substrates have C_3 symmetry and rotation (a) should also be topochemically allowed. Recalling the MM^+ calculations (Table 3.26), *cis*-cyclobutanol **116** has lower energy than *trans*-cyclobutanol **115**. As we know that the more stable product is also the one that is formed faster in many cases,[106] it is reasonable to speculate that the lower energy photoproduct cyclobutanol **116** (the major diastereomer) is formed faster than cyclobutanol **115** (the minor diastereomer) as shown in Figure 3.33 (a similar rationale was used in the studies of adamantyl ketones by Jie Yang[79]). The formation of **116(1R)** and **115(1R)**, which involve the topochemically disallowed rotation (b), should be unfavorable. This explains why high ee's for both cyclobutanol **115** and **116** were obtained for most salts **56**.
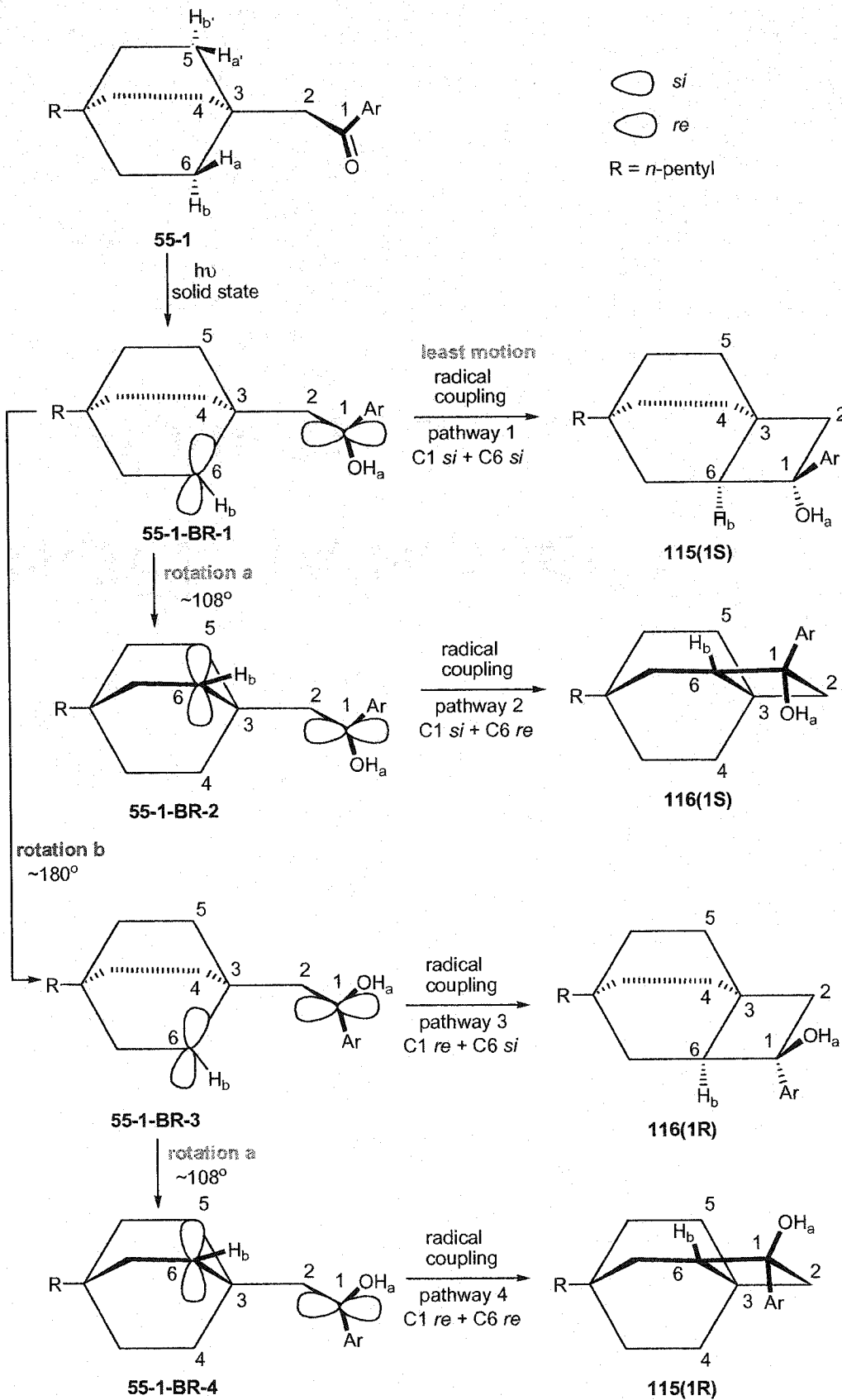
Figure 3.31 The solid state reactivity of conformer **55-1**
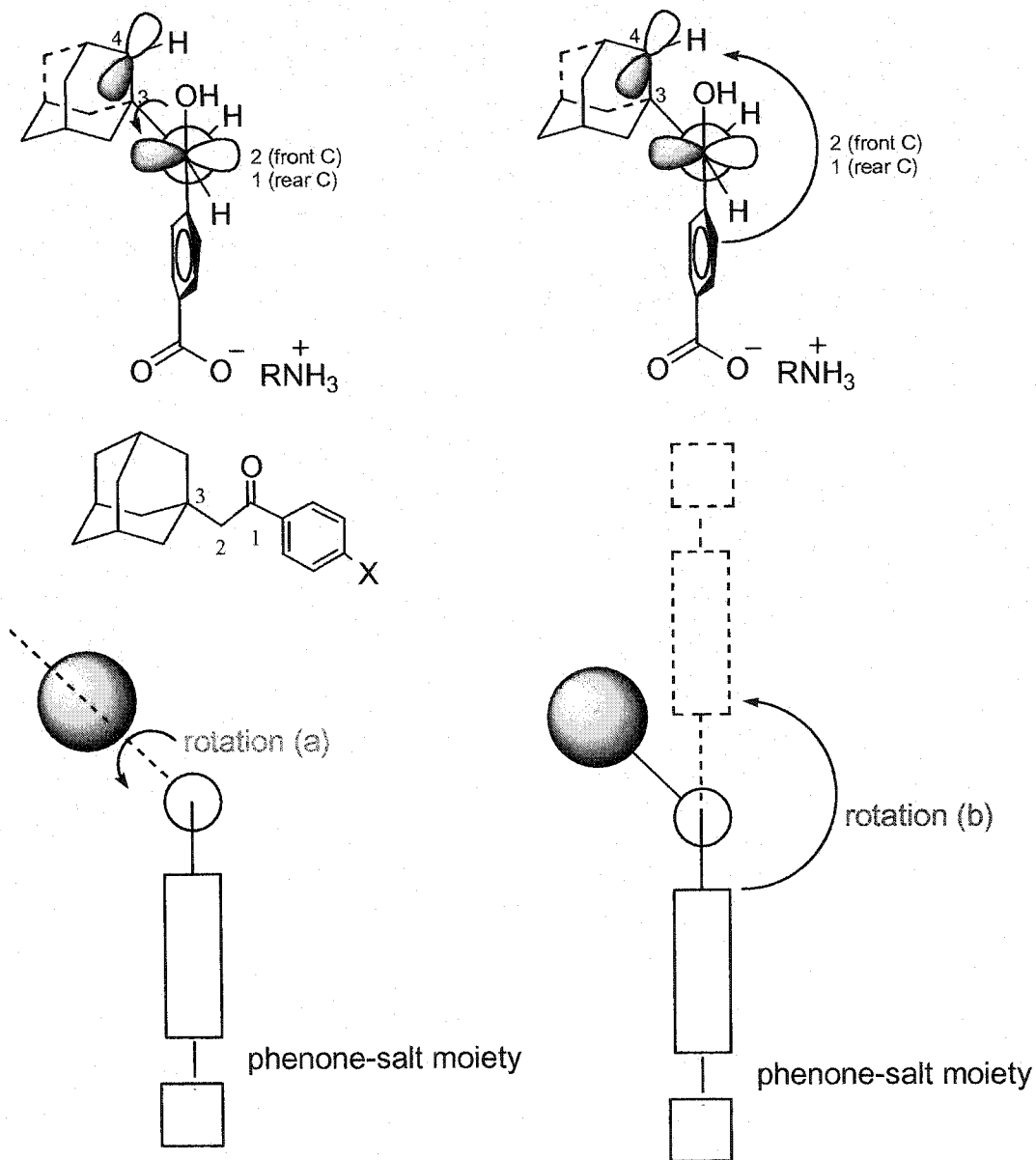
Figure 3.32 The rotations (a) and (b) (same as the rotations in pathways 2, 3, and 4 shown in Figure 3.31)
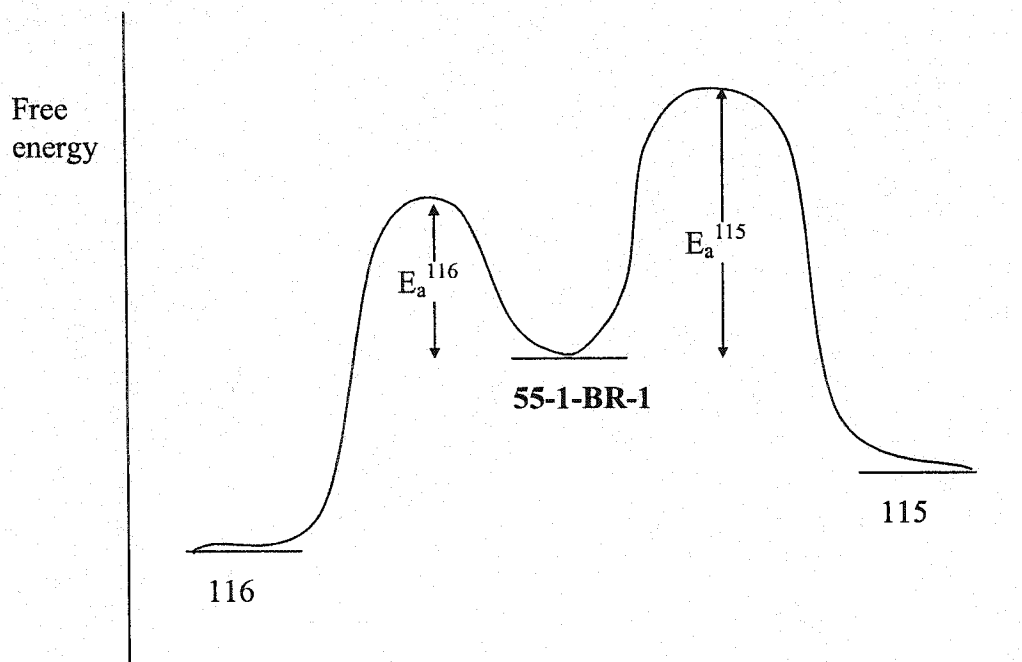
Figure 3.33 Free energy profile for rationalizing the diastereoselectivity in the photolysis of bicyclo[2.2.2]octyl ketones.

3.6.1.2 Structure-reactivity Analysis of Bicyclo[2.2.1]heptyl Substrate 59d

The X-ray crystal structure of salt **59d** (Figure 3.26(a$_2$)) shows that the carbonyl oxygen is situated nearly equidistant from γ-hydrogens H$_a$ and H$_{a'}$ (O-H$_a$, 2.58 Å; O-H$_{a'}$, 2.71 Å). Both γ-hydrogens H$_a$ and H$_{a'}$ should therefore be abstractable. As shown in Figure 3.34, abstraction of γ-hydrogen H$_a$ forms biradical **59d-BR-1** upon photolysis. Analysis similar to that used in the previous section is shown in Figure 3.34 and reveals that there are four possible pathways for forming a single bond between the two radical centers of intermediate **59d-BR-1**. Pathway 1 involves bond formation between the *re* face of the *p*-orbital at C1 and *re* face of the *p*-orbital at C6 (C1 *re* + C6 *re*) to give *trans*-cyclobutanol **119(1R)** with the C1(R) absolute configuration. Pathway 2, C1 *si* + C6 *re*, gives *cis*-cyclobutanol **120(1S)** with the C1(S) absolute configuration; pathway 3, C1 *si* + C6 *si*, gives *trans*-cyclobutanol **128(1S)** with the C1(S) absolute configuration; pathway 4, C1 *re* + C6 *si*, gives *cis*-cyclobutanol **127(1R)** with the C1(R) absolute configuration. Among these four possible pathways, pathway 1 involves the least motion (direct radical coupling without rotation (a) or (b)); therefore, *cis*-cyclobutanol **119(1R)** is the topochemically favored photoproduct. In contrast, pathways 2, 3 and 4 require certain molecular motions (rotation (a) and/or rotation (b)) to bring the corresponding *p*-orbital lobes into position for bond formation. Photochemical studies of salt **59d** (section 3.4.2.2) showed that *trans*-cyclobutanol **119** is the major photoproduct in the solid state (**119/120** ~ 69/31). This result is in agreement with the topochemical analysis: the major photoproduct is the topochemically favored *trans*-cyclobutanol **119** *via* pathway 1. This result also suggests that rotation (a) in pathway 2 (for the formation of cyclobutanol **120**), involving the rotation of the bicyclo[2.2.1]heptyl group (without C$_3$ symmetry), requires more void space than rotation of the bicyclo[2.2.2]octyl and adamantyl groups that have C$_3$ symmetry. Cyclobutanols **127** and **128** (*via* pathways 3 and 4) were not isolated in the photolysis, which might be due to the following: (1) they are highly strained (angle strain) compounds; (2) pathways 3 and 4 are non-topochemical processes involving rotation (b).

Considering another hydrogen abstraction (H$_{a'}$) in salt **59d**, biradical coupling gives *trans*-cyclobutanol **119(1S)** following direct ring-closure and *cis*-cyclobutanol **120(1R)** following rotation (a) and then ring-closure. Because the carbonyl oxygen has almost the

same distance to γ-hydrogens H_a and $H_{a'}$, low ee is expected for both *trans*-cyclobutanol **119** and *cis*-cyclobutanol **120**. Two facts account for the low but measurable 30-40 % ee's for both *trans*-cyclobutanol **119** and *cis*-cyclobutanol **120**: (1) the O-H_a and O-$H_{a'}$ distances are not exactly equal (2.58 *versus* 2.71 Å); (2) the biradical intermediates are diastereomerically related when the presence of the ammonium ion is considered, so they react at slightly different rates.
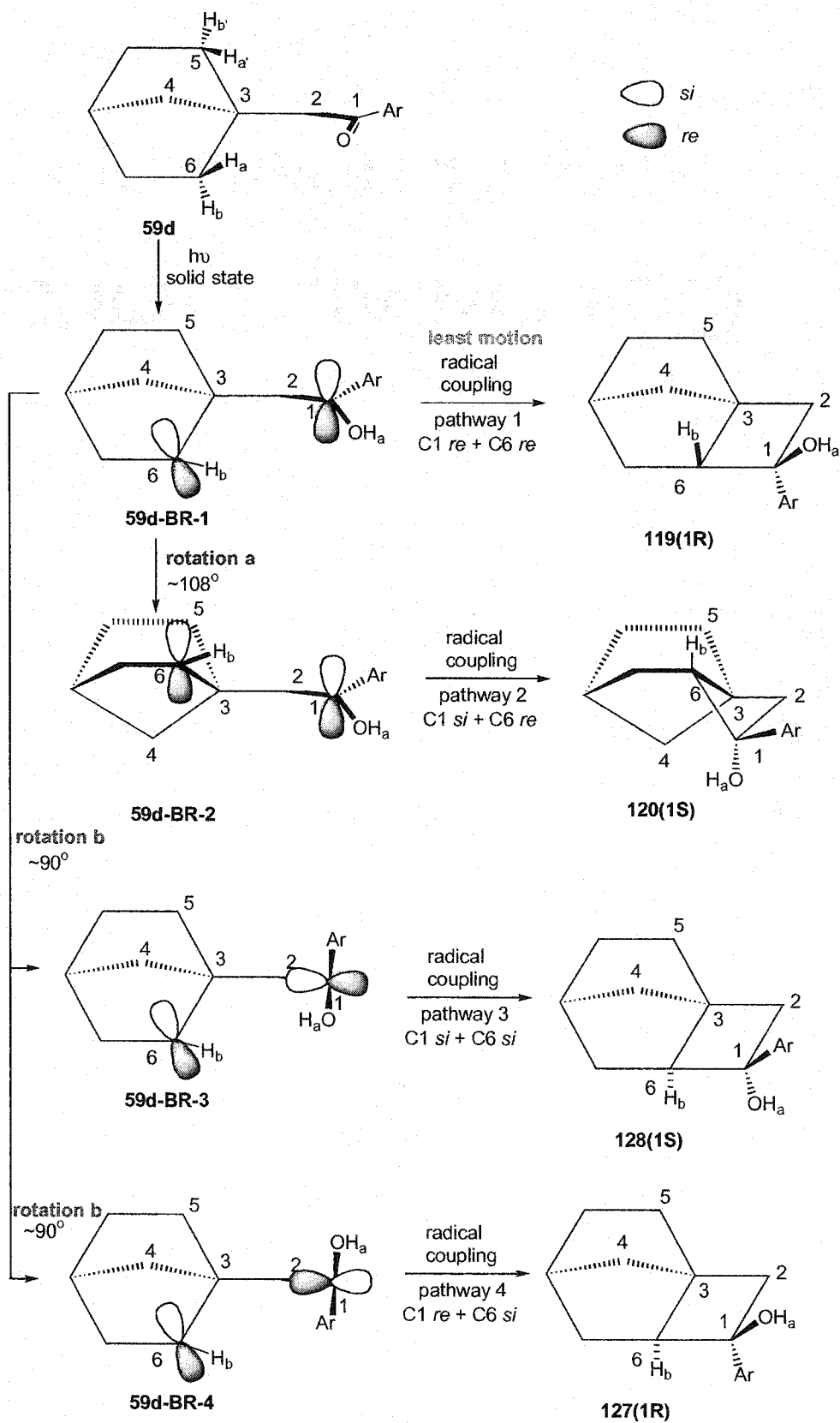
Figure 3.34 The solid state reactivity of salt **59d**

3.6.1.3 Structure-reactivity Analysis of Dimethylated Bicyclo[2.2.1]heptyl Substrate 62a

The X-ray crystal structure of salt **62a** showed that the carbonyl oxygen is situated closer to γ-hydrogen 6H$_a$ than 5H$_{a'}$ (O-6H$_a$, 2.96 Å; O-5H$_{a'}$, 5.08 Å). As a result only γ-hydrogen 6H$_a$ is abstractable. As shown in Figure 3.35, abstraction of γ-hydrogen 6H$_a$ forms biradical **62a-BR-1** upon photolysis. Similar analysis as in the previous sections is shown in Figure 3.35 and indicates that there are four possible pathways for forming a single bond between the two radicals in the intermediate **62a-BR-1**. Pathway 1 involves bond formation between the *re* face of the *p*-orbital lobe at C1 and the *re* face of the *p*-orbital lobe at C6 (C1 *re* + C6 *re*), to give *trans*-cyclobutanol **124(1R)** with the C1(R) absolute configuration. Pathway 2, C1 *re* + C6 *si*, gives *cis*-cyclobutanol **131(1R)** with the C1(R) absolute configuration; pathway 3, C1 *si* + C6 *re*, gives *cis*-cyclobutanol **125(1S)** with the C1(S) absolute configuration; pathway 4, C1 *si* + C6 *si*, gives *trans*-cyclobutanol **132(1S)** with the C1(S) absolute configuration. Among these four possible pathways, pathway 1 involves the least motion (direct radical coupling without rotation (a) or (b)); therefore, *trans*-cyclobutanol **124(1R)** is the topochemically favored photoproduct. In contrast, pathways 2, 3 and 4 require certain molecular motions (rotation (a) and/or rotation (b)) to bring the corresponding *p*-orbital lobes into position for bond formation. Photochemical studies of salt **62a** (section 3.4.3.2) showed that *trans*-cyclobutanol **124** is the dominant photoproduct in the solid state (**124/125** ~ 98/2). This result agrees that the major photoproduct is the topochemically favored *trans*-cyclobutanol **124** *via* pathway 1, and also suggests that rotation (b) in pathway 3 is disfavored to form minor photoproduct **125**. Cyclobutanols **131** and **132** (*via* pathways 2 and 4) were not isolated, and the reason might be: (1) they are highly strained (angle strain) compounds; (2) pathways 2 and 4 are non-topochemical processes involving rotations (a) and/or (b).

Hydrogen abstraction of 5H$_{a'}$ in salt **62a**, followed by biradical coupling, gives *trans*-cyclobutanol **124(1S)** (with direct ring-closure) and *cis*-cyclobutanol **125(1R)** (with rotation (b) and then ring-closure). However, hydrogen abstraction from 5H$_{a'}$ is disallowed because of a high d value (5.08 Å). This accounts for the near-quantitative ee for *trans*-cyclobutanol **124** in the photolysis of salt **62a**. The high ee in the solid state

photolysis of bicyclo[2.2.2]octyl ketones was ascribed to the differentiation in the biradical ring-closure (least motion *versus* rotation b) in section 3.6.1.1; however, the differentiation in hydrogen abstraction (H_a *versus* $H_{a'}$), which is used in bicyclo[2.2.1]heptyl ketones, also could be used in rationalizing the high ee's in bicyclo[2.2.2]octyl ketones.
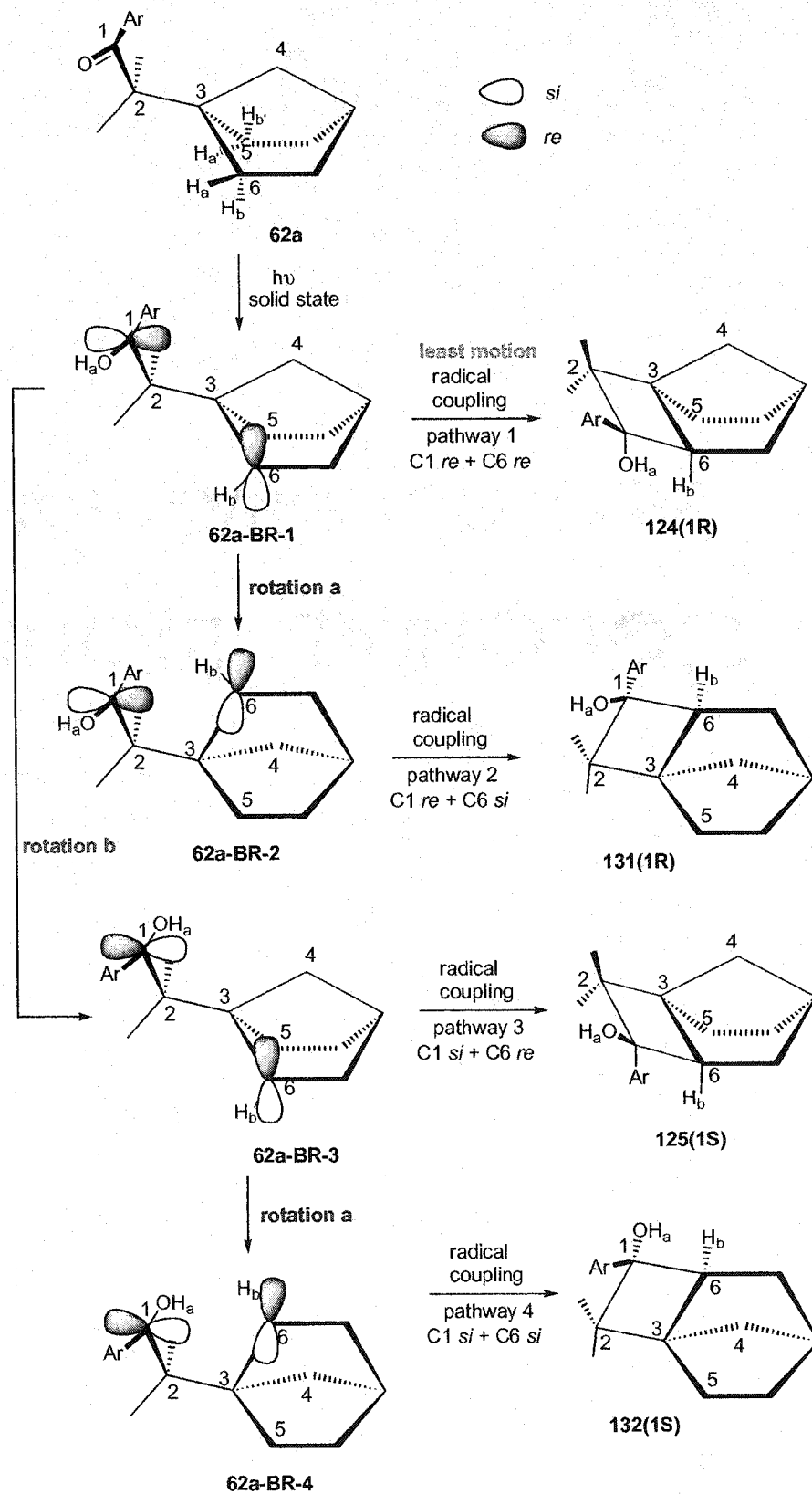
Figure 3.35 The solid state reactivity of salt **62a**

3.6.2 Non-topochemical Control Reactions

The diastereoselectivity and/or enantioselectivity (the sign of rotation for the major photoproduct) in the solid state photolysis of salts **62c**, **62e** and ester **61** in the dimethylated bicyclo[2.2.1]heptyl ketones can not be rationalized using topochemical expectations. No firm evidence can be provided to explain the results. The topochemical analysis of substrates **62e** and **61** followed by non-topochemical speculations will be described in this section. The analysis of salt **62c** is virtually the same as salt **62e** because they are near-mirror-image-related.

The X-ray structure of salt **62e** showed that the carbonyl oxygen is situated closer to γ-hydrogen $6H_a$ than $5H_{a'}$ (O-$6H_a$, 3.11 Å; O-$5H_{a'}$, 3.84 Å). Although a d value of 3.11 Å is significantly greater than the ideal d value of 2.7 ± 0.2 Å, hydrogen abstractions over distances as great as 3.15 Å have been recorded.[101] Assuming that γ-hydrogen $6H_a$ is the only abstractable hydrogen, biradical **62e-BR-1** will be formed upon photolysis as shown in Figure 3.36. Analysis similar to that used in the previous sections is shown in Figure 3.36, which indicates that there are four possible pathways for forming a single bond between the two radical centers in the intermediate **62e-BR-1**. Pathway 1 involves bond formation between the *re* face of the *p*-orbital lobe at C1 and the *re* face of the *p*-orbital lobe at C6 (C1 *re* + C6 *re*), to give *cis*-cyclobutanol **125(1R)** with the C1(R) absolute configuration. Pathway 2, C1 *re* + C6 *si*, gives *trans*-cyclobutanol **132(1R)** with the C1(R) absolute configuration; pathway 3, C1 *si* + C6 *re*, gives *trans*-cyclobutanol **124(1S)** with the C1(S) absolute configuration; pathway 4, C1 *si* + C6 *si*, gives *cis*-cyclobutanol **131(1S)** with the C1(S) absolute configuration. Among these four possible pathways, pathway 1 involves the least motion (direct radical coupling without rotation (a) or (b)); therefore, *trans*-cyclobutanol **125(1R)** is the topochemically favored photoproduct. In contrast, pathways 2, 3 and 4 require certain molecular motions (rotation (a) and/or rotation (b)) to bring the corresponding *p*-orbital lobes into position for bond formation.

Photochemical studies of salt **62e** (section 3.4.3.2) showed that *trans*-cyclobutanol **124** is the dominant photoproduct in the solid state (**124/125** ~ 88/12). This result suggests that pathway 3 (formation of **124(1S)** *via* rotations a and b) is favored over pathway 1 (formation of **125(1R)** without rotations a and b), which is seriously against topochemical

expectations. It was also found that the predicted configurations of photoproduct **124** (using topochemical analysis) were not consistent with the sign of rotation of photoproduct **124** as shown in Table 3.27. Photoproduct **124** was found to be (-), (-), and (+) from the photolysis of salts **62a, 62e, 62c** respectively (Table 3.22), but the predicted absolute configurations were (1R) (from Figure 3.35), (1S) (from Figure 3.36), (1R) (the conformation of **62c** and **62e** are near mirror-image-related, see Figure 3.27). No obvious explanation is available to rationalize these results. Due to the high d value (3.11 Å) in the crystal of salt **62e**, hydrogen abstraction might be very slow and reverse hydrogen transfer might be fast; therefore, the formation of cyclobutanol **125** *via* pathway A would be retarded in the solid state (Figure 3.37). Alternative pathway (B) might be dominant, in which reversible type I cleavage in the crystal might change the conformation (In Figure 3.37: **62e**, the carbonyl oxygen points down → **62e-Ia** → **62e-Ib** → **62e-b**, the carbonyl oxygen points up) so seriously that the d value in **62e-b** are feasible for Norrish type II reaction to form cyclobutanol **124**. Only 1-10 % type I cleavage photoproduct **135** (Figure 3.37: (i) hydrogen transfer to form the aldehyde; (ii) oxidation in the air to form the acid; (iii) treating with diazomethane to form ester **135**) was found by GCMS in the photolysis of all dimethylated bicyclo[2.2.1]heptyl ketones in both solid state and solution. Ester **135** has not been found in the photolysis of bicyclo[2.2.1]heptyl ketones.

Table 3.27 Comparison of the predicted configuration and sign of rotation

substrate	measured sign of rotation $[\alpha]^a$ for photoproduct **124**	predicted absolute configuration at C1 for photoproduct **124**
62a	-	(1R) (from Figure 3.35)
62e	-	(1S) (from Figure 3.36)
62c	+	(1R) (the anion parts of salts **62c** and **62e** are near mirror-image-related)

[a] Signs of rotation were determined at the sodium D-line.
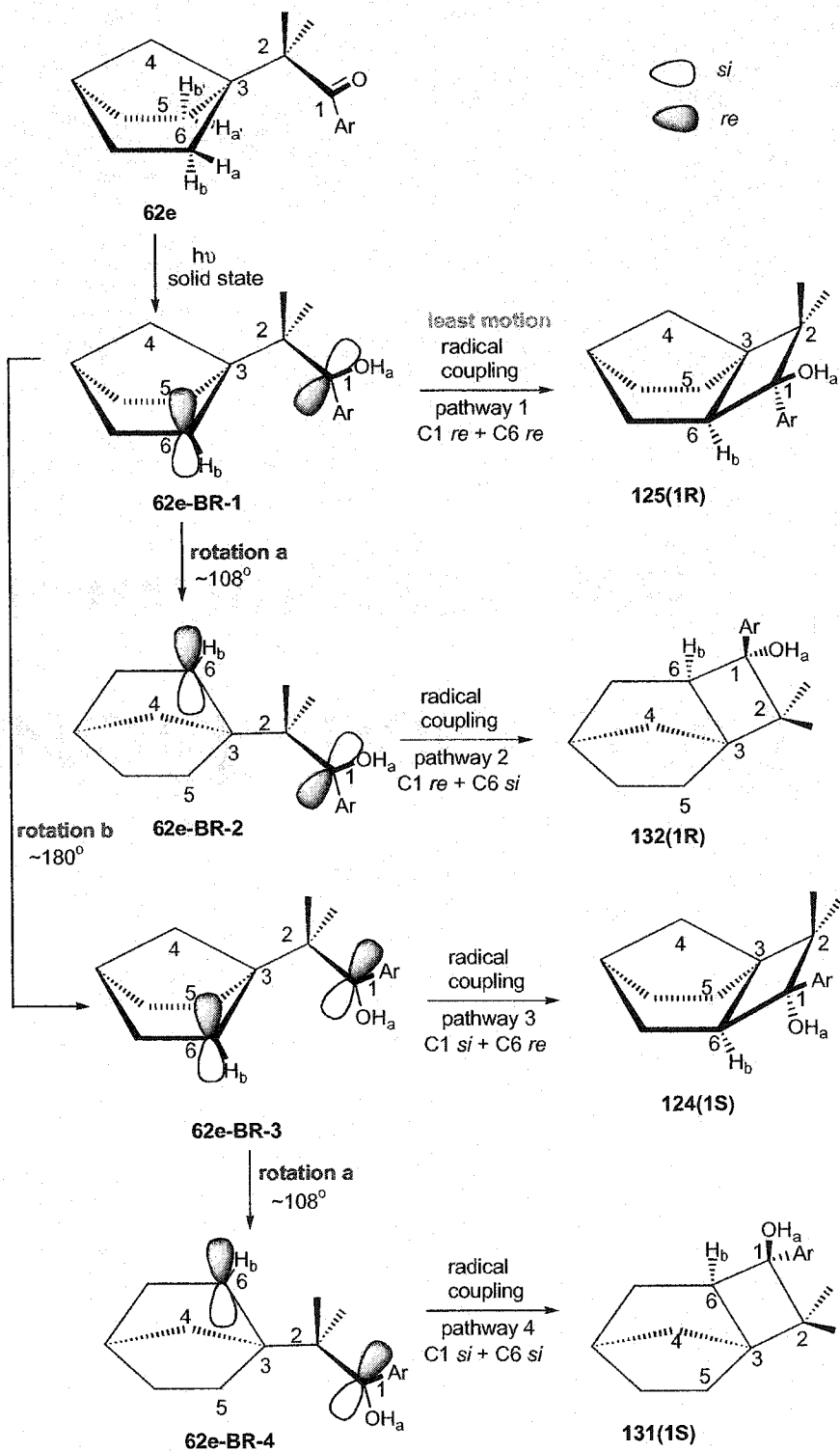
Figure 3.36 The solid state reactivity of salt **62e**
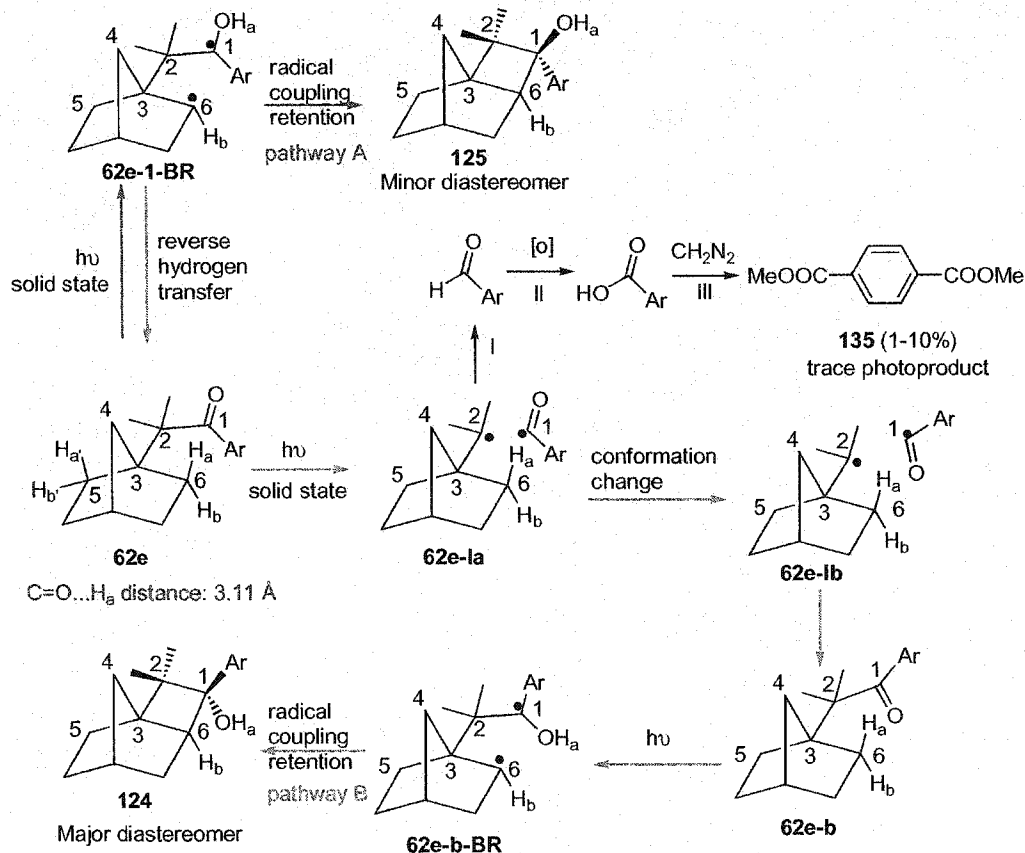
Figure 3.37 Proposed mechanism for salt **62e**

Another compound that behaves in a non-topochemical manner is ester **61**. The X-ray crystal structure of ester **61** shows that the carbonyl oxygen is situated closer to γ hydrogen $4H_{1a}$ at the one-carbon bridge (O-$4H_{1a}$, 2.61 Å; O-$4H_{1a'}$, 3.40 Å). Abstraction of hydrogen $4H_{1a}$ would form cyclobutanols **133** and **134**. However, the MM^+ calculations (Table 3.26) show that both cyclobutanols **133** and **134** are highly strained molecules; therefore, formation of these cyclobutanols should be disfavored as shown in Figure 3.38. Photochemical studies of ester **61** (section 3.3.5) showed that *trans*-cyclobutanol **124** is the dominant photoproduct in the solid state (**124/125** ~ 84/16). Again, there is no clear explanation for the formation of major photoproduct **124** from the photolysis of ester **61** in the solid state. A possible pathway is shown in Figure 3.39. The distance from the carbonyl oxygen to a γ-hydrogen $6H_{2a}$ at a two-carbon bridge is 3.06 Å, and the abstraction of $6H_{2a}$ followed by radical coupling forms cyclobutanols **124** and **125** by the same pathway as salts **62c** and **62e**. Again, due to the high d value (3.06 Å) in the crystal

of ester **61**, hydrogen abstraction might be very slow, and reversible type I cleavage in the crystal (Figure 3.39) might change the conformation so seriously (non-topochemical process, unpredictable) that the d value becomes feasible for the Norrish type II reaction.
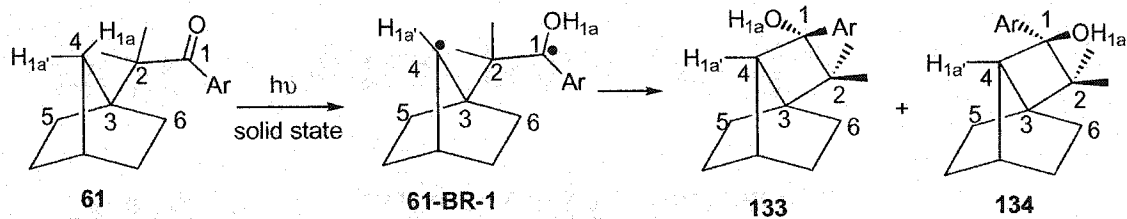
C=O...H_{1a} distance: 2.61 Å

Figure 3.38 The solid state reactivity of ester **61**

C=O...H_{2a} distance: 3.06 Å
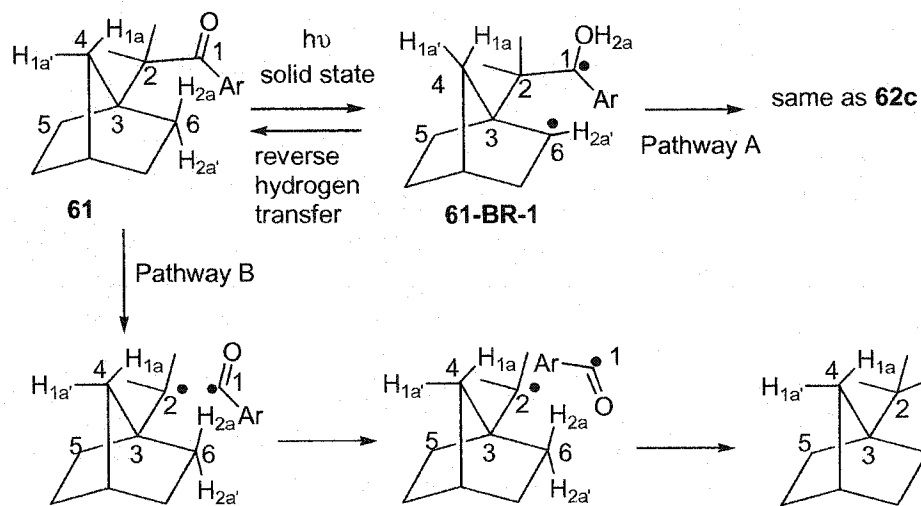
Figure 3.39 The possible pathway for the solid state photolysis of ester **61**

The conformation change *via* a reversible type I reaction must involve large motion. However, large motions during solid state reactions are certainly known. A thermal solid state reaction, illustrated in Figure 3.40, comes from the research of Toda *et al.*[107] When crystals of the thermally labile diallene **136** are heated to 150 °C, a spontaneous electrocyclic rearrangement takes place with dimethylenecyclobutene **137** being formed.
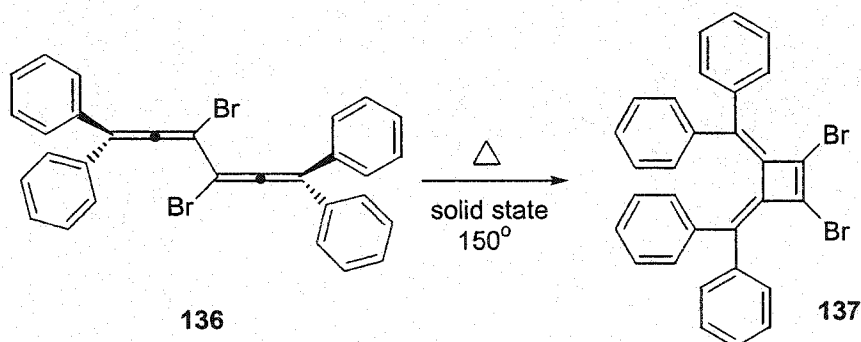
Figure 3.40 Large motions involved in a thermal crystalline state reaction.

To conclude this section, we speculate that the non-topochemical process might become dominant when the hydrogen abstraction parameter d value is significantly greater than the ideal value of 2.7 ± 0.2 Å (For salt **62e**, $O-6H_{2a} = 3.11$ Å; for salt **62c**, $O-6H_{2a} = 3.28$ Å; for ester **61**, $O-6H_{2a} = 3.06$ Å).

3.7 Summary

Solid state unimolecular reactions such as the Norrish/Yang photocyclization, are usually controlled by molecular conformation, since specific intermolecular packing arrangements are generally not required. Because organic molecules generally crystallize in or near their minimum energy conformations, it is a simple and useful matter to use molecular mechanics, which is frequently utilized in the Scheffer group,[30] to search minimum energy conformations, and thereby make predictions concerning the probable success of hypothetical type II reactions in crystals. My research project was also guided by conducting molecular mechanics calculations and comparing them with the data pool (molecular mechanics calculations and X-ray structural data) within the group.

Using molecular mechanics calculations, it was found that the distances from the carbonyl oxygen to γ-hydrogens H_a and $H_{a'}$ are 2.71 and 3.54 Å respectively in the lowest energy conformation (**55-1**) of bicyclo[2.2.2]octyl ketone **55** (Figure 3.41). It is little wonder that the ee's are high for most salts **56** of the corresponding acid. In contrast, MM^+ calculations showed that bicyclo[2.2.1]heptyl ketone **58** has a C_S-symmetric minimum energy conformation (**58-1** in Figure 3.41) in which the carbonyl oxygen is equidistant (**d** = 2.59 Å) from the enantiotopic γ-hydrogens H_a and $H_{a'}$ on the 2-carbon

bridges and much further (d = 4.80 Å) from the γ-hydrogens on the 1-carbon bridge. Such a conformation is poorly suited for high levels of asymmetric induction, since this requires selective abstraction of H_a over $H_{a'}$. The asymmetric induction studies are in agreement with this expectation, since low ee's (average ~35 %) were obtained in the solid state photolysis of bicyclo[2.2.1]heptyl ketones. In seeking ways to achieve discrimination between γ-hydrogens H_a and $H_{a'}$, ester **61** was investigated by molecular mechanics. This showed that placing two methyl groups next to the carbonyl group should have the desired effect, since the minimum energy conformation (**61-1**) of the methylated analogue (Figure 3.41) situates the ketone oxygen much closer to H_a than $H_{a'}$ (2.59 Å *versus* 5.07 Å). Again, the asymmetric induction studies are in agreement with this in that near-quantitative ee's were obtained in the photolysis of dimethylated bicyclo[2.2.1]heptyl ketones. Overall, therefore, molecular mechanics predicts that derivatives of ester **61** (salt **62**) have a much better chance of giving high levels of asymmetric induction than those from ester **58**. In this way, molecular mechanics serves as a basis for crystal engineering. Although the multistep synthesis of dimethylated bicyclo[2.2.1]heptyl ketones was challenging, MM$^+$ calculations indicated a good opportunity for achieving excellent ee for the dimethylated bicyclo[2.2.1]heptyl ketones before all laboratory work began. Moreover, high diastereoselectivity was achieved as an additional bonus.
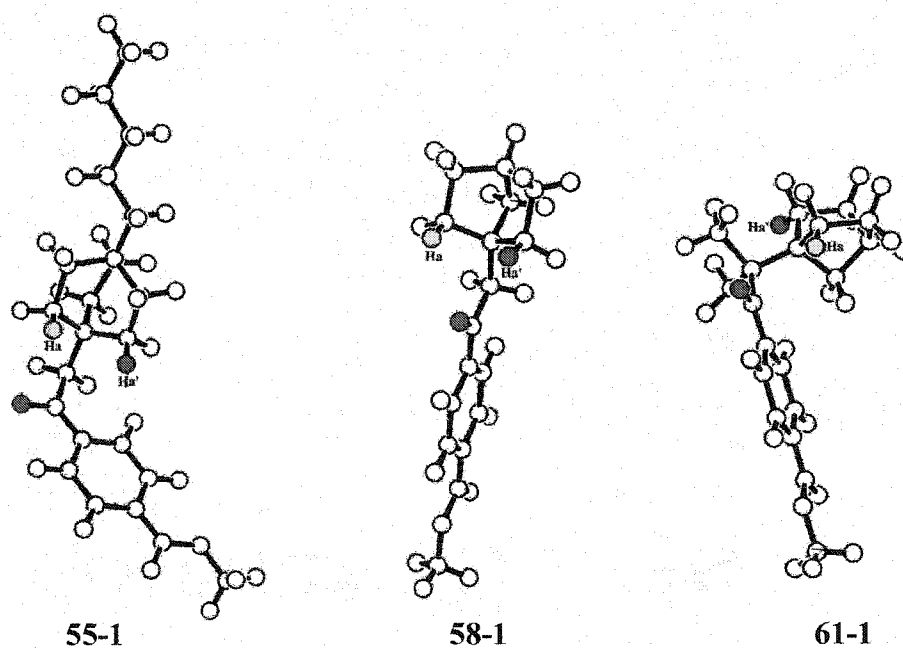
55-1   58-1   61-1

Figure 3.41 The lowest energy conformations (**55-1, 58-1, 61-1**) of esters **55, 58** and **61** identified by MM$^+$ calculation. The carbonyl oxygen is colored red, γ-hydrogen H_a (close to oxygen) green, γ-hydrogen $H_{a'}$ (enantiotopic with H_a) blue.

MM$^+$ calculations did successfully predict molecular conformations in the solid state. However, exceptions do occur, because the second or the third lowest energy conformation is sometimes adopted in the crystalline state. This is probably one of the reasons why some salts lead to low ee's while others lead to near-quantitative ee's, a typical result in solid state asymmetric induction studies. However, a large commercially available chiral amine pool can be (and has been, for my substrates) tested to find some chiral amine salts with outstanding ee and/or de. Molecular mechanics, as a crystal engineering tool, is truly useful and successful in achieving high levels of enantioselectivity and diastereoselectivity for the Yang photocyclization of bicyclic aryl ketones.

Previous studies[30,79] in the Scheffer group showed that the photoreactions in Figure 3.42(1-3) gave a clean single product, and the photoreactions in Figure 3.42(4-6) gave a mixture of photoproducts. These results suggest that rotation around the C_1-C_2 bond is

seriously hindered when the α-carbon C_2 is a quaternary carbon. The dimethyl group can not only change the conformation (change the C=O---H_a and C=O---$H_{a'}$ distances) to achieve high enantioselectivity, but also can hinder the rotation around C_1-C_2 bond to achieve high diastereoselectivity.
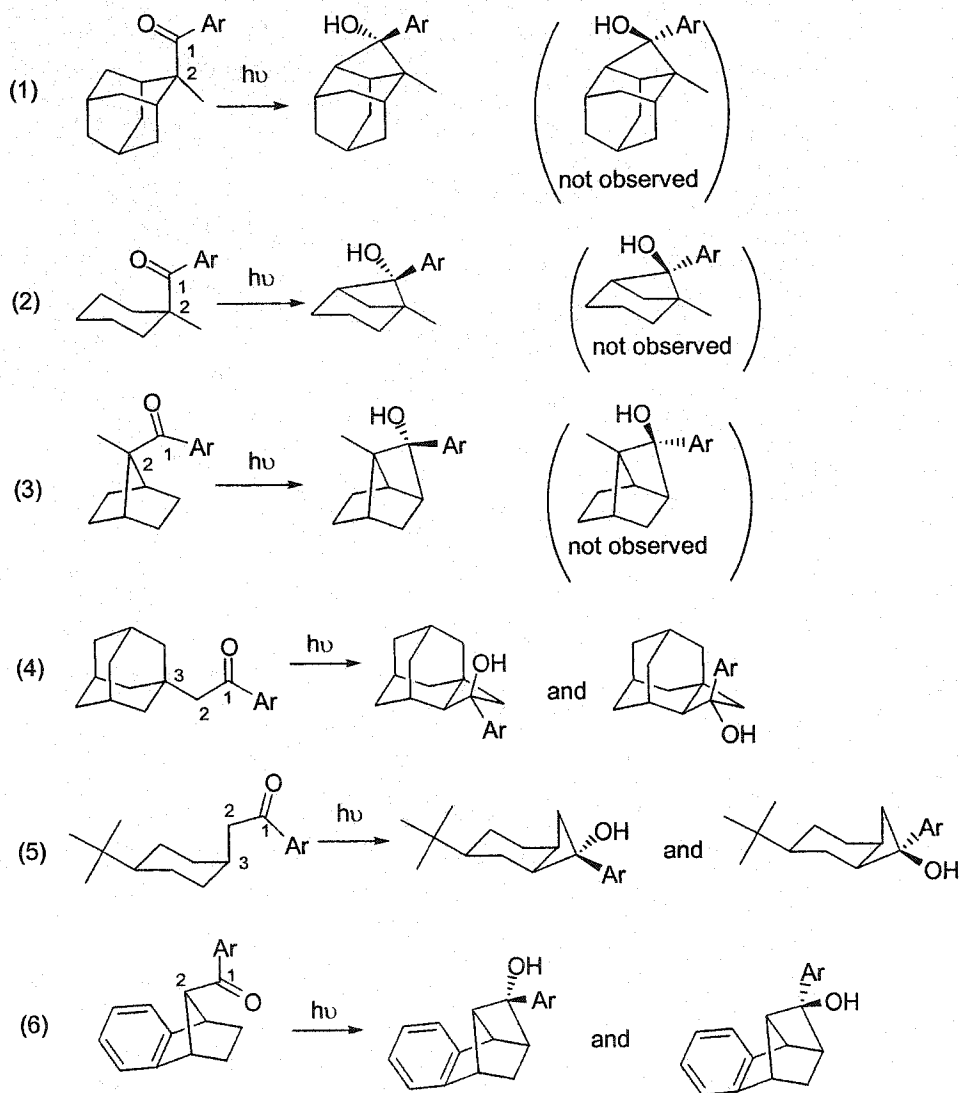
Figure 3.42 Norrish type II reactions studied previously in the Scheffer group

As with previous studies in the Scheffer group,[68] in solution photolysis, the diastereoselectivity is low compared to that observed in the solid state, and enantioselectivity is completely lost, because rotations (a) and (b) become more feasible in solution and/or because unique chiral conformation that is present in the crystal does not necessarily exist in solution (or if it does, would not be necessarily kept intact during

the photolysis). The solid state photostable substrates (with high D and β values) did react in solution phase photolyses, because the conformations with high D and β values in the solid state are not necessarily the same as those in solution, or if the same, would not be immobilized in solution.

Also in accord with previous studies,[30,92] some solid state reactivity could not be explained by topochemical control and the conformation of the starting material only. Non-topochemical processes have been found in this research and their full understanding is currently a matter of speculation. Norrish type II solid state photochemical reactivity is the overall result of the competition between the following processes: (1) γ-hydrogen abstraction (parameters: d, ω, Δ, θ); (2) Yang cyclization (parameters D and β); (3) Norrish type II cleavage (parameters φ_1 and φ_4); (4) reverse hydrogen transfer; (5) the strain energy of the photoproducts; (6) single electron transfer (as in oxoamide substrates); (7) competing type I cleavage; (8) crystal disorder, crystal defects (before photolysis); (9) crystal breakdown (after photolysis); (10) molecular/atomic motion in the crystal (e.g. rotations (a) and (b) described above). Research in solid state chemistry and crystal engineering is still in its infancy. This is both an opportunity and a challenge for the chemistry community.

EXPERIMENTAL

Chapter 4 Synthesis of Starting Materials

4.1 General Considerations

Infrared Spectra (IR)

Infrared spectra were recorded on a Perkin-Elmer 1710 Fourier-transform spectrometer. Solid samples (~2 mg) were ground with IR grade KBr (100-200 mg) in an agate mortar and pelleted in an evacuated die (Perkin-Elmer 186-0002) with a laboratory press (Carver, model B) at 17,000 psi. Liquid samples were analyzed either neat as thin films between two sodium chloride plates or as chloroform solutions in a sodium chloride cell. The positions of selected absorption maxima (ν_{max}) are reported in units of cm^{-1}.

Melting Points (mp)

Melting points were determined on a Fisher-Johns hot stage apparatus and are uncorrected. When recrystallized samples were measured, the solvent of recrystallization is given in parenthesis.

Nuclear Magnetic Resonance (NMR) Spectra

Proton nuclear magnetic resonance (^{1}H NMR) spectra were recorded in deuterated solvents as noted. Data were collected on the following instruments: Bruker AC-200 (200 MHz), Bruker AV-300 (300 MHz), Bruker WH-400 (400 MHz), and Bruker AV-400 (400 MHz). Chemical shifts (δ) are reported in parts per million (ppm) and are referenced to the residual ^{1}H solvent signals with tetramethylsilane (δ 0.00 ppm) as an external standard: chloroform (7.24 ppm), benzene (7.16 ppm), dichloromethane (5.32 ppm), methanol (3.30 ppm), and acetonitrile (1.93 ppm). The signal multiplicity, coupling constants, number of hydrogen atoms, and assignments are given in parentheses. Multiplicities are abbreviated as follows: multiplet (m), singlet (s), doublet (d), triplet (t), quartet (q), quintet (quint), heptet (hept), and broad (br). Nuclear Overhauser Enhancement (NOE) spectra were acquired on the Bruker AV-400 spectrometer. ^{1}H-^{1}H correlation spectroscopy (COSY) was conducted on the Bruker AV-400 spectrometer.

Two-dimensional Nuclear Overhauser Enhancement Spectroscopy (**NOESY**) was conducted on the Bruker AV-400 spectrometer.

Carbon nuclear magnetic resonance (^{13}**C NMR**) spectra were recorded on the following instruments: Bruker AC-200 (50.3 MHz), Bruker AV-300 (75.4 MHz), Bruker AV-400 (100.5 MHz), Bruker AM-400 (100.5 MHz) spectrometers. All experiments were conducted using broadband ^{1}H decoupling. Chemical shifts (δ) are reported in ppm and are referenced to the center of the solvent multiplet with tetramethylsilane (δ 0.0 ppm) as an external standard: chloroform (77.0 ppm), benzene (128.0 ppm), dichloromethane (54.0 ppm), methanol (49.0 ppm), and acetonitrile (118.2 ppm). Some spectra are supported by data from the Attached Proton Test (**APT**). Where these are given, (-) denotes a negative APT peak corresponding to a methine (CH) or methyl (CH_3) carbon centre, while (+) corresponds to a quaternary (C) or methylene (CH_2) carbon centre.

Two dimensional ^{13}C-^{1}H correlation spectra were obtained on the Bruker AV-400 instrument using the Heteronuclear Multiple Quantum Coherence (**HMQC**) experiment for one-bond correlations and the Heteronuclear Multiple Bond Connectivity (**HMBC**) experiment for long-range connectivities.

Mass Spectra (MS)

Low and high resolution mass spectra (**LRMS** and **HRMS**) were recorded on a Kratos MS 50 instrument using electron impact (EI) ionization at 70 eV or on a Kratos MS 80 spectrometer using desorption chemical ionization (DCI) with the ionization gas noted. The masses of organic salts were determined on a Kratos IIHQ hybrid mass spectrometer by recording liquid secondary ionization mass spectra (LSIMS), or a Bruker Esquire~LC (low resolution) or a Micromass LCT (high resolution) spectrometer using electrospray ionization (ESI). Analyses were performed by in-house technicians under the supervision of Dr. G. Eigendorf or Dr. Yun Ling. Low resolution mass spectra and GC/MS data were also recorded on an Agilent 5973N mass selective detector, attached to a Agilent 6890+ gas chromatograph, using electron impact (EI) ionization at 70 eV.

Mass to charge ratios (m/e) are given, with relative intensities in parentheses, where applicable. Molecular ions are designated as M^+.

Ultraviolet-Visible Spectra (UV/VIS)

UV/VIS spectra were recorded on a Perkin-Elmer Lambda-4B UV/VIS spectrometer in the spectral grade solvents indicated. Absorption maxima (λ_{max}) are reported in nanometers (nm), with molar extinction coefficients (ε) reported in parentheses in units of $M^{-1}cm^{-1}$.

Microanalysis (Anal.)

Elemental analyses were obtained for new compounds when possible. These were performed in-house by Mr. Peter Borda or Minaz Lakha, under the supervision of Dr. Yun Ling, on a Carlo Erba CHN Model 1106 analyzer.

Crystallography

Single crystal X-ray analysis was performed either in-house on a Rigaku AFC6S four-circle diffractometer (Cu-Kα or Mo-Kα radiation) or a Rigaku AFC7 four-circle diffractometer equipped with a DSC Quantum CCD detector (Mo-Kα radiation), or externally (Dr. Lucia Maini under the supervision of Professor Dario Braga, Department of Chemistry, University of Bologna, Italy; and Dr. Mark Botoshansky under the supervision of Professor Menahem Kaftory, Dept of Chemistry, Technion, Haifa, Israel). Data collection and structural refinements were conducted by Dr. Brian Patrick. Some structures were refined by Keyan Wang, under the supervision of Dr. Brian Patrick. Structures are presented as ORTEP drawings at the 50% probability level. Geometric parameters for hydrogen abstraction, cleavage and cyclization were measured by WinGX v1.64.05. The average error for the parameters is within 0.01 Å (for the distances) or within 1° (for the angles).

Gas Chromatography (GC)

Gas chromatographic analyses in a helium carrier gas were performed on a Hewlett-Packard 5890A gas chromatograph fitted with a flame ionization detector, or on an Agilent 6890 gas chromatograph, equipped with an Agilent 5970N mass selective

detector. Data were collected on a Hewlett-Packard 3392A integrator (5890) or using Agilent's Chemstation software (6890). The following Hewlett-Packard fused-silica capillary columns were used: HP-5MS (30 m × 0.25 mm × 0.25 μm ID), HP-5 (30 m × 0.25 mm × 0.25 μm ID), and HP-35 (15 m × 0.25 mm × 0.25 μm). Analyses were run with a split injection port (split ratios between 25:1 and 100:1) and column head pressures ranging from 100 kPa to 250 kPa.

High Performance Liquid Chromatography (HPLC)

High performance liquid chromatography (HPLC) was performed on a Waters 600E system coupled to either a Waters 486 tunable UV detector or a Waters 994 photodiode array detector under the conditions indicated. Enantiomeric excesses (ee) were determined using a Chiralcel OD™, Chiralpak AS™, or Chiralpak AD™ column (250mm×4.6mm) from Chiral Technologies, Inc., with a hexanes:IPA eluent. Data were collected using the Waters Maxima software package.

Optical Rotations

Optical rotation data was recorded on a Jasco P-1010 polarimeter at room temperature at the sodium D-line (589.3 nm).

Silica Gel Chromatography

Analytical thin layer chromatography (TLC) was carried out on commercial pre-coated silica gel plates (E. Merck, type 5554). Preparative chromatography was performed using either the flash column method with Merck 9385 or Silicycle silica gel (particle size 230-400 mesh), or by radial chromatography on a Chromatotron (Harrison Research, model 7924T) using plates of 1 or 2 mm thickness prepared from EM Science silica gel 60 PF254 with gypsum (7749-3).

Solvents and Reagents

Tetrahydrofuran (THF) and diethyl ether were heated to reflux over the sodium ketyl of benzophenone under an argon atmosphere and distilled prior to use. Anhydrous

dichoromethane and benzene were obtained by refluxing over calcium hydride under an argon atmosphere and distilling prior to use. Unless otherwise noted, all other solvents and reagents were used without further treatment, and all the reactions were conducted under a dry argon atmosphere in oven or flame-dried glassware.

4.2 Synthesis of α-Oxoamides 38, 66, 67 and 68

4.2.1 Preparation of α-Oxoamides 38 and 66

Methyl 4-acetylbenzoate (64)
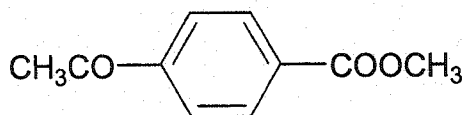
64

Following a modification of the procedure of Gerlach and Wollmann,[86] a solution of 4-bromoacetophenone (63) (10.0 g, 50.3 mmol), [1,1'-bis(diphenylphosphino)-ferrocene]dichloropalladium (II) complex with dichloromethane (1:1) (1.22 g, 1.50 mmol), in methanol (50mL), DMF (100 mL) and diisopropylethylamine (17.5 mL, 10.5 mmol) was purged for 10 min with gaseous CO. The solution was stirred under a positive pressure of CO for 5 h at 70 °C. The resulting dark red mixture was quenched with 0.5 M HCl (300 mL) and extracted with benzene (3 × 100 mL). The combined extracts were washed with sat. aq. NaCl (2 × 100 mL), dried (Na$_2$SO$_4$) and evaporated to dryness. Purification by column chromatography on silica gel (petroleum ether-diethyl ether, 5:1) afforded 8.2 g (93 %) of methyl 4-acetylbenzoate (64) as a white solid.

mp: 94-95 °C. (Lit.[108] mp 95.0-95.5 °C)

^{1}H NMR (400 MHz, CDCl$_3$): δ 8.10 (d, J = 8.5 Hz, 2H), 7.98 (d, J = 8.5 Hz, 2H), 3.93 (s, 3H), 2.62 (s, 3H).

^{13}C NMR (75 MHz, CDCl$_3$): δ 197.48, 166.19, 140.22, 133.88, 129.80, 128.17, 52.42, 26.83.

IR (KBr pellet): ν 3016, 2961, 1723, 1679, 1572, 1502, 1437, 1409, 1359, 1284, 1195, 1134, 1016, 957, 870, 851, 833, 771, 744, 698, 615, 593, 530 cm^{-1}.

LRMS (EI): *m/z* (relative intensity) 178 (M$^+$, 13.9), 163 (100), 147 (21.1), 135 (26.1), 120 (6.6), 103 (13.8), 91 (10.0), 76 (18.3).

HRMS (EI): *m/z* calcd for $C_{10}H_{10}O_3$ 178.0630, found 178.0633.

Anal. Calcd for $C_{10}H_{10}O_3$: C 67.41, H 5.66. Found: C 67.71, H 5.74.

4-(Methoxycarbonyl)-α-oxo-benzeneacetic acid (65)

65
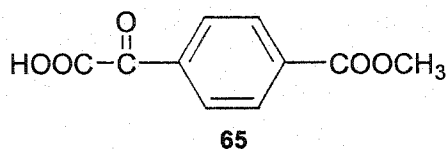
A solution of methyl 4-acetylbenzoate (**64**) (2.0 g, 11.2 mmol) in pyridine (50 mL) containing selenium dioxide (2.0 g, 18.0 mmol) was heated to be refluxing under N_2 at 100 °C for 3.5 h. The precipitate was removed by filtration and the filtrate was evaporated. The residue was neutralized with 1 M HCl (100 mL). The mixture was extracted with Et_2O (3 × 100 mL). The combined ethereal extracts were washed with water and extracted with 1N sodium bicarbonate (3 × 50 mL). After washing with diethyl ether (50 mL), the aqueous layer was acidified with concentrated hydrochloric acid, causing the precipitation of a white solid. The suspension was extracted with diethyl ether (3 × 100 mL) and the ethereal layers were washed with water (50 mL), brine (50 mL) and dried (Na_2SO_4). The solvent was removed *in vacuo* to yield crude product. Recrystallization from benzene gave 2.05 g (88 %) of 4-(methoxycarbonyl)-α-oxo-benzeneacetic acid (**65**) as a white solid.

mp 99-101 °C.

^{1}H NMR (CD$_3$CN, 300 MHz): δ 8.14 (m, 4H), 3.91 (s, 3H).

^{13}C NMR (CD$_3$CN, 75 MHz): δ 187.12, 163.96, 163.33, 136.66, 136.41, 131.18, 130.62, 53.21.

IR (KBr pellet): ν 3506 (br), 1729, 1680 (d), 1441, 1409, 1284, 1222, 1115, 753 cm^{-1}.

LRMS (DCI$^+$, isobutane): *m/z* (relative intensity) 209 (M$^+$+1, 34.8), 181 (100), 163 (56.3), 149 (58.2), 121 (5.9), 103 (3.1), 76 (1.3).

HRMS (DCI$^+$, isobutane): *m/z* calcd for C$_{10}$H$_9$O$_5$ (M$^+$+1) 209.0450, found 209.0446.

Anal. Calcd for C$_{10}$H$_8$O$_5$: C 57.70, H 3.87. Found: C 57.70, H 3.89.

Methyl *N,N'*-bis(1-methylethyl)-α-oxo-benzeneacetamide-4-carboxylate (**38**)

38
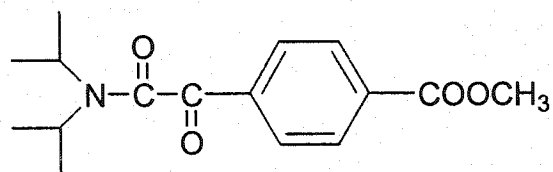
Oxalyl chloride (12.2 g, 8.4 mL, 96 mmol) was added dropwise to a cold (-5 °C) solution of compound **65** (2.0 g, 9.6 mmol) and DMF (0.7 g, 0.70 mL, 9.6 mmol) in anhydrous THF (30 mL). The solution was stirred for 2 h under N$_2$ at room temperature. Unreacted oxalyl chloride along with DMF and THF were removed *in vacuo* and the resulting yellow solid residue dissolved in anhydrous CH$_2$Cl$_2$ (30 mL). Diisopropylamine was added dropwise at –5 °C under N$_2$ and the resulting mixture stirred at room temperature for 2 h. The reaction was quenched by addition of 1 M HCl (40 mL), the layers separated, and the aqueous layer further extracted with CH$_2$Cl$_2$ (3 × 100 mL). The organic layers were combined, washed with brine (2 × 50 mL) and H$_2$O (2 × 50 mL), and dried (Na$_2$SO$_4$). Removal of the solvent *in vacuo* followed by silica gel column chromatography of the residue (petroleum ether-ethyl acetate, 9:1) afforded 2.52 g (90 %) of amide **38** as a light yellow solid.

mp 128-129 °C. (needles from diethyl ether)

UV (CH$_3$OH): λ 204.9 (1.72×10^4), 255.0 (1.56×10^4), 360.1 (226) nm (M^{-1}cm^{-1}).

^{1}H NMR (CDCl$_3$, 400 MHz): δ 8.14 (d, J = 8.2 Hz, 2H), 7.97 (d, J = 8.2 Hz, 2H), 3.93 (s, 3H), 3.67-3.55 (m, 2H), 1.56 (d, J = 6.9 Hz, 6H), 1.15 (d, J = 6.6 Hz, 6H).

^{13}C NMR (CDCl$_3$, 75 MHz): δ 190.05, 166.32, 165.97, 136.53, 134.92, 130.07, 129.39, 52.55, 50.20, 46.20, 20.57, 20.26.

IR (KBr pellet): ν 2968, 1722, 1682, 1634, 1444, 1372, 1282, 1232, 1107, 730 cm^{-1}.

LRMS (EI) *m/z* (relative intensity) 291 (M$^+$, 0.66), 260 (4.9), 163 (35.4), 135 (10.6), 128 (71.0), 104 (11.6), 86 (100), 76 (11.0).

HRMS (EI) *m/z* calcd for C$_{16}$H$_{21}$NO$_4$ 291.1471, found 291.1469.

Anal. Calcd for C$_{16}$H$_{21}$NO$_4$: C 65.96, H 7.27, N 4.81. Found: C 66.07, H 7.38, N 4.75.

This structure was confirmed by X-ray crystallographic analysis

Habit	colorless needles
Space group	$P\bar{1}$
a, Å	6.1660(5)
b, Å	11.084(1)
c, Å	24.163(2)
α (°)	90.06(1)
β (°)	93.14(1)
γ (°)	100.60(1)
Z	4
R	0.121

N,N'-Bis(1-methylethyl)-α-oxo-benzeneacetamide-4-carboxylic acid (66)
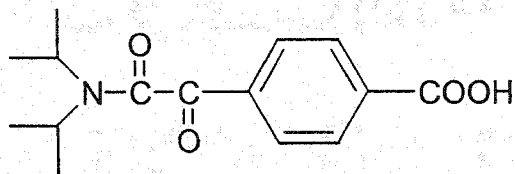
66

A solution of compound **38** (316 mg, 1.09 mmol) in methanol (10 mL) was added to a solution of lithium hydroxide monohydrate (230 mg, 5.4 mmol) in water (30 mL). The resulting solution was stirred for 0.5 h at room temperature. The solution was acidified with concentrated HCl (3 mL) and extracted with Et_2O (3 × 50 mL). The combined extracts were washed with brine (2 × 30 mL), dried (Na_2SO_4) and concentrated *in vacuo* to afford 300 mg (99 %) of acid **66** as a light yellow solid.

mp 203-205 °C.

^{1}H NMR (CD_3OD, 400 MHz): δ 8.20 (d, J = 8.6 Hz, 2H), 8.00 (d, J = 8.6 Hz, 2H), 3.70 (m, 2H), 1.56 (d, J = 6.8 Hz, 6H), 1.20 (d, J = 6.6 Hz, 6H).

^{13}C NMR (CD_3OD, 100 MHz): δ 191.46, 168.41, 168.25, 137.44, 131.44, 130.41, 52.16, 47.52, 20.49.

IR (KBr pellet): ν 2992, 1700, 1686, 1635, 1572, 1504, 1474, 1449, 1419, 1376, 1348, 1225, 1210, 1120, 992, 745, 730 cm^{-1}.

LRMS (EI$^+$) *m/z* (relative intensity) 277 (M$^+$, 3.4), 233 (2.4), 192 (3.6), 149 (48.6), 128 (100), 103 (3.0), 86 (75), 65 (7.4).

HRMS (EI$^+$) *m/z* calcd for $C_{15}H_{19}NO_4$ 277.1314, found 277.1311.

Anal. Calcd for $C_{15}H_{19}NO_4$: C 64.97, H 6.91, N 5.05. Found: C 65.12, H 6.93, N 5.15.

4.2.2 Preparation of α-Oxoamide Salts 67

L-Prolinamide salt (67a)
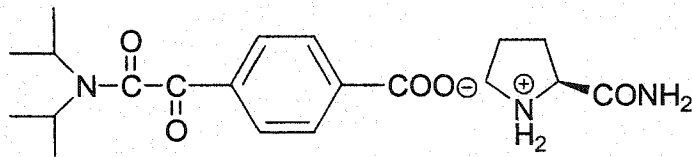
67a

A solution of acid **66** (459 mg, 1.66 mmol) in Et$_2$O (50 mL) was added with stirring to a solution of L-prolinamide (198 mg, 1.74 mmol) in Et$_2$O (100 mL). Stirring was continued for 1 h, after which time the precipitate that had formed (596 mg, 92 %) was filtered and washed with Et$_2$O. Recrystallization from MeOH afforded salt **67a** as pale yellow plates.

mp 202-206 °C

UV (CH$_3$OH): λ 205.0 (2.02×10^4), 259.9 (1.55×10^4), 349.9 (302) nm (M^{-1}cm^{-1}).

^{1}H NMR (CD$_3$OD, 300 MHz): δ 8.09 (d, J = 8.2 Hz, 2H), 7.91 (d, J = 8.2 Hz, 2H), 4.26 (m, 1H), 3.70 (m, 2H), 3.33 (m, 2H), 2.41 (m, 1H), 2.01 (m, 3H), 1.56 (d, J = 6.8 Hz, 6H), 1.18 (d, J = 6.6 Hz, 6H).

^{13}C NMR (CD$_3$OD, 75 MHz): δ 192.06, 173.21, 172.47, 168.85, 144.70, 135.46, 130.84, 130.09, 60.87, 52.23, 47.27, 31.18, 25.25, 20.44.

IR (KBr pellet): ν 3346, 2973, 1715, 1681, 1641, 1597, 1557, 1449, 1376, 1231, 1135, 993, 826, 754, 744 cm^{-1}.

LRMS (FAB: +LSIMS, matrix, thioglycerol): m/z 392 (M$^+$+1, 9.8), 278 (100), 236 (31.3), 149 (48.4), 115 (42.9), 91 (10.1).

HRMS (FAB: +LSIMS, matrix, thioglycerol): *m/z* calcd for $C_{20}H_{30}N_3O_5$ ($M^+ + 1$) 392.2185, found 392.2190.

Anal. Calcd for $C_{20}H_{29}N_3O_5$: C 61.36, H 7.47, N 10.73. Found: C 61.07, H 7.43, N 10.88.

This structure was confirmed by X-ray crystallographic analysis

Habit	colorless plates
Space group	*P2₁*
a, Å	6.9118(3)
b, Å	7.4585(3)
c, Å	20.6344(9)
α (°)	90
β (°)	97.894(2)
γ (°)	90
Z	2
R	0.051

R-(+)-Bornylamine salt (67b)
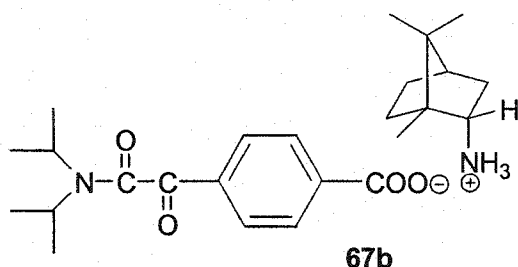
67b

A solution of acid **66** (83 mg, 0.30 mmol) in Et_2O (15 mL) was added to a solution of R-(+)-bornylamine (46 mg, 0.30 mmol) in Et_2O (5 mL). The cloudy solution was stirred for 1 h, after which time the precipitate that had formed was filtered, washed with Et_2O and dried *in vacuo* to afford salt **67b** (120 mg, 93 %) as an off-white powder. Recrystallization from MeOH afforded off-white needles.

mp 183-185 °C

UV (CH$_3$OH): λ 205.0 (2.31 × 10^4), 260.0 (1.75 × 10^4), 350.0 (276) nm (M^{-1}cm^{-1}).

^{1}H NMR (CD$_3$OD, 400 MHz): δ 8.08 (d, J = 8.3 Hz, 2H), 7.91 (d, J = 8.3 Hz, 2H), 3.70 (m, 2H), 3.38 (d × d, J_1 = 4.1 Hz, J_2 = 10.8 Hz, 1H), 2.32 (m, 1H), 1.85 (m, 1H), 1.74 (d, J = 4.5 Hz, 1H), 1.56 (d, J = 6.8 Hz, 6H), 1.52 (m, 2H), 1.31 (m, 1H), 1.18 (d, J = 6.6 Hz, 6H), 1.10 (d × d, J_1 = 4.1 Hz, J_2 = 13.6 Hz, 1H), 0.96 (s, 3H), 0.94 (s, 3H), 0.93 (s, 3H).

^{13}C NMR (CD$_3$OD, 75 MHz): δ 192.03 (+), 173.36 (+), 168.84 (+), 145.23 (+), 135.31 (+), 130.24 (-), 129.86 (-), 57.93 (-), 52.31 (-), 50.04 (+), 49.18 (+), 47.60 (-), 45.80 (-), 35.40 (+), 28.52 (+), 27.97 (+), 20.58 (-), 20.49 (-), 19.81 (-), 18.70 (-), 13.32 (-).

IR (KBr pellet): ν 3851 (br), 2961, 2199, 1675, 1640, 1585, 1542, 1460, 1374, 1236, 995, 824, 742 cm^{-1}.

LRMS (FAB: +LSIMS, matrix: thioglyerol): m/z (relative intensity) 431 (M$^+$ + 1, 15.5), 278 (12.4), 236 (5.3), 154 (100), 149 (11.2), 137 (21.4), 81 (11.0).

HRMS (FAB: +LSIMS, matrix, thioglyerol): m/z calcd for C$_{25}$H$_{39}$N$_2$O$_4$ (M$^+$ + 1): 431.2912, found 431.2905.

Anal. Calcd for C$_{25}$H$_{38}$N$_2$O$_4$: C, 69.74; H, 8.90; N 6.51. Found: C, 69.73; H, 8.93; N, 6.40.

R-(-)-1-Cyclohexylethylamine salt (67c)
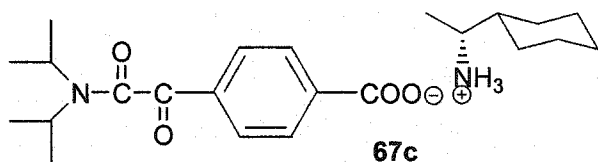
67c

A solution of acid **66** (83 mg, 0.30 mmol) in Et$_2$O (15 mL) was added to a solution of R-(-)-1-cyclohexylethylamine (38 mg, 0.30 mmol) in Et$_2$O (5 mL). The cloudy solution was stirred for 1 h, after which time the precipitate that had formed was filtered, washed with Et$_2$O and dried *in vacuo* to afford salt **67c** (118 mg, 97 %) as a white powder. Recrystallization from MeOH afforded colorless needles.

mp 178-182 °C

UV (CH$_3$OH): λ 204.9 (2.08 × 10^4), 260.0 (1.44 × 10^4), 350.1 (256) nm (M^{-1}cm^{-1}).

^{1}H NMR (CD$_3$OD, 300 MHz): δ 8.08 (d, J = 8.4 Hz, 2H), 7.90 (d, J = 8.4 Hz, 2H), 3.69 (m, 2H), 3.07 (m, 1H), 1.83-1.72 (m, 6H), 1.56 (d, J = 6.8 Hz, 6H), 1.51-1.43 (m, 1H), 1.39-1.27 (m, 2H), 1.24 (d, J = 6.8 Hz, 3H), 1.18 (d, J = 6.6 Hz, 6H), 1.11-0.99 (m, 2H).

^{13}C NMR (CD$_3$OD, 75 MHz): δ 192.08, 172.80, 168.87, 145.28, 135.31, 130.81, 130.04, 53.37, 52.15, 47.43, 42.65, 30.01, 28.78, 27.06, 26.98, 26.90, 20.52, 20.45, 15.98.

IR (KBr pellet): ν 3468, 2974, 2941, 2859, 1672, 1652, 1584, 1554, 1454, 1379, 1235, 995, 744 cm^{-1}.

LRMS (FAB: +LSIMS, matrix, thioglyerol): *m/z* (relative intensity) 405 (M$^+$ + 1, 27.8), 278 (21.1), 236 (8.0), 149 (10.2), 128 (100), 111 (8.8).

HRMS (FAB: +LSIMS, matrix, thioglyerol): *m/z* calcd for C$_{23}$H$_{36}$N$_2$O$_4$ (M$^+$ + 1): 405.2755, found 405.2752.

Anal. Calcd for C$_{24}$H$_{32}$N$_2$O$_4$: C, 68.29; H, 8.97; N 6.92. Found: C, 68.27; H, 9.04; N, 7.32.

This structure was confirmed by X-ray crystallographic analysis

Habit	colorless needles
Space group	$P2_12_12_1$
a, Å	6.3807(3)
b, Å	13.9934(7)
c, Å	25.779(1)
α (°)	90
β (°)	90
γ (°)	90
Z	4
R	0.056

S-(+)-1-Aminoindane salt (67d)
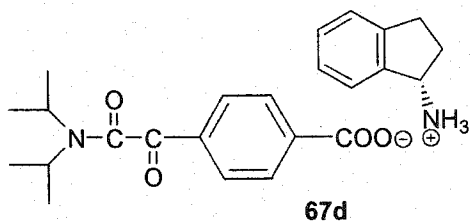
67d

A solution of acid **66** (83 mg, 0.30 mmol) in Et_2O (15 mL) was added to a solution of S-(+)-1-aminoindane (40 mg, 0.30 mmol) in Et_2O (5 mL). The cloudy solution was stirred for 1 h, after which time the precipitate that had formed was filtered, washed with Et_2O and dried *in vacuo* to afford salt **67d** (123 mg, 100 %) as a white powder. Recrystallization from MeOH afforded colorless plates.

mp 192-195 °C

UV (CH_3OH): λ 204.9 (2.43 × 10^4), 260.0 (1.52 × 10^4), 350.1 (130) nm ($M^{-1}cm^{-1}$).

^{1}H NMR (CD_3OD, 300 MHz): δ 8.07 (d, $J = 8.3$ Hz, 2H), 7.90 (d, $J = 8.3$ Hz, 2H), 7.47-7.33 (m, 4H), 4.76 (d × d, $J_1 = 5.2$ Hz, $J_2 = 7.5$ Hz, 1H), 3.69 (m, 2H), 3.18-3.10 (m,

1H), 3.02-2.92 (m, 1H), 2.62-2.54 (m, 1H), 2.11-2.03 (m, 1H), 1.56 (d, J = 6.9 Hz, 6H), 1.18 (d, J = 6.6 Hz, 6H) .

^{13}C NMR (CD$_3$OD, 75 MHz): δ 192.12, 185.87, 168.91, 145.40, 140.02, 135.33, 130.83, 130.63, 130.05, 128.25, 126.35, 125.47, 56.94, 52.16, 47.45, 31.80, 31.01, 20.51, 20.44 .

IR (KBr pellet): ν 3565, 2975, 2663, 1678, 1638, 1580, 1542, 1459, 1386, 1235, 996, 754, 743, 519 cm^{-1}.

LRMS (FAB: +LSIMS, matrix, thioglyerol): m/z (relative intensity) 411 (M$^+$ + 1, 43.8), 348 (11.6), 278 (79.3), 236 (20.4), 217 (13.6), 215 (14.3), 214 (14.5), 149 (28.6), 134 (90.6), 117 (100), 91 (25.6).

HRMS (FAB: +LSIMS, matrix, thioglyerol): m/z calcd for C$_{24}$H$_{31}$N$_2$O$_4$ (M$^+$ + 1): 411.2285, found 411.2286.

Anal. Calcd for C$_{24}$H$_{30}$N$_2$O$_4$: C, 70.22; H, 7.37; N 6.82. Found: C, 70.21; H, 7.33; N, 7.20.

(1R, 2S)-(+)-*cis*-1-Amino-2-indanol salt (67e)

67e
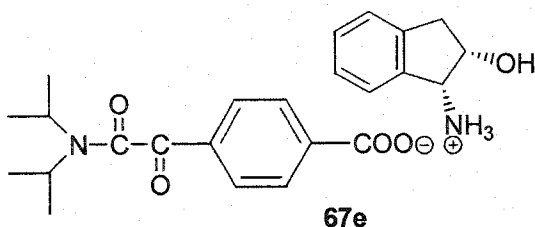
A solution of acid **66** (55 mg, 0.20 mmol) in Et$_2$O (15 mL) was added to a solution of (1R, 2S)-(+)-1-amino-2-indanol (30mg, 0.20 mmol) in Et$_2$O (5 mL). The cloudy solution was stirred for 1 h, after which time the precipitate that had formed was filtered, washed with Et$_2$O and dried *in vacuo* to afford salt **67e** (77 mg, 91 %) as a white powder. Recrystallization from MeOH afforded colorless plates.

mp 180-182 °C

UV (CH$_3$OH): λ 210.1 (2.68 × 10^4), 260.0 (2.18 × 10^4), 350.0 (173) nm (M^{-1}cm^{-1}).

^{1}H NMR (CD$_3$OD, 300 MHz): δ 8.08 (d, J = 8.1 Hz, 2H), 7.90 (d, J = 8.1 Hz, 2H), 7.44-7.30 (m, 4H), 4.69 (m, 1H), 4.55 (d, J = 5.9 Hz, 1H), 3.69 (m, 2H), 3.26-2.97 (m, 2H), 1.56 (d, J = 6.6 Hz, 6H), 1.18 (d, J = 6.5, 6H).

^{13}C NMR (CD$_3$OD, 75 MHz): δ 192.11, 174.02, 168.90, 145.08, 142.83, 138.13, 135.36, 130.90, 130.07, 128.44, 126.68, 126.19, 71.92, 58.58, 52.23, 47.51, 40.11, 20.51, 20.44.

IR (KBr pellet): ν 3324 (br), 2974, 2932, 2876, 1737, 1676, 1636, 1580, 1537, 1387, 1232, 1099, 993, 874, 741, 613 cm^{-1}.

LRMS (FAB: +LSIMS, matrix: 3-NBA): m/z (relative intensity) 427 (M$^+$ + 1, 22.6), 278 (24.9), 154 (18.5), 150 (100), 133 (47.6).

HRMS (FAB: +LSIMS, matrix: 3-NBA): m/z calcd for C$_{24}$H$_{31}$N$_2$O$_5$ (M$^+$ + 1): 427.2235, found 427.2235.

Anal. Calcd for C$_{24}$H$_{30}$N$_2$O$_5$: C, 67.59; H, 7.09; N 6.57. Found: C, 67.41; H, 7.26; N, 6.69.

This structure was confirmed by X-ray crystallographic analysis

Habit	colorless plates
Space group	*P2₁*
a, Å	7.542(2)
b, Å	6.364(2)
c, Å	24.163(9)
α (°)	90
β (°)	93.96(4)
γ (°)	90
Z	2
R	0.066

R-(+)-1-Phenylethylamine salt (67f)
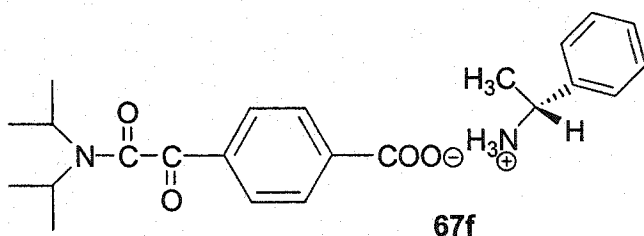
67f

A solution of acid **66** (83 mg, 0.30 mmol) in Et₂O (15 mL) was added to a solution of R-(+)-1-phenylethylamine (36mg, 0.30 mmol) in Et₂O (5 mL). The cloudy solution was stirred for 1 h, after which time the precipitate that had formed was filtered, washed with Et₂O and dried *in vacuo* to afford salt **67f** (110 mg, 92 %) as a white powder. Recrystallization from MeOH afforded colorless needles.

mp 178-181 °C

UV (CH₃OH): λ 206.6 (2.74 × 10⁴), 210.0 (2.55 × 10⁴), 259.9 (1.81 × 10⁴), 350.0 (280) nm (M⁻¹cm⁻¹).

¹H NMR (CD₃OD, 300 MHz): δ 8.08 (d, J = 8.4 Hz, 2H), 7.90 (d, J = 8.4 Hz, 2H), 7.42 (m, 5H), 4.42 (q, J = 6.9 Hz, 1H), 3.69 (m, 2H), 1.61 (d, J = 6.9 Hz, 3H), 1.56 (d, J = 6.8 Hz, 6H), 1.18 (d, J = 6.6, 6H).

¹³C NMR (CD₃OD, 100 MHz): δ 192.09, 173.38, 168.89, 145.19, 139.94, 135.33, 130.83, 130.26, 130.06, 127.63, 52.29, 52.17, 47.45, 20.87, 20.51, 20.44.

IR (KBr pellet): ν 3503, 2972, 2935, 1752, 1675, 1640, 1581, 1537, 1396, 1237, 1137, 997, 826, 745 cm⁻¹.

LRMS (FAB: +LSIMS, matrix: thioglycerol): m/z (relative intensity) 399 (M^+ + 1, 41.0), 300 (10.6), 278 (49.3), 236 (22.1), 149 (39.8), 122 (100), 105 (67.3).

HRMS (FAB: +LSIMS, matrix: thioglycerol): m/z calcd for $C_{23}H_{31}N_2O_4$ (M^+ + 1): 399.2286, found 399.2279.

Anal. Calcd for $C_{23}H_{30}N_2O_4$: C, 69.32; H, 7.59; N 7.03. Found: C, 69.23; H, 7.60; N, 7.02.

This structure was confirmed by X-ray crystallographic analysis

Habit	colorless needles
Space group	$C2$
a, Å	49.208(4)
b, Å	6.3851(4)
c, Å	13.812(1)
α (°)	90
β (°)	90.823(4)
γ (°)	90
Z	8
R	0.083

S-(-)-1-Phenylethylamine salt (67g)
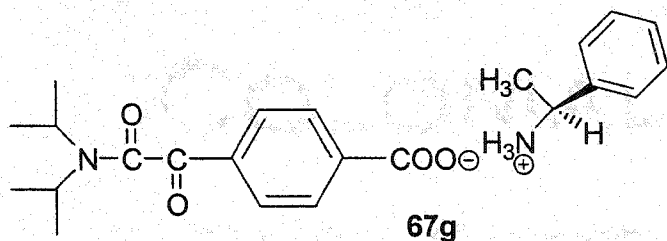
67g

A solution of acid **66** (55 mg, 0.20 mmol) in Et_2O (15 mL) was added to a solution of S-(-)-1-phenylethylamine (26 mg, 0.20 mmol) in Et_2O (5 mL). The cloudy solution was stirred for 1 h, after which time the precipitate that had formed was filtered, washed with Et_2O and dried *in vacuo* to afford salt **67g** (75 mg, 94 %) as a white powder. Recrystallization from MeOH afforded colorless needles.

mp 179-181 °C

UV (CH_3OH): λ 204.9 (2.57×10^4), 260.0 (1.50×10^4), 350.0 (218) nm ($M^{-1}cm^{-1}$).

^1H NMR (CD_3OD, 300 MHz): δ 8.09 (d, J = 8.5 Hz, 2H), 7.90 (d, J = 8.5 Hz, 2H), 7.41 (m, 5H), 4.42 (q, J = 6.9 Hz, 1H), 3.69 (m, 2H), 1.61 (d, J = 6.9 Hz, 3H), 1.56 (d, J = 6.8 Hz, 6H), 1.18 (d, J = 6.6, 6H).

^{13}C NMR (CD_3OD, 100 MHz): δ 192.09, 173.38, 168.89, 145.19, 139.94, 135.32, 130.82, 130.25, 130.06 127.63, 52.29, 52.16, 47.44, 20.88, 20.51, 20.44.

**IR** (KBr pellet): ν 3564 (br), 2972, 2935, 1751, 1674, 1640, 1581, 1537, 1382, 1237, 1137, 996, 826, 745 cm^{-1}.

LRMS (FAB: +LSIMS, matrix: thioglycerol): *m/z* (relative intensity) 399 (M^+ + 1, 53.2), 278 (100), 236 (28.8), 149 (48.4), 122 (83.3), 105 (56.2).

HRMS (FAB: +LSIMS, matrix: thioglycerol): *m/z* calcd for $C_{23}H_{31}N_2O_4$ (M^+ + 1): 399.2286, found 399.2283.

Anal. Calcd for $C_{23}H_{30}N_2O_4$: C, 69.32; H, 7.59; N 7.03. Found: C, 69.57; H, 7.43; N, 6.82.

This structure was also confirmed by X-ray crystallographic analysis and the X-ray data is identical to that of compound **67f**.

(1S, 2R)-(+)-Norephedrine salt (**67h**)
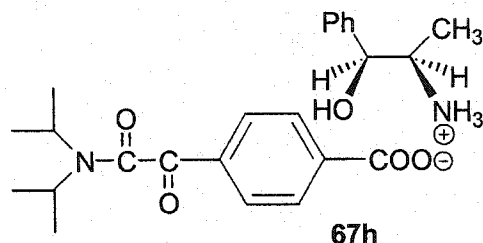
67h

A solution of acid **66** (55 mg, 0.20 mmol) in Et_2O (15 mL) was added to a solution of (1S, 2R)-(+)-norephedrine (31mg, 0.20 mmol) in Et_2O (5 mL). The cloudy solution was stirred for 1 h, after which time the precipitate that had formed was filtered, washed with Et_2O and dried *in vacuo* to afford salt **67h** (75 mg, 88 %) as a white powder. Recrystallization from MeOH afforded colorless needles.

mp 145-148 °C

^{1}**H NMR** (CD_3OD, 300 MHz): δ 7.99 (d, $J = 8.0$ Hz, 2H), 7.81 (d, $J = 8.0$ Hz, 2H), 7.29 (m, 5H), 4.85 (m, 1H), 3.60 (m, 2H), 3.21 (m, 1H), 1.47 (d, $J = 6.8$ Hz, 6H), 1.09 (d, $J = 6.5$ Hz, 6H), 0.98 (d, $J = 6.6$, 3H).

^{13}**C NMR** (CD_3OD, 75 MHz): δ 192.09, 174.01, 168.89, 145.10, 141.54, 135.34, 130.84, 130.09, 129.53, 128.99, 127.16, 73.52, 53.74, 52.23, 47.50, 20.51, 20.44, 12.36.

IR (KBr pellet): ν 3320 (br), 2977, 2076, 1734, 1675, 1636, 1540, 1382, 1232, 993, 798, 743, 703 cm^{-1}.

LRMS (FAB: +LSIMS, matrix: glycerol): *m/z* (relative intensity) 429 (M$^+$ + 1, 20.1), 278 (12.7), 152 (100), 149 (14.9), 134 (47.6).

HRMS (FAB: +LSIMS, matrix: glycerol): *m/z* calcd for $C_{24}H_{33}N_2O_5$ (M$^+$ + 1): 429.2391, found 429.2389.

Anal. Calcd for $C_{24}H_{32}N_2O_5$: C, 67.27; H, 7.53; N 6.54. Found: C, 66.85; H, 7.64; N, 6.55.

(1R, 2R)-(-)-Pseudoephedrine salt (67i)
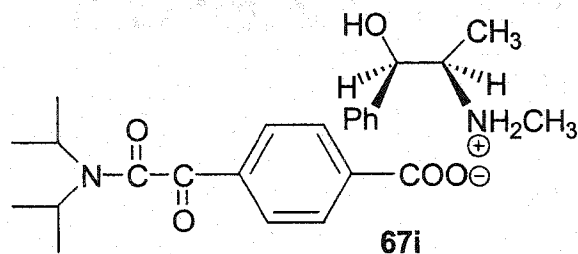
67i

A solution of acid **66** (55 mg, 0.20 mmol) in Et$_2$O (15 mL) was added to a solution of (1R, 2R)-(-)-pseudoephedrine (34mg, 0.20 mmol) in Et$_2$O (5 mL). The cloudy solution was stirred for 1 h, after which time the precipitate that had formed was filtered, washed with Et$_2$O and dried *in vacuo* to afford salt **67i** (83 mg, 94 %) as a white powder. Recrystallization from MeOH afforded colorless needles.

mp 168-172 °C

UV (CH$_3$OH): λ 205.0 (2.37 × 10^4), 260.0 (1.65 × 10^4), 350.0 (279) nm (M^{-1}cm^{-1}).

^{1}**H NMR** (CD$_3$OD, 300 MHz): δ 8.12 (d, *J* = 8.3 Hz, 2H), 7.90 (d, *J* = 8.3 Hz, 2H), 7.31-7.41 (m, 5H), 4.60 (d, *J* = 9.2 Hz, 1H), 3.60-3.68 (m, 2H), 3.20 (m, 1H), 2.63 (s, 3H), 1.52 (d, *J* = 6.8 Hz, 6H), 1.13 (d, *J* = 6.6 Hz, 6H), 1.05 (d, *J* = 6.6, 3H).

^{13}**C NMR** (CD$_3$OD, 75 MHz): δ 192.06, 173.97, 168.82, 145.18, 141.97, 135.32, 130.84, 130.06, 129.77, 129.66, 128.19, 75.55, 61.67, 52.14, 47.41, 30.45, 20.52, 20.44, 12.64.

IR (KBr pellet): ν 3412 (br), 3241, 3037, 2974, 2477, 1744, 1672, 1651, 1600, 1558, 1455, 1373, 1235, 994, 743, 614 cm^{-1}.

LRMS (FAB: +LSIMS, matrix: 3-NBA): m/z (relative intensity) 443 (M$^+$ + 1, 8.8), 278 (12.9), 166 (100), 154 (17.7), 148 (29.0), 136 (12.1).

HRMS (FAB: +LSIMS, matrix: 3-NBA): m/z calcd for $C_{25}H_{35}N_2O_5$ (M$^+$ + 1): 433.2548, found 433.2545.

Anal. Calcd for $C_{25}H_{34}N_2O_5$: C, 67.85; H, 7.74; N 6.33. Found: C, 67.65; H, 7.71; N, 6.49.

<u>(-)-*cis*-Myrtanylamine salt (**67j**)</u>
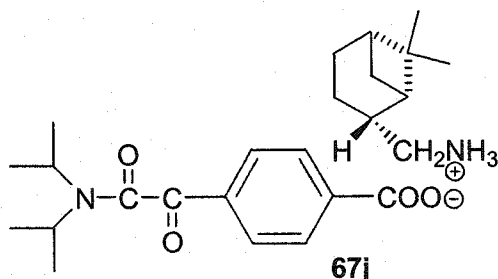
A solution of acid **66** (83 mg, 0.30 mmol) in Et$_2$O (15 mL) was added to a solution of (-)-*cis*-myrtanylamine (46mg, 0.30 mmol) in Et$_2$O (5 mL). The cloudy solution was stirred for 1 h, after which time the precipitate that had formed was filtered, washed with Et$_2$O and dried *in vacuo* to afford salt **67j** (119 mg, 92 %) as an off-white powder. Recrystallization from MeOH afforded pale yellow plates.

mp 127-130 °C

^{1}H NMR (CD$_3$OD, 300 MHz): δ 8.08 (d, J = 8.2 Hz, 2H), 7.91 (d, J = 8.2 Hz, 2H), 3.70 (m, 2H), 2.93 (d, J = 7.6 Hz, 2H), 2.40 (m, 1H), 2.31 (m, 1H), 2.04-1.92 (m, 6H), 1.56 (d, J = 6.8 Hz, 6H), 1.22 (s, 3H), 1.18 (d, J = 6.6 Hz, 6H), 1.02 (s, 3H), 0.97 (d, J = 9.8 Hz, 1H).

^{13}**C NMR** (CD$_3$OD, 75 MHz): δ 191.95 (+), 173.28 (+), 168.73 (+), 145.26 (+), 135.27 (+), 130.22 (-), 129.53 (-), 52.25 (-), 47.53 (-), 46.14 (+), 44.56 (-), 42.32 (-), 40.73 (-), 39.48 (+), 33.68 (+), 28.10 (-), 26.66 (+), 23.40 (-), 20.59 (-), 20.50 (-), 20.34 (+).

IR (KBr pellet): ν 3440, 2980, 2941, 1679, 1639, 1541, 1450, 1376, 1233, 993, 740 cm^{-1}.

LRMS (FAB: +LSIMS, matrix, thioglyerol): *m/z* (relative intensity) 431 (M$^+$ + 1, 10.7), 413 (10.4), 284 (5.3), 278 (6.4), 236 (5.0), 154 (100), 149 (14.1), 81 (16.1).

HRMS (FAB: +LSIMS, matrix, thioglyerol): *m/z* calcd for C$_{25}$H$_{39}$N$_2$O$_4$ (M$^+$ + 1): 431.2912, found 431.2913.

Anal. Calcd for C$_{25}$H$_{38}$N$_2$O$_4$: C, 69.74; H, 8.90; N, 6.51; O, 14.86. Calcd for C$_{25}$H$_{38}$N$_2$O$_4$•1/4H$_2$O: C, 69.01; H, 8.92; N 6.44. Found: C, 68.92; H, 8.96; N, 6.67.

S-(+)-2-Pyrrolidinemethanol salt (**67k**)

67k
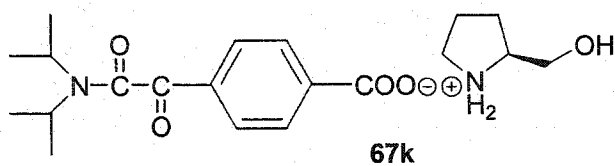
A solution of acid **66** (83 mg, 0.30 mmol) in Et$_2$O (15 mL) was added to a solution of S-(+)-2-pyrrolidinemethanol (33 mg, 0.33 mmol) in Et$_2$O (5 mL). The cloudy solution was stirred for 1 h, after which time the precipitate that had formed was filtered, washed with Et$_2$O and dried *in vacuo* to afford salt **67k** (106 mg, 93 %) as an off-white powder. Recrystallization from CH$_3$CN afforded pale yellow prisms.

mp 116-119 °C

UV (CH$_3$OH): λ 210.0 (2.67 × 10^4), 260.0 (2.47 × 10^4), 350.1 (272) nm (M^{-1}cm^{-1}).

^{1}H NMR (CD$_3$OD, 300 MHz): δ 8.08 (d, J = 8.4 Hz, 2H), 7.91 (d, J = 8.4 Hz, 2H), 3.83-3.78 (m, 1H), 3.76-3.57 (m, 4H), 3.27 (t, J = 7.4 Hz, 2H), 2.12-1.98 (m, 3H), 1.78-1.72 (m, 1H), 1.56 (d, J = 6.8 Hz, 6H), 1.18 (d, J = 6.6 Hz, 6H).

^{13}C NMR (CD$_3$OD, 75 MHz): δ 192.00, 173.51, 168.73, 145.00, 135.34, 130.78, 130.03, 61.69, 61.61, 52.07, 47.35, 46.43, 27.13, 24.88, 20.51, 20.44.

IR (KBr pellet): ν 3414, 2974, 1677, 1641, 1587, 1549, 1449, 1382, 1231, 1064, 994 cm^{-1}.

LRMS (FAB: +LSIMS, matrix, thioglyerol): m/z (relative intensity) 379 (M$^+$ + 1, 23.0), 278 (33.5), 217 (12.5), 214 (10.5), 149 (12.6), 102 (100), 91 (21.9).

HRMS (FAB: +LSIMS, matrix, thioglyerol): m/z calcd for C$_{20}$H$_{31}$N$_2$O$_5$ (M$^+$ + 1): 379.2234, found 379.2233.

Anal. Calcd for C$_{20}$H$_{30}$N$_2$O$_5$: C, 63.47; H, 7.99; N 7.40. Found: C, 63.26; H, 8.00; N, 7.14.

S-(+)-N-methyl-1-phenylethylamine salt (671)

671
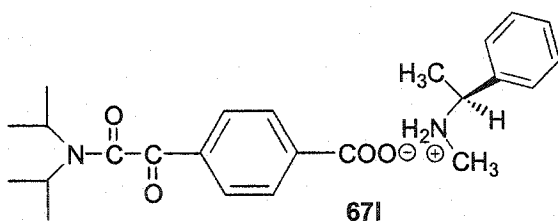
A solution of acid **66** (83 mg, 0.30 mmol) in Et$_2$O (15 mL) was added to a solution of S-(+)-N-methyl-1-phenylethylamine (41 mg, 0.30 mmol) in Et$_2$O (5 mL). The solution was stirred for 1 h. Removal of solvent *in vacuo* afforded salt **671** as a white powder. Recrystallization from ethyl acetate afforded colorless needles (103 mg, 83 %).

mp 126-128 °C.

UV (CH$_3$OH): λ 210.0 (2.43 × 10^4), 259.9 (1.72 × 10^4), 350.0 (290) nm (M^{-1}cm^{-1}).

^{1}H NMR (CD$_3$OD, 300 MHz): δ 8.09 (d, J = 8.5 Hz, 2H), 7.91 (d, J = 8.5 Hz, 2H), 7.45 (m, 5H), 4.28 (q, J = 6.9 Hz, 1H), 3.69 (m, 2H), 2.54 (s, 3H), 1.65 (d, J = 6.9 Hz, 3H), 1.56 (d, J = 6.8 Hz, 6H), 1.18 (d, J = 6.6 Hz, 6H).

^{13}C NMR (CD$_3$OD, 75 MHz): δ 192.01, 173.33, 168.76, 144.99, 137.84, 135.36, 130.82, 130.47, 130.36, 130.05, 128.63, 60.38, 52.09, 47.37, 31.44, 20.53, 20.45, 19.41.

IR (KBr pellet): ν 3443, 3002, 2972, 2938, 1670, 1646, 1540, 1455, 1383, 1373, 1234, 992, 738 cm^{-1}.

LRMS (FAB: +LSIMS, matrix, thioglyerol): m/z (relative intensity) 413 (M$^+$ + 1, 7.9), 278 (16.3), 236 (9.5), 149 (25.8), 136 (100), 105 (30.3).

HRMS (FAB: +LSIMS, matrix, thioglyerol): m/z calcd for C$_{24}$H$_{33}$N$_2$O$_4$ (M$^+$ + 1): 413.2442, found 413.2441.

Anal. Calcd for C$_{24}$H$_{32}$N$_2$O$_4$: C, 69.88; H, 7.82; N, 6.79; O, 15.51. Calcd for C$_{24}$H$_{32}$N$_2$O$_4$•1/2H$_2$O: C, 68.38; H, 7.89; N 6.65. Found: C, 68.34; H, 7.76; N, 6.36.

4.2.3 Preparation of α-Oxoamide 68

R-2-Phenylpropyl 4-[[bis(1-methylethyl)amino]oxoacetyl]benzoate (68)

68
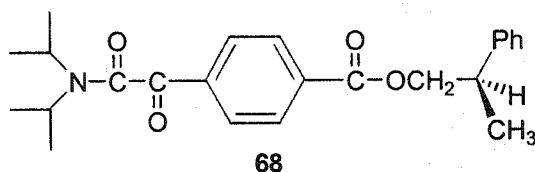
Oxalyl chloride (458 mg, 320 μL, 3.61 mmol) was added dropwise to a cold (-5 °C) solution of acid 66 (100 mg, 0.36 mmol) and DMF (1 μL) in anhydrous THF (3 mL). The solution was stirred for 3 h under N$_2$ at room temperature. Unreacted oxalyl chloride

along with DMF and THF was removed *in vacuo* and the yellow solid residue dissolved in anhydrous CH_2Cl_2 (3 mL). R-(+)-2-phenyl-1-propanol (49 mg, 49 μL, 0.36 mmol) was added dropwise at –5 °C under N_2 and the resulting mixture stirred at room temperature for 4 h. The reaction was quenched by addition of 1 M HCl (10 mL), the layers separated, and the aqueous layer further extracted with CH_2Cl_2 (3 × 10 mL). The organic layers were combined, washed with brine (2 × 10 mL) and H_2O (2 × 10 mL), and dried (Na_2SO_4). Removal of the solvent *in vacuo* followed by silica gel column chromatography of the residue (petroleum ether-ethyl acetate, 8:2) afforded 106 mg (74%) of ester **68** as a light yellow solid. Recrystallization from Et_2O afforded colorless platelets.

mp 115-117 °C

UV (CH_3OH): λ 204.9 (2.17 × 10^4), 255.0 (2.04 × 10^4), 360.0 (201) nm ($M^{-1}cm^{-1}$).

^{1}H NMR ($CDCl_3$, 400 MHz): δ 8.02 (d, J = 8.5 Hz, 2H), 7.90 (d, J = 8.5 Hz, 2H), 7.23 (m, 5H), 4.37 (m, 2H), 3.57 (m, 2H), 3.19 (m, 1H), 1.51 (d, J = 6.9 Hz, 6H), 1.33 (d, J = 7.0 Hz, 3H), 1.11 (d, J = 6.6, 6H).

^{13}C NMR ($CDCl_3$, 100 MHz): δ 190.04, 166.32, 165.35, 142.86, 136.48, 135.07, 130.01, 129.38, 128.57, 127.27, 126.82, 70.37, 50.19, 46.19, 39.00, 20.57, 20.26, 17.98.

IR (KBr pellet): ν 2974, 2934, 1714, 1678, 1646, 1452, 1281, 1230, 1108, 994, 965, 874, 732, 702 cm^{-1}.

LRMS (+CI, gas: CH_4 + NH_3): *m/z* (relative intensity) 396 (M^+ + 1, 100), 258 (14.0), 154 (16.6), 130 (50.5), 128 (60.7), 118 (27.4), 105 (17.4), 102 (25.1), 100 (20.8), 86 (13.2).

HRMS (+CI, gas: CH_4 + NH_3): *m/z* calcd for $C_{24}H_{30}NO_4$ (M^+ + 1): 396.2175, found 396.2174.

Anal. Calcd for $C_{24}H_{29}NO_4$: C, 72.89; H, 7.39; N 3.54. Found: C, 72.57; H, 7.35; N, 3.70.

This structure was confirmed by X-ray crystallographic analysis

Habit	colorless plates
Space group	$P2_1$
a, Å	12.580(4)
b, Å	6.456(2)
c, Å	13.657(4)
α (°)	90
β (°)	99.283(8)
γ (°)	90
Z	2
R	0.080

4.3 Synthesis of Bicyclo[2.2.2]octane Derivatives 85, 54, 55 and 56

4.3.1 Preparation of Ketones 85, 54 and 55

4-Pentylbicylo[2.2.2]octane-1-methanol (80)

80
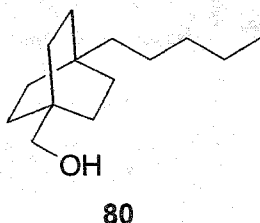
To a suspension of lithium aluminum hydride (2.18 g, 57.4 mmol) in diethyl ether (50 mL) was added dropwise a solution of acid **79** (4.3 g, 19.2 mmol) in diethyl ether (50 mL) at room temperature under an argon atmosphere. The mixture was stirred for 2.5 h. The reaction was quenched carefully with water (100 mL) at −78 °C. The resulting mixture was poured into 4 N HCl (40 mL), followed by extraction with ether (4 × 100 mL). The combined ethereal extracts were washed with brine (2 × 50 mL), dried (Na_2SO_4). Removal of the solvent *in vacuo* provided alcohol **80** (3.71 g, 92%) as a yellowish solid. The compound did not require further purification.

mp: 35.5-36.5 °C (Lit.[95 (a)] **bp**: 150 °C/0.05mmHg).

^{1}H NMR (400 MHz, $CDCl_3$): δ 3.16 (s, 2H), 2.16 (s, 1H, OH), 1.31 (m, 12H), 1.26 (m, 2H), 1.16 (m, 4H), 1.04 (m, 2H), 0.85 (t, J = 7.2 Hz, 3H).

^{13}C NMR (100 MHz, $CDCl_3$): δ 71.46, 41.58, 33.12, 32.80, 30.85, 30.74, 28.21, 23.27, 22.60, 13.98.

IR (KBr pellet): ν 3306 (br), 2925, 2856, 1457, 1376, 1044 cm^{-1}.

LRMS (EI) *m/z* 210 (M$^+$), 192, 179 (100), 163, 149, 135, 121, 109, 95, 93, 79, 67, 55.

4-Pentylbicyclo[2.2.2]octane-1-methanol methanesulfonate (**81**)

81
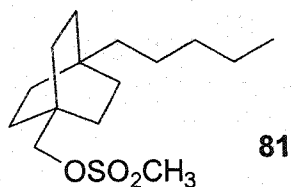
To a solution of alcohol **80** (3.66 g, 17.4 mL) in dry pyridine (30 mL) was added methanesulfonyl chloride (2.99 g, 26.1 mmol, 2.03 mL) at room temperature. The reaction was stirred for 4 h at room temperature under an argon atmosphere. The resulting mixture was poured into ice water (200 mL) and extracted with diethyl ether (4 × 120 mL). The combined ethereal extracts were washed with 4 N HCl (2 × 30 mL), water (2 × 30) mL and brine (2 × 30 mL), and dried (Na_2SO_4). Removal of the solvent *in vacuo* afforded compound **81** (5.01 g, 100 %) as a white solid. The compound did not require further purification.

mp: 73-75 °C.

^{1}H NMR (300 MHz, $CDCl_3$): δ 3.80 (s, 2H), 2.94 (s, 3H), 1.38 (m, 6H), 1.35 (m, 6H), 1.24 (m, 2H), 1.15 (m, 4H), 1.03 (m, 2H), 0.83 (t, *J* = 7.0 Hz, 3H).

^{13}C NMR (75 MHz, $CDCl_3$): δ 41.37, 36.95, 32.73, 32.09, 30.71, 30.29, 28.09, 23.23, 22.60, 14.01.

IR (KBr pellet): ν 2953, 2922, 2867, 1321, 1174, 958, 538 cm^{-1}.

LRMS (+CI: gas, CH_4 + NH_3) *m/z* 306 (M$^+$ + 18, 100), 223, 210, 192.

HRMS (+CI: gas, CH_4 + NH_3) calcd for $C_{15}H_{32}NO_3S$ (M$^+$ + 18) 306.2102, found 306.2103.

Anal. Calcd for $C_{15}H_{28}O_3S$: C, 62.46; H, 9.78. Found: C, 62.45; H, 9.84.

4-Pentylbicyclo[2.2.2]octane-1-acetonitrile (**82**)

82
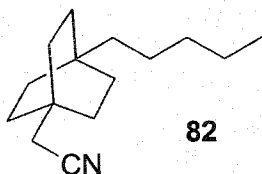
To a solution of compound **81** (4.40 g, 15.3 mmol) in dry DMF (40 mL) was added sodium cyanide (1.12 g, 22.9 mmol). The resulting mixture was heated to be refluxing at 150 °C under an argon atmosphere for 17 h. The cooled reaction mixture was poured into ice-water (150 mL) and extracted with diethyl ether (4 × 120 mL). The combined ethereal extracts were washed with Na_2CO_3 (10%, 50 mL), H_2O (50 mL), and saturated NaCl (50 mL), then dried (Na_2SO_4). Removal of solvent *in vacuo* afforded compound **82** (2.92 g, 87 %) as a yellowish solid. The compound did not require further purification.

mp: 31.5-32.5 °C (Lit.[95 (a)] **bp**: 130 °C/2mmHg).

^{1}H NMR (300 MHz, CDCl₃): δ 2.06 (s, 2H), 1.46 (m, 6H), 1.37 (m, 6H), 1.22 (m, 2H), 1.15 (m, 4H), 1.05 (m, 2H), 0.83 (t, *J* = 7.1 Hz, 3H).

^{13}C NMR (75 MHz, CDCl₃): δ 118.09, 41.21, 32.69, 31.06, 30.73, 30.69, 30.14, 29.60, 23.20, 22.57, 13.98.

IR (KBr pellet): ν 2932, 2860, 2248, 1457 cm^{-1}.

LRMS (EI) *m/z* 219, 190 (100), 176, 163, 148, 122, 107, 93, 79, 68, 55.

4-Pentylbicyclo[2.2.2]octane-1-acetic acid (**83**)

83
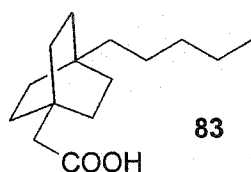
A solution of compound **82** (2.92 g) in sulfuric acid (1:1, 15 mL) and glacial acetic acid (40 mL) was heated to be refluxing at 130 °C for 24 h. Acetic acid in the cooled mixture was removed *in vacuo* and the dark residue was taken up in water (50 mL) and extracted with methylene chloride (5 × 50 mL). The combined organic extracts were washed with water (50 mL), brine (50 mL), and dried (Na_2SO_4). Removal of the solvent *in vacuo* afforded acid **83** (2.80 g, 88 %) as a white solid. The compound did not require further purification.

mp: 72-73 °C (Lit.[95 (a)] 70 °C).

^{1}H NMR (300 MHz, $CDCl_3$): δ 2.08 (s, 2H), 1.46 (m, 6H), 1.33 (m, 6H), 1.25 (m, 2H), 1.15 (m, 4H), 1.02 (m, 2H), 0.85 (t, J = 7.0 Hz, 3H).

^{13}C NMR (75 MHz, $CDCl_3$): δ 178.73, 45.91, 41.61, 32.85, 31.33, 31.09, 30.97, 30.19, 23.30, 22.69, 14.08.

IR (KBr pellet): ν 3565 (br), 2931, 2857, 1703, 1456, 1289, 1150, 962, 677 cm^{-1}.

<u>1-(4-Fluorophenyl)-2-(4'-pentylbicyclo[2.2.2]oct-1-yl) ethanone (**84**)</u>
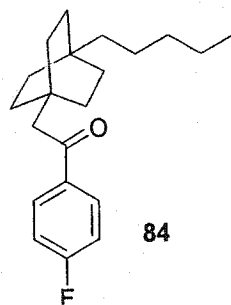
To a solid sample of acid **83** (2.23 g, 9.37 mmol) was added thionyl chloride (30 mL) at room temperature under an argon atmosphere. After stirring 20 min the solution was heated to be refluxing for 2 h. The excess thionyl chloride was removed *in vacuo* and the residue was redissolved in fluorobenzene (8 mL). The resulting solution was added dropwise to a suspension of anhydrous aluminum trichloride (5 g) in fluorobenzene (40 mL) at 0 °C (ice bath) over 30 min. The reaction was heated to be refluxing overnight (10

h) and quenched by careful addition of water (100 mL). The mixture was extracted with diethyl ether (3 × 120 mL). The combined ethereal extracts were washed with water (5 × 50 mL), brine (2 × 50 mL), and dried (Na$_2$SO$_4$). Removal of the solvent *in vacuo* afforded compound **84** (2.59 g, 88 %) as a yellowish liquid. The compound did not require further purification.

^{1}H NMR (400 MHz, CDCl$_3$): δ 7.90 (m, 2H), 7.06 (m, 2H), 2.67 (s, 2H), 1.49 (m, 6H), 1.31 (m, 6H), 1.23 (t, *J* = 7.3 Hz, 2H), 1.12 (m, 4H), 0.99 (m, 2H), 0.83 (t, *J* = 7.2 Hz, 3H).

^{13}C NMR (100 MHz, CDCl$_3$, APT: C, CH$_2$: +; CH, CH$_3$: -): δ 198.71 (+), 166.77 (+) and 164.24 (+), (^{1}J$_{C-F}$ = 253 Hz), 135.10 (+), 130.91 (-) and 130.82 (-), (^{3}J$_{C-F}$ = 9 Hz), 115.51 (-) and 115.29 (-), (^{2}J$_{C-F}$ = 22 Hz), 48.39 (+), 41.60 (+), 32.80 (+), 32.00 (+), 31.84 (+), 31.14 (+), 30.16 (+), 23.23 (+), 22.63 (+), 14.03 (-).

IR (neat): ν 2926, 2858, 1675, 1599, 1506, 1456, 1235, 1157, 832, 580 cm^{-1}.

LRMS (EI) *m/z* 316 (M$^+$), 298, 177, 163, 138, 123 (100), 95, 79, 55.

HRMS (EI) calcd for C$_{21}$H$_{29}$FO 316.2202, found 316.2202.

Anal. Calcd for C$_{21}$H$_{29}$FO: C, 79.70; H, 9.24. Found: C, 79.26; H, 9.11.

1-(4-Cyanophenyl)-2-(4'-pentylbicyclo[2.2.2]oct-1-yl) ethanone **(85)**
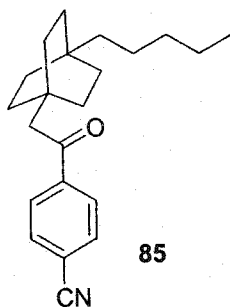
To a solution of compound **84** (1.17 g, 3.70 mmol) in dry DMF (15 mL) was added sodium cyanide (0.27 g, 5.56 mmol). The mixture was heated to be refluxing at 150 °C under an argon atmosphere for 17 h. The cooled reaction mixture was poured into ice-water (100 mL) and extracted with diethyl ether (4 × 100 mL). The combined ethereal extracts were washed with Na_2CO_3 (10%, 50 mL), H_2O (50 mL), and saturated NaCl (50 mL), then dried (Na_2SO_4). Removal of the solvent *in vacuo* afforded compound **85** (0.983 g, 82 %) as a yellowish solid. The compound did not require further purification.

mp: 89-91 °C.

UV (CH_3OH): λ 205.0 (1.33 × 10^4), 250.0 (1.50 × 10^4), 290.0 (1.15 × 10^3) nm ($M^{-1}cm^{-1}$).

^{1}H NMR (300 MHz, $CDCl_3$): δ 7.96 (d, J = 8.4 Hz, 2H), 7.72 (d, J = 8.4 Hz, 2H), 2.67 (s, 2H), 1.49 (m, 6H), 1.31 (m, 6H), 1.24 (m, 2H), 1.13 (m, 4H), 0.99 (m, 2H), 0.83 (t, J = 7.1 Hz, 3H).

^{13}C NMR (75 MHz, $CDCl_3$, APT: C, CH_2: +; CH, CH_3: -): δ 199.10 (+), 141.55 (+), 132.37 (-), 128.61 (-), 117.98 (+), 115.97 (+), 48.77 (+), 41.54 (+), 32.78 (+), 32.20 (+), 31.81 (+), 31.07 (+), 30.16 (+), 23.23 (+), 22.64 (+), 14.05 (-).

IR (KBr pellet): ν 2954, 2923, 2853, 2228, 1688, 1456, 1402, 1207, 986, 826, 572 cm^{-1}.

LRMS (EI) *m/z* 323 (M^+), 305, 252, 234, 178, 150, 130 (100), 102, 79, 55.

HRMS (EI) calcd for $C_{22}H_{29}NO$ 323.2249, found 323.2249.

Anal. Calcd for $C_{22}H_{29}NO$: C, 81.69; H, 9.04; N, 4.33. Found: C, 81.86; H, 9.19; N, 4.41.

1-(4-Carboxylphenyl)-2-(4'-pentylbicyclo[2.2.2]oct-1-yl) ethanone (54)
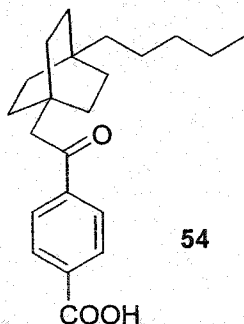
To a solution of potassium hydroxide (1.6 g) in water (8 mL) was added a solution of compound **85** (0.50g, 1.55 mmol) in ethanol (2 mL). The mixture was heated to be refluxing at 95 °C for 20 h. The reaction was quenched by adding water (50 mL). The solution was washed with methylene chloride (2 × 30 mL). The aqueous solution was carefully acidified to pH 2 with concentrated HCl. The precipitated carboxylic acid was extracted with diethyl ether (4 × 80 mL) and the combined ethereal extracts were washed with water (50 mL), brine (2 × 50 mL), and dried (Na_2SO_4). Removal of the solvent *in vacuo* provided a yellowish solid. Recrystallization from ethanol afforded acid **54** (0.434 g, 82 %) as white plates.

mp: 230-233 (decomposed) °C.

^{1}H NMR (300 MHz, $CDCl_3$): δ 8.16 (d, J = 8.3 Hz, 2H), 7.96 (d, J = 8.3 Hz, 2H), 2.76 (s, 2H), 1.50 (m, 6H), 1.32 (m, 6H), 1.24 (m, 2H), 1.14 (m, 4H), 1.01 (m, 2H), 0.84 (t, J = 7.0 Hz, 3H).

^{13}C NMR (75 MHz, $CDCl_3$): δ 200.13, 170.24, 142.65, 132.45, 130.37, 128.25, 48.97, 41.61, 32.83, 32.20, 31.86, 31.15, 30.20, 23.26, 22.67, 14.07.

IR (KBr pellet): ν 3540, 2924, 2856, 1684, 1667, 1506, 1426, 1289, 951, 875, 728 cm^{-1}.

LRMS (EI) *m/z* 342 (M$^+$), 297 (100), 204, 178, 164, 149, 79, 55.

HRMS (EI) calcd for $C_{22}H_{30}O_3$ 342.2195, found 342.2195.

Anal. Calcd for $C_{22}H_{30}O_3$: C, 77.16; H, 8.83. Found: C, 77.11; H, 8.72.

1-(4-Methoxycarbonylphenyl)-2-(4'-pentylbicyclo[2.2.2]oct-1-yl) ethanone (55)
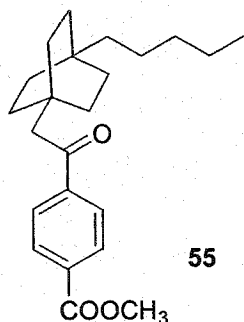
To a solution of acid **54** (0.100 g) in diethyl ether (5 mL) was added a solution of diazomethane in diethyl ether (10 mL, excess in the reaction) at room temperature. The reaction was stirred for 10 min. Removal of the solvent *in vacuo* provided a yellowish solid. Recrystallization from diethyl ether afforded ester **55** (0.104 g, 100 %) as white needles.

mp: 98-100 °C (Et$_2$O, needles).

UV (CH$_3$OH): λ 205.1 (1.46 × 10^4), 249.9 (1.69 × 10^4), 290.0 (1.38 × 10^3) nm (M^{-1}cm^{-1}).

^{1}H NMR (400 MHz, CDCl$_3$): δ 8.07 (d, J = 8.3 Hz, 2H), 7.93 (d, J = 8.3 Hz, 2H), 3.92 (s, 3H), 2.73 (s, 2H), 1.49 (m, 6H), 1.31 (m, 6H), 1.24 (m, 2H), 1.13 (m, 4H), 0.99 (m, 2H), 0.83 (t, J = 7.1 Hz, 3H).

**^{13}C NMR** (75 MHz, CDCl$_3$): δ 200.12, 166.29, 141.94, 133.49, 129.71, 128.14, 52.40, 48.90, 41.61, 32.82, 32.14, 31.84, 31.14, 30.18, 23.25, 22.66, 14.06.

IR (KBr pellet): ν 2925, 2856, 1718, 1666, 1457, 1280, 1113, 1016, 874, 734 cm^{-1}.

LRMS (EI) *m/z* 356 (M$^+$), 341, 325, 297 (100), 178, 163, 135.

HRMS (EI) calcd for $C_{23}H_{32}O_3$ 356.2352, found 356.2349.

Anal. Calcd for $C_{23}H_{32}O_3$: C, 77.49; H, 9.05. Found: C, 77.46; H, 9.17.

4.3.2 Preparation of Bicyclo[2.2.2]octyl Salts 56

<u>R-(-)-1-Cyclohexylethylamine salt (56a)</u>
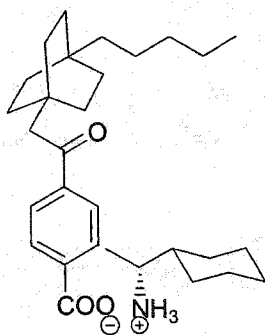
56a

A solution of acid **54** (85.5 mg, 0.25 mmol) in Et$_2$O (15 mL) was added to a solution of R-(-)-1-cyclohexylethylamine (31.8 mg, 0.25 mmol) in diethyl ether (5 mL). The cloudy solution was stirred for 1 h, after which time the precipitate that had formed was filtered, washed with diethyl ether and dried *in vacuo* to afford salt **56a** (93.5 mg, 80 %) as a white powder. Recrystallization from MeOH afforded colorless plates.

mp: 173-176 °C.

^{1}H NMR (300 MHz, CD$_3$OD): δ 7.99 (d, J = 8.5 Hz, 2H), 7.90 (d, J = 8.5 Hz, 2H), 3.07 (m, 1H), 2.77 (s, 2H), 1.84-1.70 (m, 5H), 1.56-1.50 (m, 6H), 1.37-1.32 (m, 8H), 1.28 (m, 1H), 1.24 (d, J = 6.7 Hz, 3H), 1.20-1.10 (m, 7H), 1.10-0.95 (m, 4H), 0.87 (t, J = 7.0 Hz, 3H).

^{13}C NMR (75 MHz, CD$_3$OD): δ 200.53, 172.47, 140.98, 140.16, 129.38, 127.85, 52.04, 48.79, 41.61, 41.30, 32.80, 32.07, 31.86, 31.13, 30.17, 29.31, 27.42, 25.90, 25.80, 25.69, 23.23, 22.64, 15.70, 14.05.

IR (KBr pellet): ν 3544, 2921, 2856, 2185, 1685, 1635, 1585, 1539, 1456, 1383, 1207, 984, 780 cm^{-1}.

LRMS (ESI: 0.1% formic acid in MeOH) *m/z* 470 (M$^+$ + 1, 100), 400 (20.4), 365 (18.6), 353 (55.3), 343 (15.2), 291 (14.5), 255 (30.4), 160 (19.1).

HRMS (ESI: 0.1% formic acid in MeOH) calcd for $C_{30}H_{48}NO_3$ 470.3634, found 470.3643.

Anal. Calcd for $C_{30}H_{47}NO_3$: C, 76.71; H, 10.09; N, 2.98; O, 10.22. Calcd for $C_{30}H_{47}NO_3 \cdot 1/4H_2O$: C, 75.98; H, 10.10; N, 2.95. Found: C, 75.66; H, 9.95; N, 3.17.

This structure was confirmed by X-ray crystallographic analysis:

Habit	colorless plates
Space group	*P2$_1$*
a, Å	10.0302(6)
b, Å	6.0826(3)
c, Å	23.4323(14)
α (°)	90
β (°)	91.654(2)
γ (°)	90
Z	2
R	0.092

L-Prolinamide salt (**56b**)
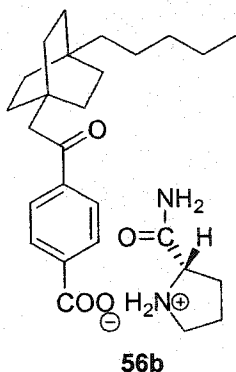
56b

A solution of acid **54** (85.5 mg, 0.25 mmol) in diethyl ether (15 mL) was added to a solution of L-prolinamide (28.5 mg, 0.25 mmol) in diethyl ether (5 mL). The cloudy solution was stirred for 1 h, after which time the precipitate that had formed was filtered, washed with diethyl ether and dried *in vacuo* to afford salt **56b** (95 mg, 83 %) as a white powder. Recrystallization from MeOH afforded colorless plates.

mp: 170-172 °C.

^{1}**H NMR** (400 MHz, CD$_3$OD): δ 8.00 (d, J = 8.3 Hz, 2H), 7.91 (d, J = 8.3 Hz, 2H), 4.26 (m, 1H), 3.34 (m, 2H), 2.77 (s, 2H), 2.40 (m, 1H), 2.00 (m, 3H), 1.52 (m, 6H), 1.34 (m, 6H), 1.27 (m, 2H), 1.16 (m, 4H), 1.02 (m, 4H), 0.86 (t, J = 7.0 Hz, 3H).

^{13}**C NMR** (75 MHz, CD$_3$OD): δ 202.59, 173.79, 172.71, 142.75, 141.34, 130.32, 129.02, 60.87, 49.64, 47.25, 42.89, 34.05, 33.03, 32.81, 32.30, 31.23, 25.31, 24.36, 23.69, 14.43.

IR (KBr pellet): ν 3544, 3081, 2925, 2856, 1688, 1673, 1584, 1542, 1456, 1380, 1204, 775 cm^{-1}.

LRMS (ESI: 0.1% formic acid in MeOH) *m/z* 457 (M$^+$ + 1, 30.9), 229 (100).

HRMS (ESI: 0.1% formic acid in MeOH) calcd for C$_{27}$H$_{41}$N$_2$O$_4$ 457.3066, found 457.3060.

Anal. Calcd for $C_{27}H_{40}N_2O_4$: C, 71.02; H, 8.83; N, 6.13. Found: C, 71.66; H, 8.81; N, 5.56.

This structure was confirmed by X-ray crystallographic analysis:

Habit	colorless plates
Space group	$P2_1$
a, Å	14.1956(14)
b, Å	9.6309(8)
c, Å	19.1279(18)
α (°)	90
β (°)	103.793
γ (°)	90
Z	4
R	0.059

(1S, 2R)-(+)-Norephedrine salt (**56c**)
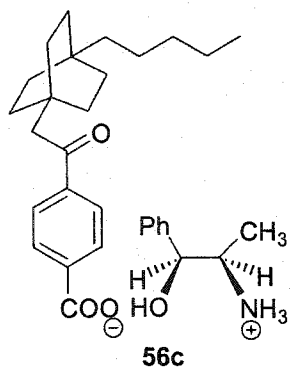
56c

A solution of acid **54** (85.5 mg, 0.25 mmol) in diethyl ether (15 mL) was added to a solution of (1S, 2R)-(+)-norephedrine (37.8 mg, 0.25 mmol) in diethyl ether (5 mL). The cloudy solution was stirred for 1 h, after which time the precipitate that had formed was filtered, washed with diethyl ether and dried *in vacuo* to afford salt **56c** (115 mg, 93 %) as a white powder. Recrystallization from MeOH afforded colorless needles.

mp: 170-173 °C.

^{1}H NMR (300 MHz, CD$_3$OD): δ 7.99 (d, J = 8.5 Hz, 2H), 7.90 (d, J = 8.5 Hz, 2H), 7.40-7.25 (m, 5H), 4.92 (d, J = 3.5 Hz, 1H), 3.48 (d × q, J_1 = 3.5 Hz, J_2 = 6.8 Hz, 1H), 2.77 (s, 2H), 1.52 (m, 6H), 1.34 (m, 8H), 1.17 (m, 4H), 1.07 (d, J = 6.8 Hz, 3H), 1.02 (m, 2H), 0.87 (t, J = 7.1 Hz, 3H).

^{13}C NMR (75 MHz, CD$_3$OD): δ 202.82, 173.95, 143.13, 141.56, 141.24, 130.29, 129.54, 128.98, 127.19, 73.79, 54.68, 49.69, 42.90, 34.05, 33.07, 32.86, 32.32, 31.26, 24.35, 23.67, 14.38, 12.61.

IR (KBr pellet): ν 3272, 2928, 2856, 2145, 1716, 1666, 1630, 1537, 1512, 1453, 1393, 1365, 1276, 763, 743, 704 cm^{-1}.

LRMS (ESI: 0.1% formic acid in MeOH) m/z 494 (M$^+$ + 1), 365 (100), 152.

HRMS (ESI: 0.1% formic acid in MeOH) calcd for C$_{31}$H$_{44}$NO$_4$ 494.3270, found 494.3275.

Anal. Calcd for C$_{31}$H$_{43}$NO$_4$: C, 74.74; H, 8.80; N, 2.81. Found: C, 74.78; H, 8.76; N, 2.68.

<u>(1R, 2R)-(-)-Pseudoephedrine salt (**56d**)</u>
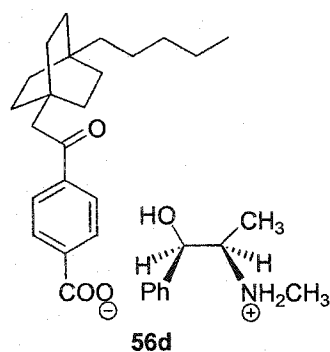
56d

A solution of acid **54** (85.5 mg, 0.25 mmol) in diethyl ether (15 mL) was added to a solution of (1R, 2R)-(-)-pseudoephedrine (41.3 mg, 0.25 mmol) in diethyl ether (5 mL). The cloudy solution was stirred for 1 h, after which time the precipitate that had formed was filtered, washed with diethyl ether and dried *in vacuo* to afford salt **56d** (110 mg, 87 %) as a white powder. Recrystallization from MeOH afforded colorless needles.

mp: 118-119 °C.

¹H NMR (300 MHz, CD$_3$OD): δ 7.99 (d, J = 8.6 Hz, 2H), 7.90 (d, J = 8.6 Hz, 2H), 7.40-7.35 (m, 5H), 4.52 (d, J = 9.2 Hz, 1H), 3.34 (m, 1H), 2.77 (s, 2H), 2.71 (s, 3H), 1.55-1.50 (m, 6H), 1.37-1.25 (m, 8H), 1.15-1.10 (m, 4H), 1.06 (d, J = 6.7 Hz, 3H), 1.05-0.95 (m, 2H), 0.87 (t, J = 7.1 Hz, 3H).

¹³C NMR (75 MHz, CD$_3$OD): δ 202.77, 174.02, 143.19, 141.99, 141.21, 130.29, 129.81, 129.72, 128.99, 128.18, 75.71, 61.76, 49.67, 42.91, 34.06, 33.06, 32.85, 32.32, 31.26, 30.55, 24.36, 23.69, 14.39, 12.72.

IR (KBr pellet): ν 3300, 2928, 2856, 2376, 1663, 1591, 1553, 1365, 1044, 1012, 762, 703 cm^{-1}.

LRMS (ESI: 0.1% formic acid in MeOH) m/z 508 (M$^+$ + 1), 482, 460, 438 (100).

HRMS (ESI: 0.1% formic acid in MeOH) calcd for C$_{32}$H$_{46}$NO$_4$ 508.3427, found 508.3420.

Anal. Calcd for C$_{32}$H$_{45}$NO$_4$: C, 75.70; H, 8.93; N, 2.76. Found: C, 75.75; H, 8.98; N, 2.77.

R-(-)-1-Aminoindane salt (**56e**)
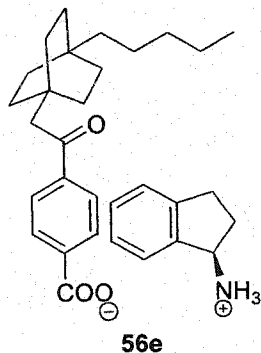
56e

A solution of acid **54** (85.5 mg, 0.25 mmol) in diethyl ether (15 mL) was added to a solution of R-(-)-1-aminoindane (33.3 mg, 0.25 mmol) in diethyl ether (5 mL). The cloudy solution was stirred for 1 h, after which time the precipitate that had formed was filtered, washed with diethyl ether and dried *in vacuo* to afford salt **56e** (99.5 mg, 84 %) as a white powder. Recrystallization from MeOH afforded colorless needles.

mp: 182-185 °C.

^{1}H NMR (300 MHz, CDCl$_3$): δ 7.71 (d, J = 8.0 Hz, 2H), 7.64 (d, J = 8.0 Hz, 2H), 7.50-7.49 (m, 1H), 7.18-7.01 (m, 3H), 4.59 (m, 1H), 2.83 (m, 1H), 2.75 (m, 1H), 2.71 (s, 2H), 2.37 (m, 1H), 1.96 (m, 1H), 1.53-1.48 (m, 6H), 1.35-1.30 (m, 6H), 1.27-1.22 (m, 2H), 1.18-1.12 (m, 4H), 1.05-0.95 (m, 2H), 0.84 (t, J = 7.1 Hz, 3H).

^{13}C NMR (75 MHz, CD$_3$OD): δ 200.52, 172.29, 143.49, 140.28, 139.76, 139.13, 129.35, 128.76, 127.75, 126.96, 124.92, 124.52, 55.58, 48.82, 41.65, 32.83, 32.09, 31.90, 31.65, 31.19, 30.22, 30.16, 23.28, 22.68, 14.08.

IR (KBr pellet): ν 3563, 2930, 2856, 2181, 1665, 1620, 1524, 1456, 1397, 808, 748 cm^{-1}.

LRMS (ESI: 0.1% formic acid in MeOH) *m/z* 476 (M$^+$ + 1, 100), 471 (13.2), 400 (27.0), 365 (39.8), 343 (22.1), 267 (96.7), 166 (58.3), 134 (38.2).

HRMS (ESI: 0.1% formic acid in MeOH) calcd for C$_{31}$H$_{42}$NO$_3$ 476.3165, found 476.3157.

Anal. Calcd for $C_{31}H_{41}NO_3$: C, 78.28; H, 8.69; N, 2.94; O, 10.09. Calcd for $C_{31}H_{41}NO_3 \cdot 1/3H_2O$: C, 77.30; H, 8.72; N, 2.91. Found: C, 77.19; H, 8.86; N, 2.75.

S-(+)-1-Aminoindane salt (56f)
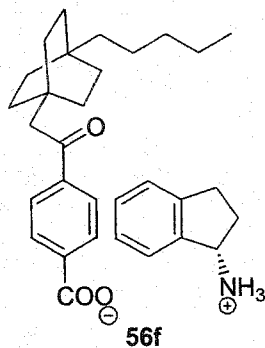
56f

A solution of acid **54** (85.5 mg, 0.25 mmol) in diethyl ether (15 mL) was added to a solution of S-(+)-1-aminoindane (33.3 mg, 0.25 mmol) in diethyl ether (5 mL). The cloudy solution was stirred for 1 h, after which time the precipitate that had formed was filtered, washed with diethyl ether and dried *in vacuo* to afford salt **56f** (90 mg, 76 %) as a white powder. Recrystallization from MeOH afforded colorless needles.

mp: 184-186 °C.

^{1}H NMR (300 MHz, CD$_3$OD): δ 7.98 (d, J = 8.1 Hz, 2H), 7.90 (d, J = 8.1 Hz, 2H), 7.45-7.20 (m, 4H), 4.75 (m, 1H), 3.12 (m, 1H), 2.97 (m, 1H), 2.77 (s, 2H), 2.59 (m, 1H), 2.07 (m, 1H), 1.52 (m, 6H), 1.34 (m, 8H), 1.18 (m, 4H), 1.03 (m, 2H), 0.87 (t, J = 7.0 Hz, 3H).

^{13}C NMR (75 MHz, CD$_3$OD): δ 202.80, 173.89, 145.37, 143.08, 141.25, 140.21, 130.59, 130.29, 128.98, 128.24, 126.34, 125.42, 57.00, 49.69, 42.91, 34.06, 33.07, 32.87, 32.33, 31.95, 31.26, 31.01, 24.35, 23.68, 14.38.

IR (KBr pellet): ν 3564, 2928, 2856, 2663, 2142, 1664, 1620, 1526, 1456, 1397, 1274, 748, 740 cm^{-1}.

LRMS (ESI: 0.1% formic acid in MeOH) *m/z* 476 ($M^+ + 1$), 347 (100), 267, 134, 117.

HRMS (ESI: 0.1% formic acid in MeOH) calcd for $C_{31}H_{42}NO_3$ 476.3165, found 476.3160.

Anal. Calcd for $C_{31}H_{41}NO_3$: C, 78.28; H, 8.69; N, 2.94; O, 10.09. Calcd for $C_{31}H_{41}NO_3 \cdot 1/2H_2O$: C, 76.82; H, 8.73; N, 2.89. Found: C, 76.57; H, 8.72; N, 2.74.

(1S, 2R)-(-)-*cis*-1-Amino-2-indanol salt (**56g**)
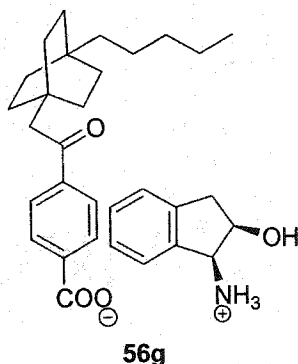
56g

A solution of acid **54** (85.5 mg, 0.25 mmol) in diethyl ether (15 mL) was added to a solution of (1S, 2R)-(-)-*cis*-1-amino-2-indanol (37.3 mg, 0.25 mmol) in diethyl ether (5 mL). The cloudy solution was stirred for 1 h, after which time the precipitate that had formed was filtered, washed with diethyl ether and dried *in vacuo* to afford salt **56g** (87.6 mg, 71 %) as a white powder. Recrystallization from MeOH afforded colorless needles.

mp: 162-165 °C.

¹H NMR (300 MHz, CD$_3$OD): δ 7.99 (d, J = 8.6 Hz, 2H), 7.91 (d, J = 8.6 Hz, 2H), 7.47-7.27 (m, 4H), 4.70 (m, 1H), 4.54 (d, J = 5.9 Hz, 1H), 3.22 (d × d, J_1 = 16.2 Hz, J_2 = 6.5 Hz, 1H), 3.01 (d × d, J_1 = 16.2 Hz, J_2 = 5.1 Hz, 1H), 2.78 (s, 2H), 1.55-1.45 (m, 6H), 1.40-1.25 (m, 8H), 1.20-1.10 (m, 4H), 1.05-0.95 (m, 2H), 0.87 (t, J = 7.3 Hz, 3H).

185

^{13}**C NMR** (75 MHz, CD$_3$OD): δ 202.78, 173.66, 145.12, 142.81, 141.33, 140.78, 130.86, 130.34, 129.00, 128.44, 126.69, 126.14, 72.03, 58.72, 49.68, 42.92, 40.12, 34.08, 33.07, 32.86, 32.33, 31.27, 24.37, 23.70, 14.39.

**IR** (KBr pellet): ν 3443, 2928, 2856, 1664, 1620, 1544, 1458, 1393, 809, 747 cm^{-1}.

LRMS (ESI: 0.1% formic acid in MeOH) *m/z* 492 (M$^+$ + 1, 0.5), 487 (4.7), 150 (100).

HRMS (ESI: 0.1% formic acid in MeOH) calcd for C$_{31}$H$_{42}$NO$_4$ 492.3114, found 492.3108.

Anal. Calcd for C$_{31}$H$_{41}$NO$_4$: C, 75.73; H, 8.41; N, 2.85; O, 13.02. Calcd for C$_{31}$H$_{41}$NO$_4$•1/2H$_2$O: C, 74.37; H, 8.46; N, 2.80. Found: C, 74.04; H, 8.07; N, 2.65.

S-(-)-*p*-Tolylethylamine salt (56h)
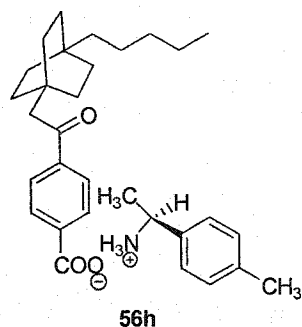
56h

A solution of acid **54** (85.5 mg, 0.25 mmol) in diethyl ether (15 mL) was added to a solution of S-(-)-*p*-tolylethylamine (33.8 mg, 0.25 mmol) in diethyl ether (5 mL). The cloudy solution was stirred for 1 h, after which time the precipitate that had formed was filtered, washed with diethyl ether and dried *in vacuo* to afford salt **56h** (110 mg, 92 %) as a white powder. Recrystallization from MeOH afforded colorless needles.

mp: 187-189 °C.

¹H NMR (300 MHz, CD₃OD): δ 7.98 (d, J = 8.4 Hz, 2H), 7.90 (d, J = 8.4 Hz, 2H), 7.31 (d, J = 8.1 Hz, 2H), 7.24 (d, J = 8.1 Hz, 2H), 4.38 (q, J = 6.9 Hz, 1H), 2.77 (s, 2H), 2.33 (s, 3H), 1.59 (d, J = 6.9 Hz, 3H), 1.55-1.45 (m, 6H), 1.40-1.25 (m, 8H), 1.20-1.10 (m, 4H), 1.05-0.95 (m, 2H), 0.87 (t, J = 7.1 Hz, 3H).

¹³C NMR (75 MHz, CD₃OD): δ 202.80, 175.49, 143.16, 141.23, 140.18, 137.07, 130.80, 130.29, 128.98, 127.52, 52.09, 49.69, 42.91, 34.06, 33.07, 32.87, 32.33, 31.26, 24.35, 23.68, 21.12, 20.89, 14.38.

IR (KBr pellet): ν 3544, 2927, 2858, 2164, 1664, 1612, 1586, 1522, 1396, 813, 763 cm⁻¹.

LRMS (ESI: 0.1% formic acid in MeOH) m/z 478 (M⁺ + 1), 349 (100), 271, 136.

HRMS (ESI: 0.1% formic acid in MeOH) calcd for $C_{31}H_{44}NO_3$ 478.3321, found 478.3329.

Anal. Calcd for $C_{31}H_{43}NO_3$: C, 77.95; H, 9.07; N, 2.93. Calcd for $C_{31}H_{43}NO_3 \cdot 1/3H_2O$: C, 76.98; H, 9.10; N, 2.90. Found: C, 76.94; H, 9.12; N, 3.01.

(1R, 2R)-(-)-Amino-1-phenyl-1, 3-propanediol salt (56i)

56i
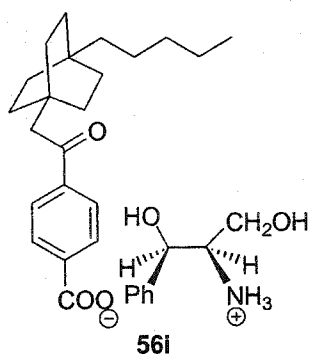
A solution of acid **54** (85.5 mg, 0.25 mmol) in diethyl ether (15 mL) was added to a solution of (1R, 2R)-(-)-amino-1-phenyl-1, 3-propanediol (41.8 mg, 0.25 mmol) in diethyl ether (5 mL). The cloudy solution was stirred for 1 h, after which time the precipitate that had formed was filtered, washed with diethyl ether and dried *in vacuo* to

afford salt **56i** (80.1 mg, 63 %) as a white powder. Recrystallization from MeOH afforded colorless prisms.

mp: 140-142 °C.

^{1}H NMR (300 MHz, CD$_3$OD): δ 7.99 (d, J = 8.4 Hz, 2H), 7.90 (d, J = 8.4 Hz, 2H), 7.43-7.32 (m, 5H), 4.72 (d, J = 8.7 Hz, 1H), 3.52 (d × d, J_1 = 3.8 Hz, J_2 = 11.6 Hz, 1H), 3.40 (d × d, J_1 = 6.1 Hz, J_2 = 11.6 Hz, 1H), 3.28-3.22 (m, 1H), 2.77 (s, 2H), 1.55-150 (m, 6H), 1.37-1.32 (m, 6H), 1.30-1.25 (m, 2H), 1.18-1.16 (m, 4H), 1.05-0.95 (m, 2H), 0.87 (t, J = 7.1 Hz, 3H).

^{13}C NMR (75 MHz, CD$_3$OD): δ 199.97, 168.50, 142.53, 139.38, 129.15, 128.11, 127.62, 127.44, 126.72, 71.37, 60.00, 58.57, 47.92, 41.23, 32.25, 31.39, 31.07, 30.71, 29.78, 22.69, 22.06, 13.88.

IR (KBr pellet): ν 3272, 2923, 2856, 2170, 1692, 1583, 1525, 1456, 1396, 1205, 1042, 781, 761, 700 cm^{-1}.

LRMS (ESI: 0.1% formic acid in MeOH) m/z 510 (M$^+$ + 1, 0.1), 168 (100), 150 (22.7).

HRMS (ESI: 0.1% formic acid in MeOH) calcd for C$_{31}$H$_{44}$NO$_5$ 510.3219, found 510.3226.

Anal. Calcd for C$_{31}$H$_{43}$NO$_5$: C, 73.05; H, 8.50; N, 2.75; O, 15.70. Calcd for C$_{31}$H$_{43}$NO$_5$•H$_2$O: C, 70.56; H, 8.60; N, 2.65. Found: C, 70.20; H, 8.42; N, 2.80.

S-(+)-2-(Methoxymethyl)pyrrolidine salt (**56j**)
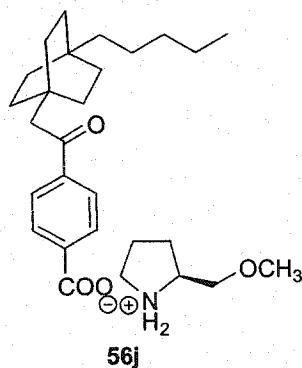
56j

A solution of acid **54** (85.5 mg, 0.25 mmol) in diethyl ether (15 mL) was added to a solution of S-(+)-2-(methoxymethyl)pyrrolidine (28.8 mg, 0.25 mmol) in diethyl ether (5 mL). The cloudy solution was stirred for 1 h, after which time the precipitate that had formed was filtered, washed with diethyl ether and dried *in vacuo* to afford salt **56j** (101.7 mg, 89 %) as a yellowish powder. Recrystallization from MeOH afforded a pale yellow powder.

mp: 76-80 °C.

^{1}H NMR (400 MHz, CD$_3$OD): δ 8.00 (d, J = 8.5 Hz, 2H), 7.91 (d, J = 8.5 Hz, 2H), 3.77 (m, 1H), 3.64 (d × d, J_1 = 3.5 Hz, J_2 = 10.5 Hz, 1H), 3.47 (d × d, J_1 = 7.9 Hz, J_2 = 10.5 Hz, 1H), 3.40 (s, 3H), 3.26 (m, 2H), 2.78 (s, 2H), 2.07 (m, 3H), 1.75 (m, 1H), 1.55-1.50 (m, 6H), 1.37-1.32 (m, 6H), 1.30-1.25 (m, 2H), 1.18-1.16 (m, 4H), 1.04-1.01 (m, 2H), 0.87 (t, J = 7.1 Hz, 3H).

^{13}C NMR (75 MHz, CD$_3$OD): δ 202.69, 173.16, 141.99, 141.56, 130.38, 129.04, 72.08, 60.74, 59.37, 49.69, 46.65, 42.91, 34.04, 33.07, 32.85, 32.32, 31.26, 27.29, 24.86, 24.36, 23.69, 14.39.

IR (KBr pellet): ν 3436, 2936, 2855, 1664, 1628, 1584, 1541, 1457, 1387, 1278, 1096, 954, 780 cm^{-1}.

LRMS (ESI: 0.1% formic acid in MeOH) *m/z* 458 (M$^+$ + 1, 0.11), 378 (5.0), 313 (27.7) 285 (100), 267 (14.4).

HRMS (ESI: 0.1% formic acid in MeOH) calcd for $C_{28}H_{44}NO_4$ 458.3270, found 458.3271.

Anal. Calcd for $C_{28}H_{43}NO_4$: C, 73.48; H, 9.47; N, 3.06; O, 13.98. Calcd for $C_{28}H_{43}NO_4 \cdot 1/2H_2O$: C, 72.07; H, 9.50; N, 3.00. Found: C, 71.99; H, 9.44; N, 2.60.

<u>R-(+)-1-Phenylethylamine salt (**56k**)</u>
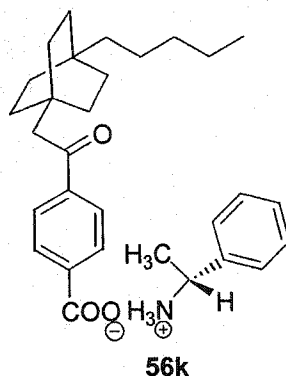
56k

A solution of acid **54** (85.5 mg, 0.25 mmol) in diethyl ether (15 mL) was added to a solution of R-(+)-1-phenylethylamine (30.3 mg, 0.25 mmol) in diethyl ether (5 mL). The cloudy solution was stirred for 1 h, after which time the precipitate that had formed was filtered, washed with diethyl ether and dried *in vacuo* to afford salt **56k** (95.2 mg, 82 %) as a white powder. Recrystallization from MeOH afforded colorless needles.

mp: 185-187 °C.

^{1}H NMR (300 MHz, CD$_3$OD): δ 7.98 (d, *J* = 8.5 Hz, 2H), 7.90 (d, *J* = 8.5 Hz, 2H), 7.45-7.35 (m, 5H), 4.42 (q, *J* = 6.9 Hz, 1H), 2.77 (s, 2H), 1.60 (d, *J* = 6.9 Hz, 3H), 1.55-1.50 (m, 6H), 1.40-1.25 (m, 8H), 1.20-1.10 (m, 4H), 1.05-0.95 (m, 2H), 0.87 (t, *J* = 7.1 Hz, 3H).

^{13}C NMR (75 MHz, CD$_3$OD): δ 200.45, 172.05, 145.71, 140.48, 139.40, 129.52, 128.84, 128.23, 127.79, 126.30, 51.15, 48.82, 41.65, 32.84, 32.08, 31.88, 31.18, 30.21, 23.28, 22.68, 21.77, 14.08.

IR (KBr pellet): ν 3544, 2927, 2856, 2559, 2198, 1716, 1661, 1627, 1581, 1532, 1456, 1394, 760, 739, 692 cm^{-1}.

LRMS (ESI: 0.1% formic acid in MeOH) *m/z* 464 (M$^+$ + 1, 94.4%), 459 (39.4%), 400 (69.7), 343 (78.7), 243 (100).

HRMS (ESI: 0.1% formic acid in MeOH) calcd for $C_{30}H_{42}NO_3$ 464.3165, found 464.3163.

Anal. Calcd for $C_{30}H_{41}NO_3$: C, 77.71; H, 8.91; N, 3.02; O, 10.35. Calcd for $C_{30}H_{41}NO_3 \cdot 1/3H_2O$: C, 76.72; H, 8.94; N, 2.98. Found: C, 76.43; H, 8.86; N, 2.98.

<u>S-(-)-1-Phenylethylamine salt (56l)</u>
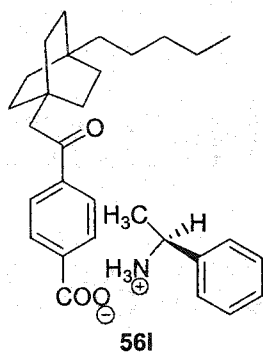
A solution of acid **54** (85.5 mg, 0.25 mmol) in diethyl ether (15 mL) was added to a solution of S-(-)-1-phenylethylamine (30.3 mg, 0.25 mmol) in diethyl ether (5 mL). The cloudy solution was stirred for 1 h, after which time the precipitate that had formed was filtered, washed with diethyl ether and dried *in vacuo* to afford salt **56l** (105 mg, 91 %) as a white powder. Recrystallization from MeOH afforded colorless needles.

mp: 185-187 °C.

^{1}**H NMR** (300 MHz, CD$_3$OD): δ 7.98 (d, J = 8.3 Hz, 2H), 7.90 (d, J = 8.3 Hz, 2H), 7.43 (m, 5H), 4.42 (q, J = 6.8 Hz, 1H), 2.77 (s, 2H), 1.61 (d, J = 6.8 Hz, 3H), 1.60-1.40 (m, 6H), 1.40-1.25 (m, 8H), 1.25-1.05 (m, 4H), 1.05-0.95 (m, 2H), 0.87 (t, J = 7.0 Hz, 3H).

^{13}**C NMR** (75 MHz, CD$_3$OD): δ 202.80, 185.93, 143.10, 141.26, 140.19, 130.29, 130.26, 130.05, 128.98, 127.58, 52.33, 49.57, 42.91, 34.06, 33.07, 32.87, 32.33, 31.26, 24.35, 23.68, 20.99, 14.38.

IR (KBr pellet): ν 3568, 2927, 2857, 2557, 2204, 1720, 1661, 1631, 1581, 1531, 1392, 760, 739, 692 cm^{-1}.

LRMS (ESI: 0.1% formic acid in MeOH) m/z 464 (M$^+$ + 1), 335 (100), 122, 105.

HRMS (ESI: 0.1% formic acid in MeOH) calcd for C$_{30}$H$_{42}$NO$_3$ 464.3165, found 464.3167.

Anal. Calcd for C$_{30}$H$_{41}$NO$_3$: C, 77.71; H, 8.91; N, 3.02; O, 10.35. Calcd for C$_{30}$H$_{41}$NO$_3$•1/2H$_2$O: C, 76.23; H, 8.96; N, 2.96. Found: C, 76.04; H, 8.85; N, 3.04.

(-)-*cis*-Myrtanylamine salt (56m)
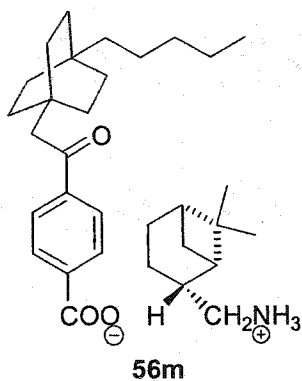
56m

A solution of acid **54** (85.5 mg, 0.25 mmol) in diethyl ether (15 mL) was added to a solution of (-)-*cis*-myrtanylamine (38.3 mg, 0.25 mmol) in diethyl ether (5 mL). The cloudy solution was stirred for 1 h, after which time the precipitate that had formed was

filtered, washed with diethyl ether and dried *in vacuo* to afford salt **56m** (112 mg, 90 %) as a white powder. Recrystallization from MeOH afforded colorless prisms.

mp: 155-157 °C.

^{1}**H NMR** (300 MHz, CD$_3$OD): δ 7.98 (d, J = 8.3 Hz, 2H), 7.90 (d, J = 8.3 Hz, 2H), 2.93 (d, J = 7.5 Hz, 2H), 2.77 (s, 2H), 2.44 (m, 1H), 2.33 (m, 1H), 1.98 (m, 5H), 1.60-1.45 (m, 7H), 1.40-1.25 (m, 8H), 1.23 (s, 3H), 1.22-1.10 (m, 4H), 1.02 (s, 3H), 1.00-0.90 (m, 3H), 0.87 (t, J = 7.0 Hz, 3H).

^{13}**C NMR** (75 MHz, CD$_3$OD): δ 202.81, 178.40, 143.33, 141.19, 130.27, 128.97, 49.69, 46.35, 44.71, 42.91, 42.46, 41.04, 39.59, 34.06, 33.72, 33.07, 32.87, 32.33, 31.26, 28.14, 26.69, 24.35, 23.68, 23.42, 20.44, 14.37.

IR (KBr pellet): ν 3544, 2925, 2856, 2145, 1671, 1620, 1585, 1537, 1367, 1272, 760, cm^{-1}.

LRMS (ESI: 0.1% formic acid in MeOH) *m/z* 496 (M$^+$ + 1), 367 (100), 307, 154.

HRMS (ESI: 0.1% formic acid in MeOH) calcd for C$_{32}$H$_{50}$NO$_3$ 496.3791, found 496.3785.

Anal. Calcd for C$_{32}$H$_{49}$NO$_3$: C, 77.53; H, 9.96; N, 2.83; O, 9.68. Calcd for C$_{32}$H$_{49}$NO$_3$•1/4H$_2$O: C, 76.83; H, 9.97; N, 2.80. Found: C, 76.49; H, 10.02; N, 2.70.

4.4 Synthesis of Bicyclo[2.2.1]heptane Derivatives 57, 58 and 59

4.4.1 Preparation of Ketones 57 and 58

2,2-Dichlorobicyclo[2.2.1]heptane (87)[97(b)]

87
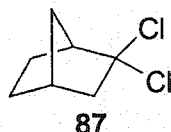
To a solution of norcamphor (25.0 g, 227 mmol) in PCl$_3$ (15.0 mL), which was cooled in an ice bath, was added, in portions, PCl$_5$ (53.0g, 255 mmol) over 15 min. The mixture was allowed to warm slowly to room temperature, and stirred overnight. The mixture was poured into 500 g of ice and extracted with n-pentane (3 × 300 mL). The combined organic extracts were washed with water (4 × 100 mL), brine (2 × 100 mL), and dried (MgSO$_4$). Purification by vacuum distillation afforded compound **87** as a white solid (31.8 g, 85%).

bp: 80-82 °C/22mmHg (Lit.[97(b)] 65.0-68.1 °C/12.0-12.4mmHg).

^{1}H NMR (400 MHz, CDCl$_3$): δ 2.71 (s, 1H), 2.60 (m, 1H), 2.30 (m, 1H), 2.08 (m, 1H), 1.96 (m, 2H), 1.54 (m, 2H), 1.41 (m, 1H), 1.17 (m, 1H).

^{13}C NMR (100 MHz, CDCl$_3$): δ 95.06, 55.79, 55.20, 37.65, 37.49, 27.38, 25.20.

LRMS (EI) m/z 165 (M$^+$), 129, 93, 68 (100).

1-Chlorobicyclo[2.2.1]heptane (88)[97(b)]

88

To a cooled (0 °C) solution of compound **87** (31.7 g, 192 mmol) in *iso*-pentane (40 mL) and *n*-pentane (140 mL) (both *iso*-pentane and *n*-pentane were purified by distillation over anhydrous aluminum trichloride) was added anhydrous aluminum trichloride (12.4 g, 92.9 mmol) in small portions as rapidly as the hydrogen chloride evolution would permit. The mixture was stirred at room temperature for 8 h. The pentane layer was decanted and the remaining dark sludge was washed with *n*-pentane (4 × 80 mL). The combined pentane extracts were washed with 5% $NaHCO_3$ (2 × 80 mL), water (2 × 80 mL), and dried (Na_2SO_4). Distillation provided compound **88** (12.2 g, 49%) as a colorless liquid.

bp: 146-152 °C (Lit.[97(b)] 70-71 °C/54 mmHg).

^{1}H NMR (300 MHz, $CDCl_3$): δ 2.17 (m, 1H), 1.80 (m, 4H), 1.67 (m, 2H), 1.45-1.10 (m, 4H).

^{13}C NMR (75 MHz, $CDCl_3$): δ 69.77, 46.79, 38.40, 34.83, 30.93.

LRMS (EI) *m/z* 130 (M^+), 101(100), 95, 79, 67.

2-(4-Fluorophenyl)oxirane (90)
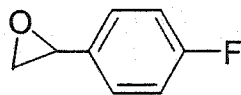
90

A solution of 3-chloroperoxybenzoic acid (*m*-CPBA ~70%, 27.3 g, 110.7 mmol) in CH_2Cl_2 (100 mL) was added to a solution of 4-fluorostyrene (8.5 g, 73.8 mmol) in CH_2Cl_2 (300 mL) at room temperature. Stirring was continued for 12 h, after which time the reaction was quenched by saturated Na_2SO_3 (300 mL). The aqueous phase was extracted with CH_2Cl_2 (3 × 200 mL). The combined organic extracts were washed with water (5 × 100 mL), brine (2 × 100 mL), and dried (Na_2SO_4). Removal of the solvent *in*

vacuo provided a yellowish liquid. Purification by column chromatography on silica gel (petroleum ether-ether, 95:5) afforded compound **90** (7.3 g, 76%) as a colorless liquid.

^{1}**H NMR** (300 MHz, CDCl$_3$): δ 7.22 (m, 2H), 7.01 (m, 2H), 3.82 (d×d, J_1 = 2.7 Hz, J_2 = 4.0 Hz, 1H), 3.11 (d×d, J_1 = 4.0 Hz, J_2 = 5.4 Hz, 1H), 2.74 (d×d, J_1 = 2.7 Hz, J_2 = 5.4 Hz, 1H).

^{13}**C NMR** (75 MHz, CDCl$_3$): δ 164.08, 160.82, 133.26, 133.23, 127.00, 126.89, 115.30, 115.01, 51.46, 50.75.

LRMS (EI) *m/z* 138 (M$^+$), 109(100), 83, 57.

1-(4'-Fluorophenyl)-2-bicylo[2.2.1]hept-1-yl ethanol **(91)**

91
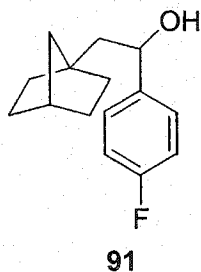
A suspension of lithium wire (0.53 g, 76.4 mmol, washed with petroleum ether and wiped with a paper towel) in dry cyclohexane (5 mL) was heated to reflux under an oxygen-free argon atmosphere. To the mixture was added a solution of 1-chloro bicyclo[2.2.1]heptane (**88**, 1.0 g, 7.6 mmol) in dry cyclohexane (5mL) over 30 min. The resulting mixture was heated to be refluxing for 10 h, after which time dry cyclohexane (20 mL) was added to dissolve the reaction mixture (the lithium carbanion solution). To a cold (-78°C) suspension of CuCN (0.34 g, 3.8 mmol, dried *in vacuo*) in THF (15 mL) was added the lithium solution over 15 min. The reaction was stirred at -78°C for 10 min before a solution of 2-(4-fluorophenyl)oxirane (**90**, 0.74 g, 5.4 mmol, 0.63mL) in THF (5 mL) was added dropwise over 15 min. The resulting solution was stirred at -78°C for 2 h followed by warming slowly to room temperature. The reaction was quenched with saturated NH$_4$Cl (100 mL), and extracted with diethyl ether (3 × 100 mL). The combined

ethereal extracts were washed with water (2 × 40 mL), brine (2 × 40 mL), and dried (Na$_2$SO$_4$). Removal of the solvent *in vacuo* provided a yellowish solid. Purification by column chromatography on silica gel (petroleum ether-ether, 9:1) afforded compound **91** (0.62 g, 50%) as a white solid.

mp: 73.5-75.0 °C.

^{1}H NMR (300 MHz, CDCl$_3$): δ 7.29 (m, 2H), 6.99 (m, 2H), 7.42 (m, 5H), 4.76 (m, 1H), 2.12 (m, 1H), 1.97 (m, 2H), 1.89 (s, 1H), 1.60-1.64 (m, 3H), 1.40-1.15 (m, 7H).

^{13}C NMR (75 MHz, CDCl$_3$): δ 163.70 and 160.46 ($^1J_{C-F}$ = 243 Hz), 141.59, 127.63 and 127.52 ($^3J_{C-F}$ = 8 Hz), 115.30 and 115.02 ($^2J_{C-F}$ = 21 Hz), 72.81, 46.19, 45.42, 44.44, 36.60, 34.88, 34.74, 30.87, 30.58.

IR (KBr pellet): ν 3255 (br), 2949, 2914, 2867, 1605, 1511, 1227, 1027, 838, 567 cm^{-1}.

LRMS ((ESI: 0.1% formic acid in MeOH) *m/z* 233 (M$^+$-1, 100), 185, 137.

HRMS ((ESI: 0.1% formic acid in MeOH) calcd for C$_{15}$H$_{18}$FO (M$^+$-1) 233.1342, found 233.1348.

Anal. Calcd for C$_{15}$H$_{19}$FO: C, 76.89; H, 8.17. Found: C, 76.96; H, 8.29.

1-(4'-Fluorophenyl)-2-bicyclo[2.2.1]hept-1-yl ethanone (92)

92
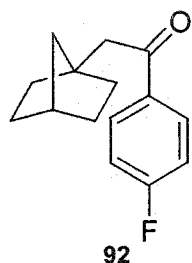
To a solution of alcohol **91** (3.0 g, 12.8 mmol) in acetone (65 mL) was added dropwise Jones' Reagent (prepared from 2.0 g chromium trioxide, 5.5 mL water and 1.8 mL of conc. sulfuric acid), maintaining the reaction temperature at 10-15 °C. After stirring for 2h, the solvent was removed *in vacuo*, and the dark residue was taken up in water (80 mL) and extracted with diethyl ether (3×100 mL). The organic extracts were combined and washed with water (30 mL), brine (2×50 mL) and dried (Na_2SO_4). Removal of the solvent *in vacuo* provided compound **92** (2.72 g, 92%) as a yellowish liquid. The compound did not require further purification.

^{1}H NMR (300 MHz, $CDCl_3$): δ 7.96 (m, 2H), 7.09 (m, 2H), 3.13 (s, 2H), 2.15 (m, 1H), 1.7-1.5 (m, 2H), 1.5-1.3 (m, 4H), 1.3-1.2 (m, 4H).

^{13}C NMR (75 MHz, $CDCl_3$): δ 198.71, 167.28 and 163.91 ($^1J_{C-F}$ = 253 Hz), 134.53 and 134.50 ($^4J_{C-F}$ = 2 Hz), 130.93 and 130.81 ($^3J_{C-F}$ = 9 Hz), 115.64 and 115.35 ($^2J_{C-F}$ = 22 Hz), 45.73, 43.90, 43.35, 36.39, 34.83, 30.57.

IR (neat): ν 3069, 2950, 2917, 2869, 1677, 1598, 1507, 1234, 1156, 833, 588 cm^{-1}.

LRMS (EI) *m/z* 232 (M$^+$), 138, 123 (100), 95.

HRMS (EI) calcd for $C_{15}H_{17}FO$ (M$^+$) 232.1263, found 232.1265.

Anal. Calcd for $C_{15}H_{17}FO$: C, 77.56; H, 7.38. Found: C, 77.90; H, 7.59.

1-(4'-Cyanophenyl)-2-bicyclo[2.2.1]hept-1-yl ethanone (**93**)
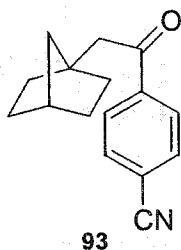
A mixture of compound **92** (2.72g, 11.7 mmol) and sodium cyanide (0.86g, 17.6 mmol) in anhydrous DMF (30 mL) was heated to be refluxing at 150 °C under an argon atmosphere for 17 h. The resulting dark mixture was quenched with water (150 mL) extracted with diethyl ether (3 × 100 mL). The combined extracts were washed with water (2 × 50 mL), brine (2 × 50 mL) and dried (Na$_2$SO$_4$). Removal of the solvent *in vacuo* provided compound **93** (2.54 g, 94%) as a yellowish solid. The compound did not require further purification.

mp: 53-54 °C.

^{1}H NMR (400 MHz, CDCl$_3$): δ 7.98 (d, J = 8.4 Hz, 2H), 7.70 (d, J = 8.4 Hz, 2H), 3.14 (s, 2H), 2.11 (m, 1H), 1.54 (m, 2H), 1.40 (m, 4H), 1.21 (m, 4H).

^{13}C NMR (100 MHz, CDCl$_3$): δ 198.72, 140.80, 132.26, 128.48, 117.85, 115.87, 45.45, 43.70, 43.55, 36.50, 34.57, 30.38.

IR (KBr pellet): ν 2948, 2870, 2224, 1691, 1402, 1206, 999, 828, 578 cm^{-1}.

LRMS (EI) *m/z* 239 (M$^+$), 210, 171, 130 (100), 102, 94, 79.

HRMS (EI) calcd for C$_{16}$H$_{17}$NO (M$^+$) 239.1310, found 239.1313.

Anal. Calcd for C$_{16}$H$_{17}$NO: C, 80.30; H, 7.16; N, 5.85. Found: C, 80.00; H, 7.33; N, 5.92.

1-(4'-carboxylphenyl)-2-bicyclo[2.2.1]hept-1-yl ethanone (57)

57   COOH
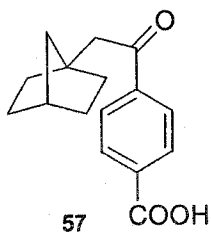
To a solution of potassium hydroxide (8.0 g, 143 mmol) in water (40 mL) was added a solution of compound **93** (2.54g, 10.6 mmol) in ethanol (10 mL). The mixture was heated to be refluxing at 95 °C for 20 h. The reaction was quenched with water (100 mL). The solution was washed with methylene chloride (2 × 30 mL). The aqueous solution was carefully acidified to pH 2 with concentrated HCl. The precipitated carboxylic acid was extracted with ether (4 × 150 mL) and the combined ethereal extracts were washed with water (2 × 30 mL), brine (2 × 30 mL), and dried (Na$_2$SO$_4$). Removal of the solvent *in vacuo* provided a yellowish solid. Recrystallization from ethanol afforded compound **57** (2.50 g, 91%) as colorless plates.

mp: 210-212 °C.

^{1}H NMR (300 MHz, CDCl$_3$): δ 8.17 (d, *J* = 8.5 Hz, 2H), 8.01 (d, *J* = 8.5 Hz, 2H), 3.20 (s, 2H), 2.17 (m, 1H), 1.58 (m, 2H), 1.41 (m, 4H), 1.27 (m, 4H).

^{13}C NMR (75 MHz, CDCl$_3$): δ 199.89, 170.83, 142.04, 132.67, 130.38, 128.22, 45.69, 43.90, 43.88, 36.68, 34.80, 30.56.

IR (KBr pellet): ν 3543, 2948, 2867, 1686, 1290, 768 cm^{-1}.

LRMS (+CI: gas, NH$_3$) *m/z* 276 (M$^+$ + 18, 27.0%), 259 (M$^+$ + 1, 66.3%), 243 (15.8%), 232 (23.3%), 215 (100%), 149 (17.9%), 124 (18.0%).

HRMS (+CI: gas, NH$_3$) calcd for C$_{16}$H$_{19}$O$_3$ (M$^+$ + 1) 259.1334, found 259.1335.

Anal. Calcd for C$_{16}$H$_{18}$O$_3$: C, 74.39; H, 7.02. Found: C, 74.65; H, 6.98.

1-(4'-Methoxycarbonylphenyl)-2-bicyclo[2.2.1]hept-1-yl ethanone (58)
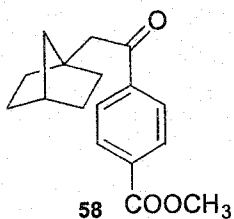
To a solution of acid **57** (0.150 g) in diethyl ether (5 mL) was added a solution of diazomethane in diethyl ether (10 mL, excess in the reaction) at room temperature. The reaction was stirred for 10 min. Removal of the solvent *in vacuo* provided a white solid. Recrystallization from ethanol afforded ester **58** (0.158 g, 100 %) as colorless plates.

mp: 76-77 °C.

UV (CH$_3$OH): λ 205.0 (1.63×10^4), 250.0 (2.15 × 10^4), 290.0 (1.73 × 10^3) nm (M^{-1}cm^{-1}).

^{1}H NMR (300 MHz, CDCl$_3$): δ 8.08 (d, J = 8.4 Hz, 2H), 7.96 (d, J = 8.4 Hz, 2H), 3.91 (s, 3H), 3.17 (s, 2H), 2.14 (m, 1H), 1.59 (m, 2H), 1.39 (m, 4H), 1.25 (m, 4H).

^{13}C NMR (75 MHz, CDCl$_3$, APT: C, CH$_2$: +; CH, CH$_3$: -): δ 199.80 (+), 166.24 (+), 141.30 (+), 133.54 (+), 129.70 (-), 128.09 (-), 52.36 (-), 45.64 (+), 43.85 (+), 43.77 (+), 36.65 (-), 34.75 (+), 30.53 (+).

IR (KBr pellet): ν 2956, 2867, 1720, 1685, 1571, 1278, 1199, 1109, 764 cm^{-1}.

LRMS (EI) *m/z* 272 (M$^+$), 213, 163 (100), 135, 104, 79.

HRMS (EI) calcd for C$_{17}$H$_{20}$O$_3$ (M$^+$) 272.1412, found 272.1412.

Anal. Calcd for C$_{17}$H$_{20}$O$_3$: C, 74.97; H, 7.40. Found: C, 75.17; H, 7.55.

This structure was confirmed by X-ray crystallographic analysis:

Habit	colorless plates
Space group	$P2_12_12_1$
a, Å	5.8460(10)
b, Å	11.314(2)
c, Å	11.914(2)
α (°)	109.17(3)
β (°)	98.08(2)
γ (°)	96.16(2)
Z	2
R	0.051

4.4.2 Preparation of Bicyclo[2.2.1]heptyl Salts 59

L-Prolinamide salt (59a)
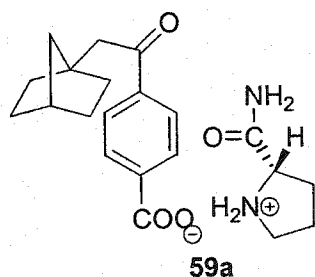
59a

A solution of acid **57** (77 mg, 0.30 mmol) in diethyl ether (15 mL) was added to a solution of L-prolinamide (34 mg, 0.30 mmol) in Et_2O (15 mL). The cloudy solution was stirred for 1 h, after which time the precipitate that had formed was filtered, washed with diethyl ether and dried *in vacuo* to afford salt **59a** (92 mg, 82 %) as a white powder. Recrystallization from MeOH afforded colorless plates.

mp: 162-163 °C.

¹H NMR (300 MHz, CD₃OD): δ 7.94 (d, J = 8.2 Hz, 2H), 7.89 (d, J = 8.2 Hz, 2H), 4.16 (m, 1H), 3.24 (m, 2H), 3.15 (s, 2H), 2.34 (m, 1H), 2.07 (m, 1H), 1.94 (m, 3H), 1.53 (m, 2H), 1.42 (m, 2H), 1.33 (m, 2H), 1.21 (m, 4H).

¹³C NMR (75 MHz, CD₃OD): δ 202.57, 173.78, 172.91, 142.66, 140.74, 130.34, 128.98, 60.95, 47.31, 46.93, 44.74, 44.51, 37.93, 35.73, 31.56, 31.25, 25.35.

IR (KBr pellet): ν 3321, 2946, 2862, 1707, 1684, 1672, 1592, 1553, 1373, 1205, 996, 776 cm⁻¹.

LRMS (ESI: 0.1% formic acid in MeOH) m/z 373 (M⁺ + 1), 328 (100), 229, 115.

HRMS (ESI: 0.1% formic acid in MeOH) calcd for $C_{21}H_{29}N_2O_4$ (M⁺ + 1) 373.2127, found 373.2131.

Anal. Calcd for $C_{21}H_{28}N_2O_4$: C, 67.72; H, 7.58; N, 7.52. Found: C, 67.46; H, 7.76; N, 7.58.

(1S, 2R)-(-)-*cis*-1-Amino-2-indanol salt (**59b**)
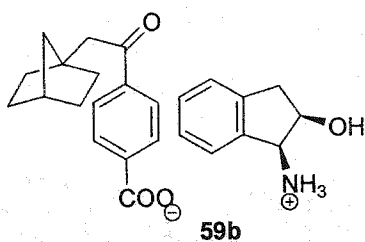
59b

A solution of acid **57** (77 mg, 0.30 mmol) in diethyl ether (15 mL) was added to a solution of (1S, 2R)-(-)-*cis*-1-amino-2-indanol (45 mg, 0.30 mmol) in diethyl ether (5 mL). The cloudy solution was stirred for 1 h, after which time the precipitate that had formed was filtered, washed with diethyl ether and dried *in vacuo* to afford salt **59b** (100 mg, 82 %) as a white powder. Recrystallization from MeOH afforded colorless needles.

mp: 166-168 °C.

¹H NMR (300 MHz, CD₃OD): δ 8.00 (d, J = 8.5 Hz, 2H), 7.94 (d, J = 8.5 Hz, 2H), 7.47 (m, 1H), 7.30 (m, 3H), 4.71 (m, 1H), 4.56 (d, J = 5.9 Hz, 1H), 3.22 (d × d, J_1 = 16.1 Hz, J_2 = 6.5 Hz, 1H), 3.21 (s, 2H), 3.02 (d × d, J_1 = 16.1 Hz, J_2 = 5.0 Hz, 1H), 2.14 (m, 1H), 1.65-1.55 (m, 2H), 1.55-1.35 (m, 4H), 1.35-1.20 (m, 4H).

¹³C NMR (75 MHz, CD₃OD): δ 202.60, 173.97, 145.03, 142.79, 140.62, 138.24, 130.81, 130.33, 128.95, 128.40, 126.63, 126.19, 71.98, 58.65, 46.93, 44.75, 44.50, 40.10, 37.93, 35.73, 31.56.

IR (KBr pellet): ν 3540, 3039, 2951, 2867, 2632, 2100, 1715, 1672, 1582, 1539, 1399, 744 cm⁻¹.

LRMS (ESI: 0.1% formic acid in MeOH) m/z (relative intensity) 408 (M⁺ + 1, 3.7), 150 (100).

HRMS (ESI: 0.1% formic acid in MeOH) calcd for $C_{25}H_{30}NO_4$ (M⁺ + 1) 408.2176, found 408.2184.

Anal. Calcd for $C_{25}H_{29}NO_4$: C, 73.68; H, 7.17; N, 3.44. Found: C, 73.44; H, 7.17; N, 3.35.

S-(-)-*p*-Tolylethylamine salt (**59c**)
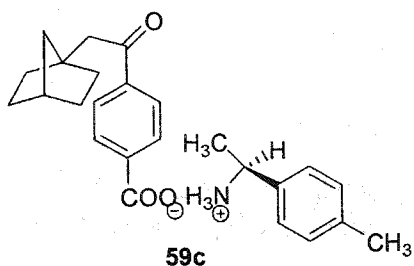
59c

A solution of acid **57** (77 mg, 0.30 mmol) in diethyl ether (15 mL) was added to a solution of S-(-)-*p*-tolylethylamine (41 mg, 0.30 mmol) in diethyl ether (5 mL). The cloudy solution was stirred for 1 h, after which time the precipitate that had formed was filtered, washed with diethyl ether and dried *in vacuo* to afford salt **59c** (105 mg, 89 %) as a white powder. Recrystallization from MeOH afforded colorless needles.

mp: 177-179 °C.

^{1}H NMR (300 MHz, CD$_3$OD): δ 7.99 (d, J = 8.5 Hz, 2H), 7.94 (d, J = 8.5 Hz, 2H), 7.31 (d, J = 8.1 Hz, 2H),), 7.23 (d, J = 8.1 Hz, 2H), 4.38 (q, J = 6.9 Hz, 1H), 3.22 (s, 2H), 2.33 (s, 3H), 2.14 (m, 1H), 1.59 (d, J = 6.9 Hz, 3H), 1.65-1.55 (m, 2H), 1.55-1.35 (m, 4H), 1.35-1.20 (m, 4H).

^{13}C NMR (75 MHz, CD$_3$OD): δ 202.64, 173.97, 143.25, 140.56, 140.17, 137.02, 130.80, 130.31, 128.94, 127.53, 52.08, 46.95, 44.75, 44.51, 37.94, 35.74, 31.57, 21.12, 20.87.

IR (KBr pellet): ν 3544, 3020, 2952, 2868, 2145, 1716, 1671, 1620, 1525, 1395, 762 cm^{-1}.

LRMS (ESI: 0.1% formic acid in MeOH) *m/z* 394 (M$^+$ + 1, 100), 281 (5.8), 271 (28.9), 259 (4.9), 242 (89).

HRMS (ESI: 0.1% formic acid in MeOH) calcd for C$_{25}$H$_{32}$NO$_3$ (M$^+$ + 1) 394.2382, found 394.2373.

Anal. Calcd for C$_{25}$H$_{31}$NO$_3$: C, 76.30; H, 7.94; N, 3.56; O, 12.20. Calcd for C$_{25}$H$_{31}$NO$_3$•1/4H$_2$O: C, 75.44; H, 7.98; N, 3.52. Found: C, 75.28; H, 8.10; N, 3.44.

R-(-)-1-Cyclohexylethylamine salt (59d)
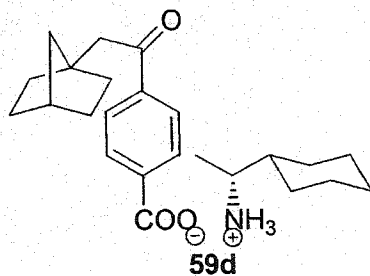
A solution of acid **57** (77 mg, 0.30 mmol) in diethyl ether (15 mL) was added to a solution of R-(-)-1-cyclohexylethylamine (38 mg, 0.30 mmol) in diethyl ether (5 mL). The cloudy solution was stirred for 1 h, after which time the precipitate that had formed was filtered, washed with diethyl ether and dried *in vacuo* to afford salt **59d** (105 mg, 91 %) as a white powder. Recrystallization from MeOH afforded colorless needles.

mp: 175-176 °C.

^{1}H NMR (300 MHz, CD$_3$OD): δ 8.00 (d, J = 8.5 Hz, 2H), 7.94 (d, J = 8.5 Hz, 2H), 3.22 (s, 2H), 3.07 (m, 1H), 2.14 (m, 1H), 1.85-1.70 (m, 5H), 1.70-1.55 (m, 2H), 1.55-1.35 (m, 5H), 1.27 (m, 7H), 1.23 (d, J = 6.7 Hz, 3H), 1.06 (m, 2H).

^{13}C NMR (75 MHz, CD$_3$OD): δ 202.62, 174.08, 143.46, 140.52, 130.29, 128.95, 53.40, 46.95, 44.76, 44.51, 42.74, 37.94, 35.75, 31.58, 30.02, 28.83, 27.08, 27.00, 26.92, 16.05.

IR (KBr pellet): ν 3564, 2943, 2865, 2164, 1716, 1681, 1624, 1584, 1532, 1382, 1208, 998, 780 cm^{-1}.

LRMS (ESI: 0.1% formic acid in MeOH) *m/z* (relative intensity) 542 (100), 386 (M$^+$ + 1, 9.5), 281 (14.1), 259 (20.0), 242 (38.4).

HRMS (ESI: 0.1% formic acid in MeOH) calcd for C$_{24}$H$_{36}$NO$_3$ (M$^+$ + 1) 386.2695, found 386.2692.

Anal. Calcd for $C_{24}H_{35}NO_3$: C, 74.77; H, 9.15; N, 3.63. Found: C, 74.53; H, 9.39; N, 3.60.

This structure was confirmed by X-ray crystallographic analysis:

Habit	colorless needles
Space group	$P2_12_12_1$
a, Å	6.197(1)
b, Å	17.606(3)
c, Å	20.766(4)
α (°)	90
β (°)	90
γ (°)	90
Z	4
R	0.065

(1S, 2R)-(+)-Norephedrine salt (59e)
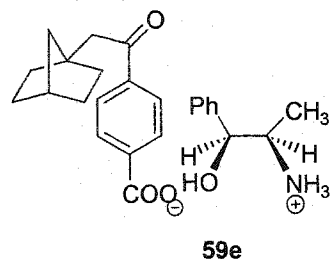
59e

A solution of acid **57** (77 mg, 0.30 mmol) in diethyl ether (15 mL) was added to a solution of (1S, 2R)-(+)-norephedrine (45 mg, 0.30 mmol) in diethyl ether (5 mL). The cloudy solution was stirred for 1 h, after which time the precipitate that had formed was filtered, washed with diethyl ether and dried *in vacuo* to afford salt **59e** (105 mg, 86 %) as a white powder. Recrystallization from MeOH afforded colorless needles.

mp: 144-147 °C.

^{1}H NMR (300 MHz, CD$_3$OD): δ 8.01 (d, J = 8.6 Hz, 2H), 7.94 (d, J = 8.6 Hz, 2H), 7.40-7.25 (m, 5H), 4.93 (d, J = 3.4 Hz, 1H), 3.49 (d × q, J_1 = 3.4 Hz, J_2 =6.6 Hz, 1H), 3.22 (s, 2H), 2.14 (m, 1H), 1.70-1.55 (m, 2H), 1.55-1.35 (4H, m), 1.35-1.20 (m, 4H), 1.07 (d, J = 6.6 Hz, 3H).

^{13}C NMR (75 MHz, CD$_3$OD): δ 202.65, 174.02, 143.23, 141.58, 140.58, 130.32, 129.53, 129.00, 128.96, 127.19, 73.74, 53.68, 46.95, 44.75, 44.51, 37.94, 35.74, 31.57, 12.56.

IR (KBr pellet): ν 3352, 2950, 2869, 2088, 1716, 1684, 1635, 1588, 1554, 1518, 1393, 1206, 1051, 780 cm^{-1}.

LRMS (ESI: 0.1% formic acid in MeOH) m/z (relative intensity) 410 (M$^+$ + 1, 0.5), 259 (2.1), 152 (100).

HRMS (ESI: 0.1% formic acid in MeOH) calcd for C$_{25}$H$_{32}$NO$_4$ (M$^+$ + 1) 410.2331, found 410.2320.

Anal. Calcd for C$_{25}$H$_{31}$NO$_4$: C, 73.32; H, 7.63; N, 3.42; O, 15.63. Calcd for C$_{25}$H$_{31}$NO$_4$•1/4H$_2$O: C, 72.95; H, 7.89; N, 3.27. Found: C, 72.68; H, 7.75; N, 3.30.

R-(+)-1-Phenylethylamine salt (59f)
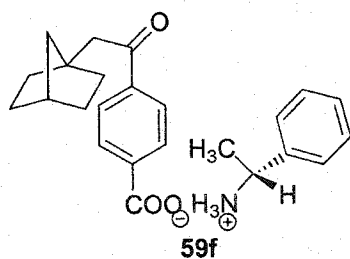
59f

A solution of acid **57** (77 mg, 0.30 mmol) in diethyl ether (15 mL) was added to a solution of R-(+)-1-phenylethylamine (36 mg, 0.30 mmol) in diethyl ether (5 mL). The cloudy solution was stirred for 1 h, after which time the precipitate that had formed was filtered, washed with diethyl ether and dried *in vacuo* to afford salt **59f** (90 mg, 79 %) as a white powder. Recrystallization from MeOH afforded colorless needles.

mp: 166-167 °C.

^{1}H NMR (300 MHz, CD$_3$OD): δ 7.92 (d, J = 8.0 Hz, 2H), 7.86 (d, J = 8.0 Hz, 2H), 7.33 (m, 5H), 4.35 (q, J = 6.7 Hz, 1H), 3.14 (s, 2H), 2.06 (m, 1H), 1.53 (d, J = 6.7 Hz, 3H), 1.51 (m, 2H), 1.41 (m, 2H), 1.32 (m, 2H), 1.20 (m, 4H).

^{13}C NMR (75 MHz, CD$_3$OD): δ 202.62, 173.97, 143.20, 140.59, 140.13, 130.31, 130.25, 130.03, 128.95, 127.60, 52.31, 46.95, 44.76, 44.51, 37.94, 35.75, 31.57, 20.97.

IR (KBr pellet): ν 3521, 2947, 2866, 2211, 1716, 1684, 1672, 1622, 1584, 1524, 1386, 1208, 996, 779, 700 cm^{-1}.

LRMS (ESI: 0.1% formic acid in MeOH) m/z 380 (M$^+$ + 1), 335 (100), 122.

HRMS (ESI: 0.1% formic acid in MeOH) calcd for C$_{24}$H$_{30}$NO$_3$ (M$^+$ + 1) 380.2226, found 380.2234.

Anal. Calcd for C$_{24}$H$_{29}$NO$_3$: C, 75.96; H, 7.70; N, 3.69. Found: C, 75.64; H, 7.79; N, 3.68.

S-(-)-1-Phenylethylamine salt (59g)
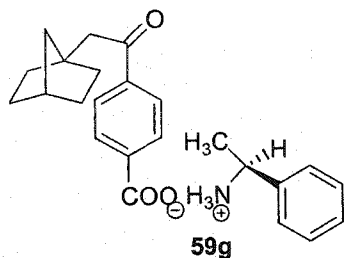
59g

A solution of acid **57** (77 mg, 0.30 mmol) in diethyl ether (15 mL) was added to a solution of S-(-)-1-phenylethylamine (36 mg, 0.30 mmol) in diethyl ether (5 mL). The cloudy solution was stirred for 1 h, after which time the precipitate that had formed was

filtered, washed with diethyl ether and dried *in vacuo* to afford salt **59g** (95 mg, 84 %) as a white powder. Recrystallization from MeOH afforded colorless needles.

mp: 165-166 °C.

¹H NMR (300 MHz, CD₃OD): δ 7.92 (d, *J* = 8.0 Hz, 2H), 7.87 (d, *J* = 8.0 Hz, 2H), 7.35 (m, 5H), 4.36 (q, *J* = 6.6 Hz, 1H), 3.15 (s, 2H), 2.07 (m, 1H), 1.54 (d, *J* = 6.6 Hz, 3H), 1.52 (m, 2H), 1.42 (m, 2H), 1..33 (m, 2H), 1.21 (m, 4H).

¹³C NMR (75 MHz, CD₃OD): δ 202.61, 173.98, 143.21, 140.59, 140.12, 130.31, 130.25, 130.03, 128.95, 127.60, 52.31, 46.95, 44.76, 44.51, 37.94, 35.74, 31.57, 20.97.

IR (KBr pellet): ν 3522, 2948, 2867, 2186, 1716, 1684, 1672, 1622, 1584, 1524, 1386, 1208, 996, 779, 700 cm⁻¹.

LRMS (ESI: 0.1% formic acid in MeOH) *m/z* 380 (M⁺ + 1), 335 (100), 122.

HRMS (ESI: 0.1% formic acid in MeOH) calcd for C₂₄H₃₀NO₃ (M⁺ + 1) 380.2226, found 380.2235.

Anal. Calcd for C₂₄H₂₉NO₃: C, 75.96; H, 7.70; N, 3.69. Found: C, 75.74; H, 7.29; N, 3.87.

(1R, 2R)-(-)-2-Amino-1-phenyl-1, 3-propanediol salt (**59h**)

210
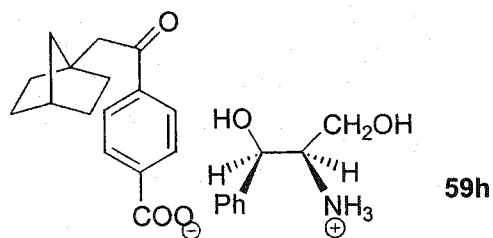
A solution of acid **57** (77 mg, 0.30 mmol) in diethyl ether (15 mL) was added to a solution of (1R, 2R)-(-)-2-amino-1-phenyl-1, 3-propanediol (50 mg, 0.30 mmol) in diethyl ether (15 mL). The cloudy solution was stirred for 1 h, after which time the precipitate that had formed was filtered, washed with diethyl ether and dried *in vacuo* to afford salt **59h** (85 mg, 67 %) as a white powder. Recrystallization from MeOH afforded a white powder.

mp: 132-133 °C.

^{1}H NMR (300 MHz, CD$_3$OD): δ 8.01 (d, J = 8.5 Hz, 2H), 7.95 (d, J = 8.5 Hz, 2H), 7.43-7.32 (m, 5H), 4.73 (d, J = 8.7 Hz, 1H), 3.53 (d × d, J_1 = 11.6 Hz, J_2 = 3.7 Hz, 1H), 3.40 (d × d, J_1 = 11.6 Hz, J_2 = 6.0 Hz, 1H), 3.28-3.25 (m, 1H), 3.22 (2H, s), 2.14 (m, 1H), 1.61-1.57 (m, 2H), 1.51-1.47 (m, 2H), 1.44-1.39 (m, 2H), 1.35-1.31 (m, 1H), 1.28 (m, 3H).

^{13}C NMR (75 MHz, CD$_3$OD): δ 202.61, 173.74, 142.92, 142.12, 140.64, 130.35, 129.77, 129.57, 128.97, 127.88, 72.34, 60.31, 59.97, 46.94, 44.75, 44.50, 37.94, 35.73, 31.57.

IR (KBr pellet): ν 3272, 2949, 2868, 1688, 1668, 1584, 1540, 1396, 1040, 760, 700 cm^{-1}.

LRMS (ESI: 0.1% formic acid in MeOH) *m/z* (relative intensity) 426 (M$^+$ + 1), 335, 259, 168 (100).

HRMS (ESI: 0.1% formic acid in MeOH) calcd for C$_{25}$H$_{32}$NO$_5$ (M$^+$ + 1) 426.2280, found 408.2184.

Anal. Calcd for C$_{25}$H$_{31}$NO$_5$: C, 70.57; H, 7.34; N, 3.29; O, 18.80. Calcd for C$_{25}$H$_{31}$NO$_5$•1/4H$_2$O: C, 69.83; H, 7.38; N, 3.26. Found: C, 69.72; H, 7.40; N, 3.03.

(-)-cis-Myrtanylamine salt (59i)
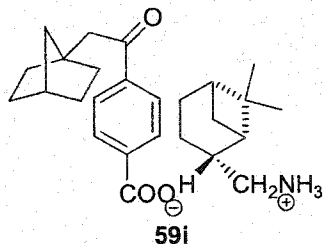
59i

A solution of acid **57** (77 mg, 0.30 mmol) in diethyl ether (15 mL) was added to a solution of (-)-cis-myrtanylamine (46 mg, 0.30 mmol) in diethyl ether (5 mL). The cloudy solution was stirred for 1 h, after which time the precipitate that had formed was filtered, washed with diethyl ether and dried *in vacuo* to afford salt **59i** (110 mg, 89 %) as a white powder. Recrystallization from MeOH afforded colorless needles.

mp: 152-154 °C.

^{1}H NMR (300 MHz, CD$_3$OD): δ 8.00 (d, J = 8.6 Hz, 2H), 7.94 (d, J = 8.6 Hz, 2H), 3.22 (s, 2H), 2.92 (m, 2H), 2.46-2.26 (m, 2H), 2.14 (m, 1H), 2.10-1.85 (m, 5H), 1.70-1.30 (m, 8H), 1.28 (m, 3H), 1.22 (s, 3H), 1.01 (s, 3H), 0.96 (d, J = 9.8 Hz, 1H).

^{13}C NMR (75 MHz, CD$_3$OD): δ 202.60, 174.11, 143.38, 140.52, 130.29, 128.95, 46.94, 46.29, 44.76, 44.70, 44.51, 42.44, 40.94, 39.56, 37.94, 35.75, 33.72, 31.57, 28.14, 26.69, 23.42, 20.43.

IR (KBr pellet): ν 3544, 2948, 2868, 2188, 1716, 1688, 1636, 1582, 1536, 1379, 1204, 996, 780 cm^{-1}.

LRMS (ESI: 0.1% formic acid in MeOH) *m/z* (relative intensity) 412 (M^{+} + 1, 18.5), 307 (15.2), 259 (0.3), 154 (100).

HRMS (ESI: 0.1% formic acid in MeOH) calcd for C$_{26}$H$_{38}$NO$_3$ (M^{+} + 1) 412.2852, found 412.2852.

Anal. Calcd for $C_{26}H_{37}NO_3$: C, 75.87; H, 9.06; N, 3.40. Found: C, 75.71; H, 9.28; N, 3.36.

S-(+)-2-(Methoxymethyl)pyrrolidine salt (59j)
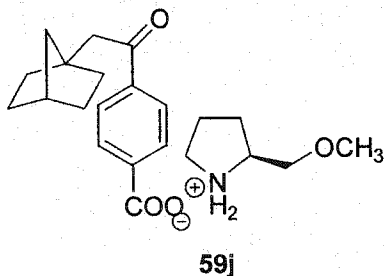
59j

A solution of acid **57** (77 mg, 0.30 mmol) in diethyl ether (15 mL) was added to a solution of S-(+)-2-(methoxymethyl)pyrrolidine (35 mg, 0.30 mmol) in diethyl ether (5 mL). The solution was stirred for 1 h, after which time no precipitate was formed and removal of solvent *in vacuo* afforded salt **59j** (112 mg, 100 %) as a pale yellow powder. Recrystallization from MeOH afforded a yellowish powder.

mp: 108-113 °C.

^{1}H NMR (300 MHz, CD_3OD): δ 8.02 (d, J = 8.5 Hz, 2H), 7.96 (d, J = 8.5 Hz, 2H), 3.78 (m, 1H), 3.64 (d × d, J_1 = 10.5 Hz, J_2 =3.6 Hz, 1H), 3.47 (d × d, J_1 = 10.5 Hz, J_2 = 7.7 Hz, 1H), 3.39 (s, 3H), 3.27 (m, 2H), 3.23 (s, 2H), 2.14 (m, 1H), 2.10-1.98 (m, 3H), 1.81-1.75 (m, 1H), 1.61-1.57 (m, 2H), 1.51-1.47 (m, 2H), 1.42-1.38 (m, 2H), 1.34-1.28 (m, 4H).

^{13}C NMR (75 MHz, CD_3OD): δ 202.52, 173.34, 142.27, 140.84, 130.39, 129.00, 72.08, 60.66, 59.36, 46.93, 46.62, 44.75, 44.52, 37.94, 35.73, 31.57, 37.32, 24.87.

IR (KBr pellet): ν 3352, 2947, 2866, 1685, 1636, 1586, 1542, 1376, 1201, 1101, 991, 783, 699 cm^{-1}.

LRMS (ESI: 0.1% formic acid in MeOH) m/z 374 ($M^+ + 1$), 353, 285 (100), 198.

HRMS (ESI: 0.1% formic acid in MeOH) calcd for $C_{22}H_{32}NO_4$ ($M^+ + 1$) 374.2331, found 374.2331.

Anal. Calcd for $C_{22}H_{31}NO_4$: C, 70.75; H, 8.37; N, 3.75. Found: C, 70.55; H, 8.28; N, 3.58.

R-(+)-Bornylamine salt (59k)
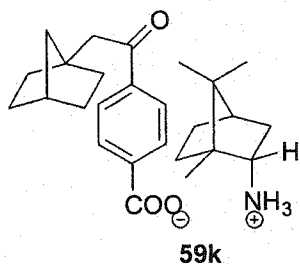
59k

A solution of acid **57** (77 mg, 0.30 mmol) in diethyl ether (15 mL) was added to a solution of R-(+)-bornylamine (46 mg, 0.30 mmol) in diethyl ether (5 mL). The cloudy solution was stirred for 1 h, after which time the precipitate that had formed was filtered, washed with diethyl ether and dried *in vacuo* to afford salt **59k** (93 mg, 75 %) as a white powder. Recrystallization from MeOH afforded colorless needles.

mp: 156-159 °C.

^{1}H NMR (300 MHz, CD$_3$OD): δ 8.00 (d, J = 8.3 Hz, 2H), 7.94 (d, J = 8.3 Hz, 2H), 3.38 (d × d, J_1 = 3.5 Hz, J_2 = 10.7 Hz, 1H), 3.22 (s, 2H), 2.33 (m, 1H), 2.14 (m, 1H), 1.82 (m, 1H), 1.72 (m, 1H), 1.70-1.30 (m, 9H), 1.29-1.24 (m, 4H), 1.10 (m, 1H), 0.95 (s, 3H), 0.93 (s, 3H), 0.92 (s, 3H).

^{13}C NMR (75 MHz, CD$_3$OD): δ 202.58, 174.05, 143.37, 140.54, 130.29, 128.95, 57.95, 50.05, 46.94, 45.85, 44.76, 44.50, 37.94, 35.74, 35.54, 31.57, 28.54, 27.96, 19.85, 18.73, 13.33.

IR (KBr pellet): ν 3544, 2953, 2869, 2136, 1716, 1686, 1669, 1624, 1588, 1514, 1379, 760 cm^{-1}.

LRMS (ESI: 0.1% formic acid in MeOH) *m/z* (relative intensity) 412 (M$^+$ + 1, 11.3), 307 (7.4), 259 (0.3), 154 (100).

HRMS (ESI: 0.1% formic acid in MeOH) calcd for $C_{26}H_{38}NO_3$ (M$^+$ + 1) 412.2852, found 412.2843.

Anal. Calcd for $C_{26}H_{37}NO_3$: C, 75.87; H, 9.06; N, 3.40. Found: C, 75.48; H, 9.27; N, 3.29.

S-(+)-1-Aminoindane salt (591)
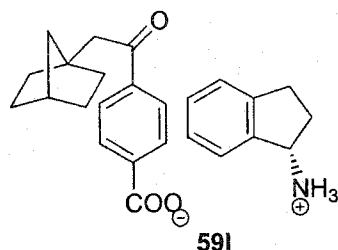
591

A solution of acid **57** (77 mg, 0.30 mmol) in diethyl ether (15 mL) was added to a solution of S-(+)-1-aminoindane (40 mg, 0.30 mmol) in diethyl ether (5 mL). The cloudy solution was stirred for 1 h, after which time the precipitate that had formed was filtered, washed with diethyl ether and dried *in vacuo* to afford salt **591** (87 mg, 74 %) as an off-white powder. Recrystallization from MeOH afforded pale yellow needles.

mp: 172-174 °C.

^{1}**H NMR** (300 MHz, CD$_3$OD): δ 7.98 (d, *J* = 8.5 Hz, 2H), 7.93 (d, *J* = 8.5 Hz, 2H), 7.49 (m, 1H), 7.30 (m, 3H), 4.75 (d × d, *J$_1$* = 5.2 Hz, *J$_2$* = 7.7 Hz, 1H), 3.21 (s, 2H), 3.11 (m, 1H), 2.96 (m, 1H), 2.57 (m, 1H), 2.14 (m, 1H), 2.05 (m, 1H), 1.65-1.55 (m, 2H), 1.55-1.35 (m, 4H), 1.35-1.25 (m, 4H).

^{13}**C NMR** (75 MHz, CD$_3$OD): δ 202.62, 173.97, 145.36, 143.19, 140.58, 140.14, 130.57, 130.30, 128.95, 128.22, 126.31, 125.47, 56.95, 46.94, 44.75, 44.50, 37.94, 35.74, 31.88, 31.57, 31.00.

IR (KBr pellet): ν 3521, 2947, 2866, 2211, 1716, 1684, 1672, 1622, 1584, 1524, 1386, 1208, 996, 779, 700 cm^{-1}.

LRMS (ESI: 0.1% formic acid in MeOH) *m/z* (relative intensity) 392 (M$^+$ + 1, 100), 281 (14.8), 267 (14.5), 259 (14.0), 242 (44.6).

HRMS (ESI: 0.1% formic acid in MeOH) calcd for C$_{25}$H$_{30}$NO$_3$ (M$^+$ + 1) 392.2226, found 392.2224.

Anal. Calcd for C$_{25}$H$_{29}$NO$_3$: C, 76.70; H, 7.47; N, 3.58. Found: C, 76.64; H, 7.70; N, 3.63.

(1R, 2R)-(-)-Pseudoephedrine salt (59m)
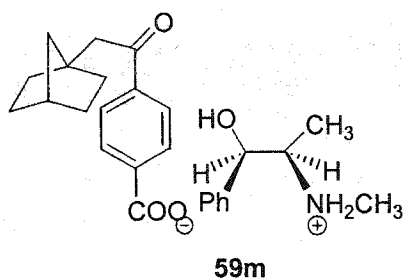
59m

A solution of acid **57** (77 mg, 0.30 mmol) in diethyl ether (15 mL) was added to a solution of (1R, 2R)-(-)-pseudoephedrine (50 mg, 0.30 mmol) in diethyl ether (5 mL). The solution was stirred for 1 h, after which time no precipitate was formed and removal of solvent *in vacuo* afforded salt **59m** (127 mg, 100 %) as a white powder.

mp: 127-129 °C.

^{1}**H NMR** (300 MHz, CD$_3$OD): δ 8.00 (d, J = 8.3 Hz, 2H), 7.95 (d, J = 8.3 Hz, 2H), 7.40-7.30 (m, 5H), 4.52 (d, J = 9.2 Hz, 1H), 3.36-3.31 (m, 1H), 3.22 (s, 2H), 2.71 (s, 3H), 2.14 (m, 1H), 1.65-1.55 (m, 2H), 1.55-1.45 (2H, m), 1.45-1.38 (m, 2H), 1.38-1.25 (m, 4H), 1.07 (d, J = 6.7 Hz, 3H).

^{13}**C NMR** (75 MHz, CD$_3$OD): δ 202.62, 174.02, 143.27, 141.98, 140.56, 130.32, 129.81, 129.73, 128.96, 128.18, 75.70, 61.76, 46.95, 44.75, 44.50, 37.94, 35.74, 31.57, 30.54, 12.72.

IR (KBr pellet): ν 3230, 3100, 2946, 2864, 2323, 1677, 1637, 1593, 1555, 1456, 1356, 1209, 1045, 780, 700 cm^{-1}.

LRMS (ESI: 0.1% formic acid in MeOH) m/z (relative intensity) 423 (M$^+$ + 1), 378 (100), 331, 166.

HRMS (ESI: 0.1% formic acid in MeOH) calcd for C$_{26}$H$_{34}$NO$_4$ (M$^+$ + 1) 424.2488, found 424.2483.

Anal. Calcd for C$_{26}$H$_{33}$NO$_4$: C, 73.73; H, 7.85; N, 3.31. Found: C, 73.79; H, 7.95; N, 3.33.

4.5 Synthesis of Dimethylated Bicyclo[2.2.1]heptane Derivatives 60, 61 and 62

4.5.1 Preparation of Ketones 60 and 61

Bicyclo[2.2.1]heptane-1-carboxylic acid (98)[97(b)]

98

A suspension of lithium wire (6.0 g, 870 mmol) in anhydrous cyclohexane (30 mL) was heated to be refluxing under an oxygen-free argon atmosphere. A solution of 1-chloronorbornane (88) (14.8 g, 113 mmol) in anhydrous cyclohexane (30 mL) was added over 30 min with stirring. The mixture was heated to be refluxing for 10 h before being cooled in an ice bath followed by addition of anhydrous cyclohexane (30 mL) and anhydrous n-pentane (40 mL). The argon stream was replaced by a stream of CO_2, which was dried over anhydrous $CaSO_4$. The reaction was stirred at 0 °C under an atmosphere of CO_2 for 3 h followed by removing unreacted lithium wire and careful quenching with ice water (100 mL). The solution was acidified with 4N HCl (100 mL) and extracted with diethyl ether (3 × 200 mL). The combined ethereal extracts were washed with water (2 × 50 mL) and then extracted with 10% aqueous KOH (4 × 100 mL). The combined basic extracts were washed with diethyl ether (2 × 50 mL) followed by acidifying with concentrated HCl to a pH of 3 after which the precipitated carboxylic acid was extracted with diethyl ether (3 × 200 mL). The combined organic extracts were washed with water (50 mL), brine (50 mL) and dried (MgSO$_4$). Removal of the solvent *in vacuo* provided acid **98** (8.41 g, 53 %) as a white solid. The compound did not require further purification.

mp: 109-111 °C (Lit.[97(b)] 113.8-115.5 °C).

^{1}H NMR (300 MHz, CDCl$_3$): δ 11.26 (s, br, 1H), 2.31 (m, 1H), 1.94-1.85 (m, 2H), 1.72-1.63 (m, 2H), 1.58-1.50 (m, 4H), 1.36-1.28 (m, 2H).

^{13}C NMR (75 MHz, CDCl$_3$, APT: C, CH$_2$: +; CH, CH$_3$: -): δ 183.49 (+), 52.04 (+), 42.33 (+), 37.79 (-), 32.92 (+), 29.95 (+).

IR (KBr pellet): ν 2958, 2873, 1699, 1420, 1311, 960, 733 cm^{-1}.

LRMS (EI) m/z 140 (M$^+$), 125, 111 (100), 95, 79, 67, 55.

Bicyclo[2.2.1]heptane-1-methanol (99)
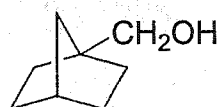
99

To a suspension of lithium aluminum hydride (4.28 g, 107.1 mmol) in diethyl ether (100 mL) was added dropwise a solution of acid **98** (5.0 g, 35.7 mmol) in diethyl ether (100 mL) at room temperature under an argon atmosphere. The mixture was stirred for 1 h. The reaction was quenched carefully with water (100 mL) at −78 °C. To the resulting mixture was added Rochelle's salt (10% sodium tartrate in water, 60 mL), followed by extraction with diethyl ether (4×150 mL). The combined ethereal extracts were washed with water (2 × 50 mL), brine (2 × 50 mL), dried (Na$_2$SO$_4$). Removal of the solvent *in vacuo* provided compound **99** (4.50 g, 100 %) as a yellowish liquid. The compound did not require further purification.

^{1}H NMR (300 MHz, CDCl$_3$): δ 3.69 (s, 2H), 2.19 (m, 1H), 1.65-1.55 (m, 2H), 1.52 (s, 1H, OH), 1.48-1.39 (m, 2H), 1.34-1.26 (m, 2H), 1.24-1.17 (m, 2H), 1.15 (m, 2H).

^{13}C NMR (75 MHz, CDCl$_3$, APT: C, CH$_2$: +; CH, CH$_3$: -): δ 67.09 (+), 50.05 (+), 40.47 (+), 37.17 (-), 31.69 (+), 30.36 (+).

IR (neat): ν 3337 (br), 2950, 2868, 1455, 1144, 1032 cm^{-1}.

LRMS (EI) *m/z* 126 (M$^+$), 108, 93, 79, 67 (100), 54.

Bicyclo[2.2.1]heptane-1-methanol methanesulfonate (**100**)

100
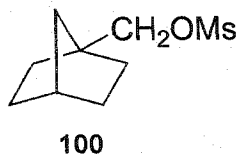
To a solution of alcohol **99** (5.0 g, 39.7 mmol) in dry pyridine (50 mL) was added dropwise methanesulfonyl chloride (6.82 g, 4.6 mL, 59.5 mmol) in dry pyridine. The reaction was stirred for 4 h under argon atmosphere at room temperature. The resulting mixture was poured into ice water (200 mL) and extracted with diethyl ether (4×150 mL). The combined ethereal extracts were washed successively with 4 N HCl (2 × 50 mL), water (2 × 50) mL and brine (2 × 50 mL), and dried (Na$_2$SO$_4$). Removal of the solvent *in vacuo* afforded compound **100** (7.45 g, 92%) as a white solid. The compound did not require further purification.

mp: 64-65 °C.

^{1}H NMR (300 MHz, CDCl$_3$): δ 4.30 (s, 2H), 2.98 (s, 3H), 2.23 (m, 1H), 1.70-1.55 (m, 2H), 1.55-1.40 (m, 2H), 1.40-1.25 (m, 4H), 1.24 (m, 2H).

^{13}C NMR (75 MHz, CDCl$_3$): δ 74.13 (+), 47.56 (+), 40.92 (+), 37.14 (-), 37.06 (-), 31.87 (+), 30.13 (+).

IR (KBr pellet): ν 2955, 2869, 1356, 1332, 1173, 943, 851, 752 cm^{-1}.

LRMS (EI) *m/z* 204 (M$^+$), 108, 93, 79 (100), 66, 54.

HRMS (EI) calcd for C$_9$H$_{16}$O$_3$S 204.0820, found 204.0821.

Anal. Calcd for C$_9$H$_{16}$O$_3$S: C, 52.91; H, 7.59. Found: C, 53.31; H, 7.89.

Bicyclo[2.2.1]heptane-1-acetonitrile (**101**)
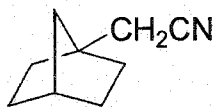
101

To a solution of compound **100** (9.2 g, 45.1 mmol) in dry DMF (60 mL) was added sodium cyanide (3.30 g, 67.6 mmol). The mixture was heated to be refluxing at 150 °C under an argon atmosphere for 17 h. The reaction was quenched by adding ice-water (200 mL) followed by extraction with diethyl ether (4×150 mL). The combined ethereal extracts were successively washed with Na_2CO_3 (10%, 80 mL), H_2O (80 mL), and saturated NaCl (80 mL), and dried (Na_2SO_4). Removal of solvent *in vacuo* gave a yellowish liquid. Silica gel chromatography (0.5 % diethyl ether in *n*-pentane) afforded compound **101** (5.05 g, 83 %) as a colorless liquid.

^{1}H NMR (300 MHz, CD_2Cl_2): δ 2.54 (s, 2H), 2.25 (m, 1H), 1.71-1.68 (m, 2H), 1.54-1.48 (m, 2H), 1.42-1.26 (m, 6H).

^{13}C NMR (75 MHz, CD_2Cl_2): δ 118.96 (+), 45.17 (+), 43.32 (+), 37.77 (-), 34.70 (+), 34.53 (+), 23.75 (+).

IR (neat): ν 2953, 2920, 2871, 2247, 1454, 1423, 1332, 739 cm^{-1}.

LRMS (EI) *m/z* 135 (M$^+$), 120, 106, 95 (100), 80, 67, 53.

HRMS (EI) calcd for $C_9H_{13}N$ 135.1048, found 135.1048.

Anal. Calcd for $C_9H_{13}N$: C, 79.95; H, 9.69; N, 10.36. Calcd for $C_9H_{13}N$ •1/12H_2O: C, 79.07; H, 9.71; N, 10.25. Found: C, 78.94; H, 9.84; N, 10.68.

Bicyclo[2.2.1]heptane-1-acetic acid (**102**)

102
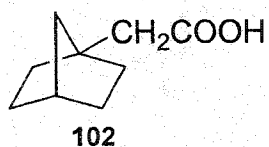
To a solution of sulfuric acid (50 %, 15 mL) and glacial acetic acid (40 mL) was added compound **101** (5.50 g). The mixture was heated to be refluxing at 130 °C for 30 h. The reaction was quenched with water (100 mL) followed by extraction with *n*-pentane (5 × 100 mL). The combined organic extracts were washed with water (5 × 30 mL), and dried (Na_2SO_4). Removal of solvent *in vacuo* gave a yellowish liquid. Silica gel chromatography (10% diethyl ether in petroleum ether) afforded acid **102** (4.89 g, 78 %) as a colorless liquid.

^{1}H NMR (300 MHz, CD_2Cl_2): δ 11.53 (s, br, 1H), 2.56 (s, 2H), 2.19 (m, 1H), 1.68-1.59 (m, 2H), 1.54-1.48 (m, 2H), 1.46-1.39 (m, 2H), 1.36-1.27 (m, 4H).

^{13}C NMR (75 MHz, CD_2Cl_2): δ 179.79, 45.41, 43.92, 40.57, 37.39, 34.86, 30.99.

IR (neat): ν 2952, 2870, 1707, 1450, 1411, 1296, 1264, 936, 657 cm^{-1}.

LRMS (EI) *m/z* 154 (M$^+$), 125, 94 (100), 79, 67, 53.

HRMS (EI) calcd for $C_9H_{14}O_2$ 154.0994, found 154.0994.

Anal. Calcd for $C_9H_{14}O_2$: C, 70.10; H, 9.15. Found: C, 69.80; H, 9.41.

Methyl bicyclo[2.2.1]hept-1-ylacetate (**103**)

103
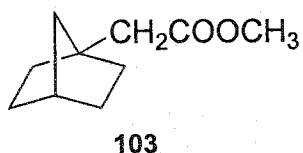
To a solution of acid **102** (4.89 g) in diethyl ether (5 mL) was added a solution of diazomethane in diethyl ether (50 mL, excess in the reaction) at room temperature. The reaction was stirred for 10 min. Removal of the solvent *in vacuo* afforded ester **103** (5.33 g, 100 %) as a yellowish liquid.

^{1}H NMR (400 MHz, CD$_2$Cl$_2$): δ 3.61 (s, 3H), 2.49 (s, 2H), 2.17 (m, 1H), 1.65-1.55 (m, 2H), 1.47-1.40 (m, 2H), 1.36-1.25 (m, 6H).

^{13}C NMR (100 MHz, CD$_2$Cl$_2$): δ 173.17 (+), 51.30 (-), 45.65 (+), 43.91 (+), 40.50 (+), 37.40 (-), 34.91 (+), 30.01 (+).

IR (neat): ν 2952, 2870, 1738, 1437, 1331, 1251, 1175, 1010 cm^{-1}.

LRMS (EI) *m/z* 168 (M$^+$), 139, 107, 94, 79 (100), 67, 53.

HRMS (EI) calcd for C$_{10}$H$_{16}$O$_2$ 168.1150, found 168.1145.

Anal. Calcd for C$_{10}$H$_{16}$O$_2$: C, 71.39; H, 9.59. Found: C, 71.54; H, 9.94.

Methyl α-(bicyclo[2.2.1]hept-1-yl)propanoate (**104**)
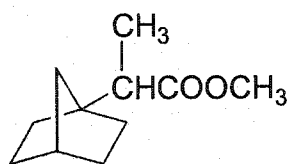
104

To a cold (-78 °C) solution of DIPA (diisopropylamine 6.5 mL, 46.5 mmol) in THF (100 mL) was added dropwise *n*-butyllithium (25.7 mL, 41.1 mmol). The mixture was warmed to 0 °C for 30 min before being cooled back to −78 °C as a cold LDA solution. To the cold (-78 °C) solution of LDA was added ester **103** (4.6 g, 27.4 mmol) in THF (40 mL) over 15 min. After stirring in the cold for 2 h, an additional portion of *n*-butyllithium (17.1 mL of a 1.6 M solution in *n*-hexane, 27.4 mmol) was added dropwise. The reaction was stirred for 30 min, followed by the addition of DMPU (6.6 mL, 54.8 mmol). After 10

min methyl iodide (5.1 mL, 82.1 mmol) was added and the reaction stirred in the cold for 3 h before warming slowly to room temperature and stirring overnight. The reaction was quenched with water (100 mL) and extracted with diethyl ether (3 × 100 mL). The combined ethereal extracts were washed with brine (2 × 30 mL), and dried (MgSO$_4$). Removal of the solvent *in vacuo* provided ester **104** (4.43 g, 89 %) as a yellowish liquid. The compound did not require further purification.

^{1}**H NMR** (400 MHz, CD$_2$Cl$_2$): δ 3.61 (s, 3H), 2.63 (q, *J* = 7.1 Hz, 1H), 2.16 (m, 1H), 1.65-1.35 (m, 4H), 1.30-1.20 (m, 6H), 1.12 (d, *J* = 7.1 Hz, 3H).

^{13}**C NMR** (100 MHz, CD$_2$Cl$_2$): δ 173.36 (+), 51.20 (-), 49.79 (+), 44.24 (-), 42.27 (+), 37.09 (-), 32.82 (+), 32.43 (+), 30.85 (+), 30.70 (+), 13.92 (-).

IR (neat): ν 2952, 2919, 2869, 1738, 1458, 1435, 1350, 1193, 1176, 1157 cm^{-1}.

LRMS (EI) *m/z* 182 (M$^+$), 167, 153, 123, 95 (100), 79, 67, 55.

HRMS (EI) calcd for C$_{11}$H$_{18}$O$_2$ 182.1307, found 182.1305.

Anal. Calcd for C$_{11}$H$_{18}$O$_2$: C, 72.49; H, 9.95. Found: C, 72.36; H, 10.11.

<u>Methyl α-methyl-α-(bicyclo[2.2.1]hept-1-yl)propanoate (**105**)</u>
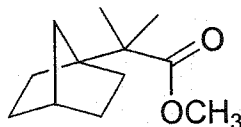
105

To a cold (-78 °C) solution of DIPA (diisopropylamine, 6.5 mL, 46.5 mmol) in THF (100 mL) was added dropwise *n*-butyllithium (25.7 mL, 41.1 mmol). The mixture was warmed to 0 °C for 30 min before being cooled back to −78 °C as a cold LDA solution. To the cold (-78 °C) solution of LDA was added ester **104** (4.43 g, 24.3 mmol) in THF (40 mL) over 15 min. After stirring in the cold for 2 h, an additional portion of *n*-

butyllithium (15.1 mL of a 1.6 M solution in *n*-hexane, 24.3 mmol) was added dropwise. The reaction was stirred for 30 min, followed by the addition of DMPU (6.6 mL, 54.8 mmol). After 10 min methyl iodide (5.1 mL, 82.1 mmol) was added and the reaction stirred in the cold for 3 h before warming slowly to room temperature and stirring overnight. The reaction was quenched with water (100 mL) and extracted with diethyl ether (3 × 100 mL). The combined ethereal extracts were washed with brine (2 × 30 mL), and dried (MgSO$_4$). Removal of the solvent *in vacuo* provided ester **105** (4.05 g, 85 %) as a yellowish liquid. The compound did not require further purification.

^{1}H NMR (400 MHz, CD$_2$Cl$_2$): δ 3.60 (s, 3H), 2.13 (m, 1H), 1.57-1.50 (m, 4H), 1.31-1.26 (m, 4H), 1.17 (s, 6H), 1.20-1.14 (m, 2H).

^{13}C NMR (100 MHz, CD$_2$Cl$_2$): δ 178.03 (+), 53.38 (+), 51.36 (-), 45.13 (+), 39.82 (+), 36.94 (-), 31.17 (+), 30.86 (+), 22.75 (-).

IR (neat): ν 2952, 2871, 1729, 1471, 1433, 1387, 1275, 1142, 988, 831 cm^{-1}.

LRMS (EI) *m/z* 196 (M$^+$), 181, 167, 137, 107, 95 (100), 81, 67, 55.

HRMS (EI) calcd for C$_{12}$H$_{20}$O$_2$ 196.1463, found 196.1466.

Anal. Calcd for C$_{12}$H$_{20}$O$_2$: C, 73.43; H, 10.27. Found: C, 73.54; H, 10.52.

2-Methyl-2-bicyclo[2.2.1]hept-1-yl-1-propanol (107)
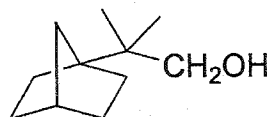
107

To a suspension of lithium aluminum hydride (1.7 g, 45.9 mmol) in diethyl ether (30 mL) was added dropwise a solution of ester **105** (3.0 g, 15.3 mmol) in diethyl ether (30 mL) under argon atmosphere at room temperature. The mixture was stirred for 2.5 h. The

reaction was quenched carefully with water (100 mL) at −78 °C. To the resulting mixture was added Rochelle's salt (10% sodium tartrate in water, 60 mL), followed by extraction with diethyl ether (4×100 mL). The combined ethereal extracts were washed with water (2 × 50 mL), brine (2 × 50 mL), dried (Na_2SO_4). Removal of the solvent *in vacuo* provided a yellowish solid. Silica gel chromatography (2 % diethyl ether in petroleum ether) afforded alcohol **107** (2.3 g, 89 %) as a white solid.

mp: 66-67 °C.

^{1}H NMR (300 MHz, $CDCl_3$): δ 3.45 (s, 2H), 2.12 (m, 1H), 1.70-1.45 (m, 4H), 1.35-1.20 (m, 3H), 1.16 (s, 1H), 1.15-1.05 (m, 3H), 0.91 (s, 6H).

^{13}C NMR (75 MHz, $CDCl_3$): δ 70.53, 53.01, 38.73, 36.88, 36.27, 30.50, 30.22, 21.52.

IR (KBr pellet): ν 3243, 2949, 2867, 1456, 1364, 1204, 1059, 1033, 1008, 754 cm^{-1}.

LRMS (EI) *m/z* 168 (M$^+$), 153, 137 (100), 95, 81, 67, 55.

HRMS (EI) calcd for $C_{11}H_{20}O$ 168.1514, found 168.1519.

Anal. Calcd for $C_{11}H_{20}O$: C, 78.51; H, 11.98. Found: C, 78.45; H, 11.64.

1-(4'-Fluorophenyl)-2-methyl-2-bicyclo[2.2.1]hept-1-yl-1-propanol (**108**)

108
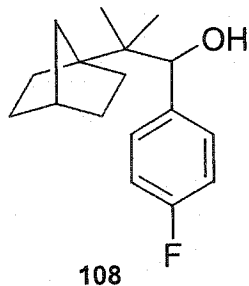
A mixture of Celite® 545 (2.4 g) and PCC (pyridinium chlorochromate, 2.4 g, 11.1 mmol) was ground with a mortar and pestle until homogeneous. This solid was suspended in a solution of alcohol **107** (1.16 g, 6.89 mmol) in anhydrous dichloromethane (40 mL) and stirred for 2.5 h at room temperature. Following the addition of anhydrous diethyl ether (200 mL), the reaction mixture was filtered through a column of Celite® 545 on Florisil® and the remaining solids triturated well with anhydrous diethyl ether. Solvent removal *in vacuo* gave a yellowish liquid (aldehyde). The residue was taken up in anhydrous THF (50 mL). To this solution was added dropwise 4-fluorophenylmagnesium bromide (8.3 mL, 8.3 mmol) at room temperature. The reaction was stirred under an atmosphere of dry argon for 2 h followed by careful quenching with ice water (50 mL) and 4N HCl (10 mL). Extraction with diethyl ether (3 × 100 mL) was followed by successive washing with water (40 mL) and saturated NaCl (2 × 30 mL), and drying (MgSO₄). Removal of the solvent *in vacuo* provided alcohol **108** (1.72 g, 95 %) as a white solid. The compound did not require further purification.

mp: 91-93 °C.

¹H NMR (300 MHz, CDCl₃): δ 7.29-7.24 (m, 2H), 7.02-6.94 (m, 2H), 4.70 (s, 1H, CH), 2.13 (m, 1H), 1.85-1.60 (m, 4H), 1.55 (s, 1H, OH), 1.40-1.20 (m, 6H), 0.93 (s, 3H, CH₃), 0.65 (s, 3H, CH₃).

¹³C NMR (75 MHz, CDCl₃): δ 163.50 and 160.40 ($^1J_{C-F}$ = 233 Hz), 138.91 and 138.88 ($^4J_{C-F}$ = 2 Hz) 129.64 and 129.53 ($^3J_{C-F}$ = 8 Hz), 114.45 and 114.17 ($^2J_{C-F}$ = 21 Hz), 79.23, 54.67, 40.28, 39.99, 36.06, 31.34, 31.13, 30.82, 30.54, 23.57, 17.67.

IR (KBr pellet): ν 3500, 2948, 2867, 1605, 1509, 1231, 1047, 840 cm⁻¹.

LRMS (EI) *m/z* 262 (M⁺), 244, 229, 215, 137 (100), 125, 95, 81, 67, 55.

HRMS (EI) calcd for C₁₇H₂₃FO 262.1733, found 262.1733.

Anal. Calcd for $C_{17}H_{23}FO$: C, 77.82; H, 8.84; F, 7.24; O, 6.10. Calcd for

$C_{17}H_{23}FO \cdot 1/8H_2O$: C, 77.16; H, 8.86. Found: C, 77.29; H, 8.75.

1-(4'-Fluorophenyl)-2,2-dimethyl-2-bicyclo[2.2.1]hept-1-yl ethanone (109)

109
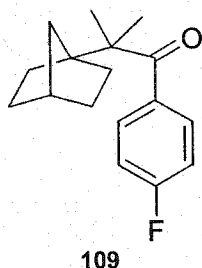
A mixture of Celite® 545 (2.5 g) and PCC (pyridinium chlorochromate, 5.16 g, 11.6 mmol) was ground with a mortar and pestle until homogeneous. This solid was suspended in a solution of alcohol **108** (1.90 g, 7.25 mmol) in anhydrous dichloromethane (50 mL) and stirred for 5 h at room temperature. Following the addition of anhydrous diethyl ether (200 mL), the reaction mixture was filtered through a column of Celite® 545 on Florisil® and the remaining solids triturated well with anhydrous diethyl ether. Solvent removal *in vacuo* was followed by silica gel chromatography (2% diethyl ether in petroleum ether) to give ketone **109** (1.88 g, 99 %) as a white solid. Recrystallization from diethyl ether provided colorless plates.

mp: 65-66 °C.

UV (CH_3OH): λ 205.0 (1.27 × 10^4), 240.0 (6.97 × 10^3), 315.0 (2.27 × 10^2) nm (M^{-1}cm^{-1}).

^{1}H NMR (400 MHz, CDCl$_3$): δ 7.56 (m, 2H), 7.02 (m, 2H), 2.13 (m, 1H, CH), 1.60-1.50 (m, 4H), 1.32 (s, 6H, 2CH$_3$), 1.30-1.20 (m, 6H).

^{13}C NMR (100 MHz, CDCl$_3$): δ 209.59 (+), 164.98 (+) and 162.48 (+) ($^1J_{C-F}$ = 250 Hz), 137.79 (+) and 137.76 (+)($^4J_{C-F}$ = 3 Hz), 130.09 (-) and 130.00 (-) ($^3J_{C-F}$ = 9 Hz), 114.95 (-) and 114.74 (-) ($^2J_{C-F}$ = 21 Hz), 53.55 (+), 50.17 (+), 39.84 (+), 36.11 (-), 31.15 (+), 30.43 (+), 24.41 (-).

IR (KBr pellet): ν 2978, 2956, 2919, 2869, 1660, 1598, 1507, 1231, 1160, 972, 845, 603 cm^{-1}.

LRMS (EI) *m/z* 260 (M$^+$), 137, 123, 95 (100), 81, 67, 55.

HRMS (EI) calcd for C$_{17}$H$_{21}$FO 260.1576, found 260.1578.

Anal. Calcd for C$_{17}$H$_{21}$FO: C, 78.43; H, 8.13. Found: C, 78.21; H, 8.19.

This structure was confirmed by X-ray crystallographic analysis:

Habit	colorless plates
Space group	*P-1*
a, Å	6.240(1)
b, Å	10.511(2)
c, Å	11.817(2)
α (°)	69.07(2)
β (°)	80.75(2)
γ (°)	76.46(2)
Z	2
R	0.046

1-(4'-Cyanophenyl)-2,2-dimethyl-2-bicyclo[2.2.1]hept-1-yl ethanone **(110)**
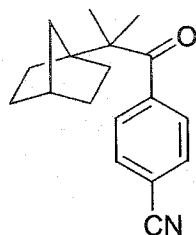
110

To a solution of ketone **109** (1.10 g, 4.23 mmol) in dry DMF (12 mL) was added sodium cyanide (0.35 g, 7.14 mmol). The resulting mixture was heated to be refluxing at 150 °C under an argon atmosphere for 20 h. The cooled reaction mixture was poured into

ice-water (100 mL) and extracted with diethyl ether (4×100 mL). The combined ethereal extracts were washed successively with Na_2CO_3 (10%, 50 mL), H_2O (50 mL), and saturated NaCl (50 mL), then dried (Na_2SO_4). Removal of solvent *in vacuo* afforded ketone **110** (0.86 g, 76 %) as a yellowish solid. The compound did not require further purification for the next reaction. Purification by silica gel chromatography (diethyl ether/petroleum ether 95/5) gave a white solid. Recrystallization from diethyl ether afforded colorless plates.

mp: 77-78 °C.

^{1}H NMR (300 MHz, CDCl$_3$): δ 7.65 (d, J = 8.6 Hz, 2H), 7.53 (d, J = 8.6 Hz, 2H), 2.14 (m, 1H, CH), 1.60-1.50 (m, 4H), 1.29 (s, 6H, 2CH$_3$), 1.28-1.20 (m, 6H).

^{13}C NMR (75 MHz, CDCl$_3$): δ 210.32 (+), 145.86 (+), 131.80 (-), 127.53 (-), 118.09 (+), 113.55 (+), 53.53 (+), 50.28 (+), 39.72 (+), 36.05 (-), 31.19 (+), 30.40 (+), 24.10 (-).

IR (KBr pellet): ν 2955, 2864, 2228, 1669, 1456, 1399, 1248, 1161, 967, 840 cm^{-1}.

LRMS (EI) *m/z* 267 (M$^+$), 239, 207, 137, 130, 102, 95, 81 (100), 67, 55.

HRMS (EI) calcd for C$_{18}$H$_{21}$NO 267.1623, found 267.1623.

Anal. Calcd for C$_{18}$H$_{21}$NO: C, 80.86; H, 7.92; N, 5.24. Found: C, 80.46; H, 7.94; N, 5.18.

This structure was confirmed by X-ray crystallographic analysis:

Habit	colorless plates
Space group	*P2₁/c*
a, Å	10.708(2)
b, Å	11.226(2)
c, Å	12.599(2)
α (°)	90
β(°)	99.17(2)
γ (°)	90
Z	4
R	0.065

1-(4'-Carboxylphenyl)-2,2-dimethyl-2-bicyclo[2.2.1]hept-1-yl ethanone (60)
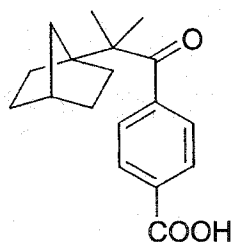
60

To a solution of potassium hydroxide (5.0 g, 89 mmol) in water (20 mL) was added a solution of ketone **110** (0.76 g, 2.85 mmol) in ethanol (6 mL). The mixture was heated to be refluxing at 95 °C for 24 h. The reaction was quenched by water (100 mL). The solution was washed with methylene chloride (2 × 50 mL). The aqueous solution was carefully acidified to a pH 2 with concentrated HCl. The precipitated carboxylic acid was extracted with Et₂O (4 × 100 mL) and the combined ethereal extracts were washed with water (50 mL), brine (50 mL) and dried (Na₂SO₄). Removal of solvent *in vacuo* provided a white solid. Recrystallization from ethanol afforded acid **60** (0.74 g, 91 %) as colorless plates.

mp: 174-176 °C.

^{1}**H NMR** (400 MHz, CDCl$_3$): δ 10.34 (s, br, 1H), 8.10 (d, J = 8.4 Hz, 2H), 7.53 (d, J = 8.4 Hz, 2H), 2.12 (m, 1H, OH), 1.58 (m, 4H), 1.31 (s, 6H, 2CH$_3$), 1.30-1.20 (m, 6H).

^{13}**C NMR** (100 MHz, CDCl$_3$): δ 211.57, 171.47, 146.99, 130.13, 129.85, 126.92, 53.53, 50.26, 39.71, 36.07, 31.19, 30.43, 24.11.

IR (KBr pellet): ν 2951, 2868, 2660, 2534, 1689, 1660, 1416, 1280, 1123, 963, 740 cm^{-1}.

LRMS (EI) m/z 286 (M$^+$, 2.81), 241 (1.93), 150 (19.55), 149 (21.09), 137 (100), 95 (35.58), 81 (77.27), 67 (14.46), 55 (8.54).

HRMS (EI) calcd for C$_{18}$H$_{22}$O$_3$ 286.1569, found 286.1568.

Anal. Calcd for C$_{18}$H$_{22}$O$_3$: C, 75.50; H, 7.74; O, 16.76. Calcd for C$_{18}$H$_{22}$O$_3$•1/6H$_2$O: C, 74.71; H, 7.78. Found: C, 74.80; H, 7.72.

This structure was confirmed by X-ray crystallographic analysis:

Habit	colorless plates
Space group	P-1
a, Å	6.2920(10)
b, Å	10.809(2)
c, Å	11.733(2)
α (°)	80.32(2)
β (°)	74.07(2)
γ (°)	82.07(2)
Z	2
R	0.064

1-(4'-Methoxycarbonylphenyl)-2,2-dimethyl-2-bicyclo[2.2.1]hept-1-yl ethanone **(61)**

61
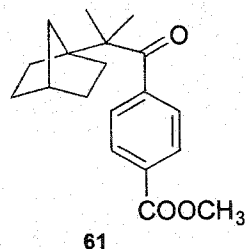
To a solution of acid **60** (0.200 g) in diethyl ether (5 mL) was added a solution of diazomethane in diethyl ether (15 mL, excess in the reaction) at room temperature. The reaction was stirred for 10 min. Removal of the solvent *in vacuo* provided a yellowish solid. Recrystallization from diethyl ether afforded ester **61** (0.210 g, 100 %) as colorless plates.

mp: 90-93 °C.

UV (CH$_3$OH): λ 205.0 (1.52 × 10^4), 245.0 (1.57 × 10^4), 280.0 (1.28 × 10^3) nm (M^{-1}cm^{-1}).

^{1}H NMR (400 MHz, CDCl$_3$): δ 8.00 (d, J = 8.3 Hz, 2H), 7.48 (d, J = 8.3 Hz, 2H), 2.12 (m, 1H, CH), 1.65-1.50 (m, 4H), 1.29 (s, 6H, 2CH$_3$), 1.28-1.20 (m, 6H).

^{13}C NMR (100 MHz, CDCl$_3$): δ 211.46, 166.38, 146.10, 131.04, 129.16, 126.85, 53.50, 52.27, 50.22, 39.69, 36.05, 31.16, 30.41, 24.09.

IR (KBr pellet): ν 3003, 2954, 2932, 2870, 1730, 1667, 1437, 1279, 1108, 959, 862, 725 cm^{-1}.

LRMS (EI) m/z 300 (M$^+$), 269, 241, 163, 137, 120, 95, 81 (100), 67, 55.

HRMS (EI) calcd for C$_{19}$H$_{24}$O$_3$ 300.1725, found 300.1728.

Anal. Calcd for C$_{19}$H$_{24}$O$_3$: C, 75.97; H, 8.05. Found: C, 75.89; H, 8.21.

This structure was confirmed by X-ray crystallographic analysis:

Habit	colorless plates
Space group	$P2_1/c$
a, Å	6.060(1)
b, Å	21.958(4)
c, Å	12.833(2)
α (°)	90.00
β (°)	107.10(3)
γ (°)	90.00
Z	4
R	0.063

4.5.2 Preparation of Dimethylated Bicyclo[2.2.1]heptyl Salts 62

R-(-)-1-Cyclohexylethylamine salt (62a)
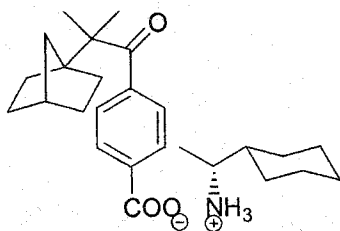
62a

A solution of acid **60** (71.5 mg, 0.25 mmol) in diethyl ether (15 mL) was added to a solution of R-(-)-1-cyclohexylethylamine (31.8 mg, 0.25 mmol) in diethyl ether (5 mL). The cloudy solution was stirred for 1 h, after which time the precipitate that had formed was filtered, washed with diethyl ether and dried *in vacuo* to afford salt **62a** (102.6 mg, 99 %) as a white powder. Recrystallization from MeOH afforded colorless plates.

mp: 187-189 °C.

^{1}H NMR (400 MHz, CD$_3$OD): δ 7.94 (d, J = 8.3 Hz, 2H), 7.47 (d, J = 8.3 Hz, 2H), 3.06 (m, 1H), 2.12 (m, 1H), 1.82-1.45 (m, 11H), 1.33 (s, 6H), 1.30-1.26 (m, 8H), 1.23 (d, J = 6.8 Hz, 3H), 1.20-1.03 (m, 2H).

^{13}C NMR (100 MHz, CD$_3$OD): δ 213.92, 174.24, 144.91, 140.53, 129.77, 127.67, 54.81, 53.38, 51.29, 42.72, 40.65, 37.39, 32.21, 31.47, 30.01, 28.81, 27.08, 27.01, 26.93, 24.59, 16.04.

IR (KBr pellet): ν 3500, 2930, 2867, 2605, 2211, 1664, 1639, 1580, 1535, 1450, 1374, 1266, 964, 755 cm^{-1}.

LRMS (ESI: 0.1% formic acid in MeOH) m/z 414 (M$^+$ + 1, 100), 291 (2.02), 287 (1.88).

Anal. Calcd for C$_{26}$H$_{39}$NO$_3$: C, 75.50; H, 9.50; N, 3.39. Found: C, 75.10; H, 9.48; N, 3.56.

This structure was confirmed by X-ray crystallographic analysis:

Habit	colorless plates
Space group	$P2_1$
a, Å	13.017(1)
b, Å	6.2546(6)
c, Å	14.544(2)
α (°)	90.00
β (°)	95.511(5)
γ (°)	90.00
Z	2
R	0.038

(1R, 2R)-(-)-Pseudoephedrine salt (62b)
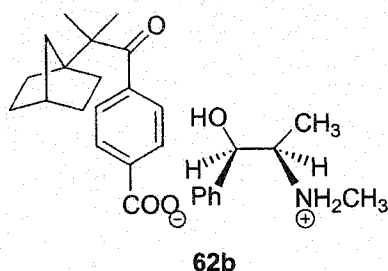
62b

A solution of acid **60** (71.5 mg, 0.25 mmol) in diethyl ether (15 mL) was added to a solution of (1R, 2R)-(-)-pseudoephedrine (41.3 mg, 0.25 mmol) in diethyl ether (5 mL). The cloudy solution was stirred for 1 h, after which time the precipitate that had formed was filtered, washed with diethyl ether and dried *in vacuo* to afford salt **62b** (86.0 mg, 76 %) as a white powder. Recrystallization from CH_3CN afforded colorless prisms.

mp: 134-135 °C.

^{1}H NMR (400 MHz, CD_3OD): δ 7.94 (d, *J* = 8.5 Hz, 2H), 7.47 (d, *J* = 8.5 Hz, 2H), 7.42-7.33 (m, 5H), 4.51 (d, *J* = 9.2 Hz, 1H), 3.33 (m, 1H), 2.70 (s, 3H), 2.12 (m, 1H), 1.67-1.56 (m, 4H), 1.33 (s, 6H), 1.30 (m, 6H), 1.06 (d, *J* = 6.7 Hz, 3H).

^{13}C NMR (100 MHz, CD_3OD): δ 213.95, 174.14, 144.96, 142.00, 140.37, 129.82, 129.81, 129.74, 128.18, 127.67, 75.73, 61.75, 54.81, 51.30, 40.65, 37.39, 32.22, 31.48, 30.55, 24.59, 12.73.

IR (KBr pellet): ν 3392, 3032, 2956, 2868, 2775, 2496, 1719, 1674, 1658, 1592, 1550, 1468, 1387, 1043, 755, 700 cm^{-1}.

LRMS (ESI: 0.1% formic acid in MeOH) *m/z* 452 (M$^+$ + 1, 0.31), 331 (2.03), 287 (0.84), 167 (4.50), 166 (100).

Anal. Calcd for $C_{28}H_{37}NO_4$: C, 74.47; H, 8.26; N, 3.10. Found: C, 73.93; H, 8.43; N, 3.48.

(1R, 2S)-(+)-cis-1-Amino-2-indanol salt (62c)

62c
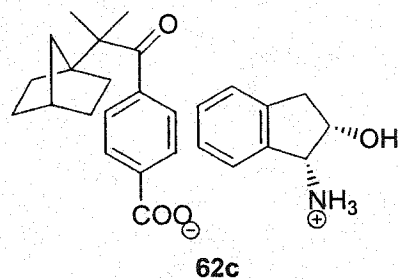
A solution of acid **60** (71.5 mg, 0.25 mmol) in diethyl ether (15 mL) was added to a solution of (1R, 2S)-(-)-cis-1-amino-2-indanol (37.3 mg, 0.25 mmol) in diethyl ether (5 mL). The cloudy solution was stirred for 1 h, after which time the precipitate that had formed was filtered, washed with diethyl ether and dried *in vacuo* to afford salt **62c** (67.0 mg, 62 %) as a white powder. Recrystallization from MeOH afforded colorless needles.

mp: 202-204 °C.

^{1}H NMR (400 MHz, CD$_3$OD): δ 7.94 (d, J = 8.1 Hz, 2H), 7.47 (d, J = 8.1 Hz, 2H), 7.40-7.26 (m, 4H), 4.70 (m, 1H), 4.54 (d, J = 5.7 Hz, 1H), 3.22 (d × d, J_1 = 16.3 Hz, J_2 = 6.4 Hz, 1H), 3.01 (d × d, J_1 = 16.3 Hz, J_2 = 4.9 Hz, 1H), 2.12 (m, 1H), 1.67-1.53 (m, 4H), 1.33 (s, 6H), 1.30-1.24 (m, 6H).

^{13}C NMR (100 MHz, CD$_3$OD): δ 213.93, 174.04, 145.05, 142.81, 140.13, 138.33, 130.85, 129.82, 128.43, 127.68, 126.68, 126.16, 72.00, 58.67, 54.81, 51.30, 40.65, 40.11, 37.39, 32.22, 31.48, 24.58.

IR (KBr pellet): ν 3221, 2960, 2869, 2628, 2243, 1719small, 1667, 1580, 1535, 1399, 751 cm^{-1}.

LRMS (ESI: 0.1% formic acid in MeOH) *m/z* 436 (M$^+$ + 1, 100), 299 (14.28), 287 (9.17), 150 (23.84).

Anal. Calcd for $C_{27}H_{33}NO_4$: C, 74.45; H, 7.64; N, 3.22. Found: C, 74.21; H, 7.69; N, 3.62.

This structure was confirmed by X-ray crystallographic analysis:

Habit	colorless needles
Space group	$P2_1$
a, Å	8.041(2)
b, Å	6.0730(10)
c, Å	23.606(5)
α (°)	90.00
β (°)	97.10(2)
γ (°)	90.00
Z	2
R	0.051

S-(-)-*p*-Tolylamine salt (**62d**)

62d
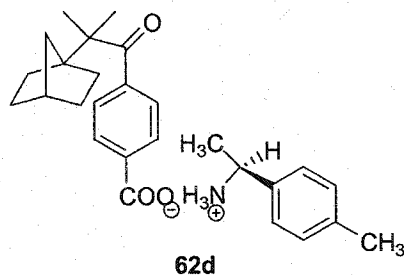
A solution of acid **60** (71.5 mg, 0.25 mmol) in diethyl ether (15 mL) was added to a solution of S-(-)-*p*-tolylamine (33.8 mg, 0.25 mmol) in diethyl ether (5 mL). The cloudy solution was stirred for 1 h, after which time the precipitate that had formed was filtered, washed with diethyl ether and dried *in vacuo* to afford salt **62d** (91.7 mg, 87 %) as a white powder. Recrystallization from MeOH afforded colorless prisms.

mp: 181-184 °C.

¹H NMR (400 MHz, CD$_3$OD): δ 7.94 (d, *J* = 8.5 Hz, 2H), 7.47 (d, *J* = 8.5 Hz, 2H), 7.31 (d, *J* = 8.1 Hz, 2H), 7.24 (d, *J* = 8.1 Hz, 2H), 4.38 (q, *J* = 6.8 Hz, 1H), 2.34 (s, 3H), 2.12 (m, 1H), 1.68-1.52 (m, 4H), 1.59 (d, *J* = 6.8 Hz, 3H), 1.33 (s, 6H), 1.32-1.25 (m, 6H).

¹³C NMR (100 MHz, CD$_3$OD): δ 213.93, 174.12, 144.96, 140.34, 140.18, 137.03, 130.80, 129.79, 127.66, 127.53, 54.81, 52.06, 51.29, 40.65, 37.39, 32.21, 31.47, 24.58, 21.13, 20.87.

IR (KBr pellet): ν 3552?, 2949, 2870, 2760, 2225, 1700, 1656, 1579, 1524, 1376, 972, 727 cm^{-1}.

LRMS (ESI: 0.1% formic acid in MeOH) *m/z* 422 (M$^+$ + 1, 100), 309 (3.41), 287 (10.68), 271 (8.27).

Anal. Calcd for C$_{27}$H$_{35}$NO$_3$: C, 76.92; H, 8.37; N, 3.32. Found: C, 76.52; H, 8.47; N, 3.49.

L-Prolinamide salt (62e)
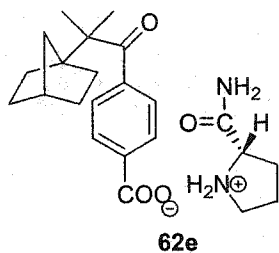
62e

A solution of acid **60** (71.5 mg, 0.25 mmol) in diethyl ether (15 mL) was added to a solution of L-prolinamide (28.5 mg, 0.25 mmol) in diethyl ether (5 mL). The cloudy solution was stirred for 1 h, after which time the precipitate that had formed was filtered, washed with diethyl ether and dried *in vacuo* to afford salt **62e** (87.3 mg, 87 %) as a white powder. Recrystallization from MeOH afforded colorless plates.

mp: 164-166 °C.

^{1}**H NMR** (400 MHz, CD$_3$OD): δ 7.95 (d, J = 8.3 Hz, 2H), 7.48 (d, J = 8.3 Hz, 2H), 4.17 (d × d, J_1 = 8.2 Hz, J_2 = 6.4 Hz, 1H), 3.32 (m, 1H), 3.27 (m, 1H), 2.38 (m, 1H), 2.12 (m, 1H), 2.00 (m, 3H), 1.67-1.56 (m, 4H), 1.33 (s, 6H), 1.30-1.26 (m, 6H).

^{13}**C NMR** (100 MHz, CD$_3$OD): δ 213.83, 172.76, 172.41, 145.68, 138.29, 129.97, 127.76, 65.23, 61.02, 54.81, 51.30, 47.30, 40.64, 37.39, 32.22, 31.47, 31.15, 26.82, 26.40, 25.25, 24.55.

IR (KBr pellet): ν 3345, 2967, 2869, 2443, 2232, 1672, 1596, 1549, 1375, 959, 759 cm^{-1}.

LRMS (ESI: 0.1% formic acid in MeOH) m/z 401 (M$^+$ + 1, 100), 325 (4.74), 287 (5.30), 229 (19.07).

Anal. Calcd for C$_{23}$H$_{32}$N$_2$O$_4$: C, 68.97; H, 8.05; N, 6.99. Found: C, 68.72; H, 8.01; N, 6.59.

This structure was confirmed by X-ray crystallographic analysis:

Habit	colorless plates
Space group	$P2_12_12_1$
a, Å	6.596(3)
b, Å	7.941(3)
c, Å	40.33(2)
α (°)	90.00
β (°)	90.00
γ (°)	90.00
Z	4
R	0.084

R-(-)-1-Aminoindane salt (62f)
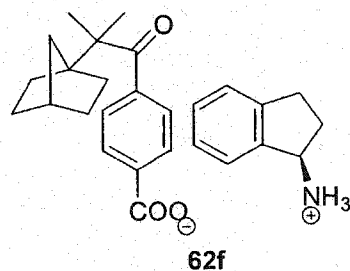
62f

A solution of acid **60** (71.5 mg, 0.25 mmol) in diethyl ether (15 mL) was added to a solution of R-(-)-1-aminoindane (33.3 mg, 0.25 mmol) in diethyl ether (5 mL). The cloudy solution was stirred for 1 h, after which time the precipitate that had formed was filtered, washed with diethyl ether and dried *in vacuo* to afford salt **62f** (85.3 mg, 81 %) as a white powder. Recrystallization from MeOH afforded colorless needles.

mp: 198-200 °C.

^{1}H NMR (400 MHz, CD$_3$OD): δ 7.94 (d, J = 8.4 Hz, 2H), 7.47 (d, J = 8.4 Hz, 2H), 7.46 (m, 1H), 7.34-7.27 (m, 3H), 4.74 (d × d, J_1 = 7.6 Hz, J_2 = 5.2 Hz, 1H), 3.19-3.10 (m, 1H), 3.01-2.93 (m, 1H), 2.63-2.55 (m, 1H), 2.12 (m, 1H), 2.10-2.00 (m, 1H), 1.67-1.56 (m, 4H), 1.33 (s, 6H), 1.30 (m, 6H).

^{13}C NMR (75 MHz, CD$_3$OD): δ 213.96, 173.95, 145.36, 145.03, 140.33, 140.21, 130.56, 129.81, 128.23, 127.64, 126.34, 125.40, 57.03, 54.83, 51.32, 40.66, 37.39, 32.23, 32.04, 31.48, 31.00, 24.58.

IR (KBr pellet): ν 3500, 2950, 2864, 2625, 2190, 1667, 1622, 1578, 1521, 1390, 1268, 749 cm^{-1}.

LRMS (ESI: 0.1% formic acid in MeOH) m/z 420 (M$^+$ + 1, 100), 341 (4.10), 323 (10.83), 287 (12.47), 267 (7.01).

Anal. Calcd for C$_{27}$H$_{33}$NO$_3$: C, 77.29; H, 7.93; N, 3.34. Found: C, 77.04; H, 7.95; N, 3.38.

R-(+)-1-Phenylethylamine salt (62g)
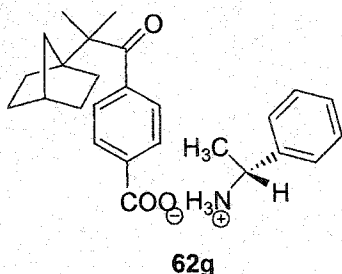
62g

A solution of acid **60** (71.5 mg, 0.25 mmol) in diethyl ether (15 mL) was added to a solution of R-(+)-1-phenylethylamine (30.3 mg, 0.25 mmol) in diethyl ether (5 mL). The cloudy solution was stirred for 1 h, after which time the precipitate that had formed was filtered, washed with diethyl ether and dried *in vacuo* to afford salt **62g** (95.4 mg, 94 %) as a white powder. Recrystallization from MeOH afforded colorless needles.

mp: 175-177 °C.

^{1}H NMR (400 MHz, CD$_3$OD): δ 7.94 (d, *J* = 8.0 Hz, 2H), 7.47 (d, *J* = 8.0 Hz, 2H), 7.43 (m, 5H), 4.42 (q, *J* = 6.8 Hz, 1H), 2.12 (m, 1H), 1.61 (d, *J* = 6.8 Hz, 3H), 1.67-1.57 (m, 4H), 1.33 (s, 6H), 1.30-1.27 (m, 6H).

^{13}C NMR (75 MHz, CD$_3$OD): δ 213.94, 173.92, 145.06, 140.20, 140.07, 130.26, 130.04, 129.82, 127.64, 127.57, 54.83, 52.34, 51.31, 40.65, 37.39, 32.22, 31.47, 24.58, 21.00.

IR (KBr pellet): ν 3500, 2952, 2869, 2558, 2178, 1657, 1627, 1579, 1528, 1456, 1394, 962, 692 cm^{-1}.

LRMS (ESI: 0.1% formic acid in MeOH) *m/z* 408 (M$^+$ + 1, 100), 309 (6.59), 287 (5.26), 243 (6.49).

Anal. Calcd for C$_{26}$H$_{33}$NO$_3$: C, 76.62; H, 8.16; N, 3.44; O, 11.78. Calcd for C$_{26}$H$_{33}$NO$_3$ •1/3 H$_2$O: C, 75.51; H, 8.21; N, 3.39. Found: C, 75.25; H, 8.05; N, 3.75.

(1R, 2S)-(-)-Norephedrine salt (**62h**)

62h
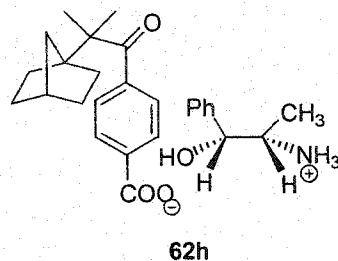
A solution of acid **60** (71.5 mg, 0.25 mmol) in diethyl ether (15 mL) was added to a solution of (1R, 2S)-(-)-norephedrine (37.8 mg, 0.25 mmol) in diethyl ether (5 mL). The cloudy solution was stirred for 1 h, after which time the precipitate that had formed was filtered, washed with diethyl ether and dried *in vacuo* to afford salt **62h** (106.0 mg, 97 %) as a white powder. Recrystallization from MeOH afforded colorless needles.

mp: 157-159 °C.

^{1}H NMR (400 MHz, CD$_3$OD): δ 7.94 (d, J = 8.5 Hz, 2H), 7.47 (d, J = 8.5 Hz, 2H), 7.38-7.35 (m, 4H), 7.32-7.28 (m, 1H), 4.92 (d, J = 3.5 Hz, 1H), 3.48 (m, 1H), 2.12 (m, 1H), 1.67-1.56 (m, 4H), 1.33 (s, 6H), 1.30-1.26 (m, 6H), 1.07 (d, J = 6.8 Hz, 3H).

^{13}C NMR (100 MHz, CD$_3$OD): δ 213.95, 174.18, 144.97, 141.60, 140.35, 129.80, 129.54, 129.00, 127.67, 127.18, 73.72, 54.81, 53.65, 51.30, 40.65, 37.39, 32.22, 31.47, 24.59, 12.54.

IR (KBr pellet): ν 3392, 2963, 2870, 2839, 2499, 2092, 1716, 1671, 1583, 1545, 1392, 983, 741 cm^{-1}.

LRMS (ESI: 0.1% formic acid in MeOH) m/z 438 (M$^+$ + 1, 100), 303 (14.46), 152 (39.30).

Anal. Calcd for $C_{27}H_{35}NO_4$: C, 74.11; H, 8.06; N, 3.20; O, 14.63. Calcd for $C_{27}H_{35}NO_4$

•1/4 H_2O: C, 72.62; H, 8.13; N, 3.14. Found: C, 72.38; H, 8.18; N, 3.34.

Chapter 5 Photochemical Studies

5.1 General Considerations

<u>Light sources and filters</u>

Irradiations were performed using either a 450 W Hanovia medium-pressure mercury lamp in a water-cooled immersion well, or a 1000 W Advanced Radiation Corporation (ARC) high-pressure Hg-Xe arc lamp in a Sciencetech model 201 air-cooled arc lamp housing controlled with a 500-1k power supply operating at 800W. Light emitted from the Hanovia lamp was filtered through Pyrex (transmits $\lambda \geq 290$ nm), and light emitted from the ARC lamp was filtered through two dichroic filters (transmits λ 200-320 nm) and Pyrex (transmits $\lambda \geq 290$ nm).

<u>Solution state photolyses</u>

Samples were dissolved in HPLC grade or spectral grade (Fisher Chemical) solvents and were purged by bubbling nitrogen through the solution for at least 15 min prior to irradiation. The reactions were performed either in sealed reaction vessels or under a positive pressure of nitrogen.

<u>Analytical solid state photolyses</u>

Solid samples (2-5 mg) were sandwiched between two microscope slides (Pyrex equivalent). The sample plates were then fastened together with tape and placed in a polyethylene bag before being heat-sealed under a positive pressure of nitrogen. Following irradiation, the sample was quantitatively washed from the plates with an appropriate solvent, and concentrated *in vacuo*. For neutral molecules, the sample was analyzed directly by GC and/or NMR spectroscopy. For salts and free acids, the sample was converted to the corresponding methyl ester with an ethereal solution of diazomethane, and subsequent analysis was based on the corresponding methyl esters. In the case of salts, the sample was filtered through silica gel to remove the amines before being analyzed by GC and/or HPLC.

Preparative scale solid state photolyses

The solid material was suspended in HPLC grade hexanes (for salts) or distilled water (for esters), purging with nitrogen for 15 min prior to irradiation, and kept under a positive pressure of nitrogen during the photolysis. Following irradiation, the reaction mixture was extracted by methanol (for salts) or dichloromethane (for esters). The extracts were combined for analysis as previously described.

Low-temperature studies

A low temperature ethanol bath contained in an unsilvered Dewar vessel (Pyrex) was maintained by a Cryocool CC-100 II Immersion Cooling System (Neslab Instruments, Inc.). Samples sealed in poly(ethylene) bags were suspended in the cold liquid and irradiated through the transparent walls of the Dewar vessel.

Reaction conversion and yield determinations

Yields for preparative scale photolyses were calculated based on the mass of the isolated products. Conversions for preparative scale photolyses were based on the average integration of at least two GC analyses. Yields and conversions for analytical photolyses were also based on the average integration of at least two GC (or HPLC, response factors calibrated) analyses. The difference in GC detector response for a particular starting material and products was found to be negligible and thus no corrections were applied to the integration data since most materials are isomers.

5.2 Photochemical Studies of α-Oxoamides

5.2.1 Preparative Photolysis of α-Oxoamide 38

Solution state photolysis

38   **39**   **40**
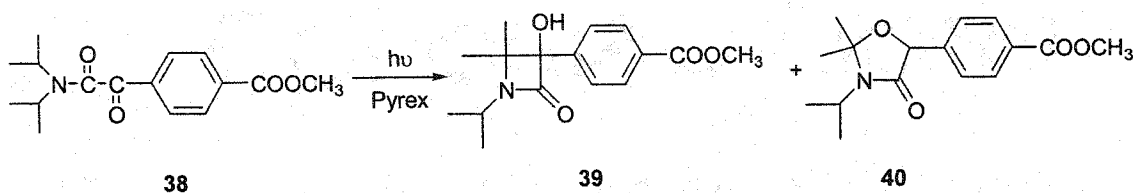
A solution of α-oxoamide **38** (50 mg) was dissolved in benzene (15 mL) in a Pyrex photolysis tube. After purging the system with N_2 for 15 min, the solution was irradiated (450 W Hanovia lamp) for 2 h. Following removal of the solvent *in vacuo* and purification by radial chromatography (ethyl acetate/petroleum ether, 3/7), racemic photoproducts **39** (8 mg) and **40** (20 mg) were obtained as white solids.

Solid state photolysis

α-Oxoamide **38** (50 mg) was sandwiched between two microscopic slides (Pyrex equivalent). The sample plates were then fastened together with tape and placed in a polyethylene bag before being heat-sealed under a positive pressure of nitrogen. Following 2 h irradiation (450 W Hanovia lamp), the sample was quantitatively washed from the plates with dichloromethane, and concentrated *in vacuo*. Purification by radial chromatography (ethyl acetate/petroleum ether, 3/7) afforded racemic photoproducts **39** (21 mg) and **40** (11 mg) as white solids.

Methyl 4-[3-hydroxy-2,2-dimethyl-1-(1-methylethyl)-4-oxo-3-azetidinyl]benzoate (39)
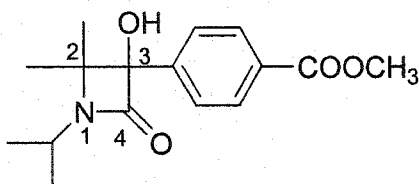
39

mp: 224-225 °C (plates, Et_2O).

^{1}H NMR (CD_2Cl_2, 300 MHz): δ 8.47 (d, J = 8.7 Hz, 2H), 8.20 (d, J = 8.7 Hz, 2H), 4.03 (s, 3H), 3.68 (hept, J = 6.8 Hz, 1H), 1.83 (s, 1H), 1.59 (s, 3H), 1.45 (d, J = 6.8 Hz, 3H), 1.42 (d, J = 6.8 Hz, 3H). 0.91 (s, 3H).

^{13}C NMR ($CDCl_3$, 100 MHz): δ 168.38, 166.77, 143.62, 129.69, 129.39, 126.66, 87.87, 67.30, 52.09, 44.20, 23.78, 22.27, 21.88, 21.74.

IR (KBr pellet): ν 3441(br), 2978, 1732, 1610, 1422, 1284, 1185, 1104, 772 cm^{-1}.

LRMS (EI) m/z 291 (M$^+$, 0.80), 260 (2.2), 206 (100), 191 (18.5), 163 (28.7), 147 (27.5), 100 (23.5).

HRMS (EI) m/z calcd for $C_{16}H_{21}NO_4$ 291.1471, found 291.1477.

Anal. Calcd for $C_{16}H_{21}NO_4$: C 65.96, H 7.27, N 4.81. Found: C 65.86, H 7.36, N 4.76.

2,2-Dimethyl-3-isopropyl-5-(4'-methoxycarbonylphenyl)oxazolidin-4-one (40)
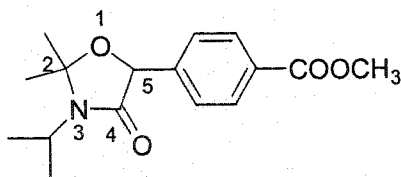
40

mp 112-114 °C (prisms from Et$_2$O)

^{1}H NMR (CDCl$_3$, 300 MHz): δ 8.02 (d, J = 8.38 Hz, 2H), 7.53 (d, J = 8.16 Hz, 2H), 5.21 (s, 1H), 3.88 (s, 3H), 3.40 (hept, J = 6.90 Hz, 1H), 1.58 (s, 3H), 1.53 (s, 3H), 1.47 (d, J = 6.83 Hz, 3H), 1.37 (d, J = 6.84 Hz, 3H).

^{13}C NMR (CDCl$_3$, 75 MHz): δ 168.17, 166.88, 142.14, 129.83, 129.65, 125.98, 94.95, 77.17, 52.07, 46.12, 27.74, 26.64, 20.39, 19.98.

IR (KBr pellet): ν 2976, 1714, 1614, 1423, 1343, 1282, 1114, 753 cm^{-1}.

LRMS (EI): m/z (relative intensity) 291 (M$^+$, 2.7), 276 (73.5), 260 (16.6), 234 (49.4), 206 (100), 191 (43.4), 165 (16.9), 147 (98.6), 133 (37.9), 105 (14.3), 84 (15.4), 77 (14.2).

HRMS (EI): m/z calcd for $C_{16}H_{21}NO_4$ 291.1471, found 291.1468.

Anal. Calcd for $C_{16}H_{21}NO_4$: C 65.96, H 7.27, N 4.81. Found: C 66.17, H 7.31, N 4.84.

5.2.2 Preparative Photolysis of Salt 67a

67a   **39** (91 %, 99% e.e.)
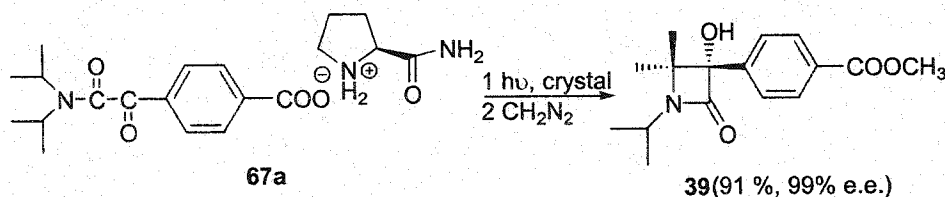
Crystals of salt **67a** (500 mg, 1.28 mmol) were crushed in a mortar and pestle and suspended in 450 mL of HPLC grade hexanes (450mL) in a standard photochemical immersed well apparatus. The suspension was thoroughly degassed under N_2 and irradiated (Pyrex, 450 W Hanovia) with stirring for 6.5 h (99 % conversion). After photolysis the suspension was placed in a separatory funnel and extracted with methanol (3 × 100 mL). The methanol extracts were concentrated *in vacuo* and treated with an excess of ethereal CH_2N_2 to form the corresponding methyl esters. Purification by silica gel chromatography (petroleum ethyl-ethyl acetate, 7:3) afforded compound **39** (338 mg, 91 %) as a white solid. Chiral HPLC analysis (OD column) indicated an optical purity of > 99 % ($[\alpha]^{22}$ +113.1 (c = 1.07 % in MeOH)). Recrystallization from benzene provided colorless plates. Only a trace amount of photoproduct **40** (1 % from GC analysis) was formed in this reaction as a racemate.

The structure of compound **39** was confirmed by X-ray crystallographic analysis:

Habit	colorless plates
Space group	$P2_12_12_1$
a, Å	6.7631(3)
b, Å	10.6176(5)
c, Å	22.061(1)
α (°)	90
β (°)	90
γ (°)	90
Z	4
R	0.051

5.2.3 Preparative Photolysis of α-Oxoamide 68
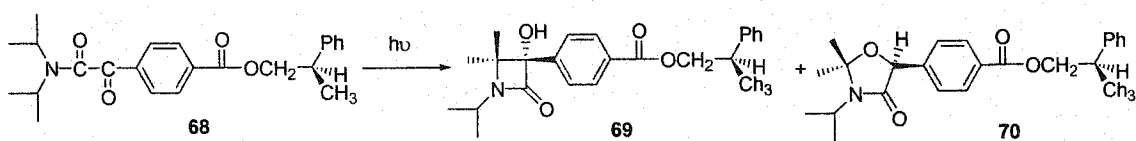
Crystals of ester **68** (200 mg) were crushed in a mortar and pestle and suspended in deionized water (40 mL) in a Pyrex photolysis tube (100 mL). The suspension was thoroughly degassed under N_2 and irradiated (Pyrex, 450 W Hanovia) with stirring for 4.5 h (100 % conversion). After photolysis the suspension was placed in a separatory funnel and extracted with dichloromethane (3 × 40 mL). The organic extracts were concentrated *in vacuo* and purified by silica gel chromatography (petroleum ethyl-ethyl acetate, 8:2) to afford compound **69** (134 mg, 67 %) as a white solid and compound **70** (15 mg) as a yellowish liquid. Chiral HPLC analysis of compound **69** indicated an optical purity of 91 %. Recrystallization in ether provided optically pure compound **69** as colorless plates. The absolute configuration of compound **69** at the newly formed chirality center was determined to be (R) by X-ray crystallography. Photoproduct **70** was determined to be a racemate by chiral HPLC analysis (OD column).

(2R, 3R*)-2-Phenylpropyl 4-[3-hydroxy-2,2-dimethyl-1-(1-methylethyl)-4-oxo-3-azetidinyl]benzoate (69)

69
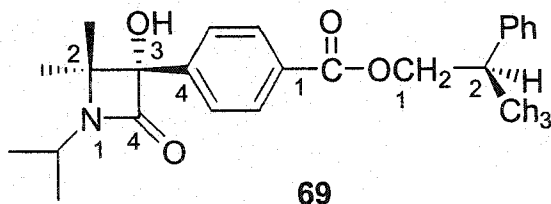
mp 191-192 °C (plates, diethyl ether)

^{1}H NMR (CDCl$_3$, 400 MHz): δ 7.76 (d, J = 8.0 Hz, 2H), 7.29 (m, 5H), 7.24 (d, J = 8.0 Hz, 2H), 5.44 (s, 1H), 4.37 (m, 2H), 3.60 (m, 1H), 3.24 (m, 1H), 1.47 (s, 3H), 1.39 (d, J = 6.9 Hz, 3H), 1.32 (d, J = 6.8 Hz, 6H), 0.74 (s, 3H).

^{13}C NMR (CDCl$_3$, 100 MHz): δ 168.47, 166.04, 143.43, 143.19, 129.70, 129.24, 128.47, 127.32, 126.65, 126.47, 87.82, 69.83, 67.33, 44.15, 38.99, 23.74, 22.27, 21.88, 21.73, 18.03.

IR (KBr pellet): ν 3246, 2975, 1727, 1703, 1671, 1407, 1273, 1099, 760 cm^{-1}.

LRMS (EI): *m/z* (relative intensity) 395 (M$^+$), 310, 192 (100), 175, 105, 91, 77.

HRMS (EI): *m/z* calcd for C$_{24}$H$_{29}$NO$_4$ (M$^+$): 395.2097, found 395.2095.

Anal. Calcd for C$_{24}$H$_{29}$NO$_4$: C, 72.89; H, 7.39; N 3.54. Found: C, 72.64; H, 7.36; N, 3.68.

This structure was confirmed by X-ray crystallographic analysis:

Habit	colorless plates
Space group	$P2_1$
a, Å	10.7830(3)
b, Å	6.8387(5)
c, Å	14.6447(1)
α (°)	90
β (°)	91.9500(10)
γ (°)	90
Z	2
R	0.063

<u>(2R, 3S*)-2-Phenylpropyl 4-[2, 2,-dimethyl-3-(1-methylethyl)-4-oxo-5-oxazolidinyl]-benzoate (70)</u>

70
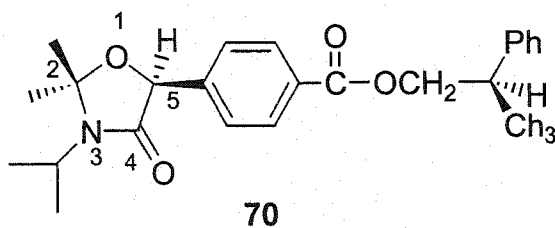
^{1}**H NMR** (CDCl$_3$, 300 MHz): δ 7.97 (d, J = 8.2 Hz, 2H), 7.52 (d, J = 8.2 Hz, 2H), 7.28 (m, 5H), 5.20 (s, 1H), 4.38 (m, 2H), 3.41 (hept, J = 6.8 Hz, 1H), 3.24 (m, 1H), 1.58 (s, 3H), 1.54 (s, 3H), 1.48 (d, J = 6.8 Hz, 3H), 1.38 (d, J = 6.8 Hz, 3H), 1.37 (d, J = 6.8 Hz, 3H).

^{13}**C NMR** (CDCl$_3$, 100 MHz): δ 168.20, 166.27, 143.18, 142.14, 130.01, 129.64, 128.51, 127.32, 126.70, 125.97, 94.96, 77.19, 69.84, 46.14, 39.07, 27.77, 26.67, 20.41, 19.84, 17.99.

IR (KBr pellet): ν 2976, 2937, 1713, 1708, 1613, 1430, 1351, 1272, 1109, 701 cm^{-1}.

LRMS (EI): *m/z* (relative intensity) 395 (M⁺), 380, 310, 278, 260, 147, 118 (100), 105, 91, 77.

HRMS (EI): *m/z* calcd for $C_{24}H_{29}NO_4$ (M⁺): 395.2097, found 395.2095.

Anal. Calcd for $C_{24}H_{29}NO_4$: C, 72.89; H, 7.39; N 3.54. Calcd for $C_{24}H_{29}NO_4 \cdot 1/2H_2O$: C, 72.26; H, 7.48; N 3.46. Found: C, 72.21; H, 7.20; N, 3.49.

5.3 Photolysis of Bicyclo[2.2.2]octane Derivatives 85 and 55

5.3.1 Preparative Photolysis of Bicyclo[2.2.2]octyl Ketone 85
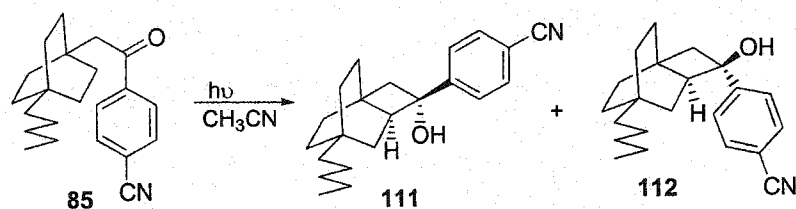
A solution of ketone **85** (82 mg) in acetonitrile (10 mL) was purged with N_2 and irradiated (450 W Hanovia lamp) for 2 h. Removal of the solvent *in vacuo* and purification by chromatography (ether/petroleum ether, 3/7) afforded cyclobutanols **112** (50 mg, 61%, white solid), and **111** (28 mg, 34%, white solid).

(3R*, 4S*)-3-(4'-Cyanophenyl)-6-pentyltetracyclo[4.2.2.0^{1,4}]decan-3-ol (112)
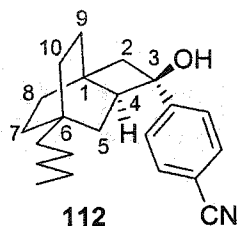
mp: 105.0-106.0 °C (plates, diethyl ether).

^{1}**H NMR** (400 MHz, CDCl$_3$): δ 7.58 (d, J = 8.2 Hz, 2H), 7.41 (d, J = 8.2 Hz, 2H), 2.54 (m, 1H), 2.36 (t, J = 9.9 Hz, 1H), 2.20 (d, J = 12.0 Hz, 1H), 2.03 (d, J = 12.0 Hz, 1H), 2.01 (s, 1H, OH), 1.65-1.48 (m, 6H), 1.40-1.05 (m, 11H), 0.85 (t, J = 7.1 Hz, 3H).

^{13}**C NMR** (75 MHz, CDCl$_3$): δ 153.02, 132.29, 125.89, 118.84, 110.61, 78.91, 46.82, 44.56, 41.26, 33.64, 32.76, 32.71, 32.43, 32.02, 31.02, 29.12, 28.74, 23.47, 22.65, 14.04.

IR (KBr pellet): ν 3458, 3037, 2921, 2852, 2235, 1607, 1456, 1377, 1171, 1020, 848, 516 cm^{-1}.

LRMS (EI) m/z 323 (M$^+$), 305, 252, 234, 178, 130 (100), 102, 79.

HRMS (EI) calcd for C$_{22}$H$_{29}$NO 323.2249, found 323.2253.

Anal. Calcd for C$_{22}$H$_{29}$NO: C, 81.69; H, 9.04; N, 4.33. Found: C, 81.83; H, 9.17; N, 4.21.

(3S*, 4S*)-3-(4'-Cyanophenyl)-6-pentyltetracyclo[4.2.2.0^{1,4}]decan-3-ol (**111**)
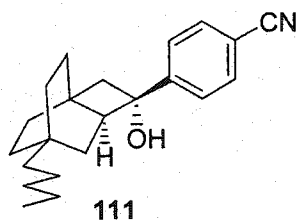
mp: 157.0-159.0 °C (plates, Et$_2$O).

^{1}**H NMR** (300 MHz, CDCl$_3$): δ 7.66 (d, J = 8.3 Hz, 2H), 7.48 (d, J = 8.3 Hz, 2H), 2.70 (d, J = 12.2 Hz, 1H), 2.57 (t, J = 9.9 Hz, 1H), 2.10 (s, 1H, OH), 2.07 (d, J = 12.2 Hz, 1H), 1.63-1.48 (m, 4H), 1.23-0.99 (m, 14H), 0.83 (t, J = 7.1 Hz, 3H).

^{13}**C NMR** (75 MHz, CDCl$_3$): δ 147.92, 132.21, 128.60, 118.74, 111.30, 78.70, 51.62, 43.02, 40.94, 33.55, 32.74, 32.47, 32.38, 31.80, 31.50, 27.70, 26.56, 23.36, 22.61, 14.06.

IR (KBr pellet): ν 3515, 2924, 2856, 2228, 1607, 1449, 1393, 1168, 1060, 840, 559 cm^{-1}.

LRMS (EI) *m/z* 323 (M$^+$), 305, 281, 252, 234, 178, 130 (100), 102, 79.

HRMS (EI) calcd for $C_{22}H_{29}NO$ 323.2249, found 323.2250.

Anal. Calcd for $C_{22}H_{29}NO$: C, 81.69; H, 9.04; N, 4.33. Calcd for $C_{22}H_{29}NO \cdot 1/4H_2O$: C, 80.57; H, 9.07; N, 4.27. Found: C, 80.78; H, 9.23; N, 4.17.

This structure was confirmed by X-ray crystallographic analysis:

Habit	colorless plates
Space group	*P-1*
a, Å	6.5607(5)
b, Å	8.6511(7)
c, Å	17.3882(12)
α (°)	73.114(8)
β (°)	77.067(9)
γ (°)	85.352(11)
Z	2
R	0.055

5.3.2 Preparative Photolysis of Bicyclo[2.2.2]octyl Ketone 55
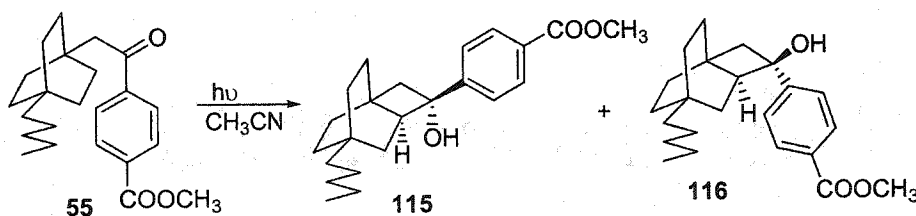
A solution of ketone **55** (190 mg) in acetonitrile (120 mL) was purged with N$_2$ and irradiated (450 W Hanovia lamp) for 3 h. Removal of the solvent *in vacuo* and purification by chromatography (ethyl acetate/petroleum ether, 1/9) afforded

cyclobutanols **116** (117 mg, 62%, yellowish liquid or white solid when solidified upon standing for months) and **115** (52 mg, 27%, white solid).

(3R*, 4S*)-3-(4'-Carbomethoxyphenyl)-6-pentyltetracyclo[4.2.2.0^{1,4}]decan-3-ol (**116**)

116
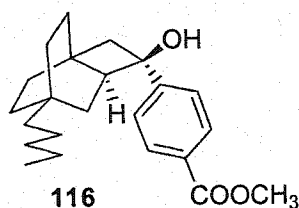
mp: 75.0-75.5 °C (needles, diethyl ether).

^{1}H NMR (400 MHz, CDCl$_3$): δ 7.98 (d, J = 8.5 Hz, 2H), 7.36 (d, J = 8.5 Hz, 2H), 3.89 (s, 3H), 2.57 (m, 1H), 2.40 (m, 1H), 2.23 (d, J = 12.0 Hz, 1H), 2.04 (d, J = 12.0 Hz, 1H), 1.82 (s, 1H, OH), 1.65 (m, 1H), 1.60-1.48 (m, 6H), 1.38-1.06 (m, 10H), 0.86 (t, J = 7.1 Hz, 3H).

^{13}C NMR (75 MHz, CDCl$_3$): δ 166.89, 153.04, 129.87, 128.78, 125.07, 79.22, 52.07, 46.65, 44.47, 41.37, 33.70, 32.83, 32.75, 32.57, 32.11, 31.02, 29.28, 28.75, 23.52, 22.70, 14.07.

IR (KBr pellet): ν 3499, 2929, 2858, 1700, 1611, 1283, 776 cm^{-1}.

LRMS (EI) m/z 356 (M$^+$), 341, 325, 297 (100), 281, 253, 178, 163, 135.

HRMS (EI) calcd for C$_{23}$H$_{32}$O$_3$ 356.2352, found 356.2354.

Anal. Calcd for C$_{23}$H$_{32}$O$_3$: C, 77.49; H, 9.05. Found: C, 77.49; H, 9.36.

(3S*, 4S*)-3-(4'-Carbomethoxyphenyl)-6-pentyltetracyclo[4.2.2.0^{1,4}]decan-3-ol (**115**)

115
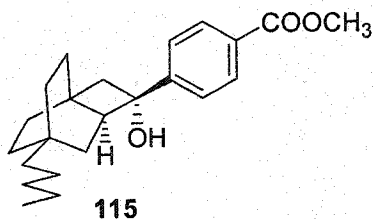
mp: 72-73 °C.

^{1}H NMR (400 MHz, CDCl$_3$): δ 8.02 (d, J = 8.3 Hz, 2H), 7.44 (d, J = 8.3 Hz, 2H), 3.90 (s, 3H), 2.72 (d, J = 12.1 Hz, 1H), 2.58 (m, 1H), 2.06 (d, J = 12.1 Hz, 1H), 1.90 (s, 1H, OH), 1.62-1.48 (m, 4H), 1.25-0.96 (m, 14H), 0.83 (t, J = 7.1 Hz, 3H).

^{13}C NMR (75 MHz, CDCl$_3$): δ 166.89, 147.81, 129.64, 129.14, 127.81, 78.76, 52.11, 51.38, 42.96, 41.01, 33.60, 32.76, 32.53, 32.34, 31.83, 31.60, 27.59, 26.50, 23.36, 22.61, 14.06.

IR (KBr pellet): ν 3312, 2930, 2856, 1726, 1611, 1436, 1279, 1112 cm^{-1}.

LRMS (EI) m/z 356 (M$^+$), 341, 297 (100), 178, 163.

HRMS (EI) calcd for C$_{23}$H$_{32}$O$_3$ 356.2352, found 356.2347.

Anal. Calcd for C$_{23}$H$_{32}$O$_3$: C, 77.49; H, 9.05. Found: C, 77.06; H, 9.14.

## 5.4 Photolysis of Bicyclo[2.2.1]heptane Derivatives 58 and 61

5.4.1 Preparative Photolysis of Bicyclo[2.2.1]heptyl Ketone 58
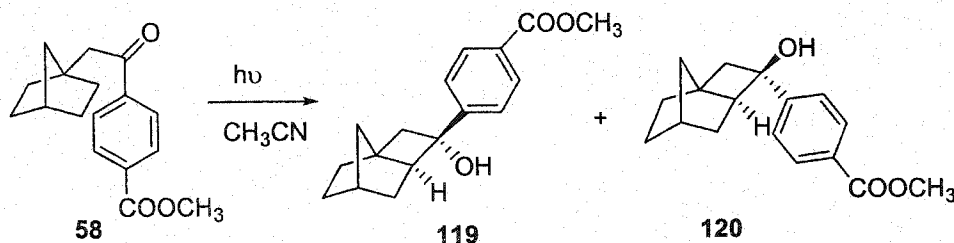
A solution of ketone **58** (67 mg) in acetonitrile (20 mL) was purged with N_2 and irradiated (450 W Hanovia lamp) for 4 h. Removal of the solvent *in vacuo* and purification by chromatography (diethyl ether/petroleum ether, 2/8) afforded cyclobutanols **119** (29 mg, 43%, white solid) and **120** (23 mg, 34%, white solid).

(1S*, 3R*, 4S*, 6S*)-3-(4'-Carbomethoxyphenyl)tetracyclo[4.2.1.0^{1,4}]nonan-3-ol (120)
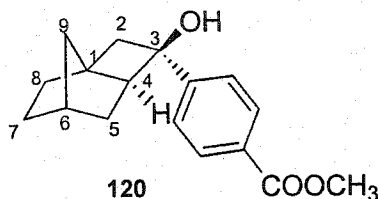
mp: 96-98 °C.

^{1}H NMR (300 MHz, CDCl$_3$): δ 7.98 (d, J = 8.3 Hz, 2H), 7.40 (d, J = 8.3 Hz, 2H), 3.88 (s, 3H, CH$_3$O), 2.51 (d, J = 12.4 Hz, 1H), 2.36 (d, J = 12.4 Hz, 1H), 2.22 (m, 1H), 2.11 (m, 1H), 2.02 (m, 1H), 1.95-1.88 (m, 1H), 1.87 (s, 1H, OH), 1.7-1.6 (m, 1H), 1.6-1.4 (m, 2H), 1.4-1.3 (m, 1H), 1.3-1.2 (m, 2H).

^{13}C NMR (100 MHz, CDCl$_3$): δ 166.91, 153.11, 129.76, 128.66, 125.13, 77.24, 52.06, 50.76, 45.12, 42.08, 38.26, 37.44, 33.63, 33.61, 28.74.

IR (KBr pellet): ν 3499, 2951, 2866, 1698, 1607, 1437, 1282, 1156, 770, 704 cm^{-1}.

LRMS (+CI: gas, NH_3) *m/z* (relative intensity) 290 (M^+ + 18, 17.0), 273 (M^+ + 1, 75.0), 271 (100), 255 (78.7), 288 (12.8).

HRMS (+CI: gas, NH_3) calcd for $C_{17}H_{21}O_3$ (M^+ + 1) 273.1490, found 273.1492.

Anal. Calcd for $C_{17}H_{20}O_3$: C, 74.97; H, 7.40. Found: C, 74.67; H, 7.37.

(1S*, 3S*, 4S*, 6S*)-3-(4'-Carbomethoxyphenyl)tetracyclo[4.2.1.0^{1,4}]nonan-3-ol (**119**)

119
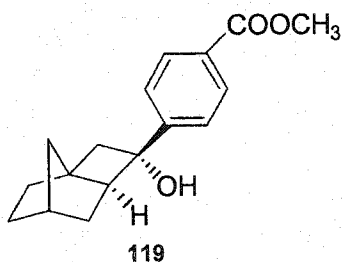
mp: 132-133 °C.

^{1}**H NMR** (300 MHz, $CDCl_3$): δ 8.01 (d, *J* = 8.4 Hz, 2H), 7.44 (d, *J* = 8.4 Hz, 2H), 3.89 (s, 3H, CH_3O), 3.10 (d, *J* = 12.6 Hz, 1H), 2.40 (s, 1H, OH), 2.31 (d, *J* = 12.4 Hz, 1H), 2.23 (m, 1H), 1.94 (m, 1H), 1.60-1.50 (m, 3H), 1.40-1.25 (m, 2H), 1.25-1.15 (m, 1H), 1.05 (m, 1H), 0.82 (m, 1H).

^{13}**C NMR** (75 MHz, $CDCl_3$): δ 168.76, 148.27, 129.69, 129.47, 128.52, 79.03, 56.93, 52.32, 41.84, 41.05, 38.79, 37.25, 35.99, 34.52, 28.49.

IR (KBr pellet): ν 3428, 2950, 2860, 1730, 1695, 1612, 1447, 1279, 1195, 1020, 856, 775, 711 cm^{-1}.

LRMS (+CI: gas, NH_3) *m/z* (relative intensity) 290 (M^+ + 18, 6.5), 273 (M^+ + 1, 30.4), 271 (100), 255 (32.9).

HRMS (+CI: gas, NH_3) calcd for $C_{17}H_{21}O_3$ (M^+ + 1) 273.1490, found 273.1492.

Anal. Calcd for $C_{17}H_{20}O_3$: C, 74.97; H, 7.40. Found: C, 74.67; H, 7.62.

5.4.2 Preparative Photolysis of Dimethylated Bicyclo[2.2.1]heptyl Ketone 61
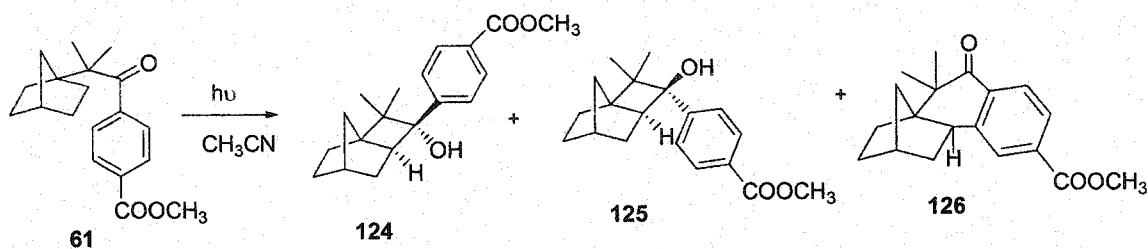
A solution of ketone **61** (200 mg) in acetonitrile (50 mL) was purged with N_2 and irradiated (450 W Hanovia lamp) for 11 h. Removal of the solvent *in vacuo* and purification by chromatography (ether/petroleum ether, 2/8) afforded cyclobutanols **124** (101 mg, 51%, yellowish liquid or white solid when solidified upon standing for months), **125** (50 mg, 25%, white solid), and ketone **126** (7 mg, 3.5%, white solid).

2,2-Dimethyl-(4'-carbomethoxy)benzo[4, 5]tetracyclo[6.2.1.0^{1,6}]undeca-3-one (**126**)

126
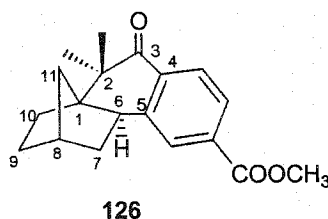
mp: 105-107 °C.

^{1}H NMR (400 MHz, CDCl$_3$): δ 7.93-7.91 (m, 1H), 7.86-7.83 (m, 2H), 3.91 (s, 3H), 3.06 (d × d, J_1 = 9.5 Hz, J_2 = 4.7 Hz, 1H), 2.30 (m, 1H), 2.29-2.22 (m, 1H), 1.74-1.70 (m, 1H), 1.69-1.63 (m, 2H), 1.45-1.42 (m, 2H), 1.26 (s, 3H), 1.24 (m, 1H), 1.10 (s, 3H), 1.06-1.03 (m, 1H).

^{13}C NMR (100 MHz, CDCl$_3$): δ 203.42 (+), 166.53 (+), 148.34 (+), 134.43 (+), 132.89 (+), 130.12 (-), 127.21 (-), 126.64 (-), 54.10 (+), 52.37 (-), 45.58 (+), 42.59 (-), 41.69 (+), 37.70 (-), 37.38 (+), 29.85 (+), 29.74 (+), 23.33 (-), 18.69 (-).

IR (KBr pellet): ν 2975, 2951, 2869, 1730, 1681, 1576, 1436, 1284, 1198, 1103, 975, 751 cm^{-1}.

LRMS (EI) m/z 298 (M$^+$, 100), 283, 189, 115.

HRMS (EI) calcd for C$_{19}$H$_{22}$O$_3$ 298.1569, found 298.1570.

Anal. Calcd for C$_{19}$H$_{22}$O$_3$: C, 76.48; H, 7.43; O, 16.09. Calcd for C$_{19}$H$_{22}$O$_3$•1/6H$_2$O: C, 75.72; H, 7.47. Found: C, 75.74; H, 7.48.

(1R*, 3S*, 4S*, 6S*)-2,2-Dimethyl-3-(4'-carbomethoxyphenyl)tetracyclo[4.2.1.0^{1,4}]nonan-3-ol (125)

125
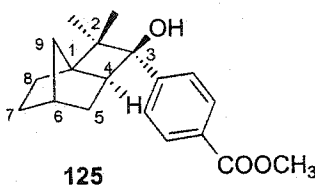
mp: 110-115 °C (plates, CH$_2$Cl$_2$).

^{1}H NMR (400 MHz, CDCl$_3$): δ 7.97 (d, J = 8.5 Hz, 2H), 7.35 (d, J = 8.5 Hz, 2H), 3.89 (s, 3H), 2.47-2.43 (m, 1H), 2.22 (m, 1H), 2.04-2.02 (m, 1H), 1.80-1.68 (m, 1H), 1.65 (s, 1H, OH), 1.63-1.56 (m, 2H), 1.34-1.30 (m, 1H), 1.29-1.22 (m, 3H), 1.21 (s, 3H), 0.72 (s, 3H).

^{13}C NMR (100 MHz, CDCl$_3$): δ 166.98, 155.15, 129.53, 128.79, 126.43, 81.13, 53.84, 52.07, 43.12, 42.70, 39.07, 37.53, 32.33, 29.49, 28.20, 24.20, 19.93.

IR (KBr pellet): ν 3489, 2956, 2934, 2860, 1699, 1611, 1440, 1285, 1196, 1100, 768 cm^{-1}.

LRMS (EI) *m/z* 300 (M$^+$), 282, 267, 253, 239, 207, 191, 163, 147, 135, 120 (100), 107, 91, 79, 67, 55.

HRMS (EI) calcd for $C_{19}H_{24}O_3$ 300.1725, found 300.1727.

Anal. Calcd for $C_{19}H_{24}O_3$: C, 75.97; H, 8.05. Calcd for $C_{19}H_{24}O_3$ •1/3 H_2O: C, 74.48; H, 8.11. Found: C, 74.05; H, 7.92.

This structure was confirmed by X-ray crystallographic analysis:

Habit	colorless plates
Space group	*P2$_1$/C*
a, Å	13.2582(6)
b, Å	6.2949(3)
c, Å	20.0604(9)
α (°)	90
β (°)	103.283(2)
γ (°)	90
Z	4
R	0.057

(1R*, 3R*, 4S*, 6S*)-2, 2-Dimethyl-3-(4'-

carbomethoxyphenyl)tetracyclo[4.2.1.0^{1,4}]nonan-3-ol (**124**)

124

mp: 77-78 °C.

^{1}H NMR (400 MHz, CDCl$_3$): δ 7.95 (d, J = 8.5 Hz, 2H), 7.58 (d, J = 8.5 Hz, 2H), 3.88 (s, 3H), 2.28-2.25 (m, 1H), 2.21-2.04 (m, 1H), 2.02 (s, 1H, OH), 1.71-1.65 (m, 1H), 1.60-1.55 (m, 1H), 1.42-1.34 (m, 2H), 1.33 (s, 3H, CH$_3$), 1.20 (m, 1H), 1.19 (s, 3H, CH$_3$), 1.12-1.05 (m, 2H).

^{13}C NMR (100 MHz, CDCl$_3$): δ 166.92 (+), 149.43 (+), 129.05 (-), 128.81 (-), 128.44 (+), 82.02 (+), 54.31 (-), 52.06 (-), 51.79 (+), 44.71 (+), 39.54 (+), 37.78 (-), 36.75 (+), 28.72 (+), 28.03 (+), 25.38 (-), 23.32 (-).

IR (neat): ν 3456 (br), 2952, 2864, 1725, 1611, 1436, 1281, 1187, 1109, 1004, 716 cm^{-1}.

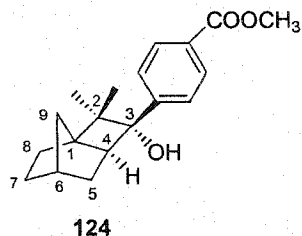**LRMS** (EI) m/z 300 (M$^+$), 282, 267, 253, 239, 207, 191, 163, 147, 135, 120 (100), 107, 91, 79, 67, 55.

HRMS (EI) calcd for C$_{19}$H$_{24}$O$_3$ 300.1725, found 300.1726.

Anal. Calcd for C$_{19}$H$_{24}$O$_3$: C, 75.97; H, 8.05. Found: C, 75.57; H, 8.13.

References

1   Wöhler, F. *Ann. Phys. Chem.* **1828**, *12*, 253.

2   Trommsdroff, H. *Ann. Chem. Pharm.* **1834**, *11*, 190.

3   Ramamurthy, V.; Venkatesan, K. *Chem. Rev.* **1987**, *87*, 433.

4   (a) Byrn, S. R. *Solid-state Chemistry of Drugs*; Academic Press: New York, 1982.
    (b) Yoshioka, S.; Stella, J. S. *Stability of Drugs and Dosage Forms*; Kluwer
    Academic/Plenum Publishers: New York, 2000.

5   Desiraju, G. R. J. *Crystal Engineering: The Design of Organic Solids*; Elsevier:
    Amsterdam, 1989.

6   (a) Horspool, W. M. *Synthetic Organic Photochemistry;* Plenum Press: New York,
    1984. (b) Schaffner, K; Demuth, M. In *Modern Synthetic Methods*; Scheffold R.
    Ed.; Springer-Verlag: Berlin Heidelberg, 1986; p.61.

7   Richards, A.; McCague, R. *Chem. Ind.* **1997**, (6), 422.

8   (a) Agranat, I.; Caner, H.; Caldwell, J. *Nature Reviews Drug Discovery* **2002**, *1*,
    753. (b) Burke, D.; Henderson, D. J. *British Journal of Anaesthesia* **2002**, *88*, 563.
    (c) Agranat, I.; Caner, H. *Drug Discovery Today* **1999**, *4*, 313. (d) Caldwell, J.
    Human Psychopharmacol. Clin. Exp. **2001**, *16*, S67. (e) Tucker, G. T. *The Lancet*
    2000, *355*, 1085.

9   (a) Rau, H. *Chem. Rev.* **1983**, *83*, 535; (b) Inoue, Y. *Chem. Rev.* **1992**, *92*, 741; (c)
    Pete, J. P. *Adv. Photochem.* **1996**, *21*, 135; (d) Everitt, S. R. L.; Inoue, Y. In
    Molecular and Supramolecular Photochemistry; Ramamurthy, V.; Schanze, K. S.,
    Eds.; Marcel Dekker: New York, 1999; Chapter 2. (d) Buschmann, H.; Scharf, H.
    D.; Hoffmann, N.; Esser, P. *Angew. Chem. Intl. Ed. Engl.* **1991**, *30*, 477.

10 Schmidt, G. M. J. *Pure Appl. Chem.* **1971**, *27*, 647.

11 (a) Nangia, A. *CrystEngComm* **2002**, *4*, 93. (b) Caira, M. R. *Top. Curr. Chem.* **1998**,
    198, 164. (c) Bernstein, J.; Davey, R. J.; Henck, J. O. *Angew. Chem. Intl. Ed.* **1999**,
    38, 3440.

12 Evans O. R.; Lin, W. *Acc. Chem. Res.* **2002**, *35*, 511.

13 Steiner, T. *Angew. Chem. Intl. Ed.* **2002**, *41*, 48.

14 (a) Hung, J. D.; Lahav, M.; Luwich, M.; Schmidt, G. M. J. *Isr. J. Chem.* **1972**, *10*, 585. (b) Cohen, M. D.; Cohen, R.; Lahav, M.; Nie, P. L. *J. Chem. Soc., Perkin Trans.* **1973**, *2*, 1095. (c) Green, B. S.; Heller, L. *J. Org. Chem.* **1974**, *39*, 1960.

15 Desiraju, G. R. J., In *Stimulating Concepts in Chemistry*, Vogtle, F.; Stoddart, J. F.; Shibasaki, S., ed.; Wiley-VCH: Weinheim, 2000; p.293.

16 Nangia, A. *Curr. Opin. Solid State Mater. Sci.* **2001**, *5*, 115.

17 Braga, D.; Grepioni, F. *Acc. Chem. Res.* **2000**, *33*, 601.

18 Beatty, A. M. *CrystEngComm* **2001**, *3*, 51.

19 Braga, D.; Desiraju, G. R.; Miller, J. S.; Orpen, A. G.; Price, S. L. . *CrystEngComm* **2002**, *4*, 500.

20 The quotation of "a crystal is a chemical cemetery" used by Nobel Prize laureate Leopold Ruzicka is from: Dunitz, J. D. *Trans. Am. Cryst. Assoc.* **1984**, *20*, 1.

21 Kohlshütter, H. W. Z. *Anorg. Allg. Chem.* **1918**, *105*, 121.

22 (a) Cohen, M. D.; Schmidt, G. M. J. *J. Chem. Soc.* **1964**, 1996. (b) Cohen, M. D.; Schmidt, G. M. J; Sonntag, F. I. *J. Chem. Soc.* **1964**, 2000. (c) Schmidt, G. M. J. *J. Chem. Soc.* **1964**, 2014.

23 Schmidt, G. M. J. *Pure Appl. Chem.* **1971**, *27*, 647.

24 Ramasubbu, N.; Guru Row, T. N.; Venkatesan, K; Ramamurthy, V.; Rao, C. N. R. *J. Chem. Soc., Chem. Commun.* **1982**, 178.

25 Nakanishi, H.; Hasegawa, M. *Acta Cryst.* **1985**, *C41*, 70.

26 Kearsley, S. K.; Desiraju, G. R. *Proc. R. Soc. London* **1985**, *A397*, 157.

27 Cohen, M. D. *Angew. Chem. Intl. Ed.* **1975**, *14*, 386.

28 Weiss, R. G.; Ramamurthy, V.; Hammond, G. S. *Acc. Chem. Res.* **1993**, *26*, 530.

29 Theocharis, C. R; Jones, W. In *Organic Solid State Photochemistry*; Desiraju, G. R., Ed.; Elsevier: Amsterdam, 1987; Chapter 2, p.47-68.

30 Scott, C. J. PhD thesis, The University of British Columbia, 2003.

31 Gavezzotti, A. *J. Am. Chem. Soc.* **1983**, *105*, 5220.

32 McBride, J. M. *Acc. Chem. Res.* **1983**, *16*, 304.

33   (a) Ariel, S.; Askari, S.; Scheffer, J. R.; Trotter, J.; Walsh, L. *J. Am. Chem. Soc.* **1984**, *106*, 5726. (b) Ariel, S.; Askari, S.; Scheffer, J. R.; Trotter, J. *Tetrahedron lett.* **1986**, *27*, 783.

34   Some examples of latent reactivity in solid state reaction include: (a) Heggie, W.; Sutherland, J. K. *Chem. Commun.* **1972**, 957. (b) Ariel, S.; Askari, S.; Scheffer, J. R.; Trotter, J. *J. Org. Chem.*, **1989**, *54*, 4324, (c) Pokkuluri, P. R.; Scheffer, J. R.; Trotter, J.; Yap, M. *J. Org. Chem.* **1992**, *57*, 1486. (d) Cheung, E.; Kang, T.; Scheffer, J. R.; Trotter, J. *Chem. Commun.* **2000**, 2309. (e) Kang, T.; Scheffer, J. R. *Org. Lett.* **2001**, *3*, 3361.

35   For a recent review on the Norrish/Yang type II reaction, see (a) Wagner, P. J.; Klán, Petr In *CRC Handbook of Organic Photochemistry and Photobiology*; Horspool, W.; Lenci, F., Eds.; CRC Press: Boca Raton, 2004; Chapter 52; (b) Wagner, P. J. In *CRC Handbook of Organic Photochemistry and Photobiology*; Horspool, W.; Lenci, F., Eds.; CRC Press: Boca Raton, 2004; Chapter 58.

36   Wagner, P.; Park, B. In *Organic Photochemistry*, Volume. 11; Padwa, A., Ed.; Marcel Dekker Inc.: New York, 1991; Chapter 4.

37   Turro, N. J. *Modern Molecular Photochemistry*; Benjamin/Commings: Menlo Park, 1978; p364.

38   (a) Coyle, J. D. *Introduction to Organic Photochemistry*; John Wiley and Sons, Inc.; Toronto, 1986; pp. 119-125. (b) Kagan, J. *Organic Photochemistry: Principles and Applications*; Academic Press: San Diego, 1993; p.58-59. (c) Horspool, W. M. *Aspects of Organic Photochemistry*; Academic Press: New York, 1976; p.172-174.

39   (a) Wagner, P. J. *Acc. Chem. Res.* **1971**, *4*, 168; (b) Wagner, P.; Park, B-S. In *Organic Photochemistry*; Padwa, A., Ed.; Marcel Dekker: New York, 1991; Chapter 4.

40   Cyclobutanol products in type II photochemistry were first reported by: Yang, N. C; Yang, D. H. *J. Am. Chem. Soc.* **1958**, *80*, 2913

41   (a) Wilson, R. M. In *Organic Photochemistry*; Padwa, A., Ed.; Marcel Dekker: New York, 1985; Volume 7, pp 339-446; (b) Adam, W.; Grabowski, W.; Wilson, R. W. *Chem. Ber.* **1989**, *122*, 561-564.

42 Lamola, A. A.; Hammond, G. S. *J. Phys. Chem.* **1965**, *43*, 2129.

43 Chairlike transition state arguments in (a) Wagner, P. J.; Kelso, P. A.; Kemppainen, A. E.; Zepp, R. G. *J. Am. Chem. Soc.* **1972**, *94*, 7500. (b) Doering, W. V. E.; Roth, W. R. *Tetrahedron* **1962**, *18*, 67. (c) Hill, R. K.; Gilman, N. W. *Chem. Commun.* **1967**, 619. (d) Dorigo, A. E.; McCarrick, M. A.; Loncharrich, R. J.; Houk, K. N. *J. Am. Chem. Soc.* **1990**, *112*, 7508.

44 Scheffer, J. R.; Scott, C. In *The CRC Handbook of Organic Photochemistry and Photobiology; 2nd Edition*; Horpool, W. M.; Lenci, F. Eds., CRC Press: Boca Raton. 2004; Chapter 54 and references cited therein.

45 Benchikh le-Hocine, M.; Do Khac, D.; Fetizon, M; Guir, F.; Guo, Y.; Prange, T. *Tetrahedron Lett.* **1992**, *33*, 1443.

46 Kraus, G.; Thomas, P. J.; Schwinden, M. D. *Tetrahedron Lett.* **1990**, *31*, 1819.

47 Nuss, J. M.; Murphy, M. M. *Tetrahedron Lett.* **1994**, *35*, 37

48 Kraus, G.; Chen, L. *J. Am. Chem. Soc.* **1990**, *112*, 3464.

49 Paquette, L.A.; Ternansky, R.J.; Balogh, D.W.; Kentgen, G. *J. Am. Chem. Soc.* **1983**, *105*, 5446.

50 Breslow, R. In *Comprehensive Organic Synthesis;* Trost, B. M. ed.; Pergamon Press: New York, 1991; p.39-52.

51 (a) Kraus, G.; Wu, Y. *J. Am. Chem. Soc.* **1992**, *114*, 8705. (b) Kraus, G.; Zhang, W. Wu, Y. *Chem. Commun.* **1996**, 2439.

52 (a) Kraus, G. A.; Schwinden, M. D. *Studies in Natural Products Chemistry*, **1994**, *14*, 645. (b) Kraus, G. A.; Schwinden, M. D. *J. Photochem. Photobiol. A: Chem.* **1991**, *62*, 241.

53 (a) Paquette, L. A.; Sugimura, T. *J. Am. Chem. Soc.* **1986**, *108*, 3841. (b) Sugimura, T.; Paquette, L. A. *J. Am. Chem. Soc.* **1987**, *109*, 3017.

54 Kraus, G.; Shi, J. *Synth. Commun.* **1990**, *20*, 1837.

55 Nath, A.; Mal, J.; Venkateswaran, R. V. *J. Org. Chem.* **1996**, *61*, 4391.

56 Kraus, G.; Zhang, N. *J. Org. Chem.* **2000**, *65*, 5644.

57 Wagner, P. J. In *CRC Handbook of Photochemistry and Photobiology;* CRC Press: Boca Raton. 1995; Chapter 38.

58   Moule, D. C.; Walsh, A. D. *Chem. Rev.* **1975**, *75*, 67.

59   Netherton, M. R. PhD thesis, The University of British Columbia, 2000.

60   For studies relating to the selectivity of hydrogen atom abstraction as a function of abstraction distance and geometry, see (a) Ihmels, H.; Scheffer, J. R. *Tetrahedron* **1999**, *55*, 885. (b) Leibovich, M.; Olovsson, G.; Scheffer, J. R.; Trotter, J. *J. Am. Chem. Soc.* **1998**, *120*, 12755. (c) Gudmundsdottir, A. D.; Lewis, T. J.; Randall, L. H.; Scheffer, J. R.; Rettig, S. J.; Trotter, J.; Wu, C. *J. Am. Chem. Soc.* **1996**, *118*, 6167.

61   (a) Bondi, A. *J. Phys. Chem.* **1964**, *68*, 441. (b) Edward, J. T. *J. Chem. Educ.* **1970**, *47*, 261.

62   Wagner, P. J. *Top. Curr. Chem.* **1976**, *66*, 1.

63   Dorigo, A. E.; McCarrick, M. A.; Loncharich, R. J.; Houk, K. N. *J. Am. Chem. Soc.* **1990**, *112*, 7508 and references therein.

64   (a) Kasha, M. *Radiat. Res.* 1960, Suppl. 2, 243. (b) Zimmerman, H. E. *Tetrahedron* **1963**, *19*, 393.

65   Burdett, J.K. *Molecular Shapes*; Wiley-Interscience: New York, 1980; p.6.

66   (a) Pasteur, L. C. R. *Acad. Sci.* **1853**, *37*, 162. (b) For discussion of Pasteur's work on sodium ammonium tartrate, see: Fieser, M. *Advanced Organic Chemistry;* Reinhold: New York, 1961; p.69.

67   (a) Morrison, J. D.; Mosher, H. S. *Asymmetric Reactions*; Prentice-Hall: Englewookd Cliffs, New Jersey; Revised Ed. 1976, ACS Books: Washington, D.C. (b) Sheldon, R. A. *Drug Inform. J.* **1990**, *24*, 129.

68   For recent reviews on asymmetric photochemistry see: (a) Inoue, Y. *Chem. Rev.* **1992**, *92*, 741. (b) Rau, H. *Chem. Rev.* **1983**, *83*, 535. (c) Pete, J. P. *Adv. Photochem.* **1996**, *21*, 135. (d) Everitt, S. R. L.; Inoue, Y. *In Molecular and Supramolecular Photochemistry* Vol. *3*; Ramamurthy, V., Schanze, K. S., Eds.; Marcel Dekker: New York, 1999; Chapter 2. (e) Griesbeck, A. G.; Meierhenrich, U. J. *Angew. Chem. Intl. Ed.* **2002**, *41*, 3147.

69   Griesbeck, A. G.; Heckroth, H. *J. Am. Chem. Soc.* **2002**, *124*, 396.

70   Bach, T.; Aechtner, T.; Neumüller, B. *Chem. Commun.* **2001**, 607.

71 For reviews on organized media and/or solid state asymmetric photochemistry see:
(a) Ohashi, Y., Ed. *Reactivity in Molecular Crystals*; VCH Publishers: New York,
1993; Chapter 5. (b) Feringa, B. L.; van Delden, R. A. *Angew. Chem. Intl. Ed.* **1999**,
38, 3418. (c) Green, B. S.; Arad-Yellin, R.; Cohen, M. D. In *Topics in
Stereochemistry*; Eliel, E. I.; Wilen, S. H.; Allinger, N. L., Eds. John Wiley &
Sonds: NY, 1986. Vol. 16, p.131. (d) Green, B. S.; Lahav, M.; Rabinovich, D. *Acc.
Chem. Res.* **1979**, *12*, 191. (e) Ito, Y. In *Molecular and Supramolecular
Photochemistry*, Ramamurthy, V.; Schanze, K. S., Eds.; Marcel Dekker: New York,
1999; Vol. *3*, Chapter 1. (f) Griesbeck, A. G.; Meierhenrich, U. J. *Angew. Chem.
Intl. Ed.* **2002**, *41*, 3147.

72 Addadi, L.; Lahav, M. *Pure Appl. Chem.* **1979**, *51*, 1269.

73 Penzien, K.; Schmidt, G. M. J. *Angew. Chem., Intl. Ed. Engl.* **1969**, *8*, 608.

74 Elgavi, A.; Green, B. S.; Schmidt, G. M. J. *J. Am. Chem. Soc.* **1973**, *95*, 2058.

75 Evans, S. V.; Garcia-Garibay, M,; Omkaram, M.; Scheffer, J. R.; Trotter, J.; Wireko,
F. *J. Am. Chem. Soc.* **1986**, *108*, 5648.

76 (a) Vaida, M; Popovitz-Biro, R; Leiserowitz, L.; Lahav, M. In *Photochemistry in
Organized and Constrained Media*; Ramamurthy, V., Ed.; VCH Publishers: New
York, 1991, Chapter 6.

77 Jacques, J.; Collet, A.; Wilen, S. H. *Enantiomers, Racemates and Resolutions*;
Wiley: New York, 1981; p.14-18.

78 For reviews of the ionic chiral auxiliary concept see: (a) Scheffer, J. R. *Can. J.
Chem.*, **2001**, *79*, 349-357. (b) Gamlin, J. N.; Jones, R.; Leibovith, M. Patrick, B.;
Scheffer, J. R.; Trotter, J. *Acc. Chem. Res.* **1996**, *29*, 203.

79 Yang J. PhD Dissertation, Unversity of British Columbia, 1993.

80 (a) Aoyama, H.; Hasegawa, T.; Omote, Y. *J. Am. Chem. Soc.* **1979**, *101*, 5343. (b)
Aoyama, H.; Hasegawa, T.; Watabe, M.; Shiraishi, H.; Omote, Y. *J. Org. Chem.*
1978, *43(3)*, 419. (c) Aoyama, H.; Sakamoto, M.; Kuwabara, K.; Yoshida, K.;
Omote, Y. *J. Am. Chem. Soc.* **1983**, *105*, 1958. (d) Aoyama, H.; Sakamoto, M.;
Omote, Y. *J. Chem. Soc. Perkin Trans. 1* **1981**, 1357. (e) Aoyama, H.; Miyazaki,
K.; Sakamoto, M.; Omote, Y. *J. Chem. Soc. Chem Commun.* **1983**, 333.

81 (a) Toda, F.; Miyamoto, H.; Matsukawa, R. *J. Chem. Soc. Perkin Trans. 1* **1992,** 1461. (b) Toda, F.; Tanaka, K.; Yagi, M. *Tetrahedron* **1987,** *43(7),* 1495. (c) Sekine, A.; Hori, K.; Ohashi, Y.; Yagi, M.; Toda, F. *J. Am. Chem. Soc.* **1989,** *111,* 697. (d) Toda, F.; Miyamoto, H. *J. Chem. Soc. Perkin Trans. 1* **1993,** 1129. (e) Toda, F.; Yagi, M.; Soda, S. *J. Chem. Soc., Chem. Commun.,* **1987,** 1413. (f) Kaftory, M.; Yagi, M.; Tanaka, K.; Toda, F. *J. Org. Chem.* **1988,** *53,* 4391. (g) Hashizume, D.; Kogo, H.; Kekine, A.; Ohashi, Y.; Miyamoto, H.; Toda, F. *J. Chem. Soc. Perkin Trans. 2,* **1996,** 61.

82 Chesta C. A.; Whitten, D. A. *J. Am. Chem. Soc.* **1992,** *114,* 2188.

83 Wang, R.; Chen, C.; Duesler, E.; Mariano, P.S. *J. Org. Chem.* **2004,** *69,* 1215.

84 (a) Hu, S.; Neckers, D. C. *Tetrahedron* **1997,** *53(8),* 2751. (b) Henery-Logan, K. R.; Chen, G. Chester *Tetrahedron Letters,* **1973,** *13,* 1103. (c) Akermark, B.; Johansson, N. *Tetrahedron Letters,* **1969,** *5,* 371.

85 The calculations were performed using HyperChem/ChemPlus soft package (version 5.11/2.0) with MM+ force parameters: Department of Chemistry, Columbia University, New York, 1994. The MM+ force field is an extension of MM2 which was developed by Allinger and co-workers [Allinger, N. L. *J. Am. Chem. Soc.,* **1977,** *99,* 8127; Burkert, U. and. Allinger, N. L *Molecular Mechanics,* ACS Monograph 177 (1982)] and is designed primarily for small organic molecules.

86 Gerlach, U.; Wollmann, T. *Tetrahedron Lett.* **1992,** *33,* 5499.

87 (a) Hallman, G.; Hagele, K. *Ann. Chem.* **1963,** *662,* 147. (b) Stadler, von Paul Albert *Helvetica Chimica Acta,* **1978,** *61,* 1675.

88 Seto, C. T. US Patent 2003120073, 2003.

89 Microanalysis was used wherever possible to confirm the 1:1 composition of the salts, but this was hindered by the absorption of water during the crystallization process in many cases.

90 Dolphin, D.; Wick, A. In *Tabulation of Infrared Spectral Data*; John Wiley and Sons: New York, 1977; p.295.

91 (a) Wagner P.J.; Kelso, Q.A.; Zepp, R.G. *J. Am. Chem. Soc.* **1972,** *94,* 7480. (b) Wagner, P.J.; Liu, K.; Noguchi, Y. *Ibid.* **1981,** *103,* 3837. (c) Small, R. D., Jr.;

Scaiano, J.C. *Chem. Phys. Lett.* **1977**, *50*, 431. (d) Kaptein, R.; de Kanter, F.J.J.; Rist, G.H. *J. Chem. Soc., Chem. Commun.* **1981**, 499.

92 Braga, D.; Chen, S.; Filson, H.; Maini, L.; Netherton, M. R.; Patrick, B. O.; Scheffer, J. R.; Scott, C.; Xia, W. *J. Am. Chem. Soc.* **2004**, *126*, 3511.

93 Cheung, E.; Netherton, M. R.; Scheffer, J. R.; Trotter, J. *J. Am. Chem. Soc.* **1999**, *121*, 2919.

94 Cheung, E.; Kang, T.; Netherton, M. R.; Scheffer, J. R.; Trotter, J. *J. Am. Chem. Soc.* **2000**, *122*, 11753.

95 (a) Carr, N., Gray G. W. *Liquid Crystal*, **1989**, *6*, 467. (b) Leibovitch, M. PhD Thesis, The University of British Columbia, 1997.

96 Boymond, L.; Rottlander, M.; Caihiez, G.; Knochel, P. *Angew. Chem. Int. Ed.* **1998**, *37*, 1701.

97 (a) Wiberg, K. B.; Lowry, B. R.; Colby, T. H. *J. Am. Chem. Soc.*, **1961**, *83*, 3998. (b) Bixler R. L.; Niemann, C. *J. Org. Chem.* **1958**, *23*, 742.

98 (a) Von S. Herberg, V. S.;Naumann, D. *Z. Anorg. Allg. Chem.*, **1982**, *494*, 151-158. (b) Ruck, R. T.; Jones M. Jr. *Tetrahedron Lett.* **1998**, *39*, 4433.

99 (a) Scott, L. T.; Carlin, K. J.; Schultz, T. H. *Tetrahedron Lett.* **1978**, *19*, 4637. (b) Kowalski, C.; Creary, X.; Rollin, A. J.; Burke, M. C. *J. Org. Chem.* **1978**, *43*, 2601. (c) Ashby, E. C.; Goel, A. B.; DePriest, R. N. *Tetrahedron Lett.* **1981**, *22*, 4355. (d) Hoare, J. H; Yates, P. *J. Org. Chem.* **1983**, *48*, 3333. (e) Romesberg, F. E.; Collum, D. B. *J. Am. Chem. Soc.* **1995**, *117*, 2166.

100 The X = F and CN substrates are not all studied in the second project since their photochemical behaviors should be the same as that of X=COOMe substrates in solution. From previous studies in adamantyl acetophenones, the photochemical behaviors for X= F and CN and COOMe substrates are same, see reference: Yang J. PhD thesis, University of British Columbia).

101 Koshima, H.; Matsushige, D.; Miyauchi, M. *CrystEngComm* **2001**, *33*, 1.

102 Lewis, T. J.; Rettig, S. J.; Scheffer, J. R.; Trotter, J. *Mol. Cryst. Liq. Cryst.* **1992**, *219*, 17.

103 Scheffer, J. R.; Xia, W. *Org. Lett.* **2004**, submitted.

104 The interaction potential (total energy) describes both bonding and non-bonding interactions. The bonding interactions are usually formulated as a strain energy. The bonding interactions (strain energy) usually refer to atoms in the following relationships: (a) directly bonded (bond stretching, a 1-2 stretch relationships); (b) geminal to each other (bond angle bending or angle strain, a 1-3 angle bending relationship); (3) vicinal to each other (a 1-4 dihedral angle rotation relationship). The non-bonding interactions usually include the following: (1) an exchange repulsion when atoms get too close; (2) a long range attraction arising form dispersion forces; (3) electrostatic interactions coming from the interaction of charges, dipoles, quadrupoles, etc. The combination of (1) and (2) is referred to as a van der Waals term. See reference: Hyperchem Computational Chemistry, Hypercube, Inc. April, 1994.

105 Angle strain: "Strain due to a departure in bond angle from 'normal' values. The term is often used in the context of non-aromatic cyclic compounds in which the internal angles differ from the regular tetrahedral angle of $109°28'$; in this sense angle strain is also know as *Baeyer strain*". IUPAC Compendium of Chemical Terminology, 2nd Edition (1997).

106 Smith, M.B.; March, J. *Advanced Organic Chemistry* Wiley Interscience: New York, 1992.

107 Toda, F.; Tanka, K.; Kato, M. *Angew. Chem., Int. Ed. Engl.* **1998**, *37*, 2724.

108 Smissman, E. E.; Israili, Z. H. *J. Org. Chem.* **1968**, *33*, 4231.